

National Technical University of Athens

Doctoral Thesis

**Hydrophobically Modified Ethoxylated
Urethane (HEUR) synthesis: Process
Intensification and Insight into the
Structure-Rheology Relationship for
Waterborne Coatings**

Author:
Ioanna Tzortzi

Supervisor:
Georgios D. Stefanidis

A thesis submitted in fulfillment of the requirements

for the degree of Doctor of Philosophy

in the

Chemical Engineering Department

Athens 2023

«Η έγκριση της διδακτορικής διατριβής από την Ανωτάτη Σχολή Χημικών
Μηχανικών του Ε.Μ.Πολυτεχνείου δεν υποδηλώνει αποδοχή των γνώμων του
συγγραφέα. (Ν. 5343/1932, Άρθρο 202)»

Table of Contents

Summary.....	ii
Περίληψη	vii
Chapter 1 Introduction.....	1
1.1. The role of HEUR thickeners in waterborne coatings.....	2
1.2. HEUR manufacturing process.....	3
1.2.1. HEUR structure and polymerization reaction.....	3
1.2.2. Industrial HEUR production process	5
1.2.3. Industrial Challenges	6
1.3. Scope of the thesis and main research objectives	7
1.4. Thesis outline.....	10
Chapter 2 Evaluation of PU Sampling Protocols and Effect of Critical Process Parameters on the one-step HEUR Synthesis	20
2.1. INTRODUCTION.....	22
2.2. MATERIALS AND METHODS.....	24
2.3. Materials.....	24
2.4. Synthesis of polymers.....	25
2.5. Sampling of the produced polymers.....	27
2.6. Homogeneity of the bulk polymers.....	27
2.7. Description of parametric studies	27
2.8. Analytical methods.....	31
2.3. RESULTS AND DISCUSSION.....	34
2.3.1. Comparative analysis of in-situ and solid sampling methods for molecular weight determination and chemical characterization of polyurethane melts	34
2.3.2. Effect of polyol moisture concentration.....	36
2.3.3. Effect of the catalyst concentration.....	43
2.3.4. Effect of reaction temperature	46
2.3.5. Effect of mixing speed	48
2.3.6. Mixing limitations in the system.....	51

2.4. CONCLUSIONS	52
Chapter 3 One-step versus Two-step Synthesis of Hydrophobically Modified Ethoxylated Urethanes (HEURs): Benefits and Limitations.....	58
3.1. Introduction.....	60
3.2. MATERIALS AND METHODS	63
3.2.1. Materials.....	63
3.2.2. Synthesis procedure & Parametric studies	64
One-step HEUR synthesis	64
Two-step HEUR synthesis.....	64
3.2.3. Analytical Methods.....	66
3.3. RESULTS AND DISCUSSION	68
3.3.1. One-step HEUR and prepolymer synthesis – Effect of the reaction stoichiometry	68
3.3.2. Rheological behavior of HEURs produced via the one-step process.....	72
3.3.3. Two-step HEUR synthesis: Prepolymer molecular weight effects and end-capping efficiency.....	75
3.4. Conclusions.....	89
Chapter 4 Intensification of HEUR synthesis via unsteady -state thermal operation using microwaves	101
4.1. Introduction.....	103
4.2. MATERIALS AND METHODS	104
4.2.1. Materials.....	104
4.2.2. Experimental set-up.....	106
4.2.3. Temperature measurement and control.....	107
4.2.4. Synthesis procedure.....	110
4.2.5. Analytical Methods.....	111
4.3. RESULTS AND DISCUSSION	112
4.3.1. Effect of MW irradiation on the Pretreatment of PEG	112
4.3.2. Effect of MW irradiation on the polymerization	119
4.3.3. Estimation and comparison of the theoretical energy requirements for CH and MW heating HEUR synthesis.....	126

4.4. CONCLUSIONS.....	131
Chapter 5 Tailoring Waterborne Coatings Rheology with Hydrophobically Modified Ethoxylated Urethanes (HEURs): Molecular Architecture Insights Supported by CG-MD Simulations	141
5.1. INTRODUCTION.....	143
5.2. MATERIALS, METHODS AND MD SIMULATIONS	145
5.2.1. Materials.....	145
5.2.2. Synthesis of HEUR-X and formulation in water	145
5.2.3. Preparation of the HEUR-latex based emulsion and full paint formulation.....	146
5.2.4. Analytical Methods.....	147
5.2.5. Coarse grained molecular dynamics simulation.....	149
5.2.5.1. Automated micelle identification and quantification.....	151
5.3. RESULTS AND DISCUSSION	152
5.3.1. Structural characterization of HEUR	152
5.3.2. Impact of the chemical structure of HEUR on micelle formation and rheological behavior in aqueous solutions	155
5.3.3. Effects of latex and HEUR chemical structure on rheology and phase stability of waterborne latex–HEUR mixtures	166
5.3.4. Rheological characterization and performance evaluation of waterborne paints thickened with HEURs: Insights from Steady Shear and Oscillatory Rheology, Levelling, Sagging, and Heat Stability measurements.....	168
5.3.5. CONCLUSIONS.....	176
Chapter 6 Conclusions and Recommendations for future work	186
6.1. Conclusions.....	187
6.2. Recommendations for future work	192
Supporting Information for all Chapters.....	193
SI for Chapter 2	194
A. Sampling of the produced polymers.....	194
B. Homogeneity of the bulk polymers.....	199
C. Chemical structures and basic chemical reactions.....	200

D. Analysis results	213
SI for Chapter 3	222
SI for Chapter 5	237
Aqueous solutions.....	237
Latex-formulations.....	238
Paint formulations.....	239

*And for the curious minds wondering if I'd willingly embrace this journey again
— without a doubt, absolutely yes....*

Acknowledgments

Acknowledgments

Completing my PhD has been a long and significant journey. It was a time filled with doubt and struggle, but these challenges were crucial for my personal growth. During the difficult moments, I found myself wondering if I could handle the external pressures and whether I could manage my own emotions to overcome each obstacle that stood in my way. However, with each hurdle surpassed, not only did I find my inner strength, but also a deeper understanding of myself. This journey reaffirmed my love for science, particularly igniting a passion for polymers and coatings. Now as I reflect, I realize this success isn't just a personal achievement, but a collective triumph shared with the numerous wonderful individuals who supported me throughout. This achievement is not only mine but belongs to everyone who has been a part of this demanding yet fulfilling journey.

First and foremost, I would like to extend my sincere gratitude to my supervisor, Georgios Stefanidis, for choosing me as his first PhD researcher during his transition from KU Leuven to NTUA. A major milestone that significantly impacted our research environment was George's initiative in bringing the Simplify project to NTUA. The substantial funding associated with this project was instrumental in renovating our lab with new equipment, modernizing our workspace, and thereby significantly enhancing our research capabilities. Moreover, it fostered a collaborative platform, enabling me to work alongside proficient and supportive colleagues. I am thankful to George for his continual support and for giving me the freedom to explore thoroughly my research interests. His critiques, although challenging and demanding at times, prompted a more thorough examination of my research, thereby bolstering the robustness and academic merit of my findings.

Additionally, I extend my warm appreciation to Prof. Tom Van Gerven from KULeuven. His insightful feedback during our monthly meetings was valuable. His kind invitation to work at KULeuven for a couple of weeks at the beginning of the project provided me with a supportive environment to kickstart my PhD, for which I am truly thankful.

Acknowledgments

Another colleague I would like to thank is Christos Xiouras, a valued co-author in two of my published papers. His assistance in refining the text significantly elevated the quality of the manuscript. Additionally, his insight into microwave processing enriched my understanding and contributed immensely to the depth of the research. His mentoring spirit and expertise were invaluable, and I am looking forward to the possibility of future endeavors together.

A special acknowledgment goes to Prof. Anastasia Detsi and her post-doctoral researcher, Andromachi Tzani, with whom I had the privilege of co-authoring two of my published works. Their invaluable support and profound expertise in NMR-analysis were pivotal in elevating the quality of our research, adding a level of depth and precision that significantly enhanced the final outcomes. The wealth of knowledge imparted by Prof. Detsi and Ms. Tzani, and their collaborative approach, have greatly enriched my PhD journey, and their contributions to our joint work are highly valued.

Moreover, my gratitude extends to Prof. Mihalis Kavousanakis within our department, with whom I had the honor of collaborating during my final year. His profound expertise in molecular dynamics, extensive experience, and insightful feedback significantly elevated the level of our research on HEURs and their self-assembly structures. Your guidance and support, Mihalis, have been instrumental in advancing our work, and I am immensely grateful for the insight and dedication you brought to our collaborative efforts. In conjunction with this, a warm acknowledgment goes out to Dora Spirouni from Scienomics, whose meticulous work on the molecular dynamics simulations, in collaboration with Mihalis, was indispensable. The effort and expertise that Mihalis and Dora brought to our project greatly contributed to the successful completion of my final research project, and for that, I am deeply grateful.

Furthermore, I am deeply grateful for the opportunity to collaborate with the remarkable R&D team in ARKEMA's Rheology and Specialty Additives department as part of the Simplify project. The team, full of expertise and willingness to support me, greatly enriched my research journey. They generously provided indispensable industrial insights and enabled me to focus my research on real-world applications, increasing their relevance and impact. A heart-filled gratitude goes out to Guillaume Michaud, Jean-Marc SUAU, Antoine Baldin, and Imane Joundi. Working with such proficient

Acknowledgments

and supportive colleagues transformed the often-turbulent waters of research into a manageable and exciting endeavor. The mixture of hearty laughter, serious discussions and a shared sense of collective achievement shaped a memorable and valued chapter of my PhD journey. For me, the work we have done together goes beyond mere academic contributions; It is a testament to the incredible experience we have shared in the pursuit of knowledge, research and innovation, for which I am deeply grateful.

Moreover, I would like to thank my committee members, for their availability and for their effort dedicated to reading and evaluating this thesis.

Throughout this journey, I had the privilege of supervising and guiding a lot of master students from our Chemical Engineering department. I am profoundly grateful for the experimental work they conducted and the trust they placed in me regarding the experimental design. Each one of them left a mark on my academic journey, and I am thankful for the shared experiences and the knowledge exchanged.

Among them, some very special individuals transitioned from being mentees to becoming close friends, whose support was instrumental in the culmination of this PhD. Yannis Papaioanou, Chrysi Choustoulaki, and Valantis Tserpes, your involvement was more than a cornerstone in this endeavor. Your continuous support, both in extensive experimental work and emotional support through the myriad challenges we had to face, were my strength. Thank you for embracing my unconventional ideas and managing my over-sentimental personality. Our shared journey, with its highs and lows, made the destination more meaningful and the voyage much more enjoyable than I could have ever imagined.

When the letters 'PhD' cross and will cross my mind, it is your faces and our shared experiences that will always resonate profoundly within me.

Chrysi and Valantis, I am excited for your promising next steps in your careers, and I wish you nothing but the utmost success and happiness. Yannis, you are one of the most hard-working people I know. The way you know the lab equipment inside and out, it almost seems like you've spent more hours there than at home! Your thoroughness and persistence are not just inspiring to me, but to everyone who has the pleasure of working

Acknowledgments

with you. The finish line of your PhD journey is within sight; keep your enthusiasm ignited and continue the exemplary work. The friendship and steady support from each one of you turned every challenge into something manageable and made every success sweeter. I cherish our time together and am excited for all the future adventures in our friendships and careers.

Panos Vettas and Thanos Arampatzis, who initiated their PhD's during my final year, brought a refreshing burst of energy and insight into our academic environment. Our time together, both in the lab and during casual hangouts, added a touch of enjoyment and enthusiasm to my Ph.D. experience. Both Panos and Thanos are amazing researchers, and I learned a lot from them. I wish we had more time to work together and I'm looking forward to the possibility of future endeavors.

Ariana Bampouli, a cherished colleague from KU-Leuven, made our collaboration on the Simplify project and on our PhD a delightful experience. Our collaboration was really fruitful, marked by shared experimental work and the joint effort of co-authoring a manuscript. Your work ethic, professionalism, and insightful advice have been invaluable, Ariana. We not only supported each other until the submission of our paper but continued to do so until the submission of our PhDs. The enjoyable moments we shared during our trips enriched our working relationship, making the professional journey as fulfilling as it was fun. I am truly fortunate not only to have collaborated with you but also to have forged a good friendship along the way.

I extend my warm appreciation to Katerina Zerva, post-doctoral researcher in our laboratory, for her indispensable assistance with the experimental aspect of my PhD, especially during its initial phase when everything was new to me. Her in-depth knowledge, extensive experience, and boundless patience were pivotal in aiding my progression. Katerina, your calming presence in my moments of heightened sentimentality was like a balm, and you embody a blend of tranquility and strength that I greatly admire.

I am very grateful to my colleagues at ICT, whose hard-work in realizing the reactive extrusion process provided a practical lens through which we could better understand and envision our laboratory efforts within the larger context of continuous processing.

Acknowledgments

Their practical work and shared insights were helped us bridge the gap between scalability, batch and continuous processing. Each interaction, though mostly virtual due to the pandemic, broadened our collective knowledge and empowered our mutual quest for innovation. As I reflect on the missed opportunities for closer interaction, I am hopeful for a future filled with shared explorations. I wish them the best in the continuation of the SIMPLE-DEMO project and their personal research careers.

I wish to extend my deepest gratitude to my cherished friends, my sister and my parents, whose endless support was my stronghold throughout this challenging journey. They constantly reminded me that it's my choice to decide which aspects of the experience I hold onto, and that we don't have to accept everything that's handed to us by others. Their love, understanding, and wise advice have been my guiding light, and for that, I am forever grateful.

Last but certainly not least, my deepest gratitude goes to my beloved partner, George Patridas, for the endless support throughout this academic endeavor. Your presence, both in moments of triumph and through challenges, has been nothing short of a blessing. Your enduring faith in my abilities, even when I doubted myself, and your constant reminders of my strength and capability have been my silent driving force. Your love, patience, and encouragement have not only made the difficult days bearable but have also added immense value and joy to the good days. Your presence by my side has been a source of comfort, joy, and inspiration, making this challenging journey not only worthwhile but also a beautiful, shared adventure. Thank you, George, for being my pillar of positivity in the whirlwind of this PhD project. Your support has truly meant the world to me and made this success infinitely sweeter. I am thrilled to have you by my side as we celebrate this milestone together

Summary

Hydrophobically Modified Ethoxylated Urethanes (HEUR) synthesis: Process Intensification and Insight into the Structure-Rheology Relationship for Waterborne Coatings

This dissertation addresses key research gaps in the synthesis and application of Hydrophobically Modified Ethoxylated Urethanes (HEURs), which despite being well-established as urethane rheology modifiers in waterborne coatings, lack comprehensive scientific inquiry in certain crucial aspects. The primary focus is on addressing the shortcomings related to HEUR production processes and their rheological behavior across various waterborne systems. Four main areas of investigation have been identified: (1) examination of the sampling procedure for urethane rheology modifiers and the process conditions of the solventless one-step HEUR synthesis, which is the current industrial standard; (2) comparison of the benefits and limitations of one-step and two-step synthesis processes; (3) exploration of the potential of microwave (MW) heating for process intensification; and (4) investigation of the structure-rheology relationship in different waterborne dispersions.

HEURs are amphiphilic polymers which can be prepared by the solventless step-growth polymerization of PEG with diisocyanates and subsequently end-capped with hydrophobic mono-alcohols. First, a careful evaluation of the solvent-free one-step synthesis of HEURs was performed, focusing on both the sampling protocols for polyurethane (PU) testing and the effect of critical process parameters. Specifically, polyethylene glycol (PEG) moisture content, reaction temperature, mechanical mixing speed and catalyst concentration were investigated in terms of their effect on product quality. Results showed that the sampling method significantly influences the molecular weight determination and the chemical characterization of PU, with the solid method (analysis of a solid piece of PU) displaying molecular weights up to 115% higher than

the in-situ method (direct dissolution of the PU melt into dry solvent) when determined by Gel Permeation Chromatography (GPC). This phenomenon was attributed to chain-extension between NCO-terminated urethane prepolymers and ambient moisture, leading to the formation of urea linkages and an extended polyurea structure. Additionally, the study revealed that the moisture concentration in the initial polyol plays a significant role in HEUR polymerization. Maintaining moisture content below the threshold of 1000 ppm was proven to be crucial to foster the primary urethane reaction while suppressing undesirable side reactions that could adversely affect the viscosity of HEUR aqueous solutions. Further investigation revealed that both elevated mixing speeds and higher reaction temperatures (within the range 80-110°C) lead to faster molecular weight development, albeit reaching the same molecular weight plateau. Notably, when the molecular weight of polyurethanes approaches 21,000 g/mol, the polymer turns into a viscous gel exhibiting the Weissenberg effect. At industrial scale, if this state is reached too rapidly, it could jeopardize the homogeneous distribution of reactants within the viscous PEG, leading to batch inconsistencies. Therefore, in the event of viscous polyurethane polymerizations carried out in industrial-scale batch reactors, it is recommended to use moderate mixing speeds adapted to the specific polymerization scale. Given PEG's susceptibility to thermal degradation, maintaining reaction temperatures between 80-85°C is recommended, especially during extended polymerization periods in industrial-scale batch reactors.

In addition, a comparison between the one-step (simultaneous chain growth and end-capping) and two-step (chain growth followed by end-capping) processes for HEUR synthesis was carried out, primarily emphasizing on the advantages and disadvantages of each method and highlighting their impact on the final HEUR properties. In the conventional one-step process (current industrial practice) there are inherent limitations in producing high molecular weight polymers due to the complex competition between end-capping and polymerization. We showed that the two-step method allows for much higher molecular weight polymers than the one-step method, while using less amount of toxic diisocyanates. Additionally, using the two-step method, the polymerization can be simply and efficiently controlled by the addition timepoint of the end-capping agent, which can be tailored to provide HEURs with a wide range of molecular weights and polydispersity indices. However, the efficient end-capping of high molecular weight polymers remains a challenge when using conventional mixing equipment in batch

reactors, due to mass transfer and mixing limitations associated with significant increase in the bulk viscosity of the reaction mixture. To overcome these limitations, alternative, more efficient mixing technologies, such as reactive extruders, should be considered for the efficient end-capping of high molecular weight polymers.

The application of MW irradiation as an alternative energy source for HEUR synthesis was explored due to the inherent heat and mass transfer limitations encountered in highly viscous systems. Given these challenges, the application of MW irradiation, known for its rapid volumetric heating capability, was investigated with the aim of reducing both the energy consumption and process time. We studied the effect of microwave heating on both the HEUR synthesis step and the initial pretreatment step of the reagents. During the reactants pretreatment step, MW heating can reduce the overall process time through tenfold faster melting of the solid PEG. However, in the subsequent PEG dehydration step, use of MW should be avoided, as faster degradation of PEG was observed compared to conventional heating (CH) dehydration at a similar bulk temperature. In the polymerization reaction, it was shown that both the polymer molecular weight, M_n , and the polydispersity index, PDI, of the HEUR prepolymer are independent of the heating source when the same reaction temperature was applied. However, it was concluded that operation of the batch reactor in a rapid unsteady-state (transient) temperature profile, only attainable with MW heating, resulted in production of HEURs with comparable molecular weights to those produced via isothermal CH experiments at process times multifold lower (4 min in MW vs. 45 or 120 min in CH at a temperature of 110 °C and 80 °C, respectively), due to the rapid thermal response of the polymerization mixture under MW irradiation. A comparison of the energy requirements of the transient MW heating process and the isothermal CH one (at comparable mean temperatures) shows that the former one needs approximately 3 times less energy to achieve the same molecular weight polymer, due to the shorter processing times (and subsequently lower heat losses to the surroundings) and the elimination of the additional energy needed to heat up the heat transfer fluid.

Acknowledging the academic and industrial need for deeper understanding of the rheological properties of urethane thickeners, the effects of hydrophilic and hydrophobic segments of HEURs on the rheological properties of various waterborne dispersions, including aqueous solutions, latex-based emulsions, and commercial

waterborne paint formulations were investigated. Utilizing both experimental and computational methodologies significant insights were gained in this area that can help advance the transition from empirical to systematic optimization of rheological performance of paints. Linear HEUR thickeners with different hydrophilic and hydrophobic segments were synthesized through a controlled one-step polymerization process by employing PEGs with molecular weights ranging from 2000 to 10,000 g/mol, resulting in HEUR molecular weights ranging from 8,000 to 33,000 g/mol. To investigate variations in molecular weight, we used HMDI-C8 as the terminal hydrophobic group. To investigate the effect of hydrophobic segment, we selected a HEUR molecular weight of 23,000 g/mol. Utilizing diisocyanates, such as HMDI, IPDI and HDI, we standardized the end-capping with C8. When mono-alcohol lengths were altered (C6 to C12), HMDI was retained as diisocyanate linker.

The rheological analysis demonstrated a significant influence of the hydrophobe's structure on HEUR behavior across all studied formulations. Notably, HEUR samples with increased terminal hydrophobicity, particularly the P8-HMDI-C12, exhibited strongly pseudoplastic behavior in all formulations studied. In paint formulations, these structures demonstrated rapid structural regeneration and high TI values resulting in enhanced sag resistance. However, these benefits were offset by compromised leveling properties. In contrast, HEURs with less effective hydrophobic segments (P8-HDI/IPDI-C8 and P8-HMDI-C5/C6) displayed Newtonian rheological behavior and the corresponding paint formulations showed slower structural regeneration with superior leveling but worse anti-sag performance.

Regarding the hydrophilic segment, gradual increase in HEUR molecular weight up to 23,000 g/mol resulted in marginal viscosity changes in aqueous solutions, while a pronounced viscosity increase was observed with a molecular weight of 33,000 g/mol. In latex emulsions, lower molecular weight HEURs (8000 g/mol) displayed extended flocculated regions, a trend that appeared to be diminished with a 14,000 g/mol HEUR and absent with a 23,000 g/mol HEUR. In paint formulations, molecular weights of 14,000, 18,000, and 23,000 g/mol exhibited similar rheological response in paint formulations, but a molecular weight of 33,000 g/mol deviated, showing a shift towards higher viscosities and solid-like properties.

To complement and rationalize the experimental findings, coarse-grained molecular dynamics (CG-MD) simulations were utilized to explore HEUR micellar morphology and effectively capture the spontaneous micelle formation in aqueous solutions. Guided by the DBSCAN algorithm and Monte-Carlo techniques, metrics, such as the volume of the hydrophobic cluster, the total micellar volume, the aggregation number (N_{agg}), and the number of interconnected chains ($N_{bridged}$) with other micelles were employed. By performing CG-MD simulations for various concentration values in aqueous solutions, we observed variations in the micellar network density correlating with experimental viscosity trends, while as the hydrophilic length of HEUR increased, the micellar volume continued to grow, in alignment with observed experimental viscosity changes.

Περίληψη

Σύνθεση υδρόφοβων αιθοξυλιωμένων ουρεθανών (HEUR): Εντατικοποίηση της διεργασίας παραγωγής τους και σχέση δομής-ρεολογικών ιδιοτήτων σε συστήματα υδατοδιαλυτών επιστρώσεων

Οι τροποποιημένες υδρόφοβες αιθοξυλιωμένες ουρεθάνες (hydrophobically modified ethoxylated urethanes - HEUR) αποτελούν μια κατηγορία πολυουρεθανών (polyurethanes - PU) που αξιοποιείται ως πρόσθετο σε υδατικές διασπορές και επιστρώσεις για την τροποποίηση της ρεολογικής τους συμπεριφοράς. Η χημική τους δομή προκύπτει από τον σταδιακό πολυμερισμό μεταξύ ενός μακριού εύκαμπτου υδατο-διαλυτού μορίου (συνήθως πολυαιθυλενογλυκόλη - PEG) που αποτελεί το κύριο κορμό του πολυμερούς, ενός δισοκυανίου (diNCO) που χρησιμοποιείται για το πολυμερισμό της PEG και ενός μικρού υδρόφοβου μορίου (μονο-αλκόολη- R-OH) που προσδίδει τον υδρόφοβο χαρακτήρα στα άκρα του πολυμερούς. Η εκτεταμένη χρήση τους, ειδικά στη βιομηχανία χρωμάτων και επικαλύψεων, έχει δημιουργήσει την ανάγκη για παραγωγή πολυμερών HEUR με τις κατάλληλες ρεολογικές ιδιότητες, χωρίς τη χρήση διαλυτών, λόγω οικονομικών και περιβαλλοντικών περιορισμών. Επίσης, πέρα από την αναγκαιότητα απομάκρυνσης των διαλυτών, η γνώση των βέλτιστων συνθηκών πολυμερισμού είναι απαραίτητη τόσο για την εξοικονόμηση ενέργειας στην βιομηχανική παραγωγή των HEUR όσο και για την παραγωγή HEUR ελεγχόμενου μοριακού βάρους με στόχο την εφαρμογή τους σε συστήματα επιστρώσεων με διαφορετικές απαιτήσεις στις ρεολογικές ιδιότητες.

Η διατριβή επικεντρώθηκε σε τέσσερις βασικούς ερευνητικούς άξονες: (1) τη μελέτη της επίδρασης της μεθόδου δειγματοληψίας PU και των συνθηκών αντίδρασης για τη σύνθεση HEUR με τεχνική πολυμερισμού μάζας ενός σταδίου (μέθοδος παραγωγής σε βιομηχανική κλίμακα), στις ιδιότητες του πολυμερούς, (2) τη σύγκριση των μεθόδων παραγωγής HEUR με πολυμερισμό μάζας ενός και δύο σταδίων, (3) τη μελέτη της εντατικοποίησης της διεργασίας παραγωγής HEUR με χρήση μικροκυμάτων και (4) τη μελέτη της επίδρασης της αμφίφυλης δομής HEUR στην ρεολογική συμπεριφορά υδατοδιαλυτών διασπορών και επιστρώσεων.

Σε πρώτο στάδιο, μελετήθηκε η επίδραση των συνθηκών αντίδρασης με τεχνική πολυμερισμού μάζας ενός σταδίου καθώς και διαφορετικές μέθοδοι δειγματοληψίας της PU στις ιδιότητες του παραγόμενου προϊόντος. Ειδικότερα αναλύθηκε η επίδραση της υγρασίας της PEG, η θερμοκρασία της αντίδρασης πολυμερισμού, η ταχύτητα της μηχανικής ανάδευσης και η συγκέντρωση του καταλύτη στην ποιότητα της παραγόμενης PU. Τα αποτελέσματα κατέδειξαν ότι η ανάλυση στερεών δειγμάτων PU όπου το τήγμα έχει στερεοποιηθεί σε ατμοσφαιρικές συνθήκες δύναται, ανάλογα με την ποσότητα diNCO στο τήγμα, να οδηγήσει μέχρι και σε 115% υψηλότερα μοριακά βάρη από την in-situ μέθοδο, κατά την οποία το τήγμα PU διαλύεται κατευθείαν σε άνυδρο χλωροφόρμιο χωρίς να εκτεθεί σε ατμοσφαιρικές συνθήκες. Το φαινόμενο αυτό οφείλεται στον μετα-πολυμερισμό (chain extension) των ισοκυανικά τερματισμένων αλυσίδων προπολυμερούς των HEUR με την ατμοσφαιρική υγρασία προς παραγωγή πολυουρίας. Επιπλέον, η μελέτη απέδειξε ότι η συγκέντρωση υγρασίας στην αρχική PEG καθορίζει το βαθμό πολυμερισμού των HEUR. Η διατήρηση της υγρασίας της PEG κάτω από 1000 ppm αποδείχθηκε ότι ευνοεί την παραγωγή PU, ενώ ταυτόχρονα καταστέλλει ανεπιθύμητες παράλληλες αντιδράσεις προς παραγωγή ουρίας που θα μπορούσαν επίσης να επηρεάσουν τόσο το βαθμό πολυμερισμού αλλά και το ιξώδες του υδατικού διαλύματος των HEUR. Περαιτέρω μελέτη απέδειξε ότι τόσο οι αυξημένες ταχύτητες ανάμειξης όσο και οι υψηλότερες θερμοκρασίες αντίδρασης (εντός του εύρους των 80-110°C) ευνοούν την ταχύτερη ανάπτυξη του μοριακού βάρους της PU, αν και φθάνουν στο ίδιο βαθμό πολυμερισμού. Συγκεκριμένα, όταν το μέσου αριθμού μοριακό βάρος των πολυουρεθανών πλησιάζει τα 21000 g/mol με δείκτη πολυδιασποράς (PDI)≈1.65, το πολυμερές μετατρέπεται σε παχύρρευστο πήκτωμα και συρρικνώνεται στη κάθετη ράβδο του αναδευτήρα, γνωστό ως φαινόμενο Weissenberg. Σε βιομηχανική κλίμακα, εάν αυτό το φαινόμενο εμφανισθεί πολύ

γρήγορα, θα μπορούσε να διαταράξει την ομοιογενή κατανομή των αντιδρώντων, οδηγώντας σε ασυνέπεια των τελικών ιδιοτήτων του παραγόμενου προϊόντος από παρτίδα σε παρτίδα. Επομένως, για παραγωγή πολυουρεθάνης με πολυμερισμό μάζας σε αντιδραστήρες διαλείποντος έργου βιομηχανικής κλίμακας, συνιστάται η χρήση μετρίων ταχυτήτων ανάδευσης. Δεδομένης της ευαισθησίας της PEG στη θερμική και οξειδωτική της αποικοδόμηση, συνιστάται η διατήρηση των θερμοκρασιών αντίδρασης μεταξύ 80-85°C, ειδικότερα αν η διάρκεια του πολυμερισμού είναι μεγάλη.

Στη συνέχεια, πραγματοποιήθηκε μια σύγκριση μεταξύ των μεθόδων παραγωγής HEUR ενός σταδίου και δύο σταδίων με πολυμερισμό μάζας, δίνοντας έμφαση στα πλεονεκτήματα και τα μειονεκτήματα της χρήσης είτε ενός σταδίου (ταυτόχρονος πολυμερισμός και τερματισμός της πολυμερικής αλυσίδας με R-OH) είτε δύο σταδίων (προηγείται ο πολυμερισμός και ακολουθείται ο τερματισμός της πολυμερικής αλυσίδας με R-OH) στις τελικές ιδιότητες του HEUR. Στη διαδικασία ενός σταδίου (βιομηχανική πρακτική), υπάρχουν εγγενείς περιορισμοί στην παραγωγή πολυμερών υψηλού μοριακού βάρους λόγω του ανταγωνισμού μεταξύ του πολυμερισμού και του τερματισμού της πολυμερικής αλυσίδας με R-OH. Δείξαμε ότι η μέθοδος δύο σταδίων επιτρέπει την ανάπτυξη πολυμερών πολύ υψηλότερου μοριακού βάρους από τη μέθοδο ενός σταδίου, ενώ χρειάζεται λιγότερη ποσότητα τοξικών δυσοκυανικών. Επιπλέον, χρησιμοποιώντας τη μέθοδο δύο σταδίων ο βαθμός πολυμερισμού μπορεί να ελεγχθεί μέσω της χρονικής στιγμής της προσθήκης της ένωσης τερματισμού (R-OH), η οποία μπορεί να προσαρμοστεί ώστε να παραχθούν HEUR με ένα ευρύ φάσμα μοριακών βαρών και PDI. Ωστόσο, η αποτελεσματική υδρόφοβη τροποποίηση των άκρων της πολυμερικής αλυσίδας υψηλού μοριακού βάρους με R-OH παραμένει μια πρόκληση όταν χρησιμοποιείται μηχανική ανάδευση σε αντιδραστήρες διαλείποντος έργου, λόγω περιορισμών στη μεταφοράς μάζας που σχετίζονται με τη σημαντική αύξηση του ιξώδους του πολυμερικού τήγματος. Συνεπώς, για την παραγωγή πολυουρεθανών υψηλού μοριακού βάρους συνιστάται η εξώθηση με ταυτόχρονη αντίδραση (reactive extrusion) που επιτρέπει την αποτελεσματική ανάμειξη και παραγωγή πολυμερών με πολύ υψηλά ιξώδη.

Η χρήση της μικροκυματικής ακτινοβολίας (MW) ως εναλλακτικός τρόπος μεταφοράς ενέργειας για τη σύνθεση HEUR διερευνήθηκε λόγω των εγγενών περιορισμών μεταφοράς μάζας και θερμότητας που χαρακτηρίζουν τα πολυμερή υψηλού ιξώδους.

Δεδομένων αυτών των περιορισμών, η εφαρμογή MW, η οποία συγκρινόμενη με τις συμβατικές μεθόδους θέρμανσης (CH) οδηγεί σε ταχεία ογκομετρική θέρμανση, σε μείωση των χρόνων αντίδρασης και της καταναλισκόμενης ενέργειας αλλά και σε υψηλότερες αποδόσεις αντίδρασης για διάφορες διεργασίες σύμφωνα με την βιβλιογραφία, διερευνήθηκε με στόχο τη μείωση τόσο της κατανάλωσης ενέργειας όσο και του χρόνου της διεργασίας. Η επίδραση των MW ερευνήθηκε τόσο στο στάδιο σύνθεσης των HEUR όσο και στο αρχικό στάδιο προεπεξεργασίας των μονομερών τους. Κατά τη διάρκεια του σταδίου προεπεξεργασίας των μονομερών, η θέρμανση με MW μπορεί να μειώσει τον συνολικό χρόνο της διεργασίας παραγωγής των HEUR μέσω της κατά δέκα φορές ταχύτερης τήξης της στερεής PEG. Ωστόσο, στο επόμενο στάδιο αφυδάτωσής της, η χρήση MW θα πρέπει να αποφεύγεται, καθώς παρατηρήθηκε ταχύτερη αποικοδόμηση της PEG σε σύγκριση με την αφυδάτωση της με CH σε παρόμοια θερμοκρασία. Στην αντίδραση πολυμερισμού, αποδείχθηκε ότι τόσο το μέσου αριθμού μοριακό βάρος, M_n , όσο και ο PDI του προπολυμερούς των HEUR είναι ανεξάρτητα από τη χρησιμοποιούμενη πηγή θέρμανσης, καθώς δεν υπήρξαν σημαντικές διαφορές για κανένα από τα δύο όταν η σύνθεση πραγματοποιήθηκε σε παρόμοιες ισοθερμοκρασιακές συνθήκες. Ωστόσο, διαπιστώθηκε ότι η λειτουργία του αντιδραστήρα διαλείποντος έργου σε μεταβατικές συνθήκες και η πραγματοποίηση του πολυμερισμού με ταχέως αυξανόμενο θερμοκρασιακό προφίλ, που μπορεί να επιτευχθεί μόνο με MW, είχε ως αποτέλεσμα την παραγωγή HEUR με συγκρίσιμα μοριακά βάρη, όπως αυτά που παράγονται μέσω CH σε ισοθερμοκρασιακές συνθήκες, σε χρόνους διεργασίας σημαντικά χαμηλότερους (4 λεπτά έναντι 45 ή 120 λεπτά σε θερμοκρασία 110 °C και 80 °C, αντίστοιχα). Το τελευταίο αποδόθηκε στην ταχεία θερμική απόκριση του αντιδρώντος μίγματος στα MW. Η ενεργειακή ανάλυση της παραγωγής HEUR που πραγματοποιήθηκε για αντιδραστήρες διαλείποντος έργου σε σταθερές ισοθερμοκρασιακές συνθήκες με CH και σε μεταβατική κατάσταση με αυξανόμενο θερμοκρασιακό προφίλ με χρήση MW (σε συγκρίσιμες μέσες θερμοκρασίες), δείχνει ότι η παραγωγή HEUR με MW χρειάζεται περίπου 3 φορές λιγότερη ενέργεια για να επιτύχει το ίδιο μοριακό βάρος, λόγω μικρότερων χρόνων αντίδρασης, προ-επεξεργασίας της PEG (και επακόλουθως μικρότερων απωλειών θερμότητας προς το περιβάλλον) και εξοικονόμηση της επιπρόσθετης ενέργειας που απαιτείται για την θέρμανση του θερμαντικού ρευστού στην περίπτωση θέρμανσης του αντιδραστήρα με μανδύα.

Τέλος, δεδομένου της επιτακτική ανάγκης της βιομηχανίας για καλύτερη κατανόηση των ρεολογικών ιδιοτήτων των HEUR και του σχετικού κενού στην υπάρχουσα βιβλιογραφία, η παρούσα διδακτορική διατριβή αναλύει συστηματικά την επίδραση των υδρόφιλων και υδρόφοβων τμημάτων των HEUR σε διάφορες υδατοδιαλυτές διασπορές, συμπεριλαμβανομένων υδατικών διαλυμάτων, ακρυλικών γαλακτωμάτων με βάση το λάτεξ και εμπορικών υδατοδιαλυτών βαφών. Χρησιμοποιώντας τόσο πειραματικές όσο και υπολογιστικές μεθόδους με κύριο στόχο την κατανόηση και τον προσδιορισμό της σχέσης δομής-ρεολογίας των HEUR, η μελέτη μας συμβάλει ουσιαστικά στην μετάβαση από την εμπειρική στη συστηματική βελτιστοποίηση της ρεολογικής συμπεριφοράς των υδατοδιαλυτών διασπορών μέσω της προσθήκης HEUR. Με πολυμερισμό μάζας ενός σταδίου συντέθηκαν γραμμικά HEUR με ποικίλα υδρόφιλα και υδρόφοβα τμήματα. Η μεταβολή του υδρόφιλου τμήματος των HEUR επιτεύχθηκε χρησιμοποιώντας PEG που κυμαίνονται από 2000 έως 10000 g/mol, οδηγώντας σε μοριακά βάρη HEUR από 8000 έως 33000 g/mol. Η μελέτη του υδρόφοβου τμήματος πραγματοποιήθηκε μέσω χρήσης διαφορετικών δομών δισοκυανίων (HMDI, IPDI, HDI) και διαφορετικού μήκους μονο-αλκόολης (C6, C8, C12).

Η ρεολογική ανάλυση ανέδειξε τη κυρίαρχη επίδραση του υδρόφοβου τμήματος των HEUR στη ρεολογική συμπεριφορά των υδατοδιαλυτών διασπορών. Για παράδειγμα, τα HEUR με ισχυρά υδρόφοβα άκρα τα οποία δημιουργούνται είτε από τη χρήση πιο όγκώδων diNCO, είτε μεγαλύτερου μήκους R-OH, παρουσιάζουν έντονα ψευδοπλαστική συμπεριφορά όταν αυτά προστεθούν σε υδατικά διαλύματα, ακρυλικά γαλακτώματα αλλά και σε υδατοδιαλυτές βαφές. Οι υδατοδιαλυτές βαφές με υψηλά ιξώδη και έντονα ψευδοπλαστική συμπεριφορά παρουσίασαν πολύ γρήγορη ανάκτηση του ιξώδους τους μετά από υψηλό ρυθμό διάτμησης, ενώ σε δοκιμαστικά τεστ που προσομοιώνουν την εφαρμογή των βαφών στους τοίχους παρουσίασαν αυξημένη αντοχή ενάντια στην κατακόρυφη ροή τους (good anti-sagging behavior) αλλά η επίστρωση αυτή ήταν πολύ τραχεία και με πολλά σημάδια (bad levelling behavior). Αντιθέτως, τα HEUR με λιγότερο υδρόφοβα άκρα παρουσίασαν μικρότερα ιξώδη και Νευτώνική συμπεριφορά η οποία συνοδεύτηκε από αργή ανάκτηση του ιξώδους τους, μικρότερη αντοχή στην κατακόρυφη ροή τους και πιο λείες επιστρώσεις. Η μεταβολή του μοριακού βάρους των HEUR δεν είχε τόσο σημαντική επίδραση στη ρεολογική του συμπεριφορά τους όσο είχε η επίδραση του υδρόφοβου τμήματός τους. Η μεταβολή

του μοριακού βάρους των HEUR από 8000-23000 g/mol οδήγησε στην αύξηση του ιξώδους των υδατοδιαλυτών διασπορών αλλά όχι με πολύ σημαντικές διαφορές, ενώ περαιτέρω αύξηση του στα 33,000 g/mol οδήγησε σε σημαντική διαφοροποίηση του ιξώδους και της ρεολογικής συμπεριφοράς των υδατοδιαλυτών διασπορών των HEUR. Αναφορικά με την ευστάθεια των ακρυλικών γαλακτωμάτων των HEUR, παρατηρήθηκε ότι η αύξηση του μοριακού βάρους του πολυμερούς που οφείλεται στο μέγεθος της χρησιμοποιούμενης PEG, οδηγεί σε διεύρυνση των συγκεντρώσεων λάτεξ και HEUR, στις οποίες δεν παρατηρείται διαχωρισμός φάσεων.

Συμπληρωματικά με τα πειραματικά αποτελέσματα της επίδρασης της υδρόφιλης και υδρόφοβης συστάδας των HEUR στη ρεολογική συμπεριφορά των υδατικών διασπορών, χρησιμοποιήθηκαν προσομοιώσεις ενός αδροποιημένου (coarse-grained) μοντέλου μοριακής δυναμικής (CG-MD) για να προσδιοριστεί η μορφολογία και η αυτοοργάνωση των μικκυλίων των HEUR σε υδατικά διαλύματα. Με χρήση του αλγορίθμου DBSCAN και τεχνικές Monte-Carlo, ποσοτικοποιήθηκαν δείκτες όπως ο όγκος του υδρόφοβου πυρήνα, ο όγκος των μικκυλίων, ο αριθμός συσσωμάτωσης (N_{agg}) και ο αριθμός των γεφυρωμένων αλυσίδων ($N_{bridged}$) με άλλα μικκύλια. Τέλος, οι προσομοιώσεις περιέγραψαν με επιτυχία την επίδραση της συγκέντρωσης των HEUR και του μεγέθους της υδρόφιλης συστάδας τους στην αυτοοργάνωση και την μορφολογία των μικκυλίων στο υδατικό περιβάλλον, το οποίο εξηγεί τα πειραματικά αποτελέσματα της ρεολογικής συμπεριφοράς των HEUR στο νερό.

Introduction

1.1. The role of HEUR thickeners in waterborne coatings

The use of coatings spans a wide range of applications between industrial and architectural fields such as wood, automotive, coil, packaging, protective and marine, and fulfils a variety of functions such as protection, aesthetics, and specialized performance.¹⁻³ Solvent-based coatings have traditionally dominated the market and are known for their robust mechanical properties and high-quality finish. In the quest for safer and more user-friendly coatings, waterborne latex-based options have emerged as a viable alternative to solvent-borne formulations, largely due to their reduced health risks associated with volatile organic compounds (VOCs) and absence of noxious odors.^{1,2} However, these waterborne systems present rheological challenges, including suboptimal flow, leveling, film build-up and application spattering. To overcome these deficiencies and improve the rheological performance of solvent-borne coatings, latex formulations require the inclusion of rheology modifiers.^{1,2,4}

Historically, early development of rheological modifiers were based on starch and casein, but these materials were both biodegradable and exhibited poor film-forming and flow characteristics.¹ Subsequent advances led to the adoption of high molecular weight cellulosic thickeners and clays, which offered improved properties through polymer chain entanglement. Despite these enhancements, cellulosic additives still exhibited limitations, such as unsatisfactory spatter resistance, suboptimal flow, and leveling properties, along with biodegradability issues.^{1,5}

The shortcomings of cellulosic additives led to the development of associative thickeners for latex coatings, which were introduced in the 1980s and offered superior rheological performance, including improved flow and leveling properties.¹ These modern rheological modifiers have thus emerged as critical components for achieving the desired rheological profiles in waterborne latex coatings. Within the associative thickeners family, Hydrophobically Modified Ethoxylated Urethanes (HEURs) constitute a representative class of rheological polyurethane (PU) modifiers, characterized by their excellent performance and versatility. Their chemical structure stems from the polycondensation reaction between a long flexible water-soluble diol (usually polyethylene glycol), a small hydrophobic alcohol and a diisocyanate (which connects the two aforementioned groups), as schematically shown in Figure 1.1.

Chapter 1

HEURs offer the advantage of effective rheological control without the need for solvents, thereby aligning with the environmental mandate that governs the coatings industry.

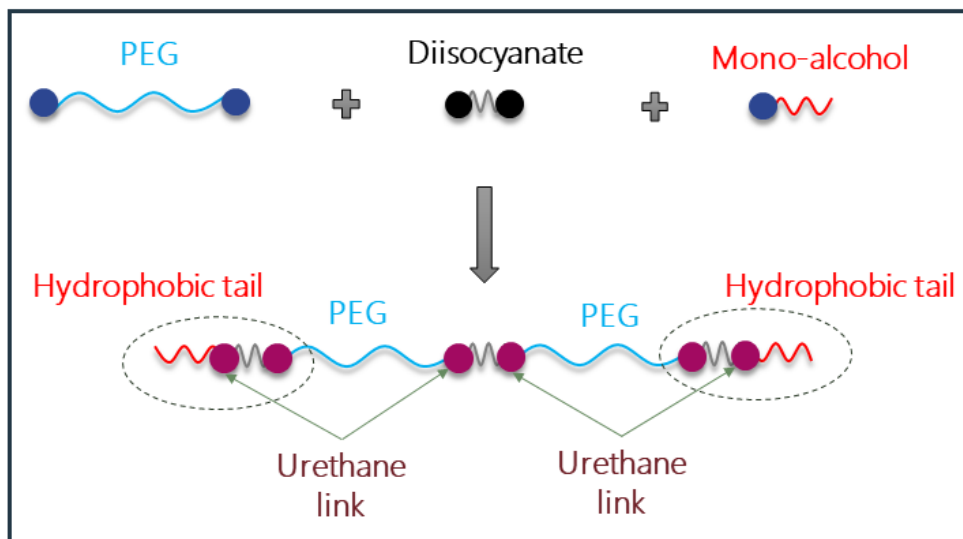


Figure 1.1. Schematic representation of the molecular structure of HEUR thickeners.

However, the status quo is not without challenges and unexplored areas. On the one hand, the synthesis of HEURs has its own complexities, often requiring high energy input, facing mass transfer limitations, and sometimes leading to batch-to-batch inconsistencies. On the other hand, there is a significant knowledge gap in understanding how the molecular architecture of HEURs can be designed to achieve specific rheological profiles. While rheology modifier market is expected to reach \$6.83 billion by 2024³, the scientific community has yet to fully decipher the connection between HEUR structure and its rheological performance, a necessity for the future of sustainable, high-performance waterborne coatings.

1.2. HEUR manufacturing process

1.2.1. HEUR structure and polymerization reaction

HEURs contain both water-soluble (hydrophilic backbone) and water-insoluble segments (hydrophobic end groups). Polyethylene glycol (PEG) of various molecular weights (2000 g/mol -10,000 g/mol) is commonly used as the hydrophilic segment in HEURs, but copolymers of PEG with poly (propylene glycol) (PPG) or poly (butylene glycol) (PBG) have also been used.³ Different hydrophobic groups, such as

Chapter 1

hydrophobic alcohols or amines (C6-C20)³ and alternative groups like fluorocarbon alkyl chains⁶⁻⁸, alkylphenyl⁹⁻¹¹, and light¹² or stimuli-responsive groups^{13,14}, have also been studied in laboratories. This amphiphilic structure of HEURs allows the formation of flower-like micelles which can be linked resulting in a dynamic transient network, either with emulsion particles or with each other, due to interactions between their hydrophobic groups.^{3,15-21} Depending on the type of HEURs used, this reversible physical network can be used to impart a more Newtonian or a strongly pseudoplastic rheological behavior to the final product.²²⁻²⁴

HEURs are typically synthesized by the step growth polymerization (also called polyaddition or polycondensation) of terminal hydroxyl groups of PEG with diisocyanates and hydrophobic mono-alcohols. Unlike conventional polycondensation, this polymerization reaction does not eliminate any by-products. Two common methods are used for the production of HEURs using diisocyanates: the one-step and two-step methods.²⁵ The one-step process involves the simultaneous addition of all reactants into the reactor, while the two-step process (or prepolymer method) involves two different sequential reaction steps. In the first step, polyol reacts with the diisocyanate to form an isocyanate-terminated prepolymer. The second step involves the addition of a monofunctional component referred to as an end-capping agent (or chain stopper)^{26,27} Figure 1.2 shows a schematic representation of the one vs two-step synthetic procedure for the HEUR synthesis.

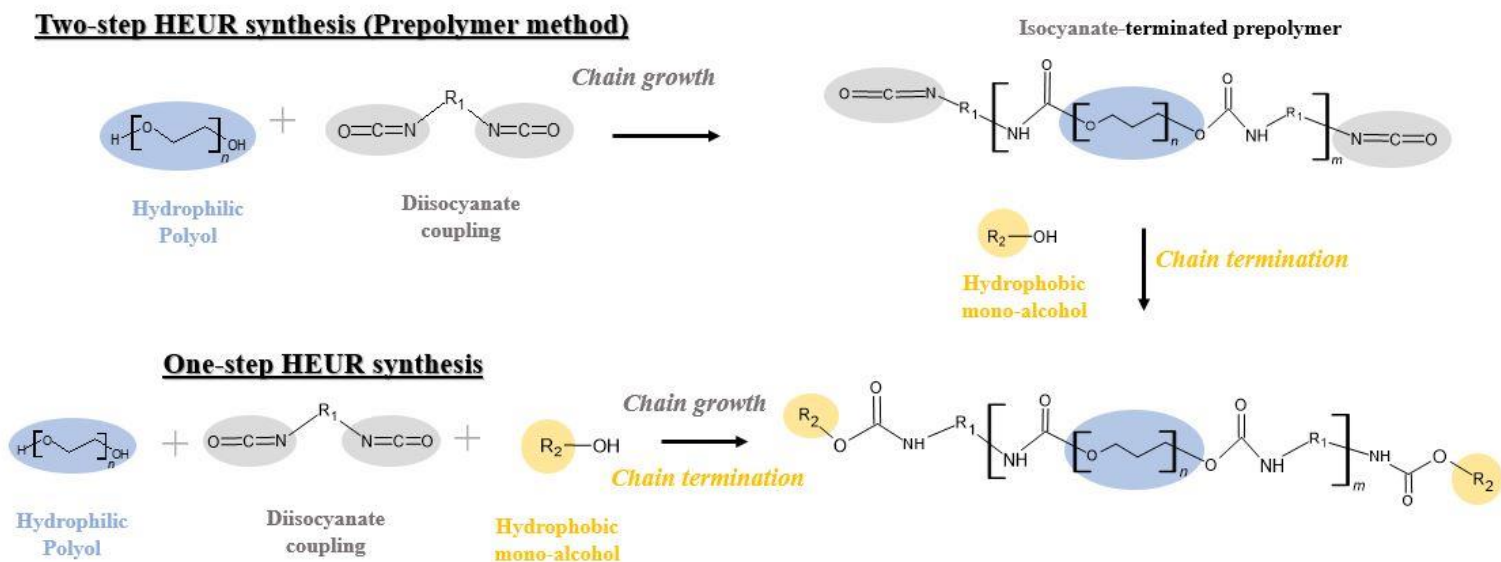


Figure 1.2. One vs two-step synthetic procedure for the HEUR synthesis. The Figure is redrafted from conference presentation²⁸ with permission of the authors.

From a reaction kinetics perspective, the one-step method used for the synthesis of HEURs has a significant disadvantage, which lies in the fact that polymerization and chain termination counteract each other based on the relative chemical reactivities of the polyol and the hydrophobe, affecting the polymer molecular weight build-up and potentially preventing the attainment of high molecular weight polymers.^{25,29-31} Conversely, the two-step process decouples the polymerization and chain termination processes, which allows for more control on the HEUR molecular weight simply by controlling the molecular weight of the prepolymer and the addition timepoint of the end-capping agent. Despite the potential for improved control using the two-step method, there is a gap in the existing literature regarding its benefits and potential limitations.

1.2.2. Industrial HEUR production process

In the chemical industry, HEUR is produced in large batches of several cubic meters ($\geq 10 \text{ m}^3$) without the use of solvents. The HEUR solution is prepared in two steps. First, the HEUR thickener (melt) is produced. The initial stage entails the synthesis of the HEUR thickening agent in its melt form. This is achieved through a one-step reaction involving PEG ($2000 < M_n < 10,000 \text{ g/mol}$), a hydrophobic molecule, a diisocyanate, and a catalyst. The reaction is carried out under vigorous stirring and stoichiometric conditions at elevated temperatures between 80 and 110°C, producing a highly viscous polyurethane thickener. Depending on the specific grade of HEUR, the resulting viscosity may range from 30 to 200 Pa·s. To facilitate subsequent handling and transfer, the product is maintained at temperatures above 80°C. The second stage involves dilution of the melt product within the same reactor. This is achieved by introducing water and a surfactant, typically in a ratio of 70% thickener, 20% water, and 10% surfactant. The mixing process continues at elevated temperatures, approximately 80°C, until complete homogenization is attained. For formulations possessing base viscosities below 50 Pa·s, a mixing period of 1 to 2 hours is usually sufficient. Conversely, formulations with higher viscosities require longer mixing times of several hours. Once complete, the product is discharged, and the reactor undergoes a thorough cleaning process with water. Before starting another batch, the reactor must

be thoroughly dried, a process that typically requires a time frame of 3 to 4 hours, and therefore represents a significant limitation on overall process efficiency.

1.2.3. Industrial Challenges

Even though established procedures for the production of HEUR exist within the industry, there are inherent limitations and challenges that pose substantial limitations, both technical and economical.

Some **challenges of the industrial HEUR production process** include:

- Due to its hygroscopic properties, PEG may exhibit elevated levels of water content, often exceeding 3000 ppm. Such elevated moisture levels can promote the undesired hydrolysis of diisocyanates, favoring urea formation over the intended urethane synthesis. This can significantly compromise the performance indicators of the final product and lead to batch-to-batch deviations. Therefore, it is common practice in the industry to purchase PEG with a reduced moisture content, approximately 700 ppm, from suppliers. If low-moisture PEG is not available, an additional dehydration step under vacuum conditions is required to achieve the requisite moisture specifications for polymerization. It should be noted that this additional vacuum step entails considerable energy and time expenditure.
- PEG (2000 g/mol – 10.000 g/mol) is in a solid state at ambient temperature and it must be pre-melted before being incorporated into the feed. Alternatively, if the feedstock is in liquid form, PEG should be kept at temperatures above 70°C to ensure fluidity.
- The influence of reaction conditions on process efficiency and product performance remains predominantly unclear. Key operational parameters such as moisture content in PEG, reaction temperature, stirring speed, reaction time, and stoichiometric ratios are typically determined by industrial empiricism rather than systematic scientific investigation.
- In industrial settings, the one-step process is commonly used for HEUR synthesis. This method presents a significant challenge due to the opposing effects of polymerization and chain termination. These competing processes are dictated by the relative chemical reactivities of the polyol and the hydrophobe.

As a result, achieving a high molecular weight polymer can become difficult. Additionally, the one-step process may require an increased isocyanate content to balance the amount reacting with the mono-alcohol, thereby affecting the reaction's stoichiometry.

- The polymerization process is inherently time-consuming, typically lasting several hours, and energy-intensive. This inefficiency is primarily attributed to the heat and mass transfer limitations, characteristic of such viscous systems.
- For certain new materials synthesized at laboratory scale, the HEUR base viscosities exceed 1000 Pa·s. These materials are not compatible with current industrial production equipment available on the market. Adapting to smaller batch sizes could theoretically enable such production, but such a modification would undermine economic feasibility. Additionally, the highly viscous media present challenges in achieving batch homogeneity, resulting in low batch-to-batch reproducibility.
- Blending of newly-developed, highly-viscous polyurethane compounds with water presents significant operational challenges and requires specialized mixing equipment or techniques to achieve satisfactory dispersion.
- Cleaning and drying procedures contribute to a substantial reduction in overall process productivity. These auxiliary steps require additional time and resources, adversely impacting the efficiency of the production cycle.

1.3. Scope of the thesis and main research objectives

The synthesis and application of HEURs in waterborne coatings is well-established in both industry and academia. Nevertheless, there is a significant lack of scientific research regarding HEUR production processes and rheological behavior in various waterborne dispersions. Remarkably, these gaps in scientific understanding reflect issues also faced by the industry, where precise control of process variables and understanding of rheological behavior can result in significant cost and product performance advantages. This doctoral thesis aims at partially addressing these shortcomings by focusing on four main topics, that is, 1) investigation of the effect process conditions in the solventless one-step HEUR process (current state of the art for HEUR synthesis), 2) comparison of one-step and two-step HEUR synthesis, 3) intensification of the synthesis process by microwave heating, and 4) investigation of

Chapter 1

the structure-rheology relationship in various waterborne dispersions. The aim is to introduce new scientific findings that are directly applicable to industrial practice in the area of waterborne coatings.

In the following paragraphs, the specific challenges and knowledge gaps in each topic are presented:

Investigation of Process Conditions in the Solventless One-step HEUR Process and Sampling Protocols for PUs: Despite the solventless one-step HEUR synthesis being standard industrial practice, there's a lack of comprehensive research into the key operating conditions that determine product quality. Parameters like moisture content of PEG, reaction temperature, agitator speed, catalyst concentration and reactant stoichiometry are often chosen empirically, rooted in technical know-how rather than scientific understanding. This empirical approach not only raises concerns about energy efficiency and reactant utilization but also hinders the industry's ability to move to a more optimized and efficient HEUR synthesis methodology. Furthermore, the lack of standardized sampling protocols for polyurethane melts further exacerbates this problem. Accurate sampling is critical for obtaining reliable polymer characterization data, which in turn is critical for understanding and optimizing the synthesis process. The lack of a methodological study of sampling procedures compromises the precision and reliability of PU analysis and thus hinders the scientific understanding required to advance the HEUR synthesis process towards a more optimized and efficient route.

One-Step vs. Two-Step Process: The one-step method in HEUR production faces kinetic challenges due to the simultaneous polymerization and chain termination processes, which counteract each other, based on the relative chemical reactivities of the polyol and the hydrophobe. In contrast, a two-step synthesis route decouples the polymerization and chain termination processes, offering a theoretical framework for precise molecular weight control through strategic adjustment of prepolymer molecular weight and timed introduction of end-capping agents. Yet, a rigorous systematic analysis that compares the two processes in terms of their performance and quality of HEUR product is absent in the existing scientific literature.

Chapter 1

Process Intensification using Microwave Heating: The HEUR synthesis process with conventional heating methods includes several thermally intensive steps, often necessitating high energy consumption due to inherent heat and mass transfer limitations in these highly viscous systems. Despite this significant operational bottleneck, existing scientific literature has largely overlooked the potential of microwave (MW) irradiation as an alternative energy source to intensify the HEUR process. Microwave irradiation offers key advantages, such as rapid and volumetric heating and eliminates the requirement for intermediary heat transfer fluids, typically used in conventional heating methods.³² These unique features of the microwave heating mechanism imply potential to reduce both time and energy consumption in HEUR syntheses under MW heating, similar to efficiency gains³³⁻⁴¹ in other liquid phase chemistries.

Structure-Rheology Relationship: Beyond the technical difficulties and inefficiencies encountered in the industrial production of HEURs, there is another fundamental, yet largely unexplored, area: the relationship between the thickener molecular structure and the rheological behavior of water-based formulations (including aqueous solutions, latex-based emulsions and paints) as well as the rheological behavior of the product in the final application. As underscored by industrial experts, gaining in-depth rheological insights isn't just an academic exercise but a practical necessity. For robust formulation design, in-depth understanding of the fundamental properties of each rheological modifier is essential to optimize the finished products across various stages, that is, manufacturing, storage, and application. Additionally, the use of advanced rheometric methodologies, encompassing rotational, oscillatory and combined measurements, is imperative for the accurate characterization of the rheological performance of formulated products. Unfortunately, current approaches of rheological optimization in waterborne dispersions are predominantly empirical, relying heavily on formulator experience. In this work, a systematic investigation towards establishment of structure-rheology relationship for HEURs has been carried out in order to develop tailored HEURs capable of fulfilling specific industrial requirements.

The subsequent section outlines the structure of this thesis according to the scope described above.

1.4. Thesis outline

The dissertation consists of six chapters. In

Table 1.1, the thesis structure is summarized. The dissertation is written in such a way that each chapter can be read on its own, without having read the other chapters. Each chapter has a short introduction which highlights the background of the topics covered in the specific chapter, therefore some topics may overlap, although this has been kept to the minimum. Additionally, to provide supplementary details, a Supporting Information (SI) section is included at the end of the thesis.

In the introductory section (Chapter 1), an overview of the coatings industry is presented with an emphasis on regulatory factors that accelerate the transition from solvent-borne to waterborne systems. The pivotal role of rheology modifiers, specifically Hydrophobically Modified Ethoxylated Urethanes (HEURs), in optimizing the rheological properties of waterborne coatings is discussed. This chapter also identifies existing technological challenges, gaps in scientific understanding, and research objectives related to the synthesis and application of HEURs. These serve as the foundation for the detailed studies conducted in the subsequent chapters.

In Chapter 2, we conduct a rigorous evaluation of the process parameters that govern the solventless one-step synthesis of HEURs, a method widely used in industrial applications. The chapter is designed to bridge the existing knowledge gap concerning the influence of specific operating conditions on product quality. We focus on key variables including the moisture content of polyethylene glycol (PEG), reaction temperature, agitator rotational speed for mechanical mixing and catalyst concentration level. Each of these parameters is subjected to quantitative analysis to assess its impact on the synthesis process. Additionally, the chapter offers a critical examination of

Chapter 1

sampling protocols for polyurethane melts, highlighting the crucial role that proper sampling plays in generating reliable polymer characterization, which, in turn, is instrumental in understanding and optimizing the synthesis process. The specific influence of reactant stoichiometry on HEUR synthesis will be further explored in Chapter 3.

In Chapter 3, we focus on a side-by-side comparison of the one-step and two-step methods for HEUR synthesis. The chapter evaluates the effectiveness of each process in terms of product quality, reactant utilization, and molecular weight control. The main research question addressed is whether the two-step method offers more precise control over these parameters compared to the conventional one-step method in an industrial setting.

In Chapter 4, the focus shifts to the application of microwave (MW) irradiation as an alternative energy source in HEUR synthesis. The chapter investigates whether MW heating can overcome the heat transfer limitations present in conventional processing, thereby enabling lower process times and energy consumption. In addition, the underlying mechanisms behind the microwave intensification process, specifically thermal vs non-thermal effects, are rigorously investigated.

In Chapter 5, the study focuses on elucidating the structure-rheology relationship in HEUR-based waterborne dispersions. Using state-of-the-art rheometric techniques, such as rotational and oscillatory measurements, the chapter is dedicated to explicitly correlate the molecular structure of HEURs with their rheological behavior in aqueous, latex-based and waterborne paints. This experimental data are complemented by Coarse-Grained Molecular Dynamics (CG-MD) simulations, providing molecular-scale insight into how HEUR self-assembly is affected by structural segments and thickener concentration. Metrics, such as aggregation number, percentage of bridged chains, and volumes of both the hydrophobic core and the entire micelle are quantified to rationalize the observed rheological phenomena at experimental level. The relevant research question to be addressed here is how the structure-rheology relationship of HEURs in waterborne dispersions can rigorously be quantified to facilitate design and optimization of urethane rheology modifiers for specific industrial applications.

Chapter 1

Table 1.1. PhD thesis composition

Chapter 1: Advances and Challenges in Rheology Modifiers for Waterborne Coatings: A Focus on Hydrophobically Modified Ethoxylated Urethanes (HEURs)	
HEUR Process	HEUR application
Chapter 2: Evaluation of PU Sampling Protocols and Effect of Critical Process Parameters on the one-step HEUR Synthesis	Chapter 5: Tailoring Waterborne Coatings Rheology with Hydrophobically Modified Ethoxylated Urethanes (HEURs): Molecular Architecture Insights Supported by CG-MD Simulations
Chapter 3: One-Step versus Two-Step Synthesis of HEURs: Benefits and Limitations	
Chapter 4: Intensification of HEUR Synthesis via Unsteady-State Thermal Operation using Microwaves	
Chapter 6: Conclusions and Recommendations for future work	

References

Chapter 1

- (1) Hester, R. D.; Squire, D. R. Rheology of Waterborne Coatings. *J. Coatings Technol.* **1997**, *69* (864), 109–114. <https://doi.org/10.1007/bf02696097>.
- (2) Javadi, A.; Cobaj, A.; Soucek, M. D. Commercial Waterborne Coatings. *Handb. Waterborne Coatings* **2020**, 303–344. <https://doi.org/10.1016/B978-0-12-814201-1.00012-3>.
- (3) Quienne, B.; Pinaud, J.; Robin, J. J.; Caillol, S. From Architectures to Cutting-Edge Properties, the Blooming World of Hydrophobically Modified Ethoxylated Urethanes (HEURs). *Macromolecules* **2020**, *53* (16), 6754–6766. <https://doi.org/10.1021/acs.macromol.0c01353>.
- (4) Wołosz, D.; Fage, A. M.; Parzuchowski, P. G.; Świdarska, A.; Brüll, R. Reactive Extrusion Synthesis of Biobased Isocyanate-Free Hydrophobically Modified Ethoxylated Urethanes with Pendant Hydrophobic Groups. *ACS Sustain. Chem. Eng.* **2022**, *10* (35), 11627–11640. <https://doi.org/10.1021/acssuschemeng.2c03535>.
- (5) Larson, R. G.; Van Dyk, A. K.; Chatterjee, T.; Ginzburg, V. V. Associative Thickeners for Waterborne Paints: Structure, Characterization, Rheology, and Modeling. *Prog. Polym. Sci.* **2022**, *129*. <https://doi.org/10.1016/j.progpolymsci.2022.101546>.
- (6) Xu, B.; Li, L.; Yekta, A.; Masoumi, Z.; Kanagalingam, S.; Winnik, M. A.; Zhang, K.; Macdonald, P. M.; Menchen, S. Synthesis, Characterization, and Rheological Behavior of Polyethylene Glycols End-Capped with Fluorocarbon Hydrophobes. *Langmuir* **1997**, *13* (9), 2447–2456. <https://doi.org/10.1021/la960799l>.
- (7) Elliott, P. T.; Xing, L. L.; Wetzel, W. H.; Glass, J. E. Influence of Terminal Hydrophobe Branching on the Aqueous Solution Behavior of Model Hydrophobically Modified Ethoxylated Urethane Associative Thickeners. *Macromolecules* **2003**, *36* (22), 8449–8460. <https://doi.org/10.1021/ma020166f>.

- (8) Cathébras, N.; Collet, A.; Viguier, M.; Berret, J. F. Synthesis and Linear Viscoelasticity of Fluorinated Hydrophobically Modified Ethoxylated Urethanes (F-HEUR). *Macromolecules* **1998**, *31* (4), 1305–1311. <https://doi.org/10.1021/ma9709011>.
- (9) Myers, R. Frequency-Dependent Rheological Characterization of Viscoelastic Materials Using Magnetic Nanoparticle Probes, Oregon State University, 2020.
- (10) Wang, F.; Peng, J.; Dong, R.; Chang, X.; Ren, B.; Tong, Z. Highly Efficient Hydrophobically Modified Ethoxylated Urethanes (HEURs) End-Functionalized by Two-Tail Dendritic Hydrophobes: Synthesis, Solution Rheological Behavior and Thickening in Latex. *Colloids Surfaces A Physicochem. Eng. Asp.* **2016**, *502*, 114–120. <https://doi.org/10.1016/j.colsurfa.2016.05.004>.
- (11) Du, Z.; Wang, F.; Chang, X.; Peng, J.; Ren, B. Influence of Substituted Structure of Percec-Type Mini-Dendritic End Groups on Aggregation and Rheology of Hydrophobically Modified Ethoxylated Urethanes (HEURs) in Aqueous Solution. *Polymer (Guildf)*. **2018**, *135*, 131–141. <https://doi.org/10.1016/j.polymer.2017.12.022>.
- (12) Guan, T.; Du, Z.; Chang, X.; Zhao, D.; Yang, S.; Sun, N.; Ren, B. A Reactive Hydrophobically Modified Ethoxylated Urethane (HEUR) Associative Polymer Bearing Benzophenone Terminal Groups: Synthesis, Thickening and Photo-Initiating Reactivity. *Polymer (Guildf)*. **2019**, *178* (April), 121552. <https://doi.org/10.1016/j.polymer.2019.121552>.
- (13) Chang, X.; Du, Z.; Hu, F.; Cheng, Z.; Ren, B.; Fu, S.; Tong, Z. Ferrocene-Functionalized Hydrophobically Modified Ethoxylated Urethane: Redox-Responsive Controlled Self-Assembly and Rheological Behavior in Aqueous Solution. *Langmuir* **2016**, *32* (46), 12137–12145. <https://doi.org/10.1021/acs.langmuir.6b03508>.
- (14) Du, Z.; Ren, B.; Chang, X.; Dong, R.; Peng, J.; Tong, Z. Aggregation and

- Rheology of an Azobenzene-Functionalized Hydrophobically Modified Ethoxylated Urethane in Aqueous Solution. *Macromolecules* **2016**, *49* (13), 4978–4988. <https://doi.org/10.1021/acs.macromol.6b00633>.
- (15) Ginzburg, V. V.; Van Dyk, A. K.; Chatterjee, T.; Nakatani, A. I.; Wang, S.; Larson, R. G. Modeling the Adsorption of Rheology Modifiers onto Latex Particles Using Coarse-Grained Molecular Dynamics (CG-MD) and Self-Consistent Field Theory (SCFT). *Macromolecules* **2015**, *48* (21), 8045–8054. <https://doi.org/10.1021/acs.macromol.5b02080>.
- (16) Ginzburg, V. V.; Chatterjee, T.; Nakatani, A. I.; Van Dyk, A. K. Oscillatory and Steady Shear Rheology of Model Hydrophobically Modified Ethoxylated Urethane-Thickened Waterborne Paints. *Langmuir* **2018**, *34* (37), 10993–11002. <https://doi.org/10.1021/acs.langmuir.8b01711>.
- (17) Tripathi, A.; Tam, K. C.; McKinley, G. H. Rheology and Dynamics of Associative Polymers in Shear and Extension: Theory and Experiments. *Macromolecules* **2006**, *39* (5), 1981–1999. <https://doi.org/10.1021/ma051614x>.
- (18) Larson, R. G.; Van Dyk, A. K.; Chatterjee, T.; Ginzburg, V. V. Associative Thickeners for Waterborne Paints: Structure, Characterization, Rheology, and Modeling. *Prog. Polym. Sci.* **2022**, *129*, 101546. <https://doi.org/10.1016/j.progpolymsci.2022.101546>.
- (19) Lu, M.; Song, C.; Wan, B. Influence of Prepolymer Molecular Weight on the Rheology and Kinetics of HEUR-Thickened Latex Suspensions. *Prog. Org. Coatings* **2021**, *156* (July 2020), 106223. <https://doi.org/10.1016/j.porgcoat.2021.106223>.
- (20) Abdala, A. A.; Wu, W.; Olesen, K. R.; Jenkins, R. D.; Tonelli, A. E.; Khan, S. A. Solution Rheology of Hydrophobically Modified Associative Polymers: Effects of Backbone Composition and Hydrophobe Concentration. *J. Rheol. (N. Y. N. Y.)* **2004**, *48* (5), 979–994. <https://doi.org/10.1122/1.1773781>.

Chapter 1

- (21) Jenkins, R. D.; Bassett, D. R.; Silebi, C. A.; El-Aasser, M. S. Synthesis and Characterization of Model Associative Polymers. *J. Appl. Polym. Sci.* **1995**, *58* (2), 209–230. <https://doi.org/10.1002/app.1995.070580202>.
- (22) Berndlmaier, R. Rheology Additives for Coatings. *Handb. Coat. Addit.* 363–403.
- (23) Wypych, G. *Handbook of Rheological Additives*, First Edit.; Elsevier, 2022; Vol. 1. <https://doi.org/10.1016/C2021-0-00266-2>.
- (24) Shun Xing Zheng. *Principles of Organic Coatings and Finishing*; Cambridge Scholars Publishing, 2019.
- (25) Król, P. Synthesis Methods, Chemical Structures and Phase Structures of Linear Polyurethanes. Properties and Applications of Linear Polyurethanes in Polyurethane Elastomers, Copolymers and Ionomers. *Prog. Mater. Sci.* **2007**, *52* (6), 915–1015. <https://doi.org/10.1016/j.pmatsci.2006.11.001>.
- (26) Odian, G. *Principles of Polymerization*, Fourth.; John Wiley & Sons, Inc, 2004. <https://doi.org/10.1002/047147875X>.
- (27) Vantomme, G.; Ter Huurne, G. M.; Kulkarni, C.; Ten Eikelder, H. M. M.; Markvoort, A. J.; Palmans, A. R. A.; Meijer, E. W. Tuning the Length of Cooperative Supramolecular Polymers under Thermodynamic Control. *J. Am. Chem. Soc.* **2019**, *141* (45), 18278–18285. <https://doi.org/10.1021/jacs.9b09443>.
- (28) Fage, A. M., Kemmerling, S., Backhaus, C. A., Deshmukh, S., B.; R., Hübner, C., Elsner, P. Synthesis of Polyurethanes through Reactive Extrusion Assisted by Alternative Energy Sources [Conference Presentation]. In *EPF European Polymer Congress*; Prague, Czech Republic, 2022.
- (29) Szycher, M. *Szycher's Handbook of Polyurethanes*, II Ind.; CRC Press, 2013; Vol. 142.
- (30) Olszewski, A.; Kosmela, P.; Żukowska, W.; Wojtasz, P.; Szczepański, M.; Barczewski, M.; Zedler, Ł.; Formela, K.; Hejna, A. Insights into Stoichiometry

- Adjustments Governing the Performance of Flexible Foamed Polyurethane/Ground Tire Rubber Composites. *Polymers (Basel)*. **2022**, *14* (18), 3838. <https://doi.org/10.3390/polym14183838>.
- (31) Prochazka, F.; Nicolai, T.; Durand, D. Molar Mass Distribution of Linear and Branched Polyurethane Studied by Size Exclusion Chromatography. *Macromolecules* **2000**, *33* (5), 1703–1709. <https://doi.org/10.1021/ma9901543>.
- (32) Li, H.; Zhao, Z.; Xiouras, C.; Stefanidis, G. D.; Li, X.; Gao, X. Fundamentals and Applications of Microwave Heating to Chemicals Separation Processes. *Renew. Sustain. Energy Rev.* **2019**, *114*, 109316. <https://doi.org/10.1016/J.RSER.2019.109316>.
- (33) Stefanidis, G. D.; Muñoz, A. N.; Sturm, G. S. J.; Stankiewicz, A. A Helicopter View of Microwave Application to Chemical Processes: Reactions, Separations, and Equipment Concepts. *Reviews in Chemical Engineering*. Walter de Gruyter GmbH 2014, pp 233–259. <https://doi.org/10.1515/revce-2013-0033>.
- (34) Komorowska-Durka, M.; Loo, M. B. t.; Sturm, G. S. J.; Radoiu, M.; Oudshoorn, M.; Van Gerven, T.; Stankiewicz, A. I.; Stefanidis, G. D. Novel Microwave Reactor Equipment Using Internal Transmission Line (INTLI) for Efficient Liquid Phase Chemistries: A Study-Case of Polyester Preparation. *Chem. Eng. Process. Process Intensif.* **2013**, *69*, 83–89. <https://doi.org/10.1016/j.cep.2013.03.003>.
- (35) Nagahata, R.; Takeuchi, K. Encouragements for the Use of Microwaves in Industrial Chemistry. *Chem. Rec.* **2019**, *19* (1), 51–64. <https://doi.org/10.1002/tcr.201800064>.
- (36) Nguyen, N. T.; Greenhalgh, E.; Kamaruddin, M. J.; El, J.; Carmichael, K.; Dimitrakis, G.; Kingman, S. W.; Robinson, J. P.; Irvine, D. J. Understanding the Acceleration in the Ring-Opening of Lactones Delivered by Microwave Heating *Q.* **2014**, *70*, 996–1003. <https://doi.org/10.1016/j.tet.2013.11.031>.

- (37) Bogdal, D.; Lukasiewicz, M.; Pielichowski, J.; Bednarz, S. Microwave-Assisted Epoxidation of Simple Alkenes in the Presence of Hydrogen Peroxide. *https://doi.org/10.1080/00397910500278479* **2006**, *35* (23), 2973–2983. <https://doi.org/10.1080/00397910500278479>.
- (38) Adlington, K.; McSweeney, R.; Dimitrakis, G.; Kingman, S. W.; Robinson, J. P.; Irvine, D. J. Enhanced ‘in Situ’ Catalysis via Microwave Selective Heating: Catalytic Chain Transfer Polymerisation. *RSC Adv.* **2014**, *4* (31), 16172–16180. <https://doi.org/10.1039/C4RA00907J>.
- (39) Kasprzyk, W.; Galica, M.; Bednarz, S. Microwave-Assisted Oxidation of Alcohols Using Zinc Polyoxometalate. **2014**, 2757–2761. <https://doi.org/10.1055/s-0034-1379211>.
- (40) Mu, S.; Liu, K.; Li, H.; Zhao, Z.; Lyu, X.; Jiao, Y.; Li, X.; Gao, X.; Fan, X. Microwave-Assisted Synthesis of Highly Dispersed ZrO₂ on CNTs as an Efficient Catalyst for Producing 5-Hydroxymethylfurfural (5-HMF). *Fuel Process. Technol.* **2022**, *233* (April), 107292. <https://doi.org/10.1016/j.fuproc.2022.107292>.
- (41) Ou, X.; Tomatis, M.; Lan, Y.; Jiao, Y.; Chen, Y.; Guo, Z.; Gao, X.; Wu, T.; Wu, C.; Shi, K.; Azapagic, A.; Fan, X. A Novel Microwave-Assisted Methanol-to-Hydrocarbons Process with a Structured ZSM-5/SiC Foam Catalyst: Proof-of-Concept and Environmental Impacts. *Chem. Eng. Sci.* **2022**, *255*, 117669. <https://doi.org/10.1016/j.ces.2022.117669>.
- (42) Bampouli, A.; Tzortzi, I.; Schutter, A. De; Xenou, K.; Michaud, G.; Stefanidis, G. D.; Gerven, T. Van. Insight Into Solventless Production of Hydrophobically Modified Ethoxylated Urethanes (HEURs): The Role of Moisture Concentration , Reaction Temperature , and Mixing Efficiency. *ACS Omega* **2022**, No. int. <https://doi.org/10.1021/acsomega.2c04530>.

Evaluation of PU Sampling Protocols and Effect of Critical Process Parameters on the one-step HEUR Synthesis

ⁱThis chapter is based on the following publication:

Bampouli, A.; ⁱⁱ **Tzortzi, I.**; ⁱⁱ Schutter, A. De; Xenou, K.; Michaud, G.; Stefanidis, G. D.; Gerven, T. Van. “*Insight Into Solventless Production of Hydrophobically Modified Ethoxylated Urethanes (HEURs): The Role of Moisture Concentration, Reaction Temperature, and Mixing Efficiency*” ACS Omega 2022, <https://doi.org/10.1021/acsomega.2c04530>.

ⁱⁱ These authors contributed equally to this work.

Additional material and discussions not included in the original publication have been incorporated to provide a more comprehensive understanding of sampling procedures for polyurethane melts.

ABSTRACT

In this work, we report for the first time on the influence of sampling methods and critical process parameters on the physicochemical and rheological properties of Hydrophobically-Modified Ethoxylated Urethanes (HEURs) and selected prepolymers without use of solvents. We find that the solid sampling method results in higher molecular weights, especially for samples with higher isocyanate concentrations, due to ambient moisture-induced chain extension phenomenon. To obtain accurate results when analyzing polyurethane melts, it is crucial to either neutralize residual NCO content or prevent its exposure to atmospheric moisture.

Additionally, we show that the polyol water concentration is detrimental for the progress of the main urethane forming reaction confirming the necessity of carefully drying the reactants below 1000 ppm to suppress the consumption of diisocyanate towards urea during HEUR synthesis. Increasing mixing speed ($\approx 30-750$ rpm), reaction temperature ($80-110$ °C) and catalyst concentration ($0.035-2.1$ wt% bismuth carboxylate) can significantly increase the rate of molecular weight buildup, but their effect decreases with time as bulk viscosity increases and mixing limitations eventually take over, leading to the Weissenberg effect and chain growth termination. Consequently, for the selected formulation the maximum product molecular weight attained lies in the range $\approx 20000-22000$ g/mol irrespective of the specific process conditions applied.

2.1. INTRODUCTION

Hydrophobically modified ethoxylated urethanes (HEURs) belong to the broader polyurethanes (PUs) family that holds a well-established position in the polymers market covering a broad range of indoor/outdoor applications.¹ HEURs, in particular, have an established share in the polymer market mainly due to their use in paints and coatings, while their application to personal care, construction and pharmaceutical products is predicted to keep rising.² HEURs are used in waterborne systems, paints and coatings, as rheology modifiers.³⁻⁷ Owing to the preference for sustainable manufacturing of environmentally friendly products, understanding of bulk polymerization and production optimization of these additives, which constitute a small but important part of a final paint formulation⁸, is crucial. When dissolved in water and above a certain concentration, HEUR polymers form flower-like micelles because of interactions between their hydrophobic ends. Further increase in the HEUR concentration can force the micelles to link between themselves resulting in a unique transient network.⁹ This dynamic reversible phenomenon imparts pseudoplastic rheological properties to the final paint or coating product; at low shear rates the viscosity is higher thereby prolonging the product shelf life, while at higher shear rates the product viscosity decreases allowing for easier paint application: from loading of the brush to the film building on the wall.^{9,10}

HEURs production follows the same principles as the production of PUs. A formulation consisting of two basic ingredients constitutes the core of the synthesis: a polyisocyanate reacts with a polyol resulting in urethane repeating groups. The presence of a catalyst, a chain extender and additives is also possible.¹¹ The quality of the reactants is paramount for the control of the reaction pathway because isocyanates can readily react with various OH-containing compounds (such as alcohols, water or carboxylic acids), amines and urethanes/ureas. In the “simple” two-reactant system described above, the reaction stoichiometry can therefore become unpredictable if moisture has physically or chemically been adsorbed by the solid polyol material (during production, handling or storage).¹¹⁻¹³ The selection and quality of reactants play a major role in the final product, as does the chosen processing method. The importance of carefully controlling both has been highlighted in various works.^{7,13-15} For PUs production, there are two processing possibilities. The first one is to add all the reactants

Chapter 2

simultaneously (one-step process). The second one is to first let the polyol and polyisocyanate react and form a chain called the prepolymer, followed by the addition of a molecule capable of terminating the reaction (two-step process).¹² Usually, some metals or amines are used as catalysts.⁹ In the current study, the one-step synthesis was used for all synthesized HEURs.

Another important aspect in the production of PUs in general and HEURs in particular is the use of a solvent phase. The most common practice reported in the literature is to apply solution polymerization, either in one or two steps.¹⁶ The use of a solvent can assist in viscosity reduction, better heat transfer, easier mixing and improved product homogeneity. In general, the chosen solvent should be inert to the isocyanate and able to dissolve the polyol and the polyurethane product.¹⁷ Examples of appropriate solvents include benzene, toluene, xylene and aromatic hydrocarbon-rich compounds¹⁷, or other commonly used ones such as dimethylformamide (DMF), tetrahydrofuran (THF), dimethyl sulfoxide (DMSO), and 1,2-dichloroethane (DCE).¹⁸ On the downside, an extra purification step is required to separate the obtained polymer from the solvent. Many examples of works with a variety of solvents are available in the literature. More specifically toluene, diethyl ether and hexane were used for polymers re-precipitation.¹⁴ Dried toluene was used in the work of Fonnum et al.⁶ Many articles by Barmar et al.^{7,13,15,19–21} discuss various parameters related to HEURs rheological behavior, emphasizing the role of the hydrophobic and hydrophilic parts of the molecule among others. In all these works, HEURs were produced in a similar way using dry toluene, THF, petroleum ether and acetone. The detailed synthesis is described in Barmar et al.¹⁹.

Despite the process related advantages when carrying out HEUR syntheses in solvents, the pressing quest for sustainability, profitability and low toxicity in chemical manufacturing requires drastic reduction or even elimination of solvents to avoid the need of their separation from the polymer product downstream, which increases the total production cost and the CO₂ equivalent emissions corresponding to the extra energy demand for solvent separation and purification. However, solventless HEUR production has never been investigated from the process point of view to shed light on the role of operating conditions that determine product quality.

Chapter 2

In the current study, all HEUR polymers were synthesized in bulk with polyethylene glycol (PEG, $M_w = 8000$ g/mol) that was coupled with 4,4-dicyclohexylmethane diisocyanate (H_{12} MDI). 1-octanol was used as a short hydrophobic molecule that terminated the developed polymeric chains. This chapter sheds light on the impact of sampling protocols for PU analysis, as well as elucidates the influence of various factors such as the moisture concentration of the polyol, catalyst concentration, reaction temperature, and mixing profile on HEUR product quality. The polymer products were characterized in terms of molecular weight, chemical structure and viscosity by means of GPC, APC, FTIR, and rotational/oscillatory testing, respectively. The crystallinity, thermal stability and heat capacity of the polymer products were also investigated through XRD, TGA and DSC characterization. Selected non-hydrophobically terminated polymers or prepolymers were also produced in order to assess the impact of the chain stopper (1-octanol) on the system.

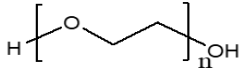
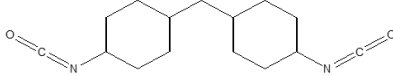
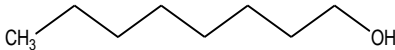
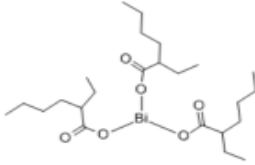
2.2. MATERIALS AND METHODS

2.3. Materials

Polyethylene glycol of molecular weight 8000 g/mol with a purity of >99.5% was kindly provided by Clariant. H_{12} MDI ((4,4-Methylenebis(cyclohexyl isocyanate), mixture of isomers, 90% purity) from Acros Organics and 1-octanol (99% purity) from Alfa Aesar were used as received. Bismuth carboxylate (KKAT XCB221), kindly provided by the King Industries, was selected as the catalyst. The structures of all main reactants and some basic properties are presented in **Error! Reference source not found.** Chloroform (>99.8% purity) stabilized with amylene was purchased from Fisher Chemicals and was dried using 4 Å molecular sieves. Chloroform-d (99.8%) for NMR was purchased from Sigma Aldrich. Extra dry methanol for synthesis was purchased from Fischer Scientific, dibutylamine (>99.5%) was obtained from Sigma Aldrich and THF (HPLC grade, >99.8%) from Chem-Lab.

Chapter 2

Table 2.1. Summary of the role, physical state at room temperature (RT) and molecular structure of the different reactants.

Reactant name [Short]	Role	M_w [g/mol]	State at RT	Structure
Polyethylene glycol [PEG]	Water soluble diol- PU backbone	8000	Solid flakes	
4,4- dicyclohexylmethane diisocyanate [H ₁₂ MDI]	Diosocyanate- Connecting diols	262.35	Liquid	
1-Octanol [Oct]	Hydrophobic part- ending of the chains build up	130.23	Liquid	
Bismuth carboxylate [kkat]	Catalyst	--	Highly viscous liquid	

2.4.Synthesis of polymers

The formulation used for all the sub-studies in the current work combines PEG, H₁₂MDI and 1-octanol, called “*HMDI*” and “*Oct*” for simplicity hereafter, in the following molar ratios: 1:1.5:1. The reactants were weighed and added to the reactor. A double-wall glass vessel with four openings was used as reactor. The vessel temperature was controlled by a heating jacket. A simplified scheme of the reactor setup is presented

Chapter 2

in Figure 2.1. The synthesis procedure applied was common for all the cases: initially, polyethylene glycol flakes were melted in the preheated reactor. The melted PEG was then subjected to a vacuum treatment step under constant mechanical mixing. The vacuum was applied until the desired moisture concentration of the PEG was reached; this was confirmed by the coulometric Karl–Fischer titration method. Polyol samples were taken from various spots of the bulk and were directly dissolved in dry chloroform. The obtained solution was titrated immediately. The moisture measurements were repeated at least three times. Immediately after the vacuum stopped, nitrogen was applied in the reactor as close as possible to the liquid surface in order to create an inert blanket that would prevent air moisture from being absorbed by the polyol. Next, the catalyst diluted in dried chloroform (2% w/w) was added to the vessel in the selected concentration. The diol and the catalyst were mixed for a few minutes before octanol was added. The reactants were left to mix properly before the isocyanate addition, which was marked as “time zero” of each experiment. A PTFE three-blade impeller connected to a stirring motor able to control the mixing speed and record torque data online was used (Hei-Torque overhead stirrer from Heidolph).

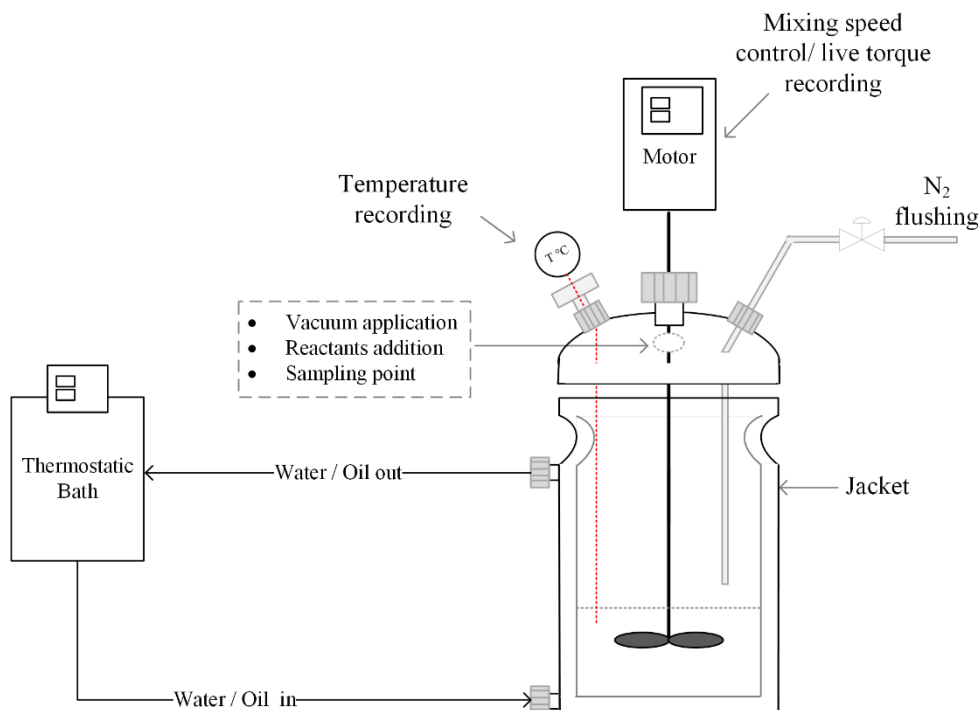


Figure 2.1. Experimental reactor setup used for the study, including a double-wall glass reactor, special openings for the various processing steps and the motor/agitator able to record on line torque data.

2.5. Sampling of the produced polymers

In the present study, two distinct sampling methods were employed: the "solid method," where the molten sample was extracted from the bulk and analyzed post-solidification, and the "liquid" or "in situ" method, where the molten sample was directly dissolved in vials containing pre-weighed dry chloroform. Uniquely in this study, various HMDI/PEG ratios were utilized to elucidate the impact of diisocyanate content on the PU melt.

2.6. Homogeneity of the bulk polymers

The homogeneity of the bulk in terms of molecular weight was investigated by collecting samples from various spots of the reactor during two selected syntheses. Specifically, in the course of two different polymerizations at 80 °C and 110 °C, polymer samples were collected in situ from five different reactor spots over 5 and 15 minutes, respectively. The formulation details can be found in Table S3.4 (Supporting Information). For both syntheses it was observed that the molecular weight of the bulk can vary up to 9% when comparing the maximum and the minimum values. The results from the two cases can be found in the Figure S3.4 and Table S3.5 (Supporting Information, Section B).

2.7. Description of parametric studies

The parametric variations applied in this work are summarized in Table 2.2. In all parametric studies, polymer products were sampled during the course of reaction for further characterization.

Chapter 2

Table 2.2. Summary of parameters investigated in the current work.

Parameter modified	Polyol moisture concentration [ppm]	Temperature [°C]	Mixing profile [rpm]	Catalyst [%]
Sampling method	≈500	80	100	0.035
Polyol moisture	≈500/800/1000/ 2000/3000/4500/6000/13000	80	100	0.035
Catalyst concentration	≈800	80	100	0.035/0.14/0.35/2.1
Reaction temperature¹	≈800	80/95/110	100	0.035
Mixing regime	≈800	80	30/100/300/750	0.035

1. Both HEURs and prepolymers were investigated in this study

Polyol moisture effect investigation

In step growth polymerizations, the production of high molecular weight polymers is aimed for. To this end, reactants of high quality in combination with strict reaction stoichiometry control are necessary. Consistency in reactants quality constitutes a challenge because the purity grade of commercially available monomers may significantly vary among different producers or even from batch to batch. In the case of HEURs synthesis, particular polyols may contain moisture due to their hydrophilic

Chapter 2

nature. As a consequence, the hydrolysis of the diisocyanate (the second main reactant in the system) can occur and, as a result, urea formation will be favored instead of the desired urethane forming reaction. The two molecules are presented below in Figure 2.2. More details on the reaction schemes in the system can be found in the Supporting information file (Section C, Figures S2.5 to S2.10).

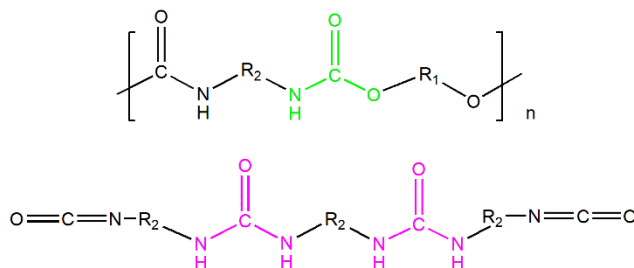


Figure 2.2. Polyurethane (top) and urea containing molecules (bottom) resulting from the main PEG- H₁₂MDI and the PEG-water reactions, respectively.

Even though multiple studies have underlined the importance of dehydrating the polyol before reacting it with isocyanate, no quantitative data are available regarding the initial moisture of polyol and its effect on the polymer weight average molecular weight (M_w) and number average molecular weight (M_n). Hence, the main goal of the study on the moisture effect is to quantitatively assess how the initial moisture of PEG affects the HEURs chain growth in terms of M_n and M_w . All processing parameters, that is, the stoichiometric ratio of the reactants (1PEG:1.5HMDI:1Oct), the mixing speed (100 rpm), the reaction temperature (80 °C) and the catalyst concentration (0.035%) remained the same for all experiments. The polymers were collected in situ at 45 minutes of reaction time. Due to the broad range of moisture concentrations (between 500 ppm and 13000 ppm) in the initial PEG materials, an excess of HMDI (1.5HMDI:1PEG) instead of the theoretical optimum molar ratio (1HMDI:1PEG or 1NCO:1OH based on Szycher¹²) was chosen for the study on the moisture effect reported herein. In order to reach the moisture level required to perform these experiments, either vacuum pretreatment was applied for a few hours under mixing at 100 °C when reduction in moisture level was desired, or distilled water was added to the mixture of reagents, which was then mixed vigorously, to reach a higher moisture level.

Chapter 2

Catalyst concentration effect investigation

In this parametric study, the initial PEG moisture concentration (≈ 800 ppm), the reactants stoichiometric ratio (1PEG:1.5HMDI:1Oct), the reaction temperature ($80\text{ }^{\circ}\text{C}$) and the mixing speed (100 rpm) were kept constant, but the catalyst concentration was modified from 0.035% to 2.1% to investigate whether higher catalyst concentrations can overcome mass transfer limitations inherent in viscous mixtures. The aim of this parametric study was to verify the maximum attainable HEUR molecular weight level for reaction times up to 120 min, which is the nominal industrial process time for this synthesis.

Reaction temperature effect investigation

In this set of experiments, all processing parameters except temperature, namely, the stoichiometric ratio of reactants (1PEG:1.5HMDI:1Oct for the HEUR synthesis and 1PEG:1.5HMDI for the prepolymer), the mixing speed (100 rpm), the initial PEG moisture concentration (≈ 800 ppm) and the catalyst concentration (0.035%) remained the same. The reaction temperature was modulated within a range of 80°C to 110°C , aligning with the operational constraints commonly encountered in industrial settings for the production of polyurethane rheology modifiers. The lower limit ($80\text{ }^{\circ}\text{C}$) is the minimum temperature required for the PEG8000 flakes to melt. The upper temperature limit of 110°C was selected in order to avoid the thermal degradation of PEG8000 and to minimize isocyanate side reactions, which become increasingly prevalent at elevated temperatures, particularly in the presence of excess isocyanate groups and certain catalysts.²²

Mixing regime effect investigation

In this study, the rotation speed of the overhead stirrer was varied between 30 rpm and 750 rpm, while keep constant the HEURs polymerization formulation ratio (1PEG:1.5HMDI:1Oct), the initial PEG moisture concentration (≈ 800 ppm), the reaction temperature ($80\text{ }^{\circ}\text{C}$) and the catalyst concentration (0.035%).

2.8. Analytical methods

Gel Permeation Chromatography (GPC): The weight/number average molecular weight (M_w/M_n) was determined by GPC from Shimadzu, using four Styragel columns from Waters. Chloroform was the mobile phase (1 ml/min) at 30 °C operating temperature. Polyethylene glycols/oxides (PEG/PEO) were used as calibration standards.

Advanced Permeation Chromatography (APC): The multimodal molecular weight distribution of the samples was determined by APC from Waters, using three Acquity APC XT columns from Waters. THF was the mobile phase (1 ml/min) at 35 °C operating temperature. Polymethylmethacrylate (PMMA) standards were used for the calibration.

Fourier Transform Infrared Spectroscopy (FTIR): The qualitative analysis of the obtained polymers was done by FTIR, which was performed using attenuated total reflectance-Fourier transform infrared spectroscopy (ATR-FTIR, Perkin Elmer, spectrum 100, USA). At least 16 scans for each sample were conducted in the span range of 4000–650 cm^{-1} . The products were collected at 45 minutes and were directly diluted in chloroform-d at a concentration of 0.05 g/ml. The liquid samples were placed in the analysis cell and the spectra were recorded after the total solvent spontaneous evaporation.

Nuclear magnetic resonance spectroscopy (NMR): The NMR spectra of a series of compounds were taken in order to identify the prepolymer and end-capped HEUR structures which are considered to be present in the synthesis. All experiments were performed on a Bruker Avance DRX 500 MHz NMR (11.7 Tesla) spectrometer (Bruker Biospin, Rheinstetten, Germany) operating at NMR frequency of 500.13 MHz for ^1H NMR, equipped with a 5 mm multi nuclear broad band inverse detection probe. All the ^1H NMR (500 MHz) were recorded with chemical shifts (δ) in parts per million (ppm) and coupling constants (J) in hertz (Hz).

Samples were added into NMR tubes (5 mm Thin Wall Precision NMR Sample Tubes 8" L, Wilmad, Vineland, NJ, USA). The obtained spectra were Fourier transformed,

Chapter 2

and their phase and baseline were automatically corrected. Prior to Fourier transformation, an exponential weighting factor corresponding to a line broadening of 1 Hz was applied. The samples were collected based on the “in situ” method³, in which the molten samples were directly dissolved in vials with pre-weighed deuterated chloroform (CDCl₃).

Thermogravimetric degradation analysis (TGA): TGA was performed using a TGA-Q500 (TA Instruments). Samples of approximately 10 mg were weighed in high-temperature platinum pans and heated from 20 °C to 550 °C at a heating rate of 10°C/min and a nitrogen gas flow of 60 mL/min for the sample and 40 mL/min for the balance.

Differential scanning calorimetry (DSC): The heat capacity curves were obtained using a DSC-Q2000 (TA Instruments). The DSC cell was purged with nitrogen gas at a flowrate of 50 ml/min. Samples of approximately 8 - 10 mg were placed in sealed aluminum pans. Samples were measured while being heated and subsequently cooled at 10 °C/min between 10 and 200 °C with 5 minutes isothermal time at the extremes. Both heating and cooling cycles were repeated twice per measurement. An empty aluminum pan was used as a reference.

Powder X-ray diffraction (PXRD): Samples were analysed in a Bruker D2 PXRD device. Each sample was scanned with *2theta* ranging from 4° to 45° with a resolution of 0.02°/s.

Rheological measurements: The rheological properties of HEURs aqueous solutions were measured on a Haake Mars 60 rheometer, using a cone and plate geometry of 25 mm diameter, 1° angle cone, made of titanium and sand blasted (C25 1°/Ti/SB). The distance of the gap was 0.056 mm. Water-HEUR solutions were prepared by directly dissolving a known amount of the HEUR in distilled water, resulting in 20% w/w solutions. The solution was stirred for few hours in order to become homogeneous and then the samples were left at rest overnight. The water amount was selected based on industrial tests performed during the commercialization stage of a thickener product. A range of 17 – 20% dilution in water is normally applied and considered representative of the downstream processing behaviour of the final product.

Chapter 2

The zero-shear viscosity and the shear stress profiles were obtained for shear rate testing from 0.01 to 10000 s⁻¹. To ensure that all samples were subjected to the same shear history, an equilibration time of 60 s was given to each shear rate. Dynamic viscoelastic properties of the solutions were measured in the oscillatory shear mode, in the frequency range of 0.05 to 100 Hz, with a constant deformation amplitude $\gamma^0 = 0.01$ s⁻¹. All rheological measurements were performed at 25 °C.

2.3.RESULTS AND DISCUSSION

2.3.1. Comparative analysis of in-situ and solid sampling methods for molecular weight determination and chemical characterization of polyurethane melts

Our study reveals significant discrepancies between the two sampling methods under consideration: the solid method and the in-situ method. In particular, for samples with lower isocyanate content, the number-average molecular weight measured via the solid method showed a 50-77% increase compared to the in-situ method (Figure S2.0.1 and Figure S2.0.2 of the Supporting Information), while this percentage further escalated to 115% when higher isocyanate concentrations were employed. Table 2.3 shows the molecular weights of HEUR measured with the in-situ and solid method when both lower and higher isocyanate concentration was employed during the HEUR synthesis.

Table 2.3. Comparative molecular weight results obtained with the in-situ and solid method for different HMDI/PEG ratios. These experiments were performed with the one-step method and PEG/Oct=1 in each case.

HMDI/PEG	Reaction time	In situ		Solid	
		Mn (g/mol)	Mw (g/mol)	Mn (g/mol)	Mw (g/mol)
1.5	3	15017	22949	26363	44766
	45	19465	32047	25762	44605
4	3	10830	13910	23137	41470
	45	11126	14516	24325	44272

Further differentiation between the two methods was evident from the FTIR spectra. For instance, samples with excess isocyanate content displayed a pronounced ($\text{N}=\text{C}=\text{O}$) at 2270 cm^{-1} the in-situ FTIR analysis, which was absent in the solid samples, where a corresponding urea peak ($-\text{NH}-\text{C}=\text{O}-\text{NH}$) appeared instead at $1627\text{-}1680\text{ cm}^{-1}$ (Figure S2.0.14 of the Supporting Information). Detailed analysis regarding the distinct urethane and urea peaks attributes are presented in Section 2.3.2. of this Chapter. Additionally, ^1H NMR analysis of the HEURs spectra in CDCl_3 strengthened the hypothesis of the formation of urea moieties after the exposure of solid samples to air moisture. (Figure S2.0.15 and Figure S2.0.16 of the Supporting Information). According to the ^1H NMR analysis, the peaks presented at range of $4.46\text{-}4.90\text{ ppm}$ correspond to the characteristic protons of the NH group of the urethane function ($-\text{NH}-\text{C}=\text{O}-\text{O}-$). However, in the ^1H NMR spectra of the solid samples, the presence of a new peak at 5.3 ppm is observed that can be assigned to the protons of urea moiety ($-\text{NH}-\text{C}=\text{O}-\text{NH}$). Furthermore, the presence of a new peak (at the solid samples) at a chemical shift of $4.37\text{ to }4.39\text{ ppm}$, could be indicative of the presence of protons of the formed amine- by products during the exposure of NCO-terminated prepolymers to air moisture. This assumption is enhanced by comparing the solid samples derived from different HMDI/PEG ratios. The integral intensity of the peak presented at 4.39 ppm (that corresponds to the sample in which the HMDI/PEG ratio is equal to 4 - Figure S2.0.16 of the Supporting Information) is up to three times higher compared to the integral of the same peak that is presented at the ^1H NMR spectrum of the solid sample having been synthesized with a lower ratio of HMDI/PEG (up to 1.5) (Figure S2.0.15 of the Supporting Information). This observation indicates the contribution of the HMDI (which is in excess) to the side reactions forming smaller molecules such as amine-terminated prepolymers or urea-urethane polymers.

Therefore, based on the results of GPC, ^1H NMR and FTIR analysis, it can be stated that the differences in molecular weight can be attributed to chain-extension reactions involving NCO-terminated urethane prepolymers and ambient moisture. This results in the formation of urea linkages and an extended polyurea structure, finally forming a solid polyurethane-urea structure. Traditional methods of moisture cured polyurethane-ureas, which involve reactions of NCO-terminated urethane prepolymers with ambient moisture, further corroborate our findings.^{23,24}

Despite the sensitivity of NCO groups towards its hydrolysis route, to the best of our knowledge, only few studies refer to the exact method applied for the samples collection. In the work of Stern²⁵, the author mentioned: “the still hot solid polymer was cut into quarters and removed from the reactor” and in the work of Arnould et al.²² the following procedure was performed: “at the end of the reaction, polyurethane prepolymers were kept under argon”. In the same work, the authors applied an extra pre-treatment step comprising quenching of the prepolymers with anhydrous methanol in order to avoid further reactions of the remaining $N = C = O$ groups in the reactive mixture that would potentially alter the obtained molar masses.²² The use of dry methanol did not show any advantages compared to the “in situ” method implemented in the current study. Nevertheless, the results of these tests can be found in Figure S2.0.3. of the Supporting Information.

Our findings therefore underline the necessity for precise sampling protocols to avoid disseminating misleading information about crucial product properties like molecular weight, composition, and viscosity. To ensure the reliability of any analytical tests conducted in polyurethane melts, it is imperative to either neutralize residual NCO content or meticulously prevent its exposure to atmospheric moisture. All of the following results of GPC, APC and FTIR presented thereafter are based on the liquid/in situ method. More details and results on comparison of the two sampling methods can be found in the Supporting information (Section A and D).

2.3.2. Effect of polyol moisture concentration

The molecular weight development is directly related to the degree of polymerization. The obtained HEUR M_n values over a range of initial PEG moisture concentrations are shown in **Figure 2.3** where it can be seen that the M_n is severely restrained when the moisture concentration of PEG is above 3000 ppm. More specifically, at this moisture level, the water is in excess compared to the PEG ($\approx 20\%$ in molar terms), which could provoke the side reaction of diisocyanate towards urea. On the contrary, when a lower moisture concentration (< 3000 ppm) is present, the M_n starts increasing and for the minimum moisture concentration of 500 ppm, the maximum $M_n \approx 21000$ g/mol is attained. In this case, the desired urethane reaction is favored. The polydispersity index (PDI) or the M_w/M_n fraction of the products is also presented in **Figure 2.3**. The PDI

values range from 1 (corresponding to pure polyol) to 1.5 for HEURs produced from polyols with low moisture concentration. For all the polymers produced in the current paper and considering that the initial moisture concentration of the polyol was controlled (≈ 800 ppm), PDI values remained approximately equal to 1.5.

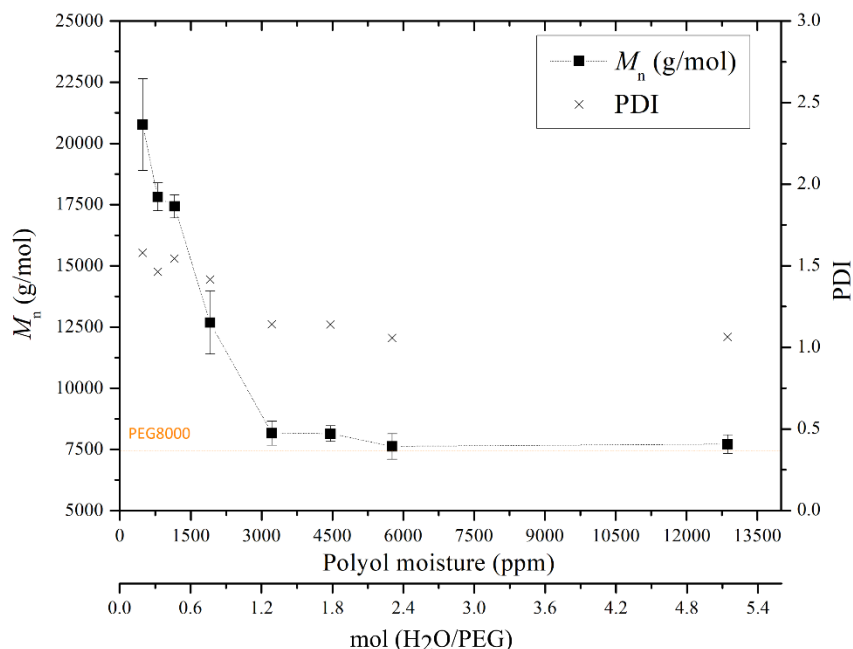


Figure 2.3. M_n and PDI values of the produced HEURs obtained for various initial PEG moisture concentrations. The second x-axis shows the corresponding molar ratio (water/PEG). The measured M_n of the PEG8000 analyzed - as received- is also shown on the graph. The dashed lines have been added to guide the eye. Experiments have been performed in at least three repetitions.

The APC analysis in Figure 2.4 shows that there is multimodal molecular weight distribution (MWD) in the HEUR samples produced both from low and high moisture concentration PEGs. Both HEURs show multiple peaks, besides the first peak which is attributed to PEG8000, corresponding to dimers, trimers and polymers consisting of higher number of connected repeating units, that are indicative of multiple distinct molecular weight populations. Direct comparison of the obtained curves showed that the HEUR produced with PEG of low moisture concentration (500 ppm) has a broader MWD and a higher molecular weight shoulder on the left of the curve. The latter is also confirmed by the PDI increase when starting from a PEG with lower moisture concentration.

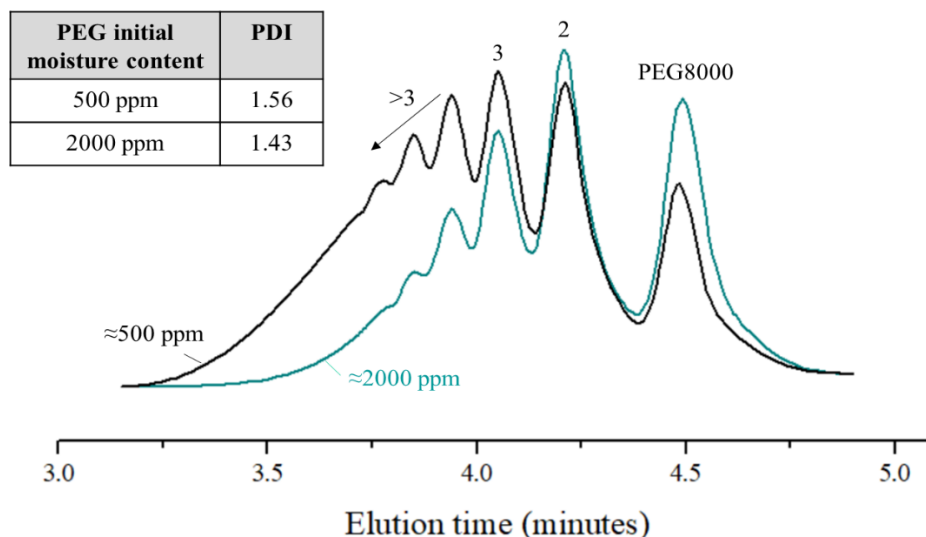


Figure 2.4. APC results for two samples from the moisture study.

Further investigation of the effect of PEG moisture concentration on the chemical composition of the produced HEUR was done with FTIR analysis, which confirms the presence of urethane or urea-related groups in the HEUR samples. Figure 2.5 shows the FTIR spectra of two samples produced from PEG with low moisture concentration (500 and 1150 ppm) and three samples produced from PEG with high moisture concentration (2000, 3200 and 5800 ppm). Band differences are spotted in two absorption regions: from ≈ 1630 to 1720 cm^{-1} corresponding to the stretching vibrations of the carbonyl $\text{C}=\text{O}$ groups and the $-\text{NH}$ bending vibration region from ≈ 1530 to 1560 cm^{-1} . For all analyzed samples, the characteristic $-\text{CH}$ stretching band appears at $\approx 2850\text{--}2900\text{ cm}^{-1}$ and the characteristic absorption peak of the isocyanate group ($\text{N}=\text{C}=\text{O}$) at 2270 cm^{-1} . The peak at 730 cm^{-1} is attributed to the solvent used for the in situ sampling.

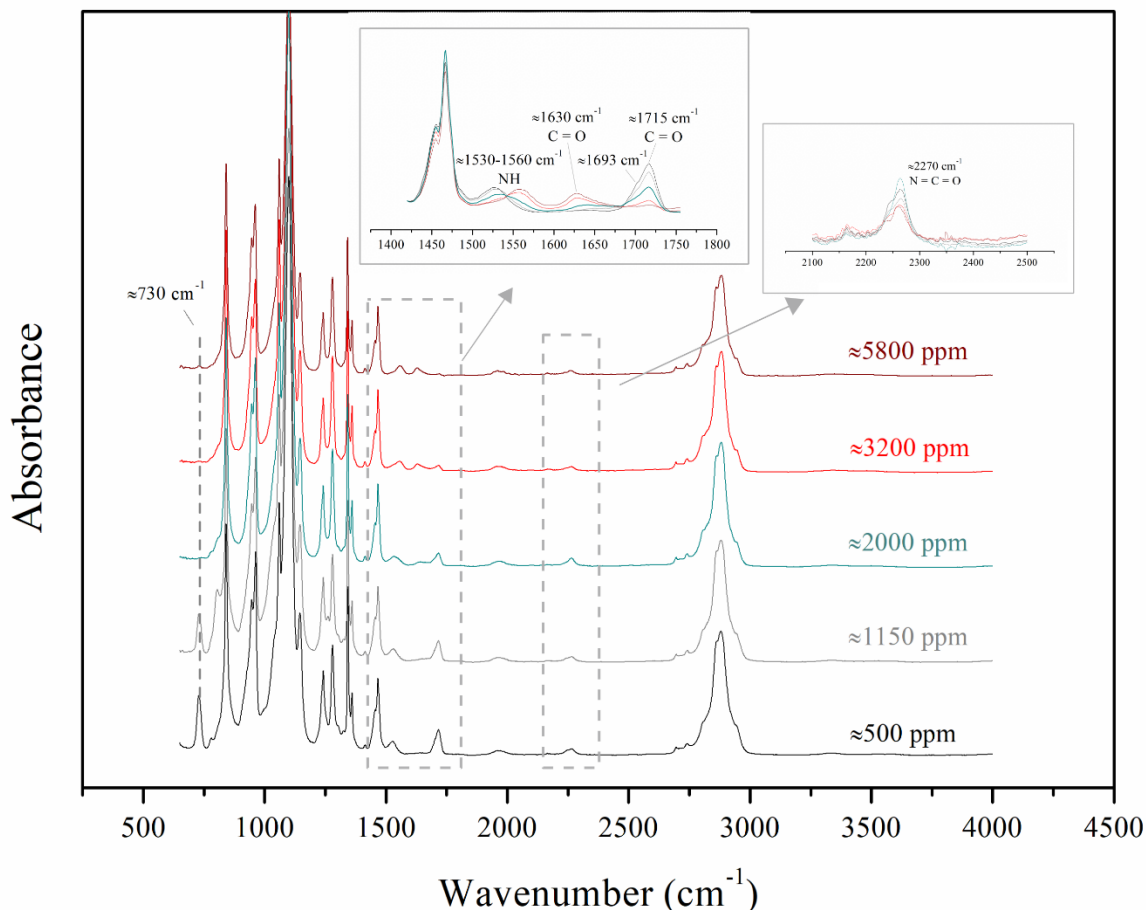


Figure 2.5. FTIR spectra of selected HEUR samples from the moisture study; The initial moisture concentration (in ppm) of the polyol is indicated on the graphs.

For the HEURs produced from PEG8000 containing the highest moisture concentrations (≈ 5800 and 3200 ppm), a discrete peak appears at 1630 cm^{-1} attributed to the ordered hydrogen bonded urea carbonyl ($\text{C}=\text{O}$).^{26–30} The peak at 1560 cm^{-1} can be associated with the bending vibrations of the NH groups in the urea bonds.²⁸ For these samples, a peak with very low intensity appears at 1715 cm^{-1} , which can be assigned to the disordered hydrogen bonded carbonyl ($\text{C}=\text{O}$) groups in the urethane molecule.^{26–29} On the contrary, the intensity of this peak at 1715 cm^{-1} increases considerably for the lower PEG8000 moisture concentration HEURs (≈ 1150 and 500 ppm). The $\text{C}=\text{O}$ of polyurethane is connected to $-\text{NH}$ and $-\text{O}$, while the $\text{C}=\text{O}$ of urea is connected to two $-\text{NH}$. This makes the three dimensional urea H –bonding stronger than the urethane one and, as a result, the frequency of the urea carbonyl is lower than the urethane one.^{26, 27}

Chapter 2

For the lower PEG8000 moisture concentration samples, a small shoulder, visible at 1693 cm^{-1} as well, can be attributed to the ordered hydrogen bonded urethane $\text{C}=\text{O}$ group.²⁶⁻²⁹ The shape of the peak representing the carbonyl of the urethane molecule is affected by the presence of free or hydrogen-bonded carbonyls.²⁹ The peak at 1530 cm^{-1} represents the bending vibrations of the NH in the urethane groups.^{25,27,31,32} The sample synthesized with PEG8000 of ≈ 2000 ppm moisture concentration shows an intermediate behavior, namely, both urea and urethane peaks are present, but the peaks intensity is lower. The spectra in Figure 2.5 clearly indicate that the moisture concentration of the polyol determines the intensity of the urea and urethane peaks, as well as the presence of characteristic bonds ($-\text{NH}-\text{C}=\text{O}-\text{O}-$ for the urethane and $-\text{NH}-\text{C}=\text{O}-\text{NH}-$ for the urea).

An interesting observation can be made by comparing the area below the two kinds of carbonyl peaks at the two extreme moisture concentrations, that is 500 ppm and 5800 ppm: the urethane peak at 1715 cm^{-1} is higher - almost double - than the urea one at 1630 cm^{-1} . Although the performed FTIR analysis is not quantitative, this difference is possibly due to the fact that during the urea forming reaction between water and diisocyanate, one molecule of CO_2 is released per urea bond formed, which is not the case in the urethane reaction. Additionally, the products of the reaction between H_{12}MDI and 1-octanol and H_{12}MDI and dibutylamine served as standards and confirmed the urea and urethane carbonyl peaks attribution experimentally. These spectra compared to targeted HEURs can be found in Figure S2.0.12 and Figure S2.0.13 (Supporting Information). The FTIR spectra interpretation confirms that above a water concentration of 3000 ppm in PEG, the urea formation severely inhibits the urethane forming reaction. The opposite occurs when the moisture concentration is below 1000 ppm and the urea peak is not detected in the spectra. Based on the obtained results, the necessity of careful storing and handling of the polyol is confirmed and a pretreatment step is necessary for controlling the reaction pathway. In practice, the initial polyol moisture concentration should be limited below ≈ 1000 ppm and the polyol should be stored under inert atmosphere, such as N_2 blanketing that is typically applied in industry, to avoid moisture uptake.

Direct comparison of the steady shear rotational testing results between 20% w/w aqueous solutions of HEURs produced with low or high PEG moisture concentration,

show differences in the Newtonian region of viscosities, as shown in Figure 2.6. The viscosity of the Newtonian plateau of HEURs synthesized with a PEG moisture concentration of ≈ 2000 ppm is higher than the ≈ 500 ppm ones, while for the former the shear thinning behavior starts at lower shear rates. This is related to the presence of urea in this HEUR molecule³³, as confirmed by the FTIR analysis (Figure 2.5). As mentioned earlier, the urea hydrogen bonds are stronger compared to the ones of urethane.^{26, 27} This effect has also been verified through TGA analysis, which is presented in Figure S2.0.17. (Supporting Information), and can explain the viscosity trends. Specifically, the HEURs containing urea, produced with PEG containing 2000 ppm of moisture, required higher temperature for mass reduction of 3%. It is remarked that the viscosity of the HEUR product at 20% concentration in water is an important property for the HEUR industrial users, as it determines its transportability through pumping lines. Viscosities in the order of ≈ 26 Pa s, corresponding to an initial moisture concentration of 2000 ppm in the PEG, as shown in Figure 2.6, are quite high in this regard and are better avoided. Therefore, limiting the initial moisture concentration below 1000 ppm, as mentioned above, is suggested to facilitate downstream HEUR transportation and post-processing.

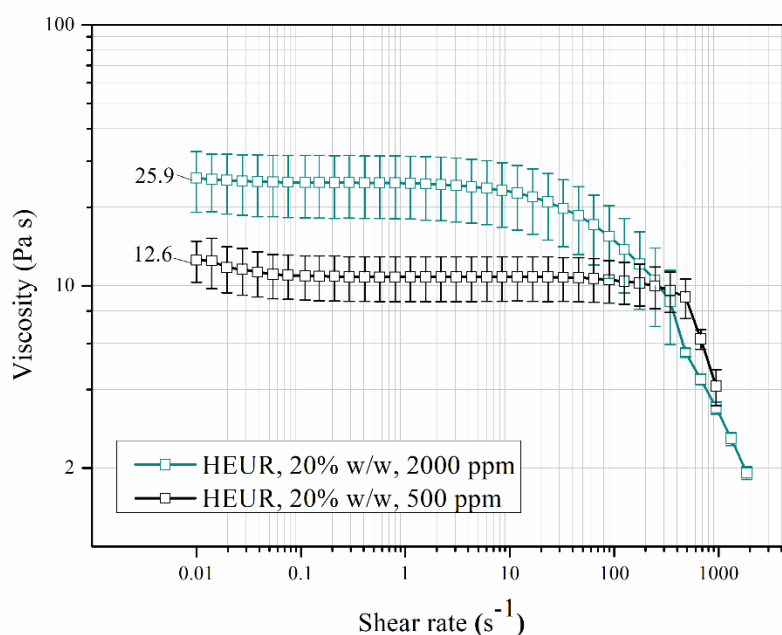


Figure 2.6. Steady shear viscosity testing of two HEUR products from the moisture study (500 and 2000 ppm initial PEG moisture concentration), diluted in water (20%) and measured at 25 °C. The zero shear viscosity values are indicated on the graphs.

Chapter 2

Oscillatory measurements were performed to characterize the viscoelastic behavior of the aforementioned HEUR samples. Both the storage modulus (G') and loss modulus (G'') increase with increasing frequency in the tested region (Figure 2.7). The G'' is related to the viscous behavior of a polymer, G' expresses the elastic response of a polymer and $\tan(\delta)$ is the ratio of the two (viscous or energy dissipation over elastic or storage behavior).^{34,35} For both evaluated samples, G'' has higher values than G' over the whole tested frequency region, and no crossover frequency is detected. The former indicates that the viscous portion of the viscoelastic performance of the HEUR aqueous solutions is predominant.³⁶ This liquid-like behavior is expected for low concentration HEURs aqueous solutions. Additionally, when comparing the $\tan(\delta)$ values of the samples (Figure 2.7), higher values were obtained for the low moisture samples which implies a more liquid-like behavior.³⁵ Therefore, less pumping energy will be required for the post processing of this type of materials. On the contrary, the high moisture samples showed lower $\tan(\delta)$ values implying that the solution shows a more elastic response and a stronger interconnected network. In this case, it is more likely that the sample will store an applied deformation load instead of dissipating it.³⁷

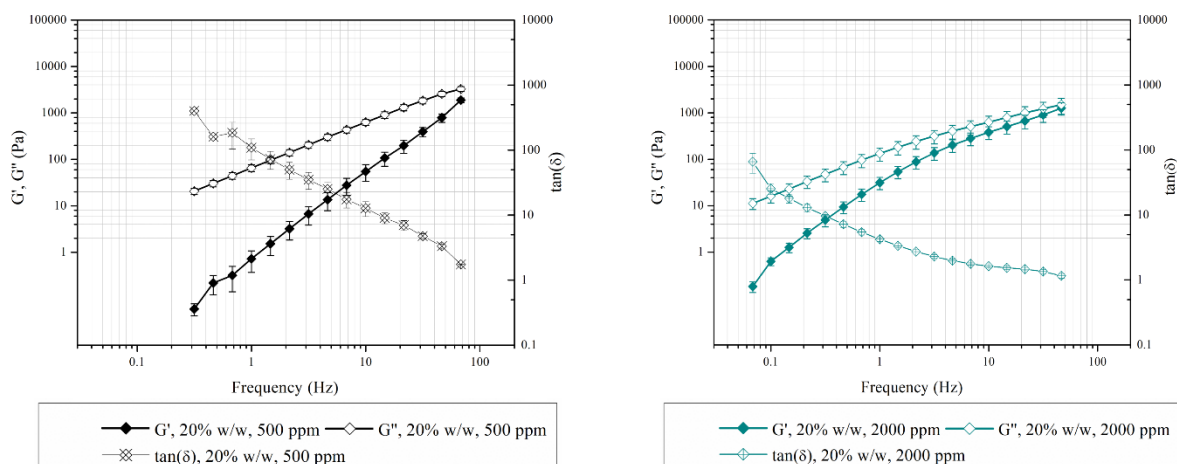


Figure 2.7. The storage (G' , solid symbols) and loss modulus (G'' , open symbols) versus frequency for two HEUR products starting from PEG with initial moisture concentration 500 ppm (left) and 2000 ppm (right), diluted in water (20%). Measurements were made at 25 °C.

Chapter 2

The crystallinity of the HEURs produced as a function of the process parameters has been investigated through XRD analysis and it is concluded that for the operating windows in this study, the product crystallinity is not affected when compared to the PEG8000 starting material (Figure S2.0.18, Supporting Information). In addition, the heat capacity of the HEURs has been investigated as a function of the PEG moisture concentrations. The results show that heat capacity remains practically unaffected when comparing HEURs starting from polyols with different initial moisture concentration. Indicative DSC graphs are presented in Figure S2.0.19. (Supporting Information). Although in situ analysis is preferred for HEURs, solid samples were used for characterization through TGA, XRD and DSC due to the technical requirements of the methods. The obtained results are considered representative of the properties of the synthesized HEURs.

2.3.3. Effect of the catalyst concentration

In order to identify the attainable molecular weight range that could be obtained for the specific stoichiometric ratios applied (1PEG:1.5HMMDI:1Oct), the modification of the catalyst concentration used in all other experiments (0.035%) was multiplied by a factor of 4, 10 and 60 and the obtained M_n values are presented in Table 2.4.

Table 2.4. Effect of catalyst concentration on the M_n of the HEURs produced. Gray highlighted region corresponds to not measured data.

Catalyst [%]	Reaction time [min]			
	3	15	45	120
	M_n [g/mol]			
0.035	9800	15900	17800	21500
0.14	15200	18100	-	-

Chapter 2

0.35	18800	20900	-	-
2.1	19900	20500	-	-

The M_n values obtained for the highest catalyst concentrations (0.35 and 2.1 wt%) resulted in approximately constant M_n values (≈ 20000 - 21000 g/mol) after 15 minutes of reaction. A similar M_n value (≈ 21500 g/mol) was obtained after 120 minutes of reaction for the working catalyst concentration (0.035 wt%). The results from this modification show that a limitation exists as regards the maximum M_n range (≈ 20000 - 22000 g/mol) for HEURs produced with the reaction stoichiometry used in this study. This range will be referred to as the “ M_n plateau” in the next paragraphs. Similar final HEUR molecular weights have been reported in relevant chemistries using catalyst concentration in the range 0.2-0.4 wt%, which is typical in HEURs synthesis (0.2 wt% of dibutyltin dilaurate (DBTDL) or tertiary amines catalyst is mentioned in the review by Quienne et al.⁹). Table 2.5 lists the operating conditions applied and final number average molecular weights in relevant published works.

Table 2.5. Summary of processing conditions and final M_n for HEURs synthesis in the literature.

[molar ratio] Reactants / <i>Catalyst</i>	Processing ¹ [min]	Temperature [°C]	M_n [g/mol]	PDI	Reference
[1]PEG8000/[1.5]IPDI/[1]1-Tetradecanol <i>DBTDL (0.2%)</i>	300	90	20500	1.2	Lu et al., 2021 ³
[1]PEG6000/[1.5]HMDI/[1.2]Cetyl alcohol	>120	45	16500	1.4	Barmar et al., 2001 ¹⁹

Chapter 2

<i>DBTDL (0.3%)</i>				
[3.2]PEG6000/[4.2]HDI/[1.1]Al kyl amine	90	45	18000	1.6
<i>DBTDL (0.4%)</i>				
				May et al., 1996 ³⁸
[3.2]PEG6000/[4.2]HMDI/[1.1] Alkyl amine	90-270	45	17600	1.7
<i>DBTDL (0.4%)</i>				
[1]PEG8000/[1.5]HMDI/[1]Oct	120	80	21500	1.5
<i>kkat (0.035%)</i>				
				This work
[1]PEG8000/[1.5]HMDI/[1]Oct	15	80	20900	1.5
<i>kkat (0.35%)</i>				

1. Refers to total processing time (prepolymer and chain stopper addition steps)

Increasing the concentration of the catalyst serves to accelerate the rate of polyurethane formation, thereby reducing the time required to achieve a targeted molecular weight within the attainable molecular weight range. This presents both energy efficiency and productivity advantages, particularly when transitioning from batch processing to continuous methods such as reactive extrusion, where higher catalyst concentrations may be strategically deployed to accelerate the reaction and operate the process in shorter extruder. However, this must be balanced against considerations such as raw material costs and energy expenditures associated with prolonged reaction times. Additionally, compliance with environmental regulations necessitates careful monitoring of residual catalyst levels in the final polyurethane product.

2.3.4. Effect of reaction temperature

For the reaction temperature study, both HEURs and prepolymers were produced in order to compare directly the effect of the chain stopper in the produced polymer. The obtained M_n results are presented in Figure 2.8.

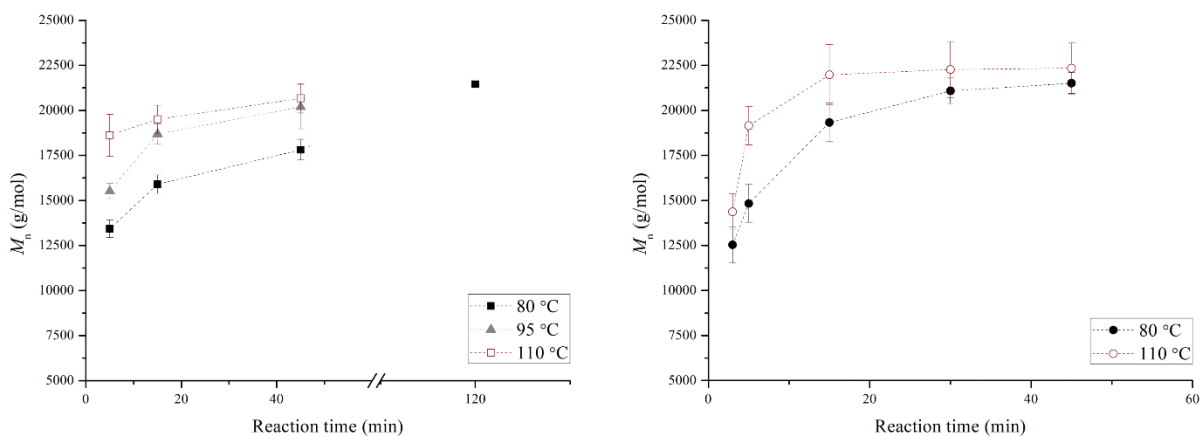


Figure 2.8. M_n of the produced HEURs obtained for reaction temperatures of 80, 95 and 110 °C (left). M_n for the prepolymers at 80 and 110 °C (right). The dashed lines have been added to guide the eye. Experiments have been performed in at least three repetitions with exception of the point of 120 min for 80 °C of the HEURs (left diagram).

In Figure 2.8 (left), the effect of the reaction temperature at short reaction times can be observed. At 110 °C, the M_n at 5 minutes of reaction (18618 g/mol) is 90% of the value at 45 minutes (20667 g/mol). At 80 °C the M_n at 5 minutes (13425 g/mol) is approximately 60% of the value at 120 minutes (21452 g/mol), which is a representative process time required to reach the M_n plateau level (≈ 21000 g/mol) when working at 80 °C in industrial batch reactors. This is a clear indication that higher temperature results in achieving the M_n plateau value faster. Taking into consideration that the plateau M_n value for all applied temperatures is approximately the same (≈ 21000 - 22000 g/mol), it can be strongly supported that no side reactions or dissociations are favored within the applied temperature range and duration of the reaction. In the moisture study presented earlier, it was shown that for the lowest reaction temperature applied (80 °C) the dominant factor controlling the urea forming side reaction is the PEG moisture concentration. Given that below 1000 ppm, no urea peaks were traced (Figure 2.5) and that for the study of reaction temperature effect, the polyol moisture concentration was

restricted well below this threshold, the urea forming side reaction can be safely excluded for all tested temperatures in the current work.

The results from the prepolymers analysis indicate a similar trend to that observed for the HEURs. In Figure 2.8 (right), it can clearly be seen that an increase in the reaction temperature shortens the required time for achieving a certain M_n value. Similar results have also been reported in the literature, but for higher temperatures applied.⁴⁰ The FTIR spectra in Figure 2.9 do not suggest the occurrence of side reactions for the prepolymers. The only difference between HEURs and prepolymer is the intensity of the N = C = O peak at 2270 cm^{-1} . The peak is higher for the prepolymer, possibly due to the absence of octanol that would attach to either free isocyanate or N = C = O ending HEUR chains.

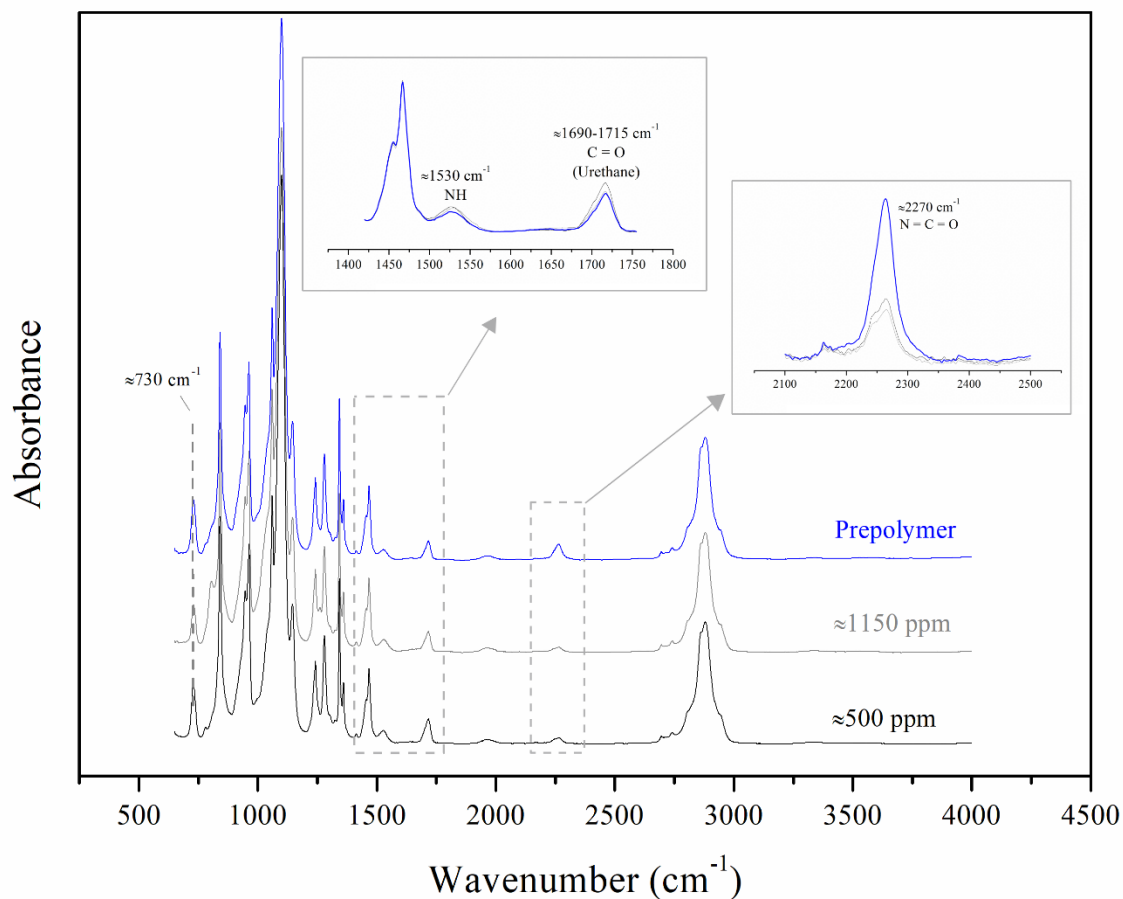


Figure 2.9. FTIR spectra of selected HEUR samples from the moisture study compared to the prepolymer produced with low moisture concentration PEG8000 (≈ 500 ppm). The initial moisture concentration (in ppm) of the polyol is also indicated on the graphs.

Chapter 2

Another observation occurs when comparing directly the M_n results of HEURs and prepolymers at the lowest temperature applied (80 °C). Figure 2.10 shows that when the chain stopper is present in the reactive mixture, the rate of the molecular weight development is restrained while the same maximum value (range of ≈ 20000 to 22000 g/mol) is reached both for the prepolymers and the HEURs products. This might be due to the mixing limitations, related to the bulk synthesis applied, and is further elaborated on in the following section of the manuscript.

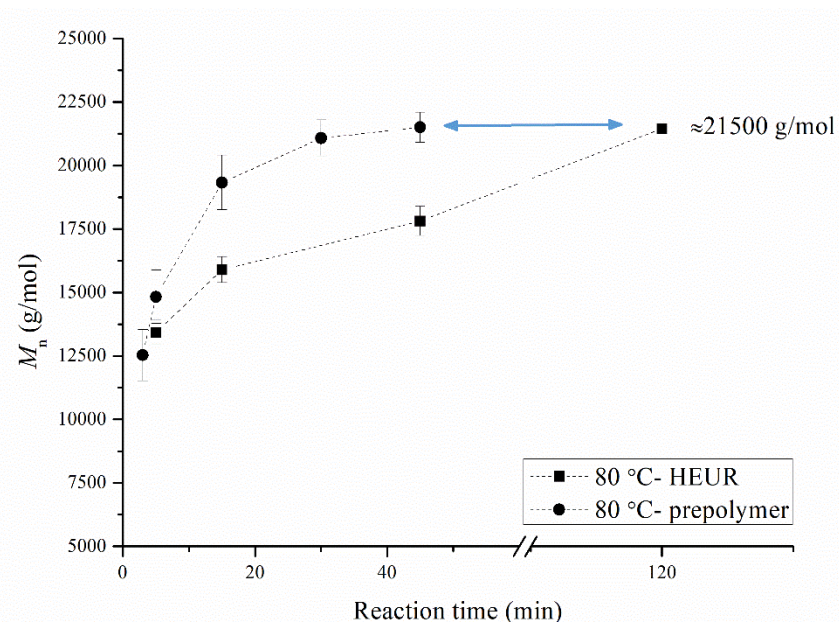


Figure 2.10. Direct comparison of M_n obtained for HEURs and prepolymers for reaction temperature of 80° C. The dashed lines have been added to guide the eye. Experiments have been performed at least in three repetitions with exception of the point of 120 min for the HEURs.

2.3.5. Effect of mixing speed

Taking into account that the inhomogeneity of the bulk can reach 9% (Figure S4, Supporting Information), it can be stated that for mixing speeds of 30-750 rpm the M_n of the produced HEURs resulted in similar values (≈ 16000 - 18000 g/mol) over time as presented in Figure 2.11. Similar to the temperature effect, the mixing speed has an impact on the molecular weight of the HEURs during the first minutes of the reaction, while the effect decreases over time.

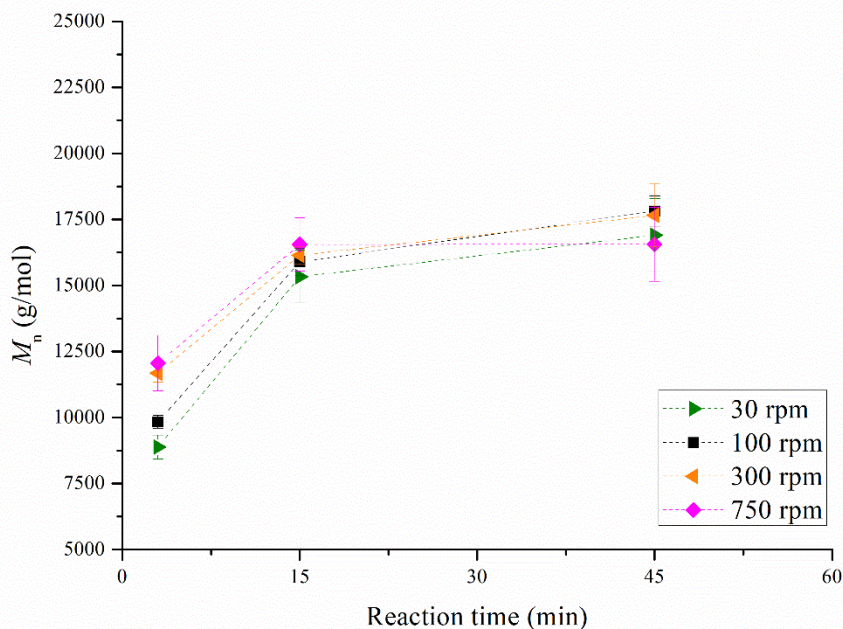


Figure 2.11. Comparison of M_n obtained for HEURs at different mixing speeds (30, 100, 300 and 750 rpm). The dashed lines have been added to guide the eye. Experiments have been performed in at least three repetitions, with the exception of the experiments at 30 rpm, which were performed in two repetitions.

Specifically, at 30 and 100 rpm, the chain build up within the first three minutes is delayed compared to the 300 and 750 rpm. As reaction time progresses, the transient behavior of the M_n evolution shows that for speeds up to 300 rpm the M_n increases monotonically. However, in the case of 750 rpm, a maximum M_n value was already reached at 15 minutes and slightly decreased thereafter. It should be noted that application of mixing speeds >300 rpm can cause very intense segregation of the bulk mixture⁴¹ and thereby entrapment of nitrogen bubbles into the melt, eventually leading to product inconsistencies and batch to batch variations. In addition, implementing excessively high mixing speeds is impractical in industrial-scale batch reactors with capacities of multiple cubic meters. Hence, moderate mixing speeds are recommended, relative to the polymerization scale in each case, to ensure uniform polymerization while minimizing air entrapment and product segregation.

During polymerizations at different mixing speeds, the torque exerted on the impeller by the motor was recorded online. Pure melted PEG8000 was used as background for all mixing speed recordings. As seen in Figure 2.12, the torque recordings for the 300 and 750 rpm showed an instant torque slope increase compared to the 100 rpm case.

Chapter 2

This behavior indicates faster polymeric chain development and molecular weight built up initiation.⁴²

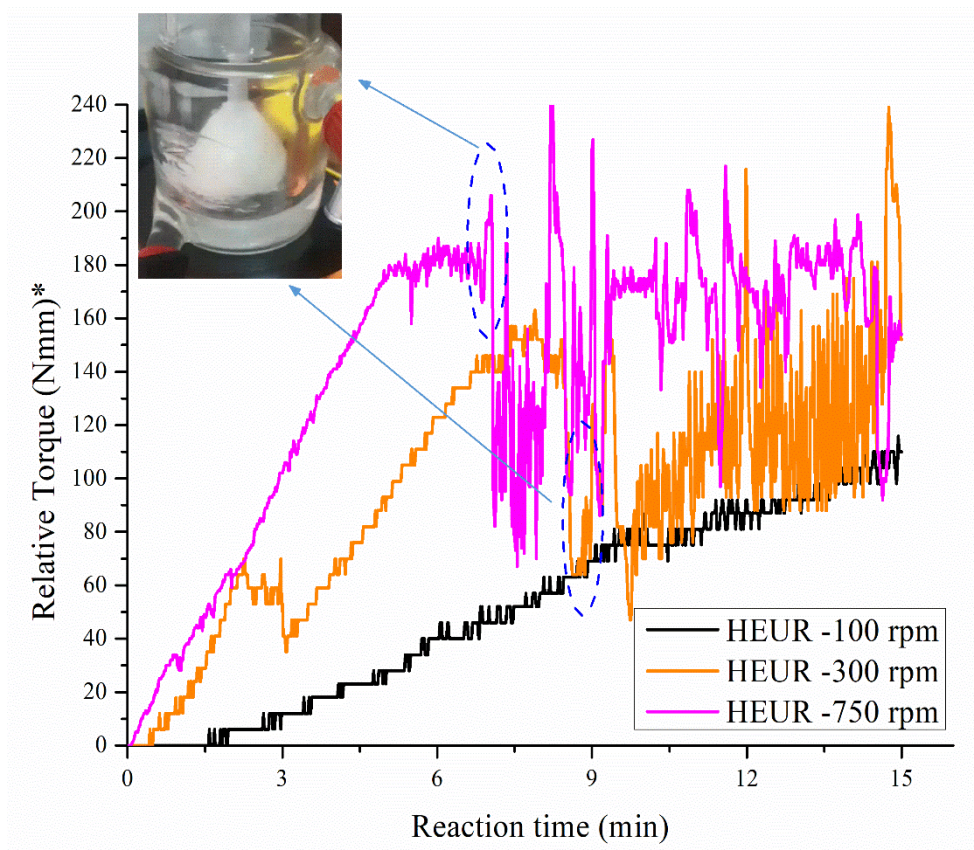


Figure 2.12. On line torque recordings during the polymerizations at different mixing speeds (100, 300, 750 rpm); the recorded signals at 300 and 750 rpm present a sharp drop indicated on the graph. At this point the bulk became a gel that crawled on the rod of the agitator as seen on the photo inside the graph. *Relative torque refers to the difference of actual torque value of the polymer relative to a baseline recording of pure PEG8000 at 80 °C.

As time proceeds, the torque signal increases consistently for all applied speeds indicating the evolution of the polymerization reaction and the increase in the M_n . Figure 2.12 shows that for the higher mixing speeds (300 and 750 rpm), the obtained signal presents a sharp drop and a vigorous oscillation starting at the indicated points in Figure 2.12. At these points, the reactive mixture became a very viscous gel that crawled on the agitator rod resulting in poor mixing of the bulk fluid, similar to what was reported by Winters et al.⁴³ for the synthesis of aromatic polyamides. As the authors⁴³ mention, “this phenomenon is known as the Weissenberg effect”. Further, the oscillations of the torque measurements are due to the constant collision of the gel with

the walls of the reactor. It is finally noted that the torque measurements were used only for qualitative analysis, as the absolute values of the torque signal are strongly affected by the frictional loads applied at the connection point of the motor with the agitator rod.⁴²

2.3.6. Mixing limitations in the system

Possible connection of the Weissenberg phenomenon with the obtained results for both the HEURs and the prepolymers was further investigated in order to understand how this effect could possibly be related to reaching similar M_n maximum values when varying different operating parameters. In order to make this correlation more clear, the temporal evolution of M_n compared to the temporal torque profile for the prepolymer at 110 °C is presented in Figure 2.13.

Figure 2.13 shows that the point of initiation of the Weissenberg effect marks the end of the M_n increase. In other words, the M_n plateau is reached exactly when the phenomenon starts occurring, due to the mixing limitations of the reactive mixture that becomes highly viscous and starts turning around together with the agitator. A similar effect was reported by Stern²⁵ during bulk polyurethane synthesis.

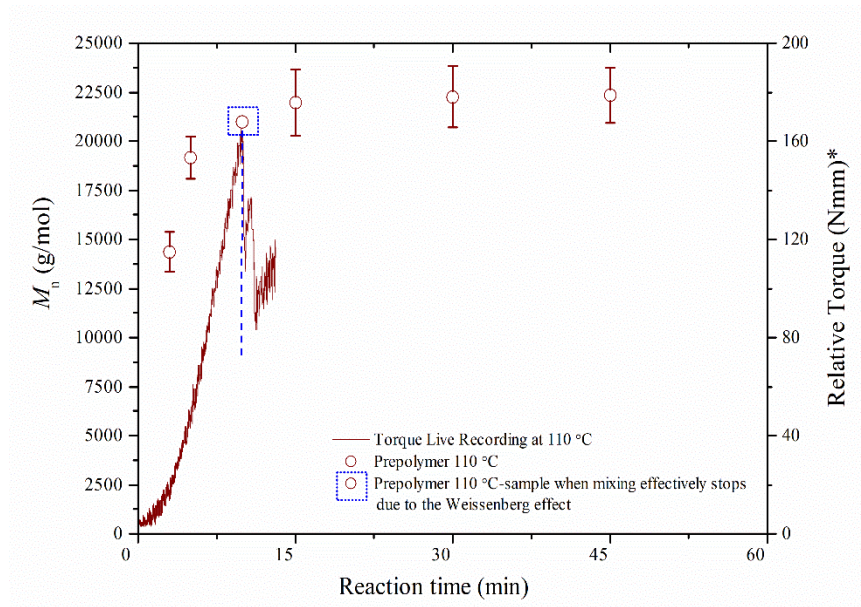


Figure 2.13. M_n development and online torque recordings during prepolymer production at 110 °C. The M_n of the sample corresponding to when mixing effectively stops due to Weissenberg effect is highlighted on the graph. *Relative torque refers to

the difference of actual torque value of the prepolymer relative to a baseline recording of pure PEG8000 at 110 °C.

2.4.CONCLUSIONS

We have investigated the effect of sampling procedure for polyurethane melts and the effect of critical process parameters of HEUR polymerization, that is, moisture concentration in the starting polyol material, reaction temperature, catalyst concentration and mixing intensity, on physicochemical and rheological properties of the obtained products. Our study emphasizes the crucial influence of sampling methods on molecular weight and chemical characterization of polyurethane melts. Specifically, we found that using the solid method resulted in number-average molecular weights that were 50-77% higher for samples with lower isocyanate content, and even 115% higher for those with elevated isocyanate concentrations, as compared to the in-situ method. This discrepancy is attributed to chain-extension reactions involving NCO-terminated urethane prepolymers and ambient moisture, which led to the formation of urea linkages and an extended polyurea structure. To obtain accurate and reliable data on key product properties like molecular weight, composition, and viscosity, it is imperative to either neutralize residual NCO content or meticulously prevent its exposure to atmospheric moisture.

Furthermore, we conclude that the modification of the moisture concentration of the polyol used in HEUR synthesis directly impacts the progress of polymerization. Below a threshold value (≈ 1000 ppm), the consumption of diisocyanate towards urea is avoided and the main urethane reaction is promoted. This moisture level is in agreement with industrial standards namely, lower than 1000 ppm. These conclusions are also supported by FTIR and TGA analyses. XRD characterization of the HEURs showed that the crystallinity of the samples remains unaffected compared to the starting polyol, while DSC measurements showed that HEURs starting from PEG with different moisture concentration result in similar heat capacity curves. Further, steady shear rotational testing of HEUR aqueous solutions (20%) revealed that the presence of urea results in significantly higher viscosities at the Newtonian plateau, while the shear thinning behavior starts at lower shear rates for the HEURs produced with PEG of high moisture concentration. Oscillatory measurements of samples from the moisture study confirmed the viscous character of the HEURs aqueous solutions and no crossover

point was detected in the tested region. However, based on the obtained values of $\tan(\delta)$, a stronger interconnected network is formed the case of high moisture concentration of PEG. Increase in catalyst concentration in the range 0.035-2.1 wt% imparts acceleration of the polymerization kinetics leading to significant reduction of processing time and required energy for synthesis of products with specific M_n . However, the maximum attainable molecular weight is not affected when varying catalyst concentration for the chosen working system, as it is mixing limitations that mark the end of the polymerization process at high bulk viscosities.

Further investigation revealed that both elevated mixing speeds and higher reaction temperatures (within the range of 80-110°C) foster faster molecular weight development, albeit reaching the same molecular weight plateau. Notably, when the molecular weight of polyurethanes approaches 21,000 g/mol, the polymer turns into a viscous gel exhibiting the Weissenberg effect. On an industrial scale, if this state is reached too rapidly, it could jeopardize the homogeneous distribution of reactants within the viscous PEG, leading to batch inconsistencies. Therefore, for viscous polyurethane polymerizations carried out in industrial-scale batch reactors, it is recommended to use moderate mixing speeds adapted to the specific polymerization scale. Given PEG's susceptibility to thermal degradation, maintaining reaction temperatures between 80-85°C is advisable, especially during extended polymerization periods in industrial-scale batch reactors. It is envisioned, however, that on process scale-up, using alternative and more efficient mixing technologies, such as static mixers and extruders, complete fluid segregation will not take place, allowing for attainment of a wider range of M_n values depending on the applied mixing efficiency.

References

- (1) Akindoyo, J. O.; Beg, M. D. H.; Ghazali, S.; Islam, M. R.; Jeyaratnam, N.; Yuvaraj, A. R. Polyurethane Types, Synthesis and Applications – a Review. *RSC Adv.* **2016**, *6* (115), 114453–114482. <https://doi.org/10.1039/C6RA14525F>.
- (2) Pulidindi, K.; Mukherjee, S. *Rheology Modifiers Market Size By Product (Organic, Inorganic), By Application (Paints & Coatings, Personal Care, Adhesives & Sealants, Textiles, Pharmaceuticals, Pulp & Paper, Construction)*.
- (3) Lu, M.; Song, C.; Wan, B. Influence of Prepolymer Molecular Weight on the Rheology and Kinetics of HEUR-Thickened Latex Suspensions. *Prog. Org. Coatings* **2021**, *156* (July 2020), 106223. <https://doi.org/10.1016/j.porgcoat.2021.106223>.
- (4) Huldén, M. Hydrophobically Modified Urethane-Ethoxylate (HEUR) Associative Thickeners 1. Rheology of Aqueous Solutions and Interactions with Surfactants. *Colloids Surfaces A Physicochem. Eng. Asp.* **1994**, *82* (3), 263–277. [https://doi.org/10.1016/0927-7757\(93\)02637-T](https://doi.org/10.1016/0927-7757(93)02637-T).
- (5) Huldén, M. Hydrophobically Modified Urethane-Ethoxylate (HEUR) Associative Thickeners 2. Interaction with Latex. *Colloids Surfaces A Physicochem. Eng. Asp.* **1994**, *88*, 207–221. [https://doi.org/https://doi.org/10.1016/0927-7757\(94\)02835-4](https://doi.org/https://doi.org/10.1016/0927-7757(94)02835-4).
- (6) Fonnum, G.; Bakke, J.; Hansen, F. K. Associative Thickeners. Part I: Synthesis, Rheology and Aggregation Behavior. *Colloid Polym. Sci.* **1993**, *271* (4), 380–389. <https://doi.org/10.1007/BF00657419>.
- (7) Barmar, M.; Barikani, M.; Kaffashi, B. Steady Shear Viscosity Study of Various HEUR Models with Different Hydrophilic and Hydrophobic Sizes. *Colloids Surfaces A Physicochem. Eng. Asp.* **2005**, *253* (1–3), 77–82. <https://doi.org/10.1016/j.colsurfa.2004.06.028>.
- (8) Lambourne, R.; Jeffs, R. A.; Jones, W. *Paint and Surface Coatings Theory and Practice*, Second Edi.; Lambourne, R., Strivens, T. A., Eds.; Woodhead Publishing, 1999. <https://doi.org/https://doi.org/10.1533/9781855737006.1>.
- (9) Quienne, B.; Pinaud, J.; Robin, J. J.; Caillol, S. From Architectures to Cutting-Edge Properties, the Blooming World of Hydrophobically Modified Ethoxylated Urethanes (HEURs). *Macromolecules* **2020**, *53* (16), 6754–6766. <https://doi.org/10.1021/acs.macromol.0c01353>.
- (10) Winnik, M. A.; Yekta, A. Associative Polymers in Aqueous Solution. *Curr. Opin. Colloid Interface Sci.* **1997**, *2* (4), 424–436. [https://doi.org/10.1016/s1359-0294\(97\)80088-x](https://doi.org/10.1016/s1359-0294(97)80088-x).
- (11) Sharmin, E.; Zafar, F. *Polyurethane: An Introduction*; Sharmin, E., Zafar, F., Eds.; IntechOpen: London, United Kingdom, 2012. <https://doi.org/10.5772/51663>.
- (12) Szycher, M. *Szycher's Handbook of Polyurethanes*, Second edi.; Szycher, M., Ed.; CRC Press, 2013.

- (13) Barmar, M.; Ribitsch, V.; Kaffashi, B.; Barikani, M.; Sarreshtehdari, Z.; Pfragner, J. Influence of Prepolymers Molecular Weight on the Viscoelastic Properties of Aqueous HEUR Solutions. *Colloid Polym. Sci.* **2004**, *282* (5), 454–460. <https://doi.org/10.1007/s00396-003-0968-0>.
- (14) Annable, T.; Buscall, R.; Ettelaie, R.; Whittlestone, D. The Rheology of Solutions of Associating Polymers: Comparison of Experimental Behavior with Transient Network Theory. *J. Rheol. (N. Y. N. Y.)*. **1993**, *37* (4), 695–726. <https://doi.org/10.1122/1.550391>.
- (15) Barmar, M. Study of the Effect of PEG Length in Uni-HEUR Thickener Behavior. *J. Appl. Polym. Sci.* **2009**, *111* (4), 1751–1754. <https://doi.org/10.1002/app.29192>.
- (16) Vermette, P.; Griesser, H. J.; Laroche, G.; Guidoin, R. *Biomedical Applications of Polyurethanes*; Vermette, P., Ed.; Landes Bioscience: Texas, U.S.A, 2001.
- (17) D. Emmons, W.; Valley, H.; E. Stevens, T.; Ambler. Polyurethane Thickeners in Latex Compositions. United States Patent number 4.079.028, 1978.
- (18) Chiono, V.; Sartori, S.; Calzone, S.; Boffito, M.; Tonda-Turo, C.; Mattu, C.; Gentile, P.; Ciardelli, G. *Synthetic Biodegradable Medical Polyurethanes*; Zhang, X., Ed.; Woodhead Publishing Series in Biomaterials, 2017. <https://doi.org/10.1016/B978-0-08-100372-5.00006-4>.
- (19) Barmar, M.; Barikani, M.; Kaffashi, B. Synthesis of Ethoxylated Urethane and Modification with Cetyl Alcohol as Thickener. *Iran. Polym. J. (English Ed.)* **2001**, *10* (5), 331–335.
- (20) Barmar, M.; Barikani, M. Investigation of the Thickening Efficiency of HEUR on the Behavior of Two Different Latex Types. *Int. Polym. Process.* **2009**, *24* (3), 218–222. <https://doi.org/10.3139/217.2191>.
- (21) Barmar, M.; Kaffashi, B. Rheological Behavior of HEUR Mixtures in Aqueous Media. *Int. Polym. Process.* **2007**, *22* (2), 146–150. <https://doi.org/10.3139/217.0046>.
- (22) Arnould, P.; Bosco, L.; Sanz, F.; Simon, F. N.; Fouquay, S.; Michaud, G.; Raynaud, J.; Monteil, V. Identifying Competitive Tin-or Metal-Free Catalyst Combinations to Tailor Polyurethane Prepolymer and Network Properties. *Polym. Chem.* **2020**, *11* (36), 5725–5734. <https://doi.org/10.1039/d0py00864h>.
- (23) Bampouli, A.; Tzortzi, I.; Schutter, A. De; Xenou, K.; Michaud, G.; Stefanidis, G. D.; Gerven, T. Van. Insight Into Solventless Production of Hydrophobically Modified Ethoxylated Urethanes (HEURs): The Role of Moisture Concentration , Reaction Temperature , and Mixing Efficiency. *ACS Omega* **2022**, No. int. <https://doi.org/10.1021/acsomega.2c04530>.
- (24) Chattopadhyay, D. K.; Prasad, P. S. R.; Sreedhar, B.; Raju, K. V. S. N. The Phase Mixing of Moisture Cured Polyurethane-Urea during Cure. *Prog. Org. Coatings* **2005**, *54* (4), 296–304. <https://doi.org/10.1016/j.porgcoat.2005.07.004>.
- (25) Tan, C.; Tirri, T.; Wilen, C.-E. Investigation on the Influence of Chain Extenders on the Performance of One-Component Moisture-Curable Polyurethane Adhesives. *Polymers (Basel)*. **2017**, *9* (12), 184.

- <https://doi.org/10.3390/polym9050184>.
- (26) Stern, T. Conclusive Chemical Deciphering of the Consistently Occurring Double-Peak Carbonyl-Stretching FTIR Absorbance in Polyurethanes. *Polym. Adv. Technol.* **2019**, *30* (3), 675–687. <https://doi.org/10.1002/pat.4503>.
- (27) Zhao, X.; Qi, Y.; Li, K.; Zhang, Z. Hydrogen Bonds and FTIR Peaks of Polyether Polyurethane-Urea. *Key Eng. Mater.* **2019**, *815 KEM*, 151–156. <https://doi.org/10.4028/www.scientific.net/KEM.815.151>.
- (28) Yilgör, E.; Burgaz, E.; Yurtsever, E.; Yilgör, I. Comparison of Hydrogen Bonding in Polydimethylsiloxane and Polyether Based Urethane and Urea Copolymers. *Polymer (Guildf)*. **2000**, *41* (3), 849–857. [https://doi.org/10.1016/S0032-3861\(99\)00245-1](https://doi.org/10.1016/S0032-3861(99)00245-1).
- (29) Teo, L. S.; Chen, C. Y.; Kuo, J. F. Fourier Transform Infrared Spectroscopy Study on Effects of Temperature on Hydrogen Bonding in Amine-Containing Polyurethanes and Poly(Urethane-Urea)S. *Macromolecules* **1997**, *30* (6), 1793–1799. <https://doi.org/10.1021/ma961035f>.
- (30) Mattia, J.; Painter, P. A Comparison of Hydrogen Bonding and Order in a Polyurethane and Poly(Urethane-Urea) and Their Blends with Poly(Ethylene Glycol). *Macromolecules* **2007**, *40* (5), 1546–1554. <https://doi.org/10.1021/ma0626362>.
- (31) Shi, Y.; Zhan, X.; Luo, Z.; Zhang, Q.; Chen, F. Quantitative IR Characterization of Urea Groups in Waterborne Polyurethanes. *J. Polym. Sci. Part A Polym. Chem.* **2008**, *46* (7), 2433–2444. <https://doi.org/10.1002/pola.22577>.
- (32) Auguścik, M.; Kurańska, M.; Prociak, A.; Karalus, W.; Lipert, K.; Ryszkowska, J. Production and Characterization of Poly(Urea-Urethane) Elastomers Synthesized from Rapeseed Oil-Based Polyols Part I. Structure and Properties. *Polimery/Polymers* **2016**, *61* (7–8), 490–498. <https://doi.org/10.14314/polimery.2016.490>.
- (33) Delpech, M. C.; Miranda, G. S. Waterborne Polyurethanes: Influence of Chain Extender in FTIR Spectra Profiles. *Cent. Eur. J. Eng.* **2012**, *2* (2), 231–238. <https://doi.org/10.2478/s13531-011-0060-3>.
- (34) János Hajas, A. W. Modified Ureas: An Interesting Opportunity to Control Rheology of Liquid Coatings. *Macromol. Symp.* **2002**, No. 187, 215–224. [https://doi.org/https://doi.org/10.1002/1521-3900\(200209\)187:1<215::AID-MASY215>3.0.CO;2-T](https://doi.org/https://doi.org/10.1002/1521-3900(200209)187:1<215::AID-MASY215>3.0.CO;2-T).
- (35) Kousaalya, A. B.; Biddappa, B. I.; Rai, S.; Pilla, S. *Mechanical Performance of Poly(Propylene Carbonate)-Based Blends and Composites*, Fourteenth.; Elsevier Ltd., 2015. <https://doi.org/10.1016/B978-1-78242-373-7.00016-0>.
- (36) Whittingstall, P. Paint Evaluation Using Rheology. *Therm. Anal. Rheol.* **2000**, RH-059.
- (37) Ren, S.; Liu, X.; Fan, W.; Wang, H.; Erkens, S. Rheological Properties, Compatibility, and Storage Stability of SBS Latex-Modified Asphalt. *Materials (Basel)*. **2019**, *12* (22). <https://doi.org/10.3390/ma12223683>.
- (38) Sadeghi, F.; Le, D. Characterization of Polymeric Biomedical Balloon: Physical

- and Mechanical Properties. *J. Polym. Eng.* **2021**, *41* (9), 799–807. <https://doi.org/10.1515/polyeng-2021-0203>.
- (39) May, R.; Kaczmarek, J. P.; Glass, J. E. Influence of Molecular Weight Distributions on HEUR Aqueous Solution Rheology. *Macromolecules* **1996**, *29* (13), 4745–4753. <https://doi.org/10.1021/ma9507655>.
- (40) Ando, T. Effect of Reaction Temperature on Polyurethane Formation in Bulk. *Polym. J.* **1993**, *25* (11), 1207–1209. <https://doi.org/10.1295/polymj.25.1207>.
- (41) Paul, E. L.; Atiemo-Obeng, V. A.; Kresta, S. M. *Handbook of Industrial Mixing: Science and Practice*; John Wiley & Sons, 2003.
- (42) Ponnuswamy, S.; Shah, S. L.; Kiparissides, C. On-line Monitoring of Polymer Quality in a Batch Polymerization Reactor. *J. Appl. Polym. Sci.* **1986**, *32* (1), 3239–3253. <https://doi.org/10.1002/app.1986.070320127>.
- (43) Winters, J.; Bolia, R.; Dehaen, W.; Binnemans, K. Synthesis of Polyaramids in γ -Valerolactone-Based Organic Electrolyte Solutions. *Green Chem.* **2021**, *23* (3), 1228–1239. <https://doi.org/10.1039/d0gc03470c>.

One-step versus Two-step Synthesis of Hydrophobically Modified Ethoxylated Urethanes (HEURs): Benefits and Limitations

ⁱ This chapter has been published as:

Tzortzi, I.; Xiouras, C.; Choustoulaki, C.; Tzani, A.; Detsi, A.; Michaud, G.; Van Gerven, T.; Stefanidis, G. D. *“One-Step versus Two-Step Synthesis of Hydrophobically Modified Ethoxylated Urethanes: Benefits and Limitations”* Ind. Eng. Chem. Res. 2023, 62 (29), 11378–11391. <https://doi.org/10.1021/acs.iecr.3c01107>.

ABSTRACT

Associative thickeners, such as hydrophobically modified ethoxylated urethanes (HEURs), are an important class of rheological modifiers allowing precise control and optimization of the rheology of waterborne coatings. In this work, we present a novel, comprehensive investigation of one-step and two-step HEUR synthesis processes, highlighting their impact on the final HEUR properties. In the conventional one-step process (current industrial practice) there are inherent limitations in producing high molecular weight polymers due to the complex competition between end-capping and polymerization. We show that the two-step method allows for much higher molecular weight polymers than the one-step method, while using less amount of toxic diisocyanates. Additionally, using the two-step method, the polymerization can be simply and efficiently controlled by the addition timepoint of the end-capping agent, which can be tailored to provide HEURs with a wide range of molecular weight and polydispersity index. However, the efficient end-capping of high molecular weight polymers remains a challenge when using conventional mixing equipment in batch reactors, due to mass transfer and mixing limitations associated with the significant increase in the bulk viscosity of the reaction mixture. To overcome these limitations, alternative and more efficient mixing technologies, such as reactive extruders, should be considered for the efficient end-capping of high molecular weight polymers.

3.1. Introduction

Hydrophobically modified ethoxylated urethanes (HEUR) are associative thickeners, widely used as rheology modifiers in waterborne systems, such as inks, paints, coatings and emulsions, among others.¹⁻⁵ HEURs contain both water-soluble (hydrophilic backbone) and water-insoluble segments (hydrophobic end groups). Polyethylene glycol (PEG) is commonly used as the hydrophilic segment in HEURs, but copolymers of PEG with poly (propylene glycol) (PPG) or poly (butylene glycol) (PBG) have also been used.¹ Different hydrophobic groups, such as hydrophobic alcohols or amines (C6-C20)¹ and alternative groups like fluorocarbon alkyl chains⁶⁻⁸, alkylphenyl⁹⁻¹¹, and light¹² or stimuli-responsive groups^{13,14}, have been studied. This amphiphilic structure of HEURs allows the formation of a dynamic transient network, either with emulsion particles or with each other, due to interactions between their hydrophobic groups.^{1,4,15-20} Depending on the type of HEURs used, this reversible physical network can be used to impart a more Newtonian or a strongly pseudoplastic rheological behavior to the final product.²¹⁻²³

The HEUR molecular weight and its polydispersity index are very important parameters directly affecting the network formation and its density, and therefore the rheological properties of the product.^{1,7,24,25} HEURs are divided into two groups based on their molecular weight distribution: Uni-HEURs and S-G-HEURs. Uni-HEURs exhibit a monomodal molecular weight distribution, while S-G HEURs exhibit a multimodal distribution respectively. For Uni-HEURs, the hydrophilic length of the polymer is determined by the length of the PEG, while for S-G-HEURs, the hydrophilic length for each HEUR oligomer (dimer, trimer, etc.) is defined by the number of PEG units coupled together. In this regard, the hydrophilic length of an S-G HEUR is determined by its molecular weight (number of PEG units coupled together), which in turn impacts the hydrophilic/hydrophobic ratio (with a constant hydrophobic group), thereby affecting the network formed in aqueous solutions. In a low molecular weight HEUR, intramolecular associations of hydrophobic groups lead to micelle formation, but the intermolecular associations that allow bridging micelles together are relatively weak. As a result, the network density is low leading to a low viscosity product.^{1,7,24,25} In contrast, by increasing the HEUR molecular weight, stronger bridging of micelles is possible and the network density, thus the viscosity, increases up to a point where the

Chapter 3

hydrophilic/hydrophobic group is too high and the hydrophobic groups are too few, resulting in the loss of associative polymer properties.^{1,7,24,25} Therefore, precise control of the molecular weight during HEURs synthesis is of utmost importance and its selection is affected by factors such as the hydrophobicity of the end-groups and the desired rheological properties for the targeted application.¹

S-G HEURs are typically synthesized by the step growth polymerization of terminal hydroxyl groups of PEG with diisocyanates and hydrophobic mono-alcohols. (For simplification purposes, S-G HEURs will be referred to as HEURs in the rest of the manuscript) However, the use of isocyanates in this process poses significant health and environmental risks, and alternative approaches have been sought.^{26–29} Among the various synthetic routes to non-isocyanate polyurethanes (NIPUS), the polyaddition of cyclic carbonates with amines has emerged as a promising method to produce polyhydroxyurethanes (PHUs).^{26,27} Despite the potential benefits of this technology, including the elimination of isocyanate-related hazards, there are challenges that hinder its broad adoption and industrial scaling up. The limitations include low reactivity of the cyclic carbonate/amine reaction, limited degree of polymerization at room temperature, resulting in low molar mass PHUs.^{26,27} Efforts have also been made to explore the use of the reactive extrusion (REX) technique to overcome the kinetic limitations associated with the aminolysis of cyclic carbonates.^{28,29} While this method shows promise to increase the reactivity and molar mass of PHUs, further studies are needed to optimize this method and make it a viable alternative for large-scale PHU production. Despite the promising future of PHUs and NIPUs, HEURs, made with diisocyanates, are still necessary in various applications.²⁶ As a result, a deeper understanding of the fine-tuning of their synthesis process continues to be of high importance.

Two common methods are used for the production of polyurethanes (PU) using diisocyanates: the one-step and two-step methods.³⁰ The one-step process involves the simultaneous addition of all raw materials into the reactor, while the two-step process (or prepolymer method) involves two different sequential reaction steps. In the first step, polyol reacts with the diisocyanate to form an isocyanate-terminated prepolymer. The second step involves the addition of either a difunctional molecule known as a chain-extender or a monofunctional component referred to as an end-capping agent (or

chain stopper)^{31,32}, depending on the type of PU being synthesized.³¹ Most of the published work on the two-step synthesis of polyurethanes focuses primarily on the use of a chain extender, which is commonly employed in the synthesis of thermoplastic polyurethane elastomers (TPUEs) and polyurethane-ureas (PUUs).^{30,33–40} However, we will not elaborate further on the findings of these studies since the chain extension step, which further builds up the molecular weight, is fundamentally different from the end-capping step employed in the HEUR synthesis. In the case of HEURs, the addition of the end-capping agent serves a dual purpose, (a) it prevents further chain extension by reacting the remaining isocyanate groups with a monofunctional compound, thereby stopping the molecular weight evolution, and (b) imparts hydrophobic character to the hydrophilic backbone developed in the pre-polymer step. Industrially, HEUR thickeners are produced using the one-step method in batch reactors⁴¹ with a typical capacity of around 10 m³. Upon completion of the reaction, the HEUR product is not subjected to any additional purification steps. The direct addition of water to the reactor allows for the formation of the HEUR aqueous solution, which is subsequently drained from the reactor and stored. From a reaction kinetics perspective, the one-step method used for industrial production of HEURs has a significant disadvantage. Its disadvantage lies in the fact that polymerization and chain termination counteract each other based on the relative chemical reactivities of the polyol and the hydrophobe, affecting the polymer molecular weight build-up and potentially preventing the attainment of high molecular weight polymers.^{30,38,42,43} Conversely, the two-step process decouples the polymerization and chain termination processes, which should in theory allow for more control on the HEUR molecular weight simply by controlling the molecular weight of the prepolymer and the addition timepoint of the end-capping agent. Despite the potential for improved control using the two-step method, there is a surprising gap in the existing literature regarding its benefits and potential limitations.

Previous research on the two-step HEUR synthesis has primarily been centered on the thickening performance of HEUR in water and latex formulations. These studies tailored the hydrophilic and hydrophobic lengths of the polymer through the use of different PEGs and types of hydrophobic agents, but largely ignored the effects of the synthesis method used.^{7,10,11,13,24,44–48} Only Glass and co-workers did a more systematic investigation on the pre-polymerization step by changing the reaction stoichiometry, but their findings are not easily applicable to industrial bulk polymerization methods

because they utilized solvents.^{7,24,47,48} A summary of relevant published works on the two-step HEUR synthesis, including details on the hydrophilic/hydrophobic length used, operating conditions, final molecular weight and polydispersity index values, is provided in Table S1 of the Supporting Information. Nonetheless, none of these studies conducted a thorough investigation into decoupling the polymerization and chain termination processes to assess the individual contribution of each step to the final properties of HEUR, nor did they compare the potential benefits and limitations of the one-step versus two-step HEUR synthesis.

For this reason, the main objective of this paper is two-fold: First, we apply the one-step HEUR synthesis at a wide range of reaction stoichiometries with the aim of identifying the range of polymer molecular weights accessible using this method. Subsequently, we prepare HEURs using the two-step prepolymer method considering the influence of each step (pre-polymerization and end-capping) on the final HEUR properties. More specifically, we investigate how the molecular weight of the prepolymers at the time of end-capping agent injection and the amount of end-capping agent affect the resulting HEUR properties. Finally, the two processes are compared in terms of their performance, and the resulting polymers are thoroughly characterized in terms of their chemical properties and their rheological performance in aqueous formulations. To the authors' knowledge, there is no previous work examining the two-step HEUR synthesis, considering the influence of each step (pre-polymerization and end-capping) on the final HEUR properties, and comparing it to its one-step counterpart.

3.2. MATERIALS AND METHODS

3.2.1. Materials

Polyethylene glycol of molecular weight 8000 g/mol with purity of >99.5% was provided by Clariant. H12MDI (4,4-Methylenebis (cyclohexyl isocyanate), mixture of isomers, 90% purity from Acros Organics and 1-Octanol (99% purity) from Alfa Aesar were used as received. Bismuth carboxylate (KKAT XCB221) provided by King Industries was used as the catalyst. Methanol was purchased from Acros Organics. Chloroform (>99.8% purity) stabilized with amylene was purchased from Fisher Chemicals and was dried using 4Å molecular sieves. Chloroform-d (99.8%) for NMR

was purchased from Sigma Aldrich. All reagents were of analytical grade and used without further purification.

3.2.2. Synthesis procedure & Parametric studies

One-step HEUR synthesis

The one-step HEUR synthesis was performed in bulk from the reaction of PEG, H12MDI and 1-octanol. It is worth noting that due to its hydrophilic nature, PEG may contain a significant amount of water, which can lead to the hydrolysis of diisocyanate towards urea formation instead of the desired urethane reaction.^{3,38} Thus, it is crucial to pretreat and dry PEG before proceeding with the polymerization reaction. Initially, 50g of PEG flakes were melted in the preheated reactor at 110°C, followed by a vacuum treatment step at 110°C and a vacuum pressure range of 1-5 mbar with constant magnetic mixing. In this study, the PEG moisture concentration was controlled at approximately 500 ppm prior to the reaction using the coulometric Karl-Fischer titration method. The pretreatment steps for the PEG were the same for both one and two-step synthesis methods. In all experiments, the reaction temperature was 80 °C, the reaction time was 45 min, and the catalyst concentration was set to 0.035% based on the total mass of the reactive mixture. The HMDI/PEG ratio was varied from 0.5 to 3, while the Oct/PEG ratio was 1. The progress of the reaction was monitored through sampling and offline GPC analysis, specifically measuring the molecular weight development of the prepolymer/HEUR over time. Indicative results are presented in Figure S3.1 of the Supporting Information. After completion of the polymerization, the entire polymer content of the reactor was diluted with water in 20% w/w solutions by adding water to the reactor, without carrying out prior purification steps in the polymer melt. The water-based HEUR formulations were obtained by stirring the mixture overnight, which resembles an industrial practice for the formulation of a thickener product.

Two-step HEUR synthesis

Two case studies were selected for investigation based on the HMDI/PEG ratios used for the pre-polymerization step and the range of obtainable prepolymer molecular weights. The HMDI/PEG ratios tested were 1.2 and 1.5, while the amount of octanol used for prepolymer end-capping was Oct/PEG=1 and 2. To study the importance of

Chapter 3

the pre-polymerization step for the HEUR molecular weight, different injection times of octanol, 2, 4 and 10 min, were used. These injection times were chosen considering the occurrence of the Weissenberg effect³, which occurs at approximately 4 min, while 2 and 10 min represent time windows before and after this effect. The Weissenberg effect is a phenomenon that occurs when a spinning rod is submerged into a solution of viscoelastic liquid or viscous polymer melt, and instead of being thrown outward, the solution is drawn towards the rod and crawls on it.⁴⁹ The Weissenberg effect is also related to the mixing limitations of the polymerization mixture, which becomes highly viscous when high molecular weights are reached.^{3,50} The total reaction time, including the pre-polymerization and end-capping step, was 45 min for all cases. Considering that the molecular weight development of the prepolymers is complete at 45 min reaction time, the latter is considered sufficient to carry out the end-capping step. Figure 3.1 shows a schematic representation of the one vs two-step synthetic procedure for the HEUR synthesis.

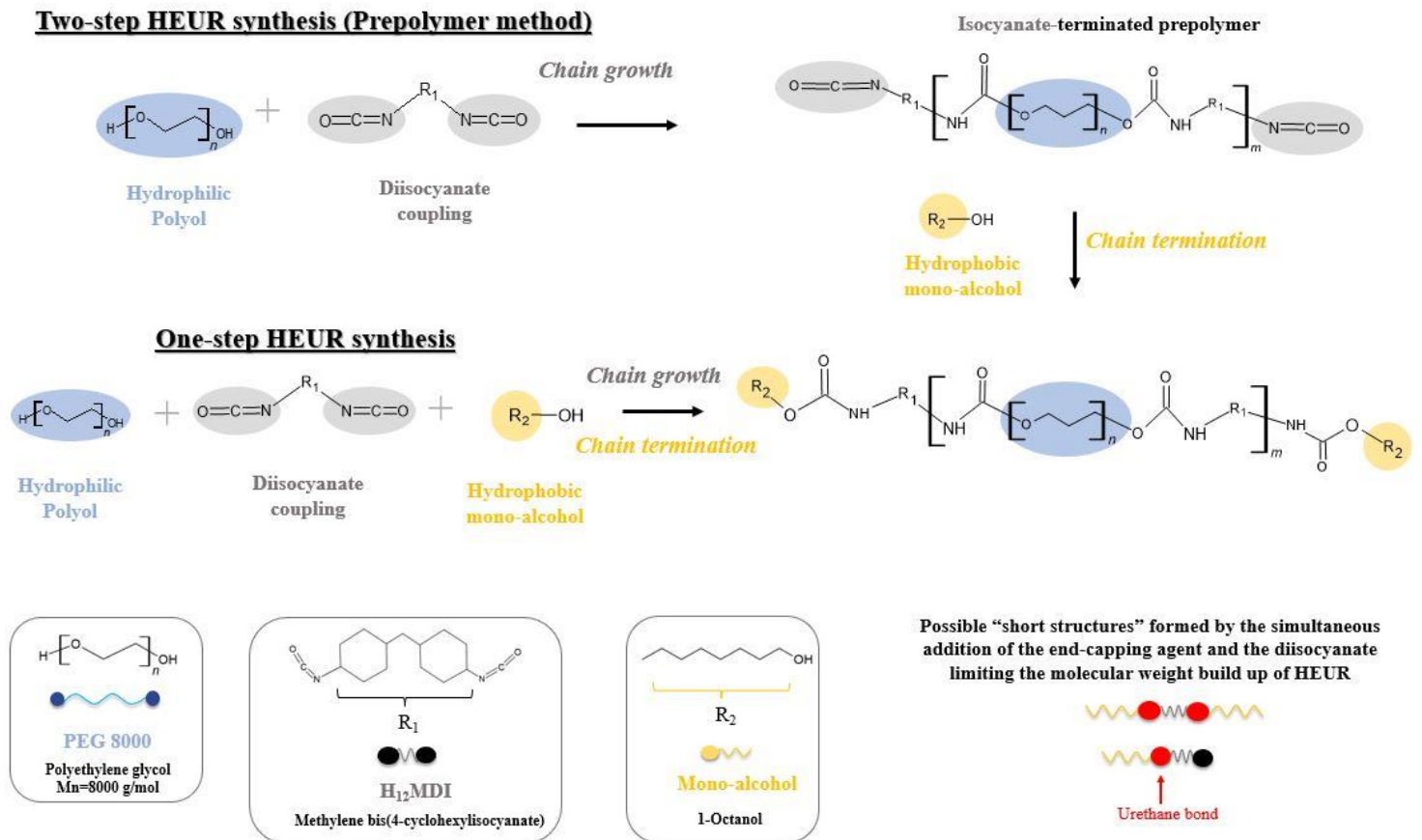


Figure 3.1. One vs two-step synthetic procedure for the HEUR synthesis. The Figure is redrafted from conference presentation⁵¹ with permission of the authors.

3.2.3. Analytical Methods

Gel Permeation Chromatography (GPC): The weight-average molecular weight (M_w) and the number-average molecular weight (M_n), were determined by GPC from Shimadzu, using four Styragel columns from Waters. The polydispersity index, PDI, was calculated as: $PDI = M_w/M_n$. Chloroform was the mobile phase (1 ml/min) at 30 °C operating temperature. Polyethylene glycol/oxide (PEG/PEO) were used as calibration standards. The samples were collected based on the “in-situ” method³, in which the molten samples were directly dissolved in vials with pre-weighed dry chloroform.

Fourier Transform Infrared Spectroscopy (FTIR): The qualitative analysis of the obtained polymers was done by FTIR, which was performed using attenuated total reflectance-Fourier transform infrared spectroscopy (ATR-FTIR, Perkin Elmer, spectrum 100, USA). At least 16 scans for each sample were conducted in the span range of 4000–650 cm^{-1} . The samples were collected based on the “in situ” method³, in which the molten samples were directly dissolved in vials with pre-weighed dry chloroform. The liquid samples were placed in the analysis cell and the spectra were recorded after total spontaneous solvent evaporation.

Gas Chromatography (GC): GC chromatography was used to measure the free octanol present in the polymer mixture and to calculate the percentage of octanol reacted under various reaction conditions. All samples were analysed in a gas chromatography (SHIMADZU – GC 2014) coupled with FID and column DB-1 HT (30 m x 0.250 mm ID x 0.10 μm film thickness) was employed for determining octanol. The carrier gas was Helium (He) and split injection mode was used with a split ratio 80:1. The program used for sample analysis was the following: the oven was set at 40 °C for 4 min, after which the temperature increased at a rate of 10 °C/min up to 250 °C and remained stable for 15min. The injector temperature was held at 270 °C while the detector temperature was set at 300 °C. The sample injection volume was 1 μL . The samples were collected based on the “in situ” method³, in which the molten samples were directly dissolved in vials with methanol and diluted at 1/20 ratio % w/w.

Nuclear magnetic resonance spectroscopy (NMR): The NMR spectra of a series of compounds were taken in order to identify the prepolymer and end-capped HEUR

Chapter 3

structures which are considered to be present in the synthesis. All experiments were performed on a Bruker Avance DRX 500 MHz NMR (11.7 Tesla) spectrometer (Bruker Biospin, Rheinstetten, Germany) operating at NMR frequency of 500.13 MHz for ^1H NMR, equipped with a 5 mm multi nuclear broad band inverse detection probe. All the ^1H NMR (500 MHz) were recorded with chemical shifts (δ) in parts per million (ppm) and coupling constants (J) in hertz (Hz).

Samples were added into NMR tubes (5 mm Thin Wall Precision NMR Sample Tubes 8" L, Wilmad, Vineland, NJ, USA). The obtained spectra were Fourier transformed, and their phase and baseline were automatically corrected. Prior to Fourier transformation, an exponential weighting factor corresponding to a line broadening of 1 Hz was applied. The samples were collected based on the "in situ" method³, in which the molten samples were directly dissolved in vials with pre-weighed deuterated chloroform (CDCl_3).

Thermogravimetric Analysis (TGA): TGA was performed using a TGA-DSC 1 Star System (METTLER TOLEDO). Samples of ~ 10 mg were weighed in aluminum oxide pans and heated from 20 to 550 $^\circ\text{C}$ at a heating rate of 10 $^\circ\text{C}/\text{min}$ and a nitrogen gas flow of 60 mL/min.

Rheological measurements: The rheological properties of HEURs in aqueous solutions were measured on a HAAKE/MARS iQ Air rheometer. A plate - cone (C35 2.0 $^\circ$ /Ti), using a cone and plate geometry of 35 mm diameter, 2 $^\circ$ angle cone, made of (C35 2 $^\circ$ /Ti). The distance of the gap was 0.096 mm. Water-HEUR solutions were prepared by direct addition of water into the reactor after the end of polymerization resulting in 20% w/w aqueous solutions. It is important to note that the 20% w/w concentration refers to the dilution of the solid content (melt) of the reactor in water. This solid content includes the total polymer melt, HEUR, unreacted monomers, and any by-products that may be present since no purification steps were performed. This experimental protocol aligns with industrial practices, which do not involve purification steps. At this point, it is important to emphasize that any side reaction of the residual NCO groups with water during the water formulation step can result in small reduction in water content, slightly changing the % w/w of HEUR in the aqueous formulation. However, based on accurate calculations this deviation in solution concentration is

considered to be entirely negligible due to the large excess of water used. The solution was stirred overnight in order to become homogeneous and then the samples were left to rest during the next day. The water amount was selected based on industrial tests performed during the commercialization stage of a thickener product. A range of 17 – 20% dilution in water is normally applied and considered representative of the downstream processing behaviour of the final product. The zero-shear viscosity and the shear stress profiles were obtained for shear rate testing from 0.01 to 1000 s⁻¹. Dynamic viscoelastic properties of the solutions were measured in the oscillatory shear mode, in the frequency range of 0.05–100 Hz, with a constant strain value of 1% (in the LVER). All rheological measurements were performed at 23 °C.

3.3. RESULTS AND DISCUSSION

Before implementing the two-step HEUR synthesis, the one-step method was used to investigate the effect of reaction stoichiometry (HMDI/PEG molar ratio) on the molecular weight of HEURs and the prepolymer. The results of this initial study serve as a framework to evaluate the performance of the one-step HEUR synthesis in terms of the range of different molecular weight polymers possible, as well as their rheological performance in aqueous formulations, and to compare it with the two-step HEUR synthesis.

3.3.1. One-step HEUR and prepolymer synthesis – Effect of the reaction stoichiometry

In HEUR synthesis, the number average molecular weight and the molecular weight distribution of the polymer depend on the ratio of the isocyanate groups to the alcohol groups $r = [\text{NCO}]/[\text{OH}]$.^{42,43,31} The theoretical relationship between the polymer molecular weight and r ratio, based on the theory of step-growth polymerizations is shown in Figure 3.2.^{31,38,52,53} As shown in Figure 3.2a, an excess of diisocyanate over diol, or vice versa, would eventually produce a polyurethane prepolymer terminated with isocyanate groups or hydroxyl groups, respectively, which are incapable of further growth. The maximum molecular weight is theoretically obtained when the diisocyanate groups are in equimolar amounts to the hydroxyl groups. However, in the one-step HEUR synthesis, the simultaneous addition of the end-capping agent with the polyol and the diisocyanate can affect the molecular weight build-up of the polymer,

since polymerization and chain termination occur simultaneously and counteract each other based on the relative chemical reactivities of the polyol and the hydrophobe.

To investigate this aspect of the one-step process, we performed the synthesis of both prepolymer and HEUR for a range of HMDI/PEG ratios, the results of which are presented in Figure 3.2b. Similar to the theoretical case, Figure 3.2b shows that the prepolymer reaches its maximum obtainable molecular weight $M_n \approx 76,000$ g/mol and $PDI \approx 1.9$, as the HMDI/PEG ratio approaches unity, which confirms equal functionality between HMDI and PEG. This maximum molecular weight of the prepolymer should in fact determine the upper limit of the obtainable HEUR molecular weight. However, when the end-capping agent is added simultaneously with the diisocyanate and the polyol (one-step method), the maximum obtainable molecular weight of HEUR is limited to $M_n \approx 21,000$ g/mol and $PDI \approx 1.6$. Additionally, relatively more HMDI is now needed to obtain this maximum molecular weight (HMDI/PEG ratio of 1.5), reflecting the competition between PEG and octanol in the consumption of HMDI.

Although enough isocyanate is added (HMDI/PEG = 1.5 and Oct/PEG = 1) to both produce the maximum molecular weight and endcap the polymer backbone, a four-fold reduction in the maximum molecular weight of HEUR is observed in the presence of an end-capping agent. This could in part be explained by the higher reactivities and lower activation energies of the reaction of diisocyanates with short mono-alcohols compared to macrodiols.^{30,54-56} Therefore, when diisocyanate is present simultaneously with mono-alcohols and macrodiols under reactive conditions, the end-capping reaction is favored resulting in a lack of truly stoichiometric conditions for the polymerization. This phenomenon can also be linked to the formation of "short structures" of HMDI with Oct, as illustrated in Figure 3.1. In addition, the increase in the molecular weight of HEUR leads to an increase in the bulk viscosity during the polymerization. As a result, diffusional limitations leading to molecular mobility limitations reduce the reactivity of the reactant functional groups, which has a critical effect on the structure and molecular weight of the polymer product.⁵⁷⁻⁵⁹ However, in order to draw further conclusions on the kinetics of these competing reactions, a detailed analysis should be performed that includes all chemical pathways and species formed using a range of advanced analytical techniques to obtain information on the concentrations of the various reactive species and intermediates, which is beyond the scope of this work.

Chapter 3

Overall, the results presented so far indicate that in the one-step HEUR synthesis, the simultaneous addition of the end-capping agent with the polyol and the diisocyanate can substantially limit the molecular weight of the final polymer, due to the competition between chain growth and chain termination. If this competition is eliminated by using the two-step method, HEURS with M_n up to 71,000 g/mol should in theory be obtainable, while also consuming less HMDI and thereby having a more efficient and cost-effective polymerization process.

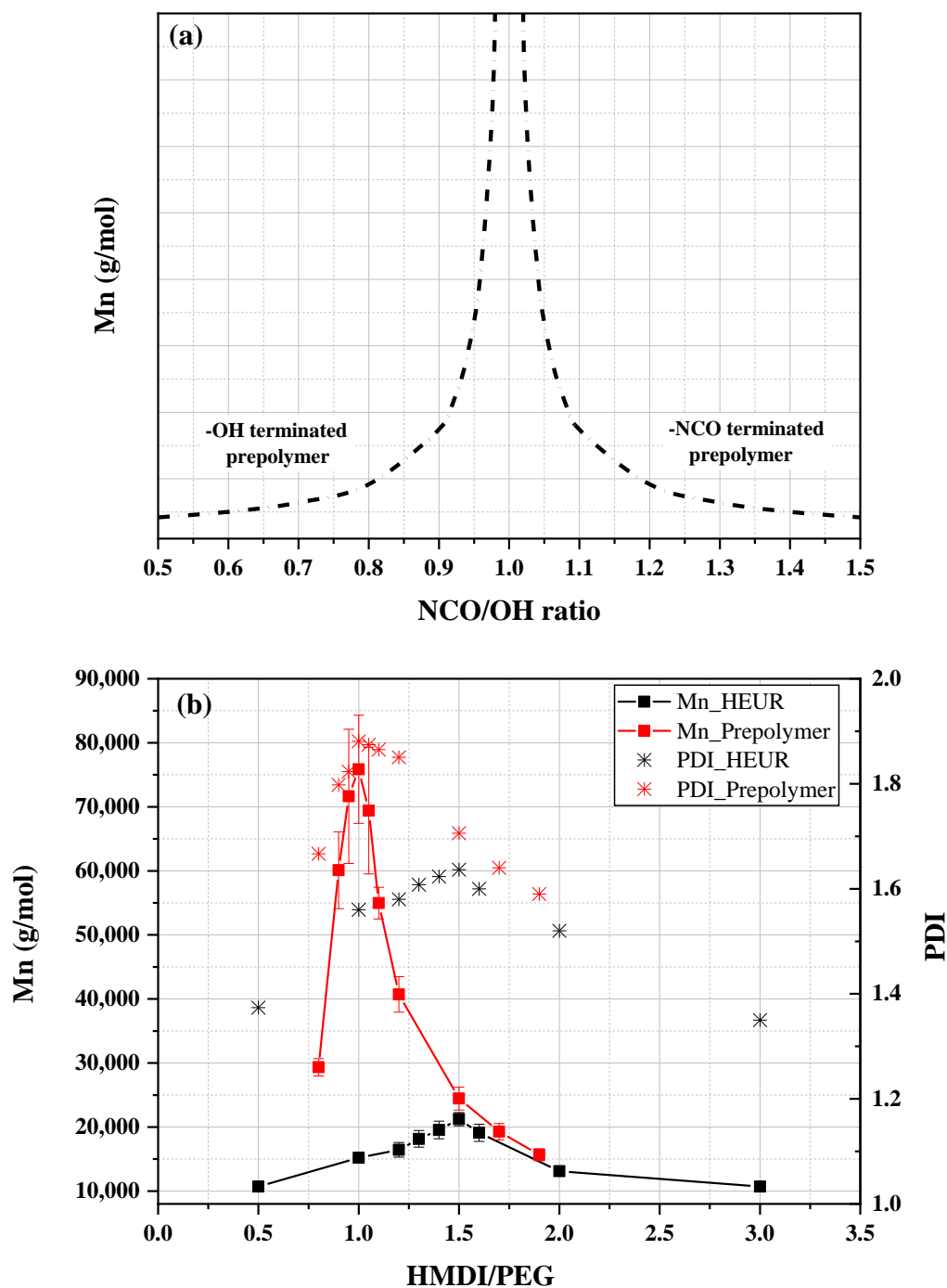


Figure 3.2. (a) Theoretical relationship between polyurethane prepolymer's molecular weight and NCO/OH ratio.³⁸ (b) M_n and PDI values of the produced prepolymers and HEURs obtained for various initial HMDI/PEG ratios and Oct/PEG=1. The lines have been added as a guide to the eye. Experiments were performed in at least three

repetitions and the error bars represent the standard deviation of the experimental data set.

3.3.2. Rheological behavior of HEURs produced via the one-step process

The rheological behavior of the different molecular weight polymers produced via the one-step method is assessed in Figure 3.3. When the HMDI/PEG ratio is varied from 1 to 1.5, an increase in the viscosity of the aqueous formulation is observed, which corresponds well with the increase in the M_w of HEUR¹, considering the same amount of reacted octanol at these ratios (Figure 3.3 and Figure S3.0.2 of the Supporting Information). As the molecular weight of the polymer increases, the degree of entanglement increases and the amount of free volume decreases, thereby reducing chain mobility and consequently increasing viscosity.^{1,60} Additionally, as the shear rate increases, these entanglements break and the viscosity begins to decrease (the shear thinning behaviour). Higher M_w polymers have a higher number of entanglements and are therefore more susceptible to shear forces, leading to the onset of shear thinning at lower shear rates, as seen in Figure 3.3.⁶⁰

Increasing the HMDI/PEG ratio beyond 1.5 up to 3 restricts polymer growth due to excess NCO groups which leads to lower molecular weights of HEUR and residual NCO groups after the reaction (Figure S3.0.4, Supporting Information). Despite having a lower molecular weight, these polymers exhibit increased viscosity, while the shear thinning behavior occurs at lower shear rates (Figure 3.3). In these cases, the viscosity is likely influenced by the higher residual free NCO groups, which can react with water during the formulation of HEUR in water (water addition into the reactor after the completion of the reaction), resulting in chain extended polyurethane-urea structures and a thicker aqueous solution.^{3,61-63} To explore the impact of chain extension on the increased viscosity of the HEUR aqueous solution, we conducted a focused analysis which is presented with more details in the Supporting Information. Our results showed that while the reaction of NCO-terminated prepolymers with water led to some degree of chain extension and a slightly higher molecular weight (Table S3.0.2 of the Supporting Information), these changes alone are insufficient to explain the substantial increase in viscosity of the aqueous solutions. Therefore, this viscosity increase observed in the HEUR aqueous solutions synthesized with HMDI/PEG ratios higher than 1.5, can be attributed to the presence of urea groups. Unlike urethane groups, urea

groups can form stronger hydrogen bonds since both hydrogens can simultaneously participate in hydrogen bonding interactions.^{3,61–63} Additionally, the presence of heteroatomic hydrogen bonding between urea and urethane groups in PUU dispersion further enhances the hydrogen bonding interactions,^{64,65} resulting in the formation of pseudo-cross-linked network structures.^{62,66,67} These structures impart physical properties similar to those of covalent cross-linked networks,^{62,66,67} resulting in thicker aqueous dispersions. This hypothesis was also confirmed with FTIR analysis, which showed the presence of free NCO residual in the analysed samples before the water addition (Figure S3.0.4 of the Supporting Information). Additionally, ¹H NMR analysis strengthened the hypothesis of the formation of urea moieties after the water addition due to the presence of a new characteristic peak at a chemical shift around 5 ppm (Figure S3.0.5 of the Supporting Information). To further support our findings, we conducted a steady shear viscosity testing on both an aqueous solution of HEUR of $M_n \approx 21,000$ g/mol containing both urethane-urea bonds (hexylamine used as end-capper) and a HEUR solution of the same molecular weight containing only urethane bonds (hexanol used as end-capper). Our results showed that the HEUR solution containing urethane-urea bonds displayed higher viscosities than the HEUR solution containing only urethane bonds. Furthermore, the onset of shear thinning occurred at lower shear rates, indicating a greater number of entanglements in the PUU dispersion. These findings are in agreement with the notion that urea groups in PUU dispersions exhibit stronger hydrogen bonding interactions, resulting in the formation of pseudo-cross-linked network structures that contribute to thicker aqueous HEUR solutions. (Figure S3.0.3 of the Supporting Information).

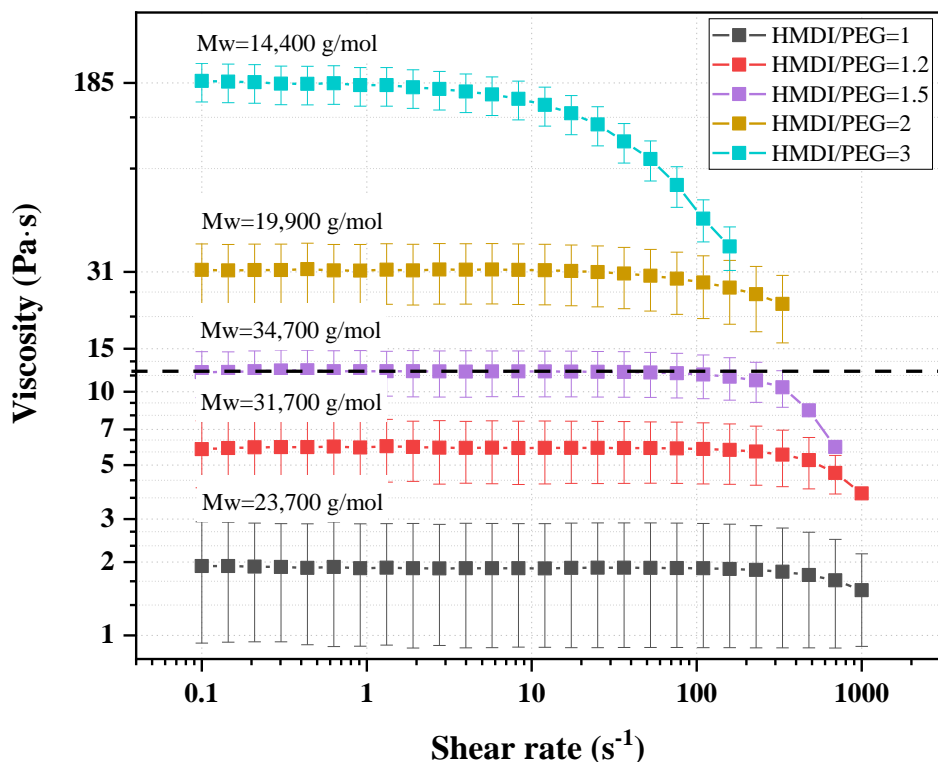


Figure 3.3. Steady shear viscosity testing of HEUR products from the one-step synthesis at different reaction stoichiometries (HMDI/PEG ratio), diluted in water (20%) and measured at 23 °C. The M_w values are also indicated in the graph.

It is important to emphasize that modified urea additives, when used in binders, show pronounced pseudoplastic properties, providing a very large viscosity increase at low shear rates while the thinning effect starts at lower shear rates compared to polyurethane additives.^{3,68} Therefore, special attention should be paid to the reaction conditions leading to urea formation, since its presence in the HEUR-water-binder formulation significantly affects the rheological performance of the formulation.

It is also noted that the viscosity of the HEUR product at 20% concentration in water is an important property for paint manufacturers since it determines its transportability through pumping lines. Viscosities higher than ≈ 10 -15 Pa·s, corresponding to HMDI/PEG ratios higher than 1.5, as shown in Figure 3.3, are quite high in this regard and are better avoided. Overall, our experimental results confirm that in the one-step process, a delicate balance between HEUR molecular weight and NCO content is

necessary to achieve optimal rheological behaviour in water formulations, which is better achieved at low NCO contents and high HEUR molecular weights.

3.3.3. Two-step HEUR synthesis: Prepolymer molecular weight effects and end-capping efficiency

The objectives of this study were to prepare HEURs using the two-step prepolymer method considering the influence of each step (pre-polymerization and end-capping) on the final HEUR properties. Two case studies were selected (described in Sections 3.3.1 and 3.3.2) for implementation. In the first, the pre-polymerization step was performed with HMDI/PEG = 1.2 and the second with HMDI/PEG=1.5. The key idea for the first case study was to synthesize a range of HEUR molecular weights by tailoring the addition time point of the end-capping agent, and to investigate how the molecular weight of the prepolymers at the time of end-capping agent injection and the amount of end-capping agent affect the resulting HEUR properties. The second case study aimed to investigate whether the polymerization process (one- or two-step process) could lead to different structural properties of HEUR when the same molecular weight is obtained by the two processes.

3.3.3.1. Effect of injection time of octanol on the degree of polymerization and molecular weight

To investigate the potential of obtaining HEURs with molecular weights higher than the one-step process ($M_n \approx 21,000$ g/mol and $PDI \approx 1.6$), the two-step process was applied, in which the prepolymer was first synthesized (at HMDI/PEG=1.2), and octanol was injected at different pre-polymerization times: 2, 4 and 10 min (The variable “**tinj**” is used to symbolize the injection time of octanol which is equal to the pre-polymerization time). Two different amounts of octanol were used Oct/ PEG = 1 and 2 for each injection time. Figure 3.4 shows the number average molecular weight (M_n) of the prepolymer and HEUR for each injection time. For comparison, the maximum molecular weight of the prepolymer at HMDI/PEG = 1.2 (i.e. when no end-capping is applied) is also given in the same figure. Additionally, Figure 3.5 shows the variation in the number-average degree of polymerization (DP_n) and PDI values for the HEURs obtained with the one (t=0) and two-step (2,4,10 min) method for HMDI/PEG=1.2 and Oct/PEG=1.

Chapter 3

Figure 3.4 shows that the synthesis of the HEUR using the two-step process (prepolymer method) allows for higher molecular weights than the one-step method (HMDI/PEG ratio=1.2). Importantly, with injection times greater than 2 min, the HEUR molecular weights and PDI values obtained are already higher than the global maximum of the one-step process $M_n \approx 21,000$ g/mol, $PDI \approx 1.6$, $DP_n \approx 3$, which was obtained at HMDI/PEG ratio=1.5 (Figure 3.2b).

From this, it can be concluded that the two-step process enables tailoring the desired molecular weight and polydispersity index simply by controlling the addition timepoint of the end-capping agent, hence the molecular weight of the prepolymer. At the same time, the amount of toxic HMDI used can be reduced significantly. Greater flexibility in obtaining a broader range of molecular weights together with tailoring the structure of the hydrophobic groups, give prospects for obtaining a range of rheological profiles based on the application properties required, due to the diverse possibilities of synthesizable structures.

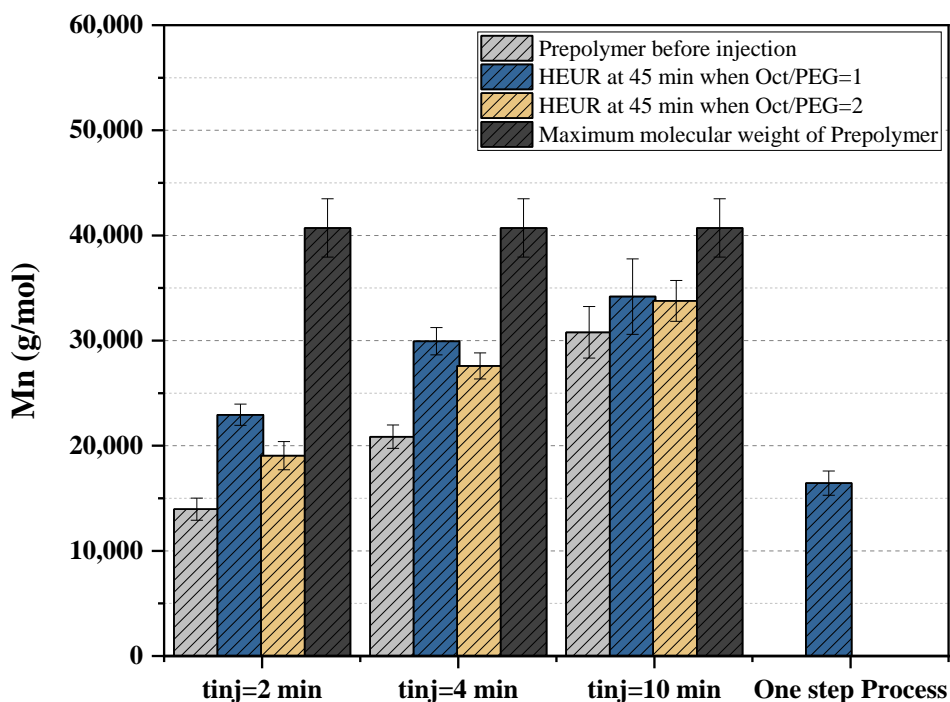


Figure 3.4. Two-step versus one-step HEUR synthesis (HMDI/PEG=1.2): Number-average molecular weight of the prepolymer before octanol injection, the HEUR at 45 min when Oct/PEG =1 and 2, the maximum molecular weight of the prepolymer and the HEUR synthesized with the one-step process at the same HMDI/PEG ratio. The variable “ t_{inj} ” is used to symbolize the injection time of octanol which is equal to the pre-polymerization time. The results are grouped based on the process used for the HEUR synthesis (one vs two step) and selected injection times (two-step process).

In particular, Figure 3.4 shows that as the pre-polymerization time (injection time) increased, the molecular weight of the prepolymer increased and approached its maximum experimental value $M_n \approx 41,000$ g/mol, $PDI \approx 1.9$, $DP_n \approx 5$. Specifically, at 2, 4 and 10 min the prepolymer had already reached 34%, 51%, and 76% of its maximum molecular weight.

Furthermore, the effect of the end-capping agent addition on the molecular weight of HEUR was more pronounced at short pre-polymerization times, while relatively lower molecular weights were obtained when a higher amount of chain stopper was added at short pre-polymerization times (Figure 3.4). Specifically, when injecting the octanol (Oct/PEG=1) at 2, 4 and 10 min allowed HEURs to obtain 56%, 74% and 84% of their maximum molecular weight, while for higher amount of octanol injections (Oct/PEG=2) these percentages were 47%, 68% and 83%. The number average molecular and PDI values of all polymers synthesized using the two-step process is shown in Table S1 of the Supporting Information. A direct comparison of the degree of polymerization and PDI values between the one and two-step HEUR synthesis (Figure 3.5) shows that the prepolymer method allows for higher degrees of polymerization and PDI values. As expected, the degree of polymerization and PDI values increase as a function of the octanol injection time. However, when injecting octanol after 4 min, the increase is less pronounced. This observation aligns well with the visually observed mixing limitations caused by the viscosity increase of the bulk (image insert in Figure 3.5), which becomes a gel and keeps rotating, violently hitting the reactor walls. a phenomenon known as the Weissenberg effect. The point of initiation of the Weissenberg effect is around $\approx 21,000$ g/mol, $PDI=1.64$ which corresponds to a pre-polymerization time of 4 min in this HMDI/PEG ratio.

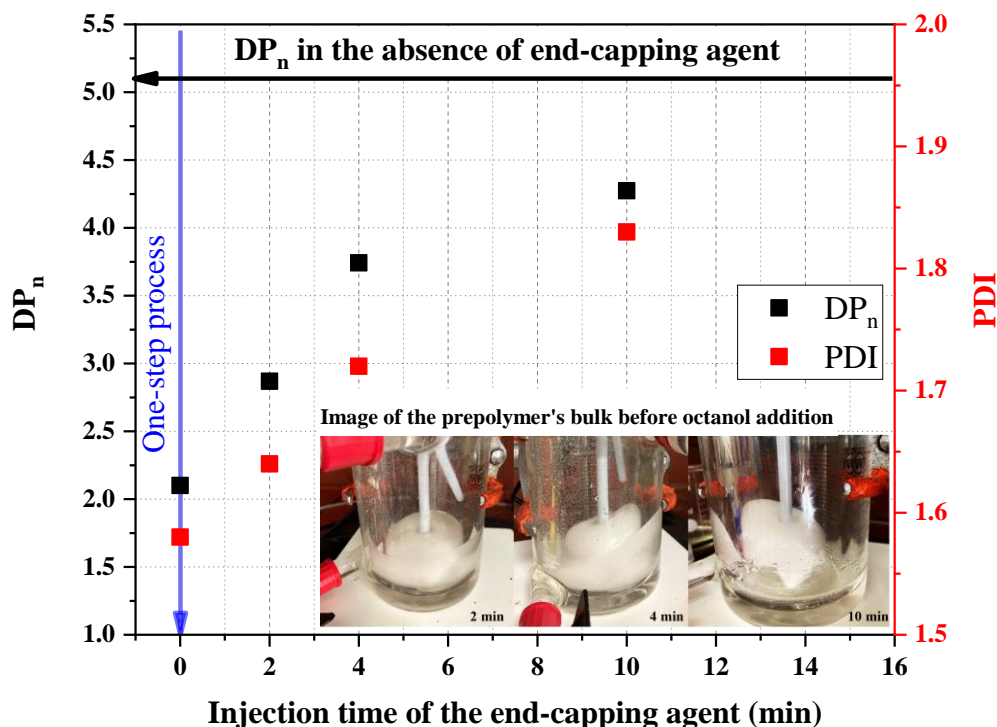


Figure 3.5. DP_n and PDI values for the HEURs obtained with the one ($t=0$) and two-step (2,4,10 min) method for HMDI/PEG=1.2 and Oct/PEG=1. The DP_n in the absence of the end-capping agent is also marked for comparison. The insert images show the prepolymer bulk appearance before octanol addition at 2, 4 and 10 min

3.3.3.2. End-capping efficiency and rheological behavior of HEURs synthesized via the two-step process

As mentioned previously, the two-step HEUR synthesis gave polymers with significantly higher molecular weights than the one-step method. Such high molecular weight polymers, while desirable in several applications, can be challenging to efficiently and homogeneously end-cap due to the mixing and processing limitations imposed by the bulk mixture viscosity increase and the occurrence of the Weissenberg effect (Figure 3.5). In turn, inefficient end-capping of the HEURs may also affect their rheological performance in aqueous formulations.

To investigate the end-capping efficiency in the two-step process, the experiment at HMDI/PEG=1.2 and octanol injection time=10min was repeated multiple times to

perform the experimental campaign statistics. The octanol content was also measured at different locations in the reactor to assess possible inhomogeneities imposed by the mixing limitations of the bulk mixture. The detailed results of this study are reported in the Supporting Information.

The results showed that it is possible to obtain good repeatability in terms of number and weight average molecular weight, but a high degree of spatial inhomogeneity of % octanol reacted is observed for each experiment performed (Figure S3.6 and Figure S3.7 of the Supporting Information). Very low values of octanol consumption indicate a high concentration of NCO-terminated prepolymer compared to regions with higher values of octanol consumption. This spatial variation indicates a corresponding difference in the NCO concentration within the bulk present in all experiments, which can be correlated with experimental observations after the HEUR was formulated with the addition of water into the reactor (Figure 3.6). Different spots of the reactor contained a transparent gel that differed in terms of quantity for each experiment. This is consistent with the findings of Braatz (1993)⁶⁹ who suggests that, when a polyurethane prepolymer is put into water, it initiates chain extension on contact with water, and after some time it starts to form a semisolid hydrogel matrix.^{34,69,70} The strength and shape of the hydrogel mainly depends on the ratio of water to prepolymer, which decreases as the amount of water increases.^{34,70}

This gelation phenomenon seems to seriously impact the rheological behavior of the aqueous solutions of HEUR. Figure 3.6 shows the corresponding steady shear rheology of the aqueous solutions of six HEURs synthesized by the two-step method (average with error bars shown) and three HEURs prepared using the one-step method. Higher standard deviations are obtained when synthesizing high molecular weight HEURs with the two-step method, despite the good repeatability obtained with respect to molecular weight. The latter can be attributed to the batch-to-batch variation of the NCO-terminated prepolymer moiety, which forms hydrogels in water, thickening it to a different extent for each experiment.

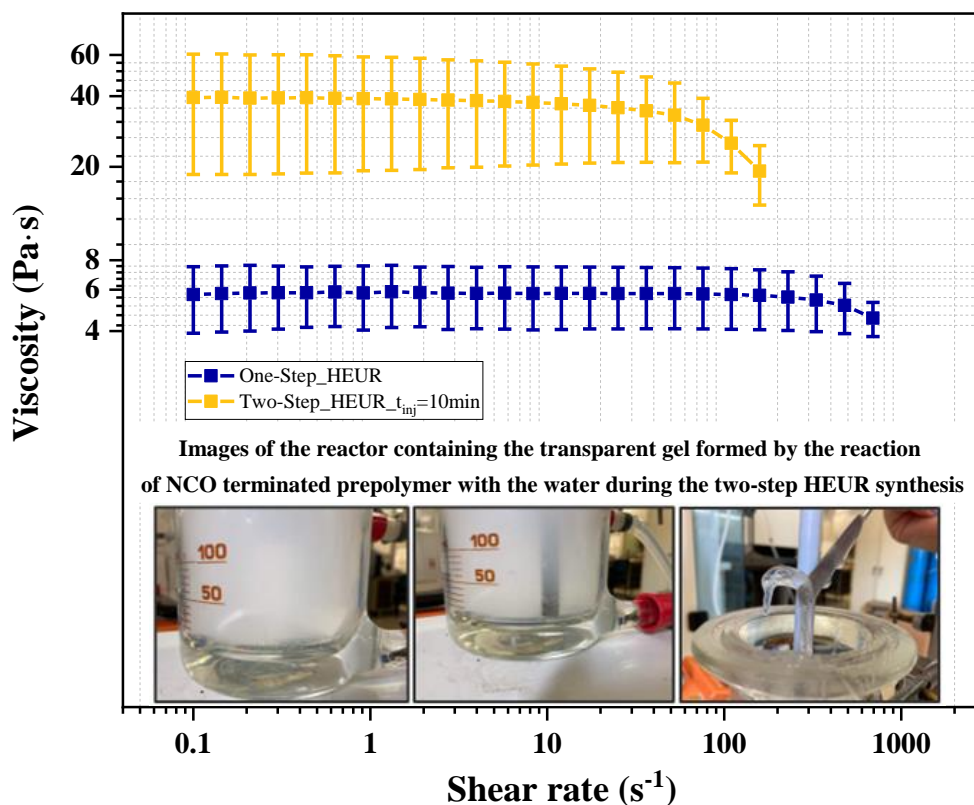


Figure 3.6. Steady shear viscosity testing of HEUR products from the one and two step process at HMDI/PEG=1.2 and injection time=10 min, diluted in water (20%) and measured at 23 °C. Experiments for the one step HEUR synthesis were performed in three repetitions and for the two-step HEUR synthesis at least six repetitions. The error bars represent the standard deviation of the experimental data set. The insert images show the reactor containing a transparent gel formed after the two-step HEUR synthesis with the addition of water.

These results suggest that the homogeneous end-capping of high molecular weight ($M_n \approx 31,000$ g/mol, $PDI \approx 1.8$) produced using the two-step process is challenging when overhead mixers are used, due to mass transfer limitations associated with the Weissenberg effect, leading to inhomogeneous distribution of the octanol in the reactor. However, in view of homogeneously end-capping high prepolymer molecular weights, alternative and more efficient mixing technologies⁷¹, such as extruders should be used to overcome the mass transfer limitations imposed by the increase in bulk viscosity in

batch mode. Intensified mixing will allow the end-capping of a wider range of prepolymers molecular weight up to $M_n \approx 76,000$ g/mol, $PDI \approx 1.9$ and $DP_n \approx 10$, depending on the applied mixing efficiency.

3.3.3.3. Structure and rheological behavior of polymers obtained via the one and two step method at the same molecular weight

In order to compare the structure of the HEURs attained using the one- and two-step methods at the same molecular weight, an experiment was performed at an HMDI/PEG ratio of 1.5, in which it was found that the maximum molecular weight of the prepolymer is approximately equal to the maximum molecular weight of the HEUR using the one-step process (Figure 3.2b). In this way, it is investigated whether a two-step approach would offer more control over polymer architecture through the prepolymer method, thereby achieving better rheological properties. Having already demonstrated the effect of injection time on HEUR molecular weight, only a 10-minute injection time is tested, and the results are shown in Figure 3.7.

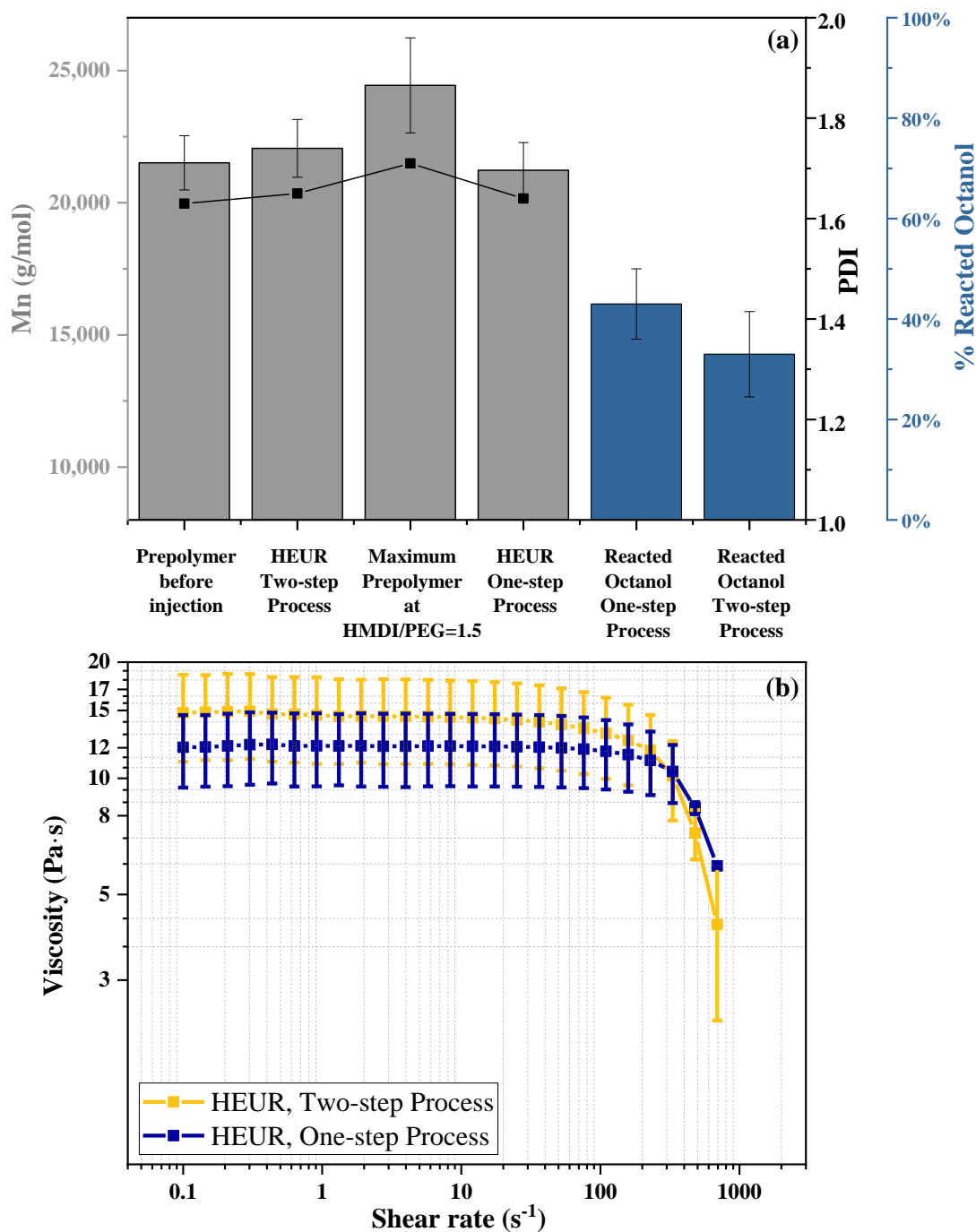


Figure 3.7. Two-step versus one-step HEUR synthesis (HMDI/PEG=1.5): (a) Number-average molecular weight of the prepolymer before octanol injection, the HEUR at 45min (one and two-step process) and the maximum molecular weight of the prepolymer at the same HMDI/PEG ratio. % Reacted Octanol and PDI values are also showed for the one and two-step HEUR synthesis. (b) Steady shear rheology of the

Chapter 3

aqueous solutions of HEURs synthesized with the one and two-step process. Water based formulations of HEUR were performed with the addition of water into the reactor.

As shown in Figure 3.7a, the molecular weight of the prepolymer before the octanol injection is already ~90% of the maximum molecular weight reached at HMDI/PEG = 1.5, while at the end of the polymerization the molecular weight of HEUR remains unchanged. The resulting values for the % reacted octanol were slightly lower than the average values observed for the one-step synthesis, because less NCO content is available at 10 min when the prepolymer is already formed.

Additionally, the steady shear rheology of the aqueous solutions of HEUR synthesized with the one and two-step process was also compared, and the results are depicted in Figure 3.7b. This figure clearly shows that the steady shear rheology of the two HEUR products is very similar, indicating that HEURs of the same molecular weight obtained by the one and two-step process have similar structure and chemical composition. In addition, it shows that despite the existing mass transfer limitations, prepolymers of $M_n \approx 21,000$ g/mol, $PDI \approx 1.6$ can be efficiently end-capped, and provide a good rheological performance, very similar to the same product of the one-step process. Furthermore, in order to characterize the viscoelastic behavior of the HEUR samples, oscillatory measurements were conducted. For both samples the storage modulus (G') and loss modulus (G'') both increased with frequency in the tested region, as shown in Figure S3.0.8 of the Supporting Information. The G'' is associated with the viscous behavior of the polymer, while G' expresses the elastic response.^{4,72,73} The ratio of the two, $\tan(\delta)$, indicates the ratio of viscous or energy dissipation to elastic or storage behavior.^{4,72,73} It is worth noting that viscoelastic measurements are strongly correlated with the microstructure and the strength of the thickener's self-assembly phenomena in a dispersion.^{72,74} The oscillatory measurements presented in Figure S8 of the Supporting Information show a remarkable degree of similarity between the two aqueous HEUR dispersions, implying that the self-assembly phenomena of HEUR in water-based formulations are analogous. These observations suggest that the structural characteristics of the HEUR products obtained via the one-step and two-step processes with the same molecular weight are nearly identical.

Chapter 3

Further FTIR tests were performed to determine the chemical composition of the produced prepolymer and HEURs and to compare the structure-property relationship with the synthesis route used. Figure 3.8 shows the FTIR spectra of the HEUR synthesized with the one-step process, the prepolymer at 10 min before the injection of octanol and the HEUR synthesized with the two-step process after the octanol addition. The peak at 530 cm^{-1} is attributed to the chloroform used for the in-situ sampling. Any differences in this range in the spectra of all samples are attributed to residual chloroform during the scan. For all analyzed samples, the characteristic absorption bands of polyethylene glycol appear in the range $840\text{-}1466\text{ cm}^{-1}$,^{75,76} the characteristic -CH stretching band appears in the range $2700\text{-}3000\text{ cm}^{-1}$, and the characteristic absorption peak of the isocyanate group ($\text{N}=\text{C}=\text{O}$) appears at 2265 cm^{-1} .^{3,76,77} Additionally, for all samples, a peak appears at 1715 cm^{-1} , which can be assigned to the disordered hydrogen-bonded carbonyl ($\text{C}=\text{O}$) groups in the urethane molecule.^{3,63,78-80} The peak at 1530 cm^{-1} represents the bending vibrations of the NH in the urethane groups while the peak at 1640 cm^{-1} , is attributed to the traces of ordered hydrogen-bonded urea carbonyl ($\text{C}=\text{O}$).^{3,76,77,79,81}

Based on the spectra obtained, no differences are observed between the prepolymer and the HEUR (two-step process) except for the intensity of the $\text{N}=\text{C}=\text{O}$ peak at 2270 cm^{-1} . The intensity of this peak is lower for the HEUR (two-step process) due to the injected octanol, which endcaps the free isocyanate molecules or the NCO-terminated prepolymer chain. In the same figure, HEUR synthesized by the one-step method is also plotted. No structural differences are observed between the HEUR synthesized with the one and two-step process. This result has also been confirmed by a TGA analysis, which is presented in Figure S3.0.9 in the Supporting Information. The TGA curves for HEUR synthesized using the one- and two-step process method show remarkable similarity, suggesting similar thermal degradation behavior for both samples. The overlapping weight loss profiles and comparable onset temperatures indicate comparable thermal stability and decomposition properties between the two samples. This similarity in thermal behavior further supports the similar structures obtained by the one- and two step processes when $\text{HMDI/PEG}=1.5$, $\text{Oct/PEG}=1$ and $t_{\text{inj}}=10\text{ min}$.

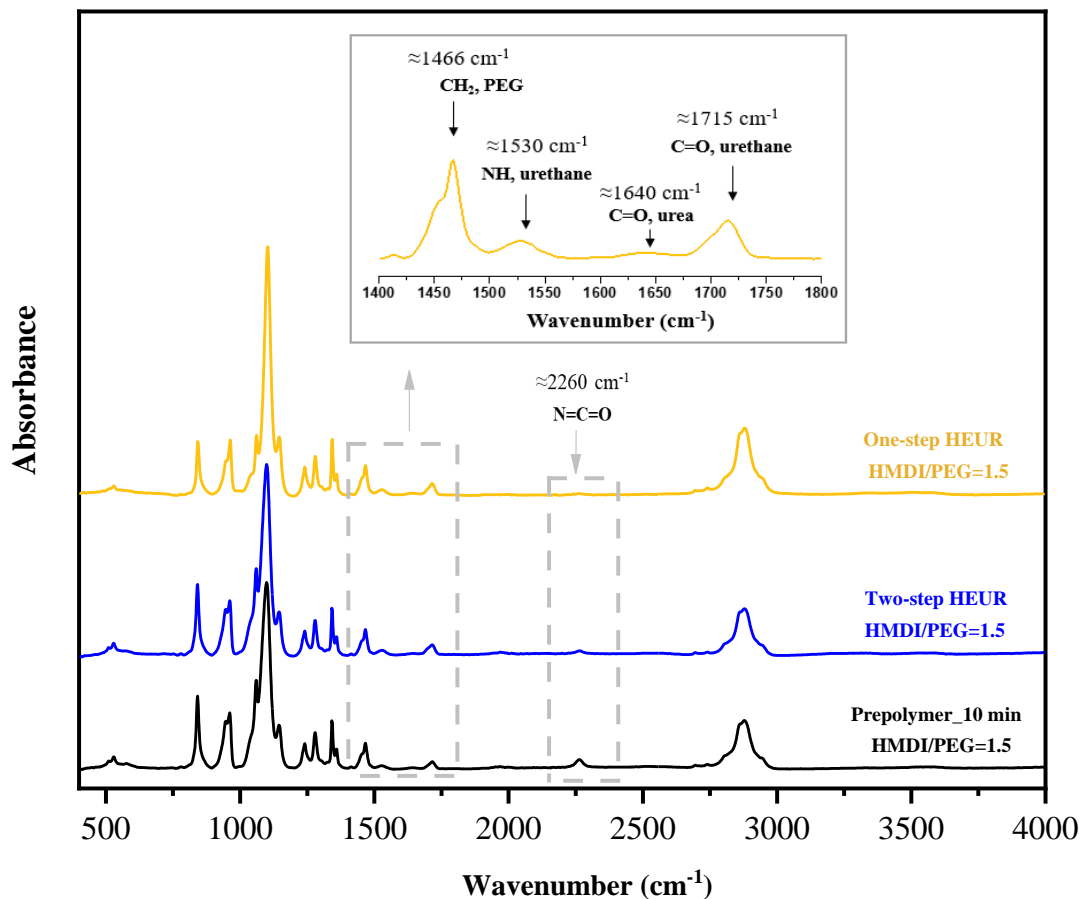


Figure 3.8. FTIR spectra of the prepolymer at 10 min and HEUR, synthesized with one and two-step process.

¹H NMR analysis was also used to confirm the HEUR structures synthesized by the one and two-step methodologies, specifically using HMDI/PEG=1.5 (Figure 3.9). The results of the ¹H NMR analysis demonstrate there are no differences in the chemical shifts of the signals indicating that both methods yield the same structures. Furthermore, the integration of the peaks in the ¹H NMR spectra follows an identical pattern for both synthesis routes. The ¹H NMR spectra of the HEURs in CDCl₃ (Figure 3.9) allow to clearly identify the region where the urethane linkages appear in the structures (3.6 - 4.9 ppm), while it can be clearly seen that new peaks are detected in the spectrum of the prepolymer after the octanol addition. These new peaks at 4.77 ppm, 4.47 ppm and 4.00 ppm correspond to the end-capping of the NCO-terminated prepolymer by octanol.

Chapter 3

The ^1H NMR spectrum of the HMDI end-capped with octanol is also presented to confirm the presence of the end-capping peaks in the HEUR.

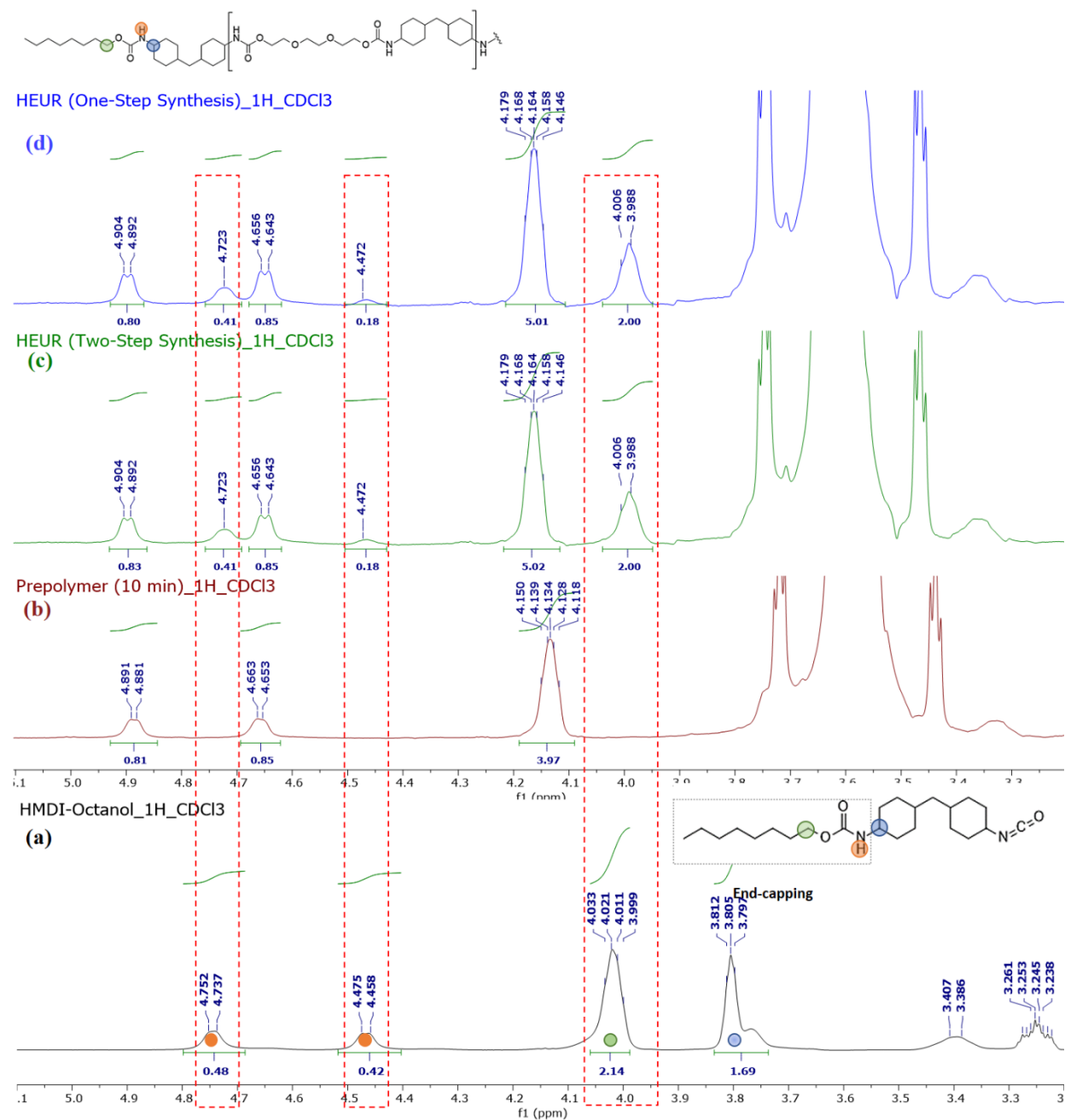


Figure 3.9. ^1H NMR (CDCl_3) spectra of (a) HMDI-Octanol (b) Prepolymer (10min) - HMDI/PEG=1.5 and (c) HEUR (two-step synthesis) after the addition of octanol (Oct/PEG=1) at 10 min and (d) HEUR (one-step synthesis), HMDI/PEG=1.5, Oct/PEG=1

Chapter 3

The findings of FTIR, TGA, ^1H NMR analysis provide strong evidence that the chemical composition and structure of the HEURs produced with the one and two-step process are identical when targeting the same molecular weight, regardless of the synthetic route used. These observations, taken together with the comparable molecular weights and similar rheological behavior of the aqueous solutions of HEURs (one and two-step method), confirm that the synthetic route does not affect the structural properties of the polymer when producing HEURs with the same molecular weights.

Table 3.1 has been included below to facilitate a clear comparison of the results obtained using the one-step and two-step methods to synthesize HEURs in the same stoichiometry. This table provides a comprehensive overview of the most important parameters, including the molar ratio between the reactants, the M_n , the PDI, and other relevant factors.

Chapter 3

Table 3.1. Comparison of HEURs obtained with the one-step and two-step methods.

Process	HMDI/ PEG	Oct/ PEG	Injection time of octanol	Mn of pre- polymer before injection of octanol min (g/mol)	PDI of pre- polymer before injection of octanol min (g/mol)	Maximum Mn/PDI of prepolymer at the selected HMDI/PEG ratio	HEUR Mn (g/mol)	PDI
One-Step	1.2	1	0 min	-	-		16,400	1.6
Two- Step	1.2	1	2 min	14,000	1.5		22,900	1.6
Two- Step	1.2	1	4 min	20,900	1.6	40,700/1.9	29,900	1.7
Two- Step	1.2	1	10 min	30,800	1.8		34,200	1.8
One-Step	1.5	1	0 min	-	-		21,200	1.7
Two- Step	1.5	1	10 min	21,500	1.6	24,400/1.7	22,100	1.7

3.4. Conclusions

We investigated for the first time the benefits and limitations of utilizing either a one-step (simultaneous chain growth and end-capping) versus a two-step (chain growth followed by end-capping) polymerization process targeting hydrophobically modified ethoxylated urethanes (HEURs) using polyethylene glycol 8000g/mol, HMDI and 1-octanol. To this end, we conducted a systematic investigation on the effect of reaction stoichiometry on both methods. The results revealed that the simultaneous addition of the end-capping agent (octanol) with the other reactants (one-step process) limits the maximum attainable molecular weight of HEUR to $M_n \approx 21,000$ g/mol, $PDI \approx 1.6$ and $DP_n \approx 3$, which is achieved at an excess of HMDI (HMDI/PEG=1.5 and Oct/PEG=1). Conversely, the two-step HEUR process enables more control over the final molecular weight simply by performing the pre-polymerization step with stoichiometric balance between HMDI and PEG and controlling the addition timepoint of the end-capping agent. In this way, the two-step method allows for a reduction of the amount of toxic HMDI used, as well as more control over the degree of polymerization and the resulting polymer molecular weight and polydispersity index of HEUR, surpassing the 21,000 g/mol threshold and reaching up to $M_n \approx 76,000$ g/mol, $PDI \approx 1.9$ and $DP_n \approx 10$. While such high molecular weight polymers are desirable, we find that their homogeneous and efficient end-capping becomes challenging with conventional mixing techniques due to mass transfer limitations imposed by the increase in the bulk viscosity of the reaction mixture. Such mass transfer limitations can possibly be overcome by use of intensified mixing process equipment, such as reactive extruders, whose unique geometry allows handling very viscous media in flow. Finally, we showed that when synthesizing HEURs with the same molecular weight, $M_n \approx 21,000$ g/mol, $PDI \approx 1.6$ using either the one-step or the two-step method, the chemical structure and rheological performance of the polymers in aqueous formulations is similar.

References

- (1) Quienne, B.; Pinaud, J.; Robin, J. J.; Caillol, S. From Architectures to Cutting-Edge Properties, the Blooming World of Hydrophobically Modified Ethoxylated Urethanes (HEURs). *Macromolecules* **2020**, *53* (16), 6754–6766. <https://doi.org/10.1021/acs.macromol.0c01353>.
- (2) Santos, F. A.; Bell, T. J.; Stevenson, A. R.; Christensen, D. J.; Pfau, M. R.; Nghiem, B. Q.; Kasprzak, C. R.; Smith, T. B.; Fernando, R. H. Syneresis and Rheology Mechanisms of a Latex-HEUR Associative Thickener System. *J. Coatings Technol. Res.* **2017**, *14* (1), 57–67. <https://doi.org/10.1007/s11998-016-9829-x>.
- (3) Bampouli, A.; Tzortzi, I.; Schutter, A. De; Xenou, K.; Michaud, G.; Stefanidis, G. D.; Gerven, T. Van. Insight Into Solventless Production of Hydrophobically Modified Ethoxylated Urethanes (HEURs): The Role of Moisture Concentration , Reaction Temperature , and Mixing Efficiency. *ACS Omega* **2022**, No. int. <https://doi.org/10.1021/acsomega.2c04530>.
- (4) Ginzburg, V. V.; Chatterjee, T.; Nakatani, A. I.; Van Dyk, A. K. Oscillatory and Steady Shear Rheology of Model Hydrophobically Modified Ethoxylated Urethane-Thickened Waterborne Paints. *Langmuir* **2018**, *34* (37), 10993–11002. <https://doi.org/10.1021/acs.langmuir.8b01711>.
- (5) Kästner, U. The Impact of Rheological Modifiers on Water-Borne Coatings. *Colloids Surfaces A Physicochem. Eng. Asp.* **2001**, *183–185*, 805–821. [https://doi.org/10.1016/S0927-7757\(01\)00507-6](https://doi.org/10.1016/S0927-7757(01)00507-6).
- (6) Xu, B.; Li, L.; Yekta, A.; Masoumi, Z.; Kanagalingam, S.; Winnik, M. A.; Zhang, K.; Macdonald, P. M.; Menchen, S. Synthesis, Characterization, and Rheological Behavior of Polyethylene Glycols End-Capped with Fluorocarbon Hydrophobes. *Langmuir* **1997**, *13* (9), 2447–2456. <https://doi.org/10.1021/la960799l>.

- (7) Elliott, P. T.; Xing, L. L.; Wetzel, W. H.; Glass, J. E. Influence of Terminal Hydrophobe Branching on the Aqueous Solution Behavior of Model Hydrophobically Modified Ethoxylated Urethane Associative Thickeners. *Macromolecules* **2003**, *36* (22), 8449–8460. <https://doi.org/10.1021/ma020166f>
- (8) Cathébras, N.; Collet, A.; Viguié, M.; Berret, J. F. Synthesis and Linear Viscoelasticity of Fluorinated Hydrophobically Modified Ethoxylated Urethanes (F-HEUR). *Macromolecules* **1998**, *31* (4), 1305–1311. <https://doi.org/10.1021/ma9709011>.
- (9) Myers, R. Frequency-Dependent Rheological Characterization of Viscoelastic Materials Using Magnetic Nanoparticle Probes, Oregon State University, 2020.
- (10) Wang, F.; Peng, J.; Dong, R.; Chang, X.; Ren, B.; Tong, Z. Highly Efficient Hydrophobically Modified Ethoxylated Urethanes (HEURs) End-Functionalized by Two-Tail Dendritic Hydrophobes: Synthesis, Solution Rheological Behavior and Thickening in Latex. *Colloids Surfaces A Physicochem. Eng. Asp.* **2016**, *502*, 114–120. <https://doi.org/10.1016/j.colsurfa.2016.05.004>.
- (11) Du, Z.; Wang, F.; Chang, X.; Peng, J.; Ren, B. Influence of Substituted Structure of Percec-Type Mini-Dendritic End Groups on Aggregation and Rheology of Hydrophobically Modified Ethoxylated Urethanes (HEURs) in Aqueous Solution. *Polymer (Guildf)*. **2018**, *135*, 131–141. <https://doi.org/10.1016/j.polymer.2017.12.022>.
- (12) Guan, T.; Du, Z.; Chang, X.; Zhao, D.; Yang, S.; Sun, N.; Ren, B. A Reactive Hydrophobically Modified Ethoxylated Urethane (HEUR) Associative Polymer Bearing Benzophenone Terminal Groups: Synthesis, Thickening and Photo-Initiating Reactivity. *Polymer (Guildf)*. **2019**, *178* (April), 121552. <https://doi.org/10.1016/j.polymer.2019.121552>.
- (13) Chang, X.; Du, Z.; Hu, F.; Cheng, Z.; Ren, B.; Fu, S.; Tong, Z. Ferrocene-Functionalized Hydrophobically Modified Ethoxylated Urethane: Redox-

- Responsive Controlled Self-Assembly and Rheological Behavior in Aqueous Solution. *Langmuir* **2016**, *32* (46), 12137–12145. <https://doi.org/10.1021/acs.langmuir.6b03508>.
- (14) Du, Z.; Ren, B.; Chang, X.; Dong, R.; Peng, J.; Tong, Z. Aggregation and Rheology of an Azobenzene-Functionalized Hydrophobically Modified Ethoxylated Urethane in Aqueous Solution. *Macromolecules* **2016**, *49* (13), 4978–4988. <https://doi.org/10.1021/acs.macromol.6b00633>.
- (15) Ginzburg, V. V.; Van Dyk, A. K.; Chatterjee, T.; Nakatani, A. I.; Wang, S.; Larson, R. G. Modeling the Adsorption of Rheology Modifiers onto Latex Particles Using Coarse-Grained Molecular Dynamics (CG-MD) and Self-Consistent Field Theory (SCFT). *Macromolecules* **2015**, *48* (21), 8045–8054. <https://doi.org/10.1021/acs.macromol.5b02080>.
- (16) Tripathi, A.; Tam, K. C.; McKinley, G. H. Rheology and Dynamics of Associative Polymers in Shear and Extension: Theory and Experiments. *Macromolecules* **2006**, *39* (5), 1981–1999. <https://doi.org/10.1021/ma051614x>.
- (17) Larson, R. G.; Van Dyk, A. K.; Chatterjee, T.; Ginzburg, V. V. Associative Thickeners for Waterborne Paints: Structure, Characterization, Rheology, and Modeling. *Prog. Polym. Sci.* **2022**, *129*, 101546. <https://doi.org/10.1016/j.progpolymsci.2022.101546>.
- (18) Lu, M.; Song, C.; Wan, B. Influence of Prepolymer Molecular Weight on the Rheology and Kinetics of HEUR-Thickened Latex Suspensions. *Prog. Org. Coatings* **2021**, *156* (July 2020), 106223. <https://doi.org/10.1016/j.porgcoat.2021.106223>.
- (19) Abdala, A. A.; Wu, W.; Olesen, K. R.; Jenkins, R. D.; Tonelli, A. E.; Khan, S. A. Solution Rheology of Hydrophobically Modified Associative Polymers: Effects of Backbone Composition and Hydrophobe Concentration. *J. Rheol. (N. Y. N. Y.)* **2004**, *48* (5), 979–994. <https://doi.org/10.1122/1.1773781>.

- (20) Jenkins, R. D.; Bassett, D. R.; Silebi, C. A.; El-Aasser, M. S. Synthesis and Characterization of Model Associative Polymers. *J. Appl. Polym. Sci.* **1995**, *58* (2), 209–230. <https://doi.org/10.1002/app.1995.070580202>.
- (21) Berndlmaier, R. Rheology Additives for Coatings. *Handb. Coat. Addit.* 363–403.
- (22) Wypych, G. *Handbook of Rheological Additives*, First Edit.; Elsevier, 2022; Vol. 1. <https://doi.org/10.1016/C2021-0-00266-2>.
- (23) Shun Xing Zheng. *Principles of Organic Coatings and Finishing*; Cambridge Scholars Publishing, 2019.
- (24) May, R.; Kaczmarek, J. P.; Glass, J. E. Influence of Molecular Weight Distributions on HEUR Aqueous Solution Rheology. *Macromolecules* **1996**, *29* (13), 4745–4753. <https://doi.org/10.1021/ma9507655>.
- (25) Barmar, M.; Barikani, M.; Kaffashi, B. The Effect of Molecular Weight on the Behaviour of Step-Growth Hydrophobically Modified Ethoxylated Urethane (S-G HEUR) End-Capped with Dodecyl Alcohol. *Iran. Polym. J. (English Ed.)* **2004**, *13* (3).
- (26) Cornille, A.; Auvergne, R.; Figovsky, O.; Boutevin, B.; Caillol, S. A Perspective Approach to Sustainable Routes for Non-Isocyanate Polyurethanes. *Eur. Polym. J.* **2017**, *87*, 535–552. <https://doi.org/10.1016/j.eurpolymj.2016.11.027>.
- (27) Quienne, B.; Pinaud, J.; Caillol, S. Synthesis of Hydrophobically Modified Ethoxylated Non-Isocyanate Urethanes (HENIURs) and Their Use as Rheology Additives. *Eur. Polym. J.* **2022**, *175* (June), 111384. <https://doi.org/10.1016/j.eurpolymj.2022.111384>.
- (28) Wołosz, D.; Fage, A. M.; Parzuchowski, P. G.; Świdorska, A.; Brüll, R. Reactive Extrusion Synthesis of Biobased Isocyanate-Free Hydrophobically Modified Ethoxylated Urethanes with Pendant Hydrophobic Groups. *ACS Sustain. Chem. Eng.* **2022**, *10* (35), 11627–11640. <https://doi.org/10.1021/acssuschemeng.2c03535>.

- (29) Wołosz, D.; Fage, A. M.; Parzuchowski, P. G.; Świdarska, A.; Brüll, R.; Elsner, P. Sustainable Associative Thickeners Based on Hydrophobically Modified Ethoxylated Poly(Hydroxy-Urethane)s End-Capped by Long Alkyl Chains. *Prog. Org. Coatings* **2023**, *179* (November 2022), 107514. <https://doi.org/10.1016/j.porgcoat.2023.107514>.
- (30) Król, P. Synthesis Methods, Chemical Structures and Phase Structures of Linear Polyurethanes. Properties and Applications of Linear Polyurethanes in Polyurethane Elastomers, Copolymers and Ionomers. *Prog. Mater. Sci.* **2007**, *52* (6), 915–1015. <https://doi.org/10.1016/j.pmatsci.2006.11.001>.
- (31) Odian, G. *Principles of Polymerization*, Fourth.; John Wiley & Sons, Inc, 2004. <https://doi.org/10.1002/047147875X>.
- (32) Vantomme, G.; Ter Huurne, G. M.; Kulkarni, C.; Ten Eikelder, H. M. M.; Markvoort, A. J.; Palmans, A. R. A.; Meijer, E. W. Tuning the Length of Cooperative Supramolecular Polymers under Thermodynamic Control. *J. Am. Chem. Soc.* **2019**, *141* (45), 18278–18285. <https://doi.org/10.1021/jacs.9b09443>.
- (33) Arnould, P.; Bosco, L.; Sanz, F.; Simon, F. N.; Fouquay, S.; Michaud, G.; Raynaud, J.; Monteil, V. Identifying Competitive Tin-or Metal-Free Catalyst Combinations to Tailor Polyurethane Prepolymer and Network Properties. *Polym. Chem.* **2020**, *11* (36), 5725–5734. <https://doi.org/10.1039/d0py00864h>.
- (34) Deng, C.; Cui, Y.; Zhao, T.; Tan, M.; Huang, H.; Guo, M. Mechanically Strong and Stretchable Polyurethane-Urea Supramolecular Hydrogel Using Water as an Additional in Situ Chain Extender. *RSC Adv.* **2014**, *4* (46), 24095–24102. <https://doi.org/10.1039/c4ra02597k>.
- (35) Ahn, T. O.; Choi, I. S.; Jeong, H. M.; Cho, K. Thermal and Mechanical Properties of Thermoplastic Polyurethane Elastomers from Different Polymerization Methods. *Polym. Int.* **1993**, *31* (4), 329–333. <https://doi.org/10.1002/pi.4990310404>.

- (36) Prisacariu, C.; Scortanu, E.; Agapie, B. New Insights into Polyurethane Elastomers Obtained by Changing the Polyaddition Procedures. *Proc. World Congr. Eng. 2011, WCE 2011* **2011**, 3, 2178–2183.
- (37) Jung, Y. S.; Lee, S.; Park, J.; Shin, E. J. One-Shot Synthesis of Thermoplastic Polyurethane Based on Bio-Polyol (Polytrimethylene Ether Glycol) and Characterization of Micro-Phase Separation. *Polymers (Basel)*. **2022**, 14 (20). <https://doi.org/10.3390/polym14204269>.
- (38) Szycher, M. *Szycher's Handbook of Polyurethanes*, 2nd ed.; CRC Press, 2013; Vol. 142.
- (39) Vlad, S. Influence of the Chain Extender Length and Diisocyanate Amount on the Thermal Stability and Mechanical Properties of Some Polyurethanes. *Mater. Plast.* **2008**, 45 (4), 394–397.
- (40) El Miloud Maafi, Fouad Malek, L. T. Synthesis and Characterization of New Polyurethane Based on Polycaprolactone. *J. Appl. Polym. Sci.* **2009**, 115 (6), 3651–3658. <https://doi.org/10.1002/app>.
- (41) Cegla, M.; Engell, S. Generation-Aware Electrified Production: Optimal Continuous Industrial Production of Paint Thickeners. *Chem. Eng. Trans.* **2022**, 96 (June), 31–36. <https://doi.org/10.3303/CET2296006>.
- (42) Olszewski, A.; Kosmela, P.; Żukowska, W.; Wojtasz, P.; Szczepański, M.; Barczewski, M.; Zedler, Ł.; Formela, K.; Hejna, A. Insights into Stoichiometry Adjustments Governing the Performance of Flexible Foamed Polyurethane/Ground Tire Rubber Composites. *Polymers (Basel)*. **2022**, 14 (18), 3838. <https://doi.org/10.3390/polym14183838>.
- (43) Prochazka, F.; Nicolai, T.; Durand, D. Molar Mass Distribution of Linear and Branched Polyurethane Studied by Size Exclusion Chromatography. *Macromolecules* **2000**, 33 (5), 1703–1709. <https://doi.org/10.1021/ma9901543>.
- (44) Peng, J.; Dong, R.; Ren, B.; Chang, X.; Tong, Z. Novel Hydrophobically

- Modified Ethoxylated Urethanes End-Capped by Percec-Type Alkyl Substituted Benzyl Alcohol Dendrons: Synthesis, Characterization, and Rheological Behavior. *Macromolecules* **2014**, *47* (17), 5971–5981. <https://doi.org/10.1021/ma500876d>.
- (45) Barmar, M.; Ribitsch, V.; Kaffashi, B.; Barikani, M.; Sarreshtehdari, Z.; Pfragner, J. Influence of Prepolymers Molecular Weight on the Viscoelastic Properties of Aqueous HEUR Solutions. *Colloid Polym. Sci.* **2004**, *282* (5), 454–460. <https://doi.org/10.1007/s00396-003-0968-0>.
- (46) Barmar, M.; Barikani, M.; Kaffashi, B. Synthesis of Ethoxylated Urethane and Modification with Cetyl Alcohol as Thickener. *Iran. Polym. J. (English Ed.)* **2001**, *10* (5), 331–335.
- (47) Lundberg, D. J.; Glass, J. E.; Eley, R. R. Viscoelastic Behavior among HEUR Thickeners. *J. Rheol. (N. Y. N. Y.)* **1991**, *35* (6), 1255–1274. <https://doi.org/10.1122/1.550174>.
- (48) Kaczmarek, J. P.; Glass, J. E. Synthesis and Characterization of Step Growth Hydrophobically-Modified Ethoxylated Urethane Associative Thickeners. *Langmuir* **1994**, *10* (9), 3035–3042. <https://doi.org/10.1021/la00021a029>.
- (49) Vlachopoulos, J.; Strutt, D. *Rheology of Molten Polymers*; Elsevier Inc., 2016. <https://doi.org/10.1016/B978-0-323-37100-1.00006-5>.
- (50) Winters, J.; Bolia, R.; Dehaen, W.; Binnemans, K. Synthesis of Polyaramids in γ -Valerolactone-Based Organic Electrolyte Solutions. *Green Chem.* **2021**, *23* (3), 1228–1239. <https://doi.org/10.1039/d0gc03470c>.
- (51) Fage, A. M., Kemmerling, S., Backhaus, C. A., Deshmukh, S., B., R., Hübner, C., Elsner, P. Synthesis of Polyurethanes through Reactive Extrusion Assisted by Alternative Energy Sources [Conference Presentation]. In *EPF European Polymer Congress*; Prague, Czech Republic, 2022.
- (52) Kamal Adibi. Synthesis and Characterization of Some Polyurethane Graft

- Copolymers, Imperial College London, 1979.
- (53) Choi, K. Y.; Mcauley, K. B. Step-Growth Polymerization. In *Polymer Reaction Engineering*; Asua, J. M., Ed.; 2007; pp 273–314.
- (54) Król, P.; Gawdzik, A. Basic Kinetic Model for the Reaction Yielding Linear Polyurethanes. II. *J. Appl. Polym. Sci.* **1995**, *58* (4), 729–743. <https://doi.org/10.1002/app.1995.070580406>.
- (55) Scott J. Moravek, R. F. S. Reaction Kinetics of Dicyclohexylmethane-4,40-Diisocyanate with 1- and 2-Butanol: A Model Study for Polyurethane Formation. *J. Appl. Polym. Sci.* **2008**. <https://doi.org/https://doi.org/10.1002/app.28320>.
- (56) Tibor Nagy, Borbala Antal, Katalin Czifrak, Ildiko Papp, Jozsef Karger-Kocsis, Miklos Zsuga, S. K. New Insight into the Kinetics of Diisocyanate-Alcohol Reactions by High_performance Liquid Chromatography and Mass Spectrometry. *J. Appl. Polym. Sci.* **2015**. <https://doi.org/DOI:10.1002/app.42127>.
- (57) Cassagnau, P.; Bounor-Legaré, V.; Fenouillot, F. Reactive Processing of Thermoplastic Polymers: A Review of the Fundamental Aspects. *Int. Polym. Process.* **2007**, *22* (3), 218–258. <https://doi.org/10.3139/217.2032>.
- (58) Moreno, G.; Valencia, C.; Franco, J. M.; Gallegos, C.; Diogo, A.; Bordado, J. C. M. Influence of Molecular Weight and Free NCO Content on the Rheological Properties of Lithium Lubricating Greases Modified with NCO-Terminated Prepolymers. *Eur. Polym. J.* **2008**, *44* (7), 2262–2274. <https://doi.org/10.1016/j.eurpolymj.2008.04.047>.
- (59) De Keer, L.; Van Steenberge, P. H. M.; Reyniers, M. F.; D’hooge, D. R. Going beyond the Carothers, Flory and Stockmayer Equation by Including Cyclization Reactions and Mobility Constraints. *Polymers (Basel)*. **2021**, *13* (15), 1–26. <https://doi.org/10.3390/polym13152410>.
- (60) Gonzalez-gutierrez, J.; Oblak, P.; Emri, I. Improving Powder Injection Moulding

- by Modifying Binder Viscosity through Different Molecular Weight Variations
12 . 5 Improving Powder Injection Moulding by Modifying Binder Viscosity
through Different Molecular Weight Variations. **2013**, No. January 2014.
- (61) Polyurethane, N.; Delebecq, E.; Pascault, J.; Boutevin, B.; Lyon, U. De. On the Versatility of Urethane / Urea Bonds : Reversibility , Blocked. **2013**.
- (62) Santamaria-Echart, A.; Fernandes, I.; Barreiro, F.; Corcuera, M. A.; Eceiza, A. Advances in Waterborne Polyurethane and Polyurethane-Urea Dispersions and Their Eco-Friendly Derivatives: A Review. *Polymers (Basel)*. **2021**, *13* (3), 1–32. <https://doi.org/10.3390/polym13030409>.
- (63) Mattia, J.; Painter, P. A Comparison of Hydrogen Bonding and Order in a Polyurethane and Poly(Urethane-Urea) and Their Blends with Poly(Ethylene Glycol). *Macromolecules* **2007**, *40* (5), 1546–1554. <https://doi.org/10.1021/ma0626362>.
- (64) Veetil, R. E.; Soundiraraju, B.; Mathew, D.; Kalamblayil Sankaranarayanan, S. K. End-Terminated Poly(Urethane-Urea) Hybrid Approach toward Nanoporous/Microfilament Morphology. *ACS Omega* **2022**, *7* (7), 6280–6291. <https://doi.org/10.1021/acsomega.1c06888>.
- (65) Marcano, A.; Fatyeyeva, K.; Koun, M.; Dubuis, P.; Grimme, M.; Marais, S. Recent Developments in the Field of Barrier and Permeability Properties of Segmented Polyurethane Elastomers. *Rev. Chem. Eng.* **2019**, *35* (4), 445–474. <https://doi.org/10.1515/revce-2017-0033>.
- (66) C. Hepburn. *Polyurethane Elastomers*; Springer Science & Business Media, 2012. <https://doi.org/https://doi.org/10.1007/978-94-011-2924-4>.
- (67) Sang, S.; Li, Y.; Wang, K.; Tang, J. Application of Blocked Isocyanate in Preparation of Polyurethane(Urea) Elastomers. *J. Appl. Polym. Sci.* **2021**, *138* (24). <https://doi.org/10.1002/app.50582>.
- (68) János Hajas, A. W. Modified Ureas: An Interesting Opportunity to Control

- Rheology of Liquid Coatings. *Macromol. Symp.* **2002**, No. 187, 215–224.
[https://doi.org/https://doi.org/10.1002/1521-3900\(200209\)187:1<215::AID-MASY215>3.0.CO;2-T](https://doi.org/https://doi.org/10.1002/1521-3900(200209)187:1<215::AID-MASY215>3.0.CO;2-T).
- (69) Braatz, J. A. A Simple Method for Determining Water-induced Gelling Times of Isocyanate Prepolymers. *J. Appl. Polym. Sci.* **1993**, 50 (9), 1545–1554.
<https://doi.org/10.1002/app.1993.070500908>.
- (70) Xue, S.; Pei, D.; Jiang, W.; Mu, Y.; Wan, X. A Simple and Fast Formation of Biodegradable Poly(Urethane-Urea) Hydrogel with High Water Content and Good Mechanical Property. *Polymer (Guildf)*. **2016**, 99, 340–348.
<https://doi.org/10.1016/j.polymer.2016.07.034>.
- (71) Li, T. T.; Feng, L. F.; Gu, X. P.; Zhang, C. L.; Wang, P.; Hu, G. H. Intensification of Polymerization Processes by Reactive Extrusion. *Ind. Eng. Chem. Res.* **2021**, 60 (7), 2791–2806. <https://doi.org/10.1021/acs.iecr.0c05078>.
- (72) Mezger, T. G. *The Rheology Handbook*; 2009; Vol. 38.
<https://doi.org/10.1108/prt.2009.12938eac.006>.
- (73) Tadros, T. F. *Rheology of Dispersions: Principles and Applications*; 2010.
<https://doi.org/10.1002/9783527631568>.
- (74) Worldwide, M. I. *Optimizing Rheology for Paint and Coating Applications [White Paper]*; 2015.
- (75) Vrandečić, N. S.; Erceg, M.; Jakić, M.; Klarić, I. Kinetic Analysis of Thermal Degradation of Poly(Ethylene Glycol) and Poly(Ethylene Oxide)s of Different Molecular Weight. *Thermochim. Acta* **2010**, 498 (1–2), 71–80.
<https://doi.org/10.1016/j.tca.2009.10.005>.
- (76) Delpech, M. C.; Miranda, G. S. Waterborne Polyurethanes: Influence of Chain Extender in FTIR Spectra Profiles. *Cent. Eur. J. Eng.* **2012**, 2 (2), 231–238.
<https://doi.org/10.2478/s13531-011-0060-3>.

- (77) Auguścik, M.; Kurańska, M.; Prociak, A.; Karalus, W.; Lipert, K.; Ryszkowska, J. Production and Characterization of Poly(Urea-Urethane) Elastomers Synthesized from Rapeseed Oil-Based Polyols Part I. Structure and Properties. *Polimery/Polymers* **2016**, *61* (7–8), 490–498. <https://doi.org/10.14314/polimery.2016.490>.
- (78) Zhao, X.; Qi, Y.; Li, K.; Zhang, Z. Hydrogen Bonds and FTIR Peaks of Polyether Polyurethane-Urea. *Key Eng. Mater.* **2019**, *815 KEM*, 151–156. <https://doi.org/10.4028/www.scientific.net/KEM.815.151>.
- (79) Yilgör, E.; Burgaz, E.; Yurtsever, E.; Yilgör, I. Comparison of Hydrogen Bonding in Polydimethylsiloxane and Polyether Based Urethane and Urea Copolymers. *Polymer (Guildf)*. **2000**, *41* (3), 849–857. [https://doi.org/10.1016/S0032-3861\(99\)00245-1](https://doi.org/10.1016/S0032-3861(99)00245-1).
- (80) Teo, L. S.; Chen, C. Y.; Kuo, J. F. Fourier Transform Infrared Spectroscopy Study on Effects of Temperature on Hydrogen Bonding in Amine-Containing Polyurethanes and Poly(Urethane-Urea)S. *Macromolecules* **1997**, *30* (6), 1793–1799. <https://doi.org/10.1021/ma961035f>.
- (81) Stern, T. Conclusive Chemical Deciphering of the Consistently Occurring Double-Peak Carbonyl-Stretching FTIR Absorbance in Polyurethanes. *Polym. Adv. Technol.* **2019**, *30* (3), 675–687. <https://doi.org/10.1002/pat.4503>

Intensification of HEUR synthesis via unsteady-state thermal operation using microwaves

[†]This chapter has been published as:

Tzortzi, I.; Xiouras, C.; Tserpes, C.; Tzani, A.; Detsi, A.; Van Gerven, T.; Stefanidis, G. D.
“Intensification of Solventless Production of Hydrophobically-Modified Ethoxylated Urethanes (HEURs) by Microwave Heating” Chem. Eng. Process. - Process Intensif. 2023, 186 (November 2022), 109315. <https://doi.org/10.1016/j.cep.2023.109315>.

ABSTRACT

Hydrophobically modified ethoxylated urethanes (HEURs) are among the most widely studied class of waterborne polyurethanes. HEURs are amphiphilic polymers that are usually composed of a polyethylene glycol (PEG) backbone, typically end-capped with aliphatic alkyl chains. HEUR synthesis in the industry is a slow and energy-intensive step-growth polymerization process, due to heat and mass transfer limitations inherent in such highly viscous systems. We investigate for the first time the effect of microwave heating on both the solvent-free HEUR synthesis step and the initial pretreatment step of the reagents prior to the HEUR synthesis. We show that microwaves can drastically reduce the overall processing time, and thereby reduce total energy consumption by: A) faster melting of solid PEG and B) faster completion of the polymerization reaction, when operating with a novel rapidly rising transient temperature profile that cannot be reproduced by conventional heating. However, it was found that PEG pretreatment/dehydration by microwaves leads to faster degradation of PEG, compared to dehydration by conventional heating at the same bulk temperature, and should therefore be avoided.

4.1. Introduction

Hydrophobically modified ethoxylated urethanes (HEURs) are among the most widely studied class of waterborne polyurethanes. HEURs are amphiphilic polymers usually composed of a polyethylene glycol (PEG) backbone, typically end-capped with aliphatic alkyl chains.¹ HEURs can be prepared by the solventless step-growth polymerization of PEG with diisocyanates, which are then reacted with hydrophobic alcohols. HEUR synthesis in the industry takes place in batch reactors and heat input is required to bring and maintain the reactants to reaction temperature. The process is slow, typically in the order of a few hours, and energy-intensive due to heat and mass transfer limitations inherent in such highly viscous systems. Therefore, the heat transfer rate, along with the total energy requirement, plays a significant role in industrial HEUR synthesis.

In conventional heating (CH) methods, currently used for HEUR synthesis, energy is transferred from the reactor wall surface to the reaction mixture by convection and conduction using heat transfer fluids (hot utilities). This is an inefficient mode of heating, as large amounts of heat transfer fluids (e.g. superheated steam) also need to be heated at a temperature higher than the reaction temperature. Additionally, the reactor surface walls must be overheated to achieve the desired core temperature.²⁻⁴ This in turn results in high energy consumption and long-term mixture exposure to high temperatures, especially in the vicinity of the reactor walls, which may lead to local product degradation and/or equipment deterioration.^{2,3} In view of rising energy costs, the development of more energy-efficient processes by applying the principles of process intensification (PI) through the use of alternative energy sources, e.g. ultrasound (US) and/or microwaves (MW) can contribute to process optimization in terms of lower costs, shorter production times and superior product quality.²⁻¹¹ Unlike CH, MW heating is fast and volumetric in nature, while it does not require the use of heat transfer fluids.¹² Therefore, MW heating has the potential to both shorten the overall total processing time and reduce energy consumption in a plethora of chemical processes.^{2,13-20}

While a limited number of studies have reported on the effect of MW on the synthesis of polyurethane foams, the solvent-based synthesis of selected polyurethane prepolymers and its curing process and the crosslinking of polyurethane elastomers²¹⁻²⁸, at this moment, to the authors' knowledge, there is no previous work examining HEUR under MW heating. The only study reporting results on the effect of MW heating on step-growth bulk polyurethane polymerization relevant to the type of polymerization used in this study is that by Kucinska Lipka et al. (2017)²⁸. In summary, this study argued that the use of MW heating can accelerate the synthesis of urethane prepolymers compared to CH at identical temperature conditions, but the final molecular weight of the urethane prepolymers was comparable for both heating modes. Additionally, the study did not investigate potential effects of MW heating on the reagent pretreatment steps, which typically constitute a large part of industrial polymerization processes. Finally, a comprehensive energy comparison between the two heating modes has not yet been performed for such polymerization processes.

Herein, we investigate, for the first time, the effect of MW heating on both solventless HEUR synthesis step and on the initial pretreatment step of the reagents for the HEUR synthesis. We show that MWs can drastically reduce the overall processing time, and thereby reduce total energy consumption by faster melting of solid PEG and faster completion of the polymerization reaction. The findings of this study can be used to optimize heat transfer and energy efficiency in this industrially relevant polymerization reaction.

4.2. MATERIALS AND METHODS

4.2.1. Materials

Polyethylene glycol of molecular weight 8000 g/mol with purity of >99.5% was provided by Clariant. H₁₂MDI (4,4-Methylenebis (cyclohexyl isocyanate), mixture of isomers, 90% purity) from Acros Organics and 1-Octanol (99% purity) from Alfa Aesar were used as received. Bismuth carboxylate (KKAT XCB221) provided by King Industries was selected as the catalyst. Chloroform (>99.8% purity) stabilized with amylene was purchased from Fisher Chemicals and was dried using 4Å molecular sieves. Chloroform-d (99.8%) for NMR was purchased from Sigma Aldrich. All

Chapter 4

reagents were of analytical grade and used without further purification. The structures of all main reactants and some basic properties are presented in Table 4.1.

Table 4.1. Summary of the various reactants used in this study, their role in polyurethane synthesis and their structures.

Reactant [Short]	Role	Simplified structure	Chemical structure
Polyethylene glycol [PEG]	Macrodiol- Hydrophillic backbone	HO-R ₁ -OH	
4,4- dicyclohexylmethan e diisocyanate [HMDI]	Diisocyanate -Connecting diols and mono- alcohols	O=C=N-R ₂ -N=C=O	
Octanol [Oct]	Hydrophobic tails	R ₃ -OH	
Bismuth carboxylate [kkat]	Catalyst	--	

4.2.2. Experimental set-up

Non-reactive and reactive experiments were performed with MW and CH. The reactive experiments using CH are reported in our previous work.²⁹ For the MW heating experiments, an identical reactor featuring the same geometry as compared to the one used for the CH experiments, but without a jacket, was used. The reactor volume was 250 mL and the same PTFE three-blade impeller was used connected to a stirrer motor capable of controlling the mixing speed from 20 rpm to 1200 rpm (Hei-Torque overhead stirrer from Heidolph).

The MW-heated experiments were performed in a MW multimode cavity (Milestone flexiWAVE MW Synthesis Platform) with a maximum output power of 1.8 kW and a built-in manual power control system (details in the next section). The volume of the MW cavity is 70.5 L. The flexiWAVE configuration is accompanied by an internal camera in the MW cavity and a touchscreen terminal from which reaction progress can be monitored. A special PTFE base was used to position the reactor in the same place within the MW cavity during the MW experiments. A snapshot of the experimental setup for CH and MW heating is shown in Figure 4.1. A schematic representation of the reactor inside the MW cavity is also shown in Figure 4.2.



Figure 4.1. Picture of the experimental reactor setup used for the study (a) Conventional Synthesis: jacketed reactors connected with oil/water bath, vacuum pump, overhead stirrer²⁹, (b) flexiWAVE MW Synthesis Platform, (c) internal of MW cavity with glass reactor.

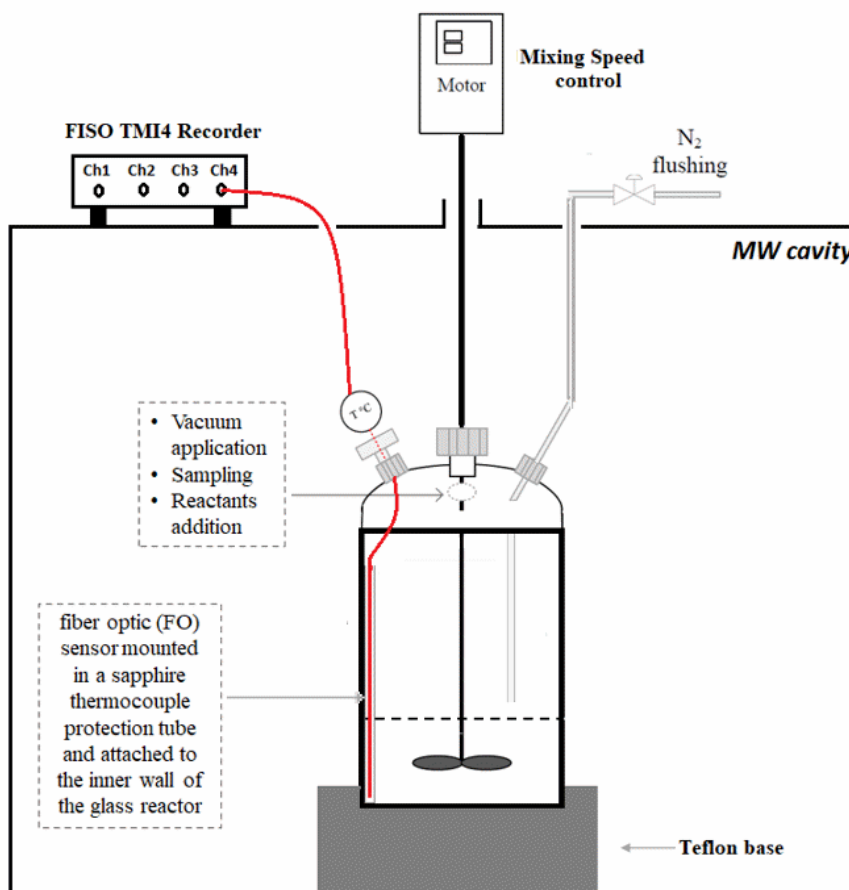


Figure 4.2. Schematic representation of the experimental reactor setup inside the MW cavity, including a Teflon base, a glass reactor, special openings for the various processing steps, fiber optic (FO) sensor mounted in a sapphire thermocouple protection tube and attached to the inner wall of the glass reactor, FISO TMI4 Recorder connected with the FO sensor and motor connected to the stirrer.

4.2.3. Temperature measurement and control

When comparing the kinetics of MW versus CH thermally activated processes, accurate and precise recording of the internal reaction mixture temperature profile is of paramount importance, and failure to ensure can lead to erroneous conclusions.³⁰ However, temperature measurement and precise control in MW-irradiated process mixtures is not trivial mainly due to: a) rapid temperature evolution upon irradiation of polar mixtures, b) inaccessibility of the cavities, and c) inability to use conventional thermocouples due to interactions with the MW field (sparking).

To alleviate these limitations and enable an accurate comparison of the MW and CH experiments in this work, the internal reaction mixture temperature during the MW

heated experiments, was measured by a fiber optic (FO) sensor (CEM Corp) mounted in a sapphire thermocouple protection tube and attached to the inner wall of the glass reactor (Figure 4.2). Readings of the FO sensor were recorded in a FISO TMI4 unit at a temporal resolution of 600 ms to ensure negligible delays in recording the temperature evolution.

To determine potential temperature gradients in the MW irradiated mixture, a series of experiments were performed in flexiWAVE with molten PEG 8000 g/mol at the reaction stirring speed. Molten PEG was added to the reactor used for the MW-assisted experiments at the same scale (50 g), and two FOs were placed in opposite positions across the inner diameter of the vessel. For verification purposes, a portable thermocouple was used to measure the temperature of the bulk material centrally at the stirrer position. Isothermal and transient temperature profiles were tested with MW heating in flexiWAVE and temperature gradients in the bulk of the PEG/reactive mixture ranged between 3-4°C, which is considered negligible.

To enable internal reaction temperature control, initially the flexiWAVE's built-in temperature control system was tested, which is based on adjusting the power generated by the magnetron upon feedback from the built-in temperature sensor. However, this control system proved insufficient for this work due to the long response time of the built-in temperature sensor (8 s). Therefore, a manual control strategy was implemented by adjusting the power based on the CEM FO sensor (response time of 600 ms). The latter was performed by constructing a pseudo-calibration using pure PEG 8000 g/mol between the applied power and the temperature recorded by TMI4. This procedure was performed with the exact same reactor and position within the MW cavity. As shown in Figure 4.3, accurate temperature control can be attained by this methodology. When the nominal MW power is set at 100–110 W, it is possible to maintain the bulk PEG temperature at 110 °C, while 71–72 W stabilize the bulk PEG temperature at 80 °C. The pseudo-calibration procedure was performed to obtain information about the applied power and the temperature change of pure PEG, since for practical reasons the temperature could not be continuously measured during the pretreatment step under vacuum. In addition, it allowed more control over the application of MW and avoidance of large oscillations/overshoots when trying to stabilize the temperature during

isothermal polymerizations. During the polymerizations, the temperature was continuously measured and recorded with the FO.

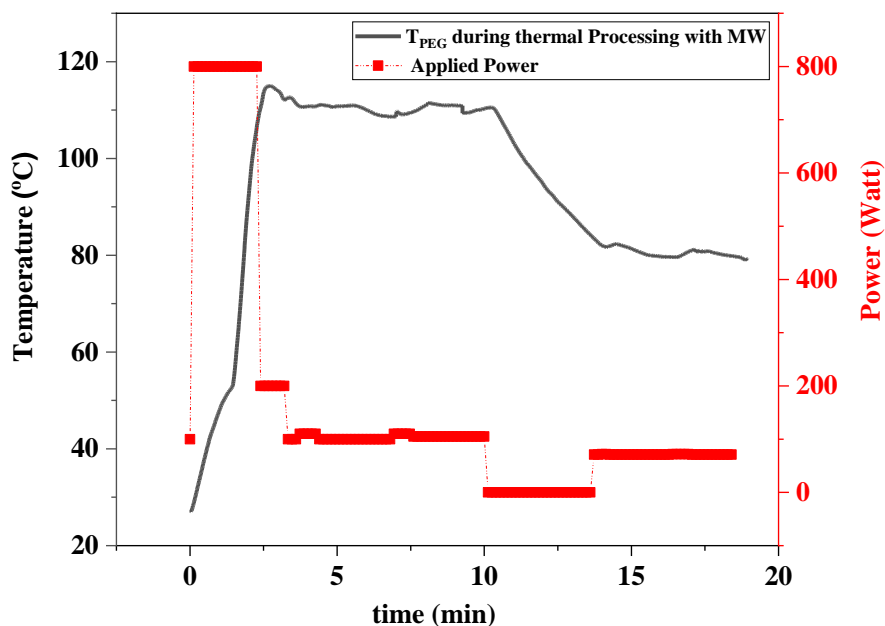


Figure 4.3. Temperature recorded by the FO sensor during the thermal processing of PEG 8000 g/mol inside the MW cavity at different power levels.

For the temperature measurement in the CH experiments, the same FO sensor and recording device were used.²⁹

During the dehydration stage, magnetic stirring was used in both heating modes to prevent vents and leaks from the overhead stirrer from affecting the applied vacuum pressure. For this reason, during the MW-heated experiments, the FO was not used to measure the bulk temperature of the PEG, and the latter was regulated with the applied power and the temperature recorded by TMI4 based on the pseudo-calibration using pure PEG 8000 g/mol, as described previously. An IR sensor was also used to measure the reactor wall temperature, and the vacuum was periodically stopped to allow the internal temperature to be measured with a portable thermocouple. During the measurement of the bulk temperature of PEG with the portable thermocouple, the MW power was turned off to exclude any influence of MW on the portable thermocouple.

During this process, the temperature gradients in the bulk of the PEG did not exceed 3°C when the latter was dehydrated by MW heating.

4.2.4. Synthesis procedure

The HEUR bulk synthesis was performed from the one-step reaction of PEG, H₁₂MDI and 1-octanol (hereafter referred to as HMDI and Oct) and the corresponding HEUR prepolymer from the reaction of HMDI and PEG. For the HEUR case the molar ratio of PEG:HMDI:Oct was 1:1.5:1 and for the prepolymer PEG:HMDI 1:1.5. The catalyst concentration was 0.035% w/w with respect to the total mass of the reactive mixture. The synthesis method used for both the prepolymer and the HEUR was the same with our previous work.²⁹ Figure 4.4 shows the chemical structures and synthetic routes of prepolymer, HEUR and urea (main byproduct). For the prepolymer case, where only HMDI and PEG react, functional groups on each end of monomer molecules (–NCO) react with functional groups on the ends of other monomers (–OH) to form functional group linkages (urethanes bonds), called step-growth/condensation polymerization. Based on the stoichiometry used the prepolymer is –NCO terminated. Similarly, HEUR follows the same synthetic route to build the HEUR backbone, but a monofunctional monomer (octanol) bearing a second chemical function that cannot react in the condensation reaction is also added to endcap the prepolymer backbone. The incorporation of hydrophobic end-groups significantly affects the thickening performance of HEURs. It is worth noting that due to its hydrophilic nature, PEG may contain a significant amount of water, which can lead to the hydrolysis of diisocyanate towards urea formation instead of the desired urethane reaction.²⁹ Therefore, it is important to pretreat and regulate the moisture of PEG below 1000 ppm before proceeding with the polymerization reaction, an aspect often overlooked during HEUR synthesis. As shown in Figure 4.4 isocyanate groups react with water to unstable carbamic acid intermediates which immediately decompose to amine and carbon dioxide, and this amine further reacts with HMDI to form urea structures. As a first step, solid polyethylene glycol flakes were melted in the reactor and subsequently subjected to a vacuum treatment step with constant mixing until the moisture content of PEG was ~800 ppm, as confirmed by Karl-Fischer titration. Immediately after the vacuum was stopped, nitrogen was introduced into the reactor near the liquid surface to prevent atmospheric moisture from being absorbed into the PEG. Next, the reactants

Chapter 4

were heated and held to the reaction temperature prior to polymerization and the catalyst was added to the vessel at the chosen concentration. Before adding the isocyanate, the PEG, catalyst and octanol were mixed for a few minutes to homogenize. Isocyanate addition is marked as time zero of each experiment. The sampling method used for all experiments is the in-situ method as described in our previous work, in which the molten sample extracted from the reactor was directly dissolved in vials with pre-weighed dry chloroform to prevent possible ongoing polymerization or post polymerization effect.²⁹

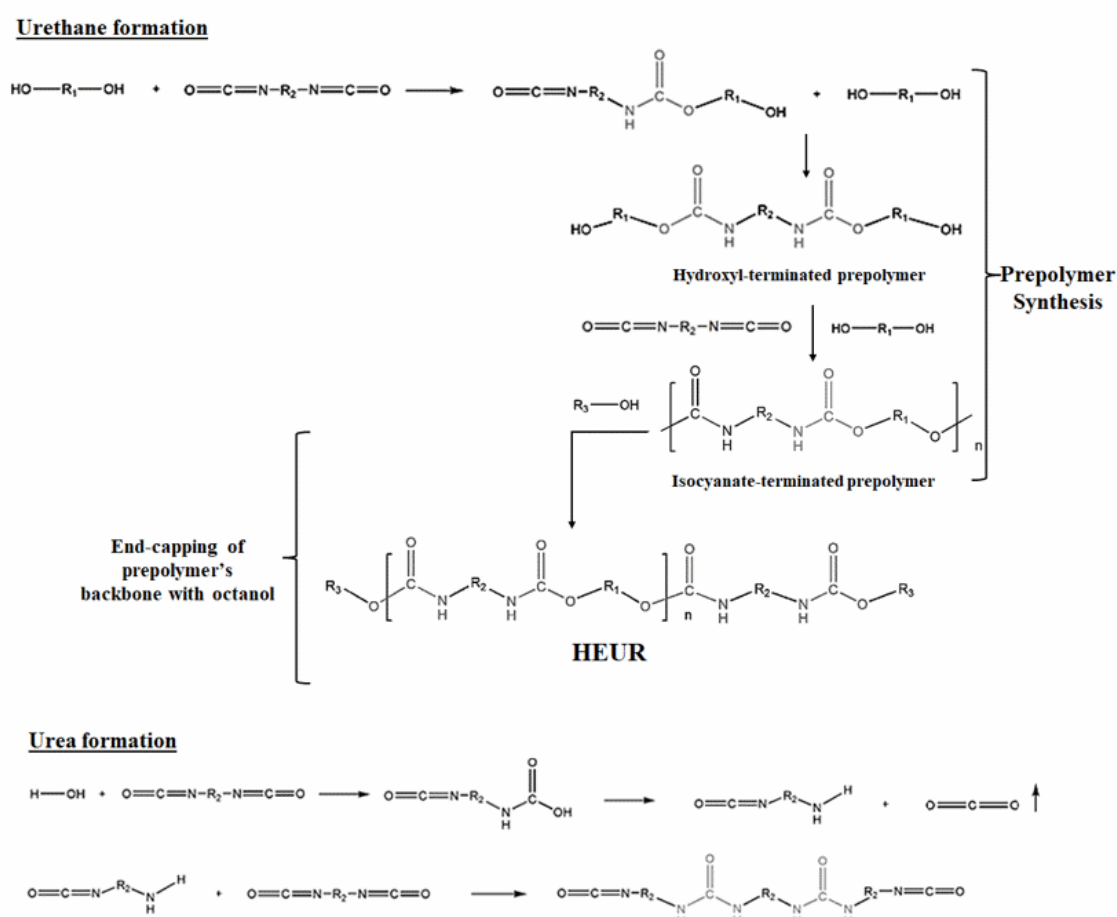


Figure 4.4. Chemical structures and synthetic routes of urea, prepolymer and HEUR synthesis.^{1,29,31-34}

4.2.5. Analytical Methods

Gel Permeation Chromatography (GPC): The weight/number average molecular weight (M_w/M_n) was determined by GPC from Shimadzu, using four Styragel columns

from Waters. Chloroform was the mobile phase (1 ml/min) at 30 °C operating temperature. Polyethylene glycols/oxides (PEG/PEO) were used as calibration standards.

Fourier Transform Infrared Spectroscopy (FTIR): The qualitative analysis of the obtained polymers was done by FTIR, which was performed using attenuated total reflectance-Fourier transform infrared spectroscopy (Bruker Alpha FTIR-ATR). Spectra were acquired in the measurement range of 4000–400 cm^{-1} at room temperature. Signals were collected in 16 scans at a resolution of 4 cm^{-1} and were rationed against a background spectrum recorded from the clean, empty cell at room temperature. The liquid samples were placed in the analysis cell, and the spectra were recorded after the total spontaneous solvent evaporation.

NMR: All ^1H NMR measurements were performed on a Bruker Avance DRX 500 MHz NMR (11.7 Tesla) spectrometer (Bruker Biospin, Rheinstetten, Germany) operating at NMR frequency of 500.13 MHz for ^1H NMR, equipped with a 5 mm multi nuclear broad band inverse detection probe. All the ^1H NMR (500 MHz) spectra were recorded with chemical shifts (δ) in parts per million (ppm) and coupling constants (J) in hertz (Hz). Samples were added into NMR tubes (5 mm Thin Wall Precision NMR Sample Tubes 8" L, Wilmad, Vineland, NJ, USA). The obtained spectra were Fourier transformed, and their phase and baseline were automatically corrected. Prior to Fourier transformation, an exponential weighting factor corresponding to a line broadening of ^1Hz was applied. ^1H NMR spectra of the samples were measured in deuterated chloroform (CDCl_3).

4.3. RESULTS AND DISCUSSION

4.3.1. Effect of MW irradiation on the Pretreatment of PEG

4.3.1.1. Effect of MW irradiation on the melting and cooling stage of PEG

A series of non-reactive heating experiments were performed both with CH and MW heating to demonstrate the effect of MW irradiation on the total time of the pretreatment stage of PEG prior to the reaction. A detailed description of the stages involved in the pretreatment of PEG are shown in Table 4.2.

Chapter 4

Additionally, process times are quoted and classified based on the type of heating source used. Solid PEG was melted and set to reach two targeted temperatures, 110°C and 80°C, which account for the vacuum and the reaction temperature, respectively. Based on initial tests, the duration of the dehydration stage of PEG under vacuum was found to be primarily dependent on the applied vacuum pressure, the bulk temperature of PEG, the stirring speed, as well as the initial and desired final moisture content in PEG. For our case the initial moisture concentration in PEG was approximately 2000 ppm and the desirable concentration was ~800 ppm. In our previous work²⁹ we have shown that the initial polyol moisture concentration should be limited below 1000 ppm in order to limit the side reaction of isocyanate to form urea.

Table 4.2. Description of the various steps involved in the pretreatment stage of PEG prior to reaction.

	Step	Process time	Temperature (°C)	CH	MW Heating
Pretreatment stage of PEG	1	Time needed for the heating fluid to reach vacuum temperature	$T_{\text{vacuum}}=110^{\circ}\text{C}$	$t_{1,\text{CH}}$	-
	2	Time needed for PEG to melt and reach vacuum temperature		$t_{2,\text{CH}}$	$t_{2,\text{MW}}$
	3	Vacuum treatment time to dehydrate PEG		$t_{3,\text{CH}}$	$t_{3,\text{MW}}$
	4	Time needed for PEG to reach reaction temperature (Cooling Stage)	$T_{\text{reaction}}=80^{\circ}\text{C}$	$t_{4,\text{CH}}$	$t_{4,\text{MW}}$

Chapter 4

The applied vacuum pressure for both heating modes was 50-100 mbar. For our experimental conditions the necessary duration for the dehydration stage of PEG is 3.5hrs ~210 min for both heating modes. Temperatures higher than 110°C favor the thermal degradation of PEG and are therefore not selected for the dehydration step.

The selection of the reaction temperature of 80°C is based on current industrial practice. Although HEUR synthesis can be performed at higher temperatures (up to 110 °C)²⁹, lower reaction temperatures are industrially preferable, mainly because prolonged exposure of the reactive mixture at higher temperature risks both the thermal stability of PEG and favor isocyanate side reactions. In the formation and processing of polyurethanes, side reactions can occur, particularly at elevated temperatures with excess isocyanate groups accelerated by the presence of certain catalysts.³⁵ Thus, in addition to urethane products, urea, allophanate, biuret and isocyanurate groups can also be present in polyurethanes, which influence their final structure and properties³⁶ It is evident that both temperature and reaction time have a profound effect on the extent of these side reactions. For example even at 108 °C and 1 h reaction time, traces of allophanates were present in a urethane prepolymer synthesis.³⁷

Figure 4.5 shows the temporal evolution of PEG temperature during the pretreatment stages for both CH and MW heating. These temperatures were measured using the same FO and recorder as described in Section 2. For the CH experiments, the reactor was initially empty, and the time required for the heating fluid to reach 110 °C was measured. Next, PEG was added to the reactor and mixing started when the outer PEG layer in contact with the reactor jacket was melted. It is worth noting that the melting point of PEG is around 65-70 °C. For the MW heated experiments, the reactor was pre-filled with PEG prior to the application of MW heating. When MW irradiation started, the reactive mixture was monitored by the internal camera and stirring started when the camera indicated that the PEG melting process had started. Figure 4.5 shows that using MW already eliminates step 1 (i.e. heating time to 110 °C), while the total time to melt PEG and reach vacuum temperature can be reduced from 40 to 4 min, corresponding to a decrease of 90%. The vacuum treatment time is excluded from the chart and is shown as a break in x-axes and has a duration of 210 min, constant for both heating modes. Regarding the cooling stage of PEG, the use of MW radiation can result in an 80% reduction in the duration of step 4 compared to CH, because in the latter, the thermal

inertia of the heating fluid slows down the cooling process from 110 °C to 80 °C. Cooling to reaction temperature is performed atmospherically by natural convection in both cases. In terms of process characteristics, the processing time for the pretreatment of PEG for HEUR synthesis in lab scale is reduced from 280 min (CH) to 220 min (MWs), which corresponds to a 21% reduction in the total pretreatment time. It is evident that the bulk of the pre-processing time is due to the isothermal vacuum treatment step, which can be shortened by further decrease in pressure, e.g. by the use of a more powerful vacuum pump.

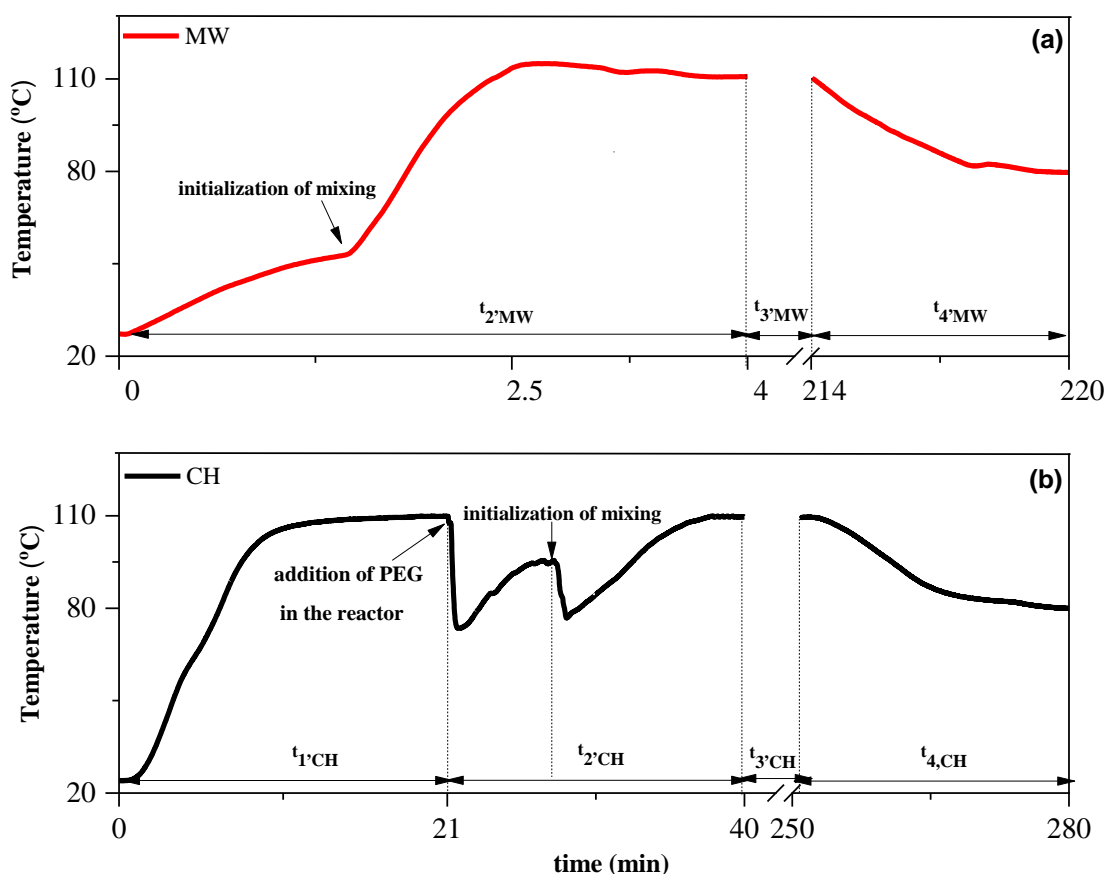


Figure 4.5. Temporal temperature profiles in bulk PEG in the internal of the reactor during its pretreatment process under CH (b) and MW (a). With MW PEG is fully melted at 4 min and with CH at 40min.

4.3.1.2. Effect of MW irradiation on the dehydration stage of PEG

Considering that the vacuum dehydration process accounts for about 80% of the total process time for the pretreatment of PEG, a series of experiments were performed to determine if MW could improve the dehydration profile of PEG by measuring the

evolution of moisture content at different dehydration times and lower temperatures with Karl Fischer titration. Figure 4.6 shows the dehydration profile of PEG at 80 °C and 110 °C for a total dehydration time of 3.5 hr.

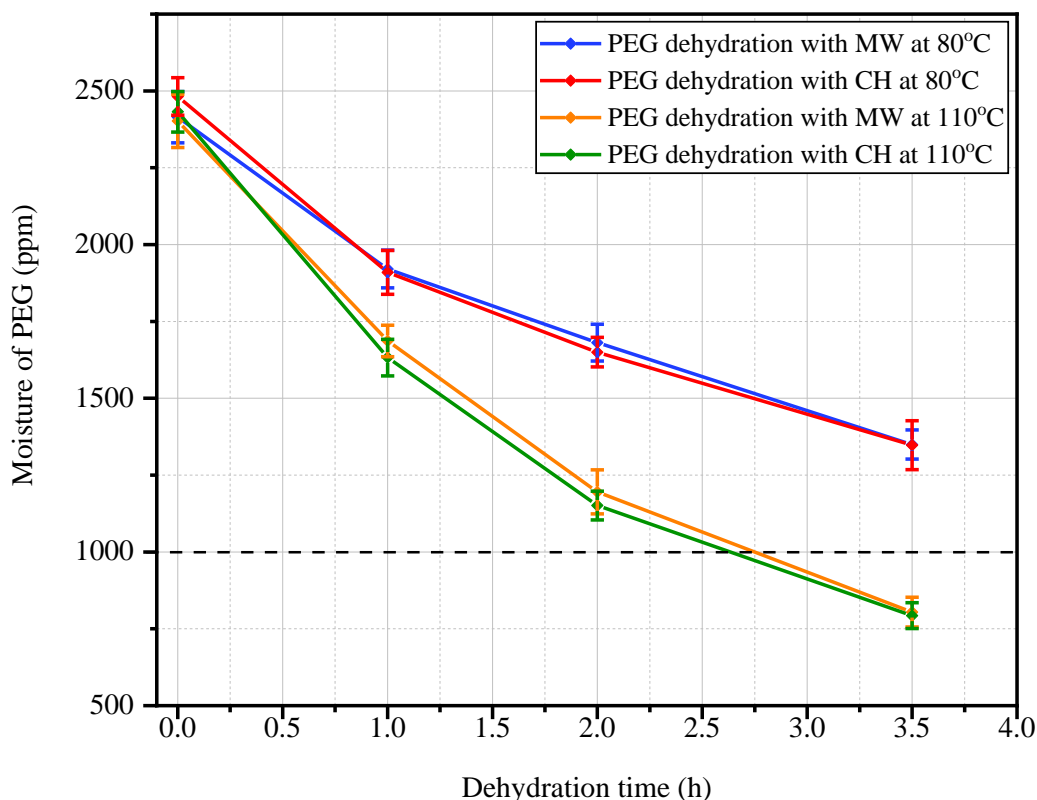


Figure 4.6. Dehydration profiles of PEG with MW and CH at 1, 2, and 3.5 h, at 80 °C and 110 °C and a vacuum pressure of 50-100 mbar. 1000 ppm is also shown in the graph as the maximum water requirement for performing the polyurethane synthesis.

As can be seen in Figure 4.6, the moisture content of PEG remained the same for all dehydration times tested for both heating modes when identical temperature and pressure conditions were applied. Additionally, it is observed that a temperature of 80 °C is not sufficient to lower the moisture content of PEG below the 1000 ppm threshold, regardless of the heating source used. These results demonstrate that the duration of the dehydration process at 80 °C or 110 °C with a vacuum pressure of 50-100 mbar cannot be shortened with MW.

However, it was observed that the bulk of the PEG became yellowish when the latter was dehydrated with MW at 110 °C, which is an indication of PEG thermal degradation.^{38,39} A series of experiments were performed to evaluate the effect of the heating source on the prolonged thermal processing of PEG during the vacuum treatment step in terms of PEG stability. To study the effects of MW heating on the thermal pretreatment of PEG under vacuum, ¹H NMR spectra of PEG thermally treated at 110 °C for 3.5 h with MW and CH were recorded. In all ¹H NMR spectra (Figure 4.7(a-c)), a peak at 3.60 ppm is present, corresponding to the protons signal of the methylene groups of the polyethylene backbone of PEG. However, in the ¹H NMR spectrum of PEG obtained by MW heating, additional peaks appeared around 2.5, 3.34, 4.10-4.29, 6.45, 8.05 and 9.69 ppm. These peaks could be attributed to PEG thermal degradation products (Figure 4.7 (c)).

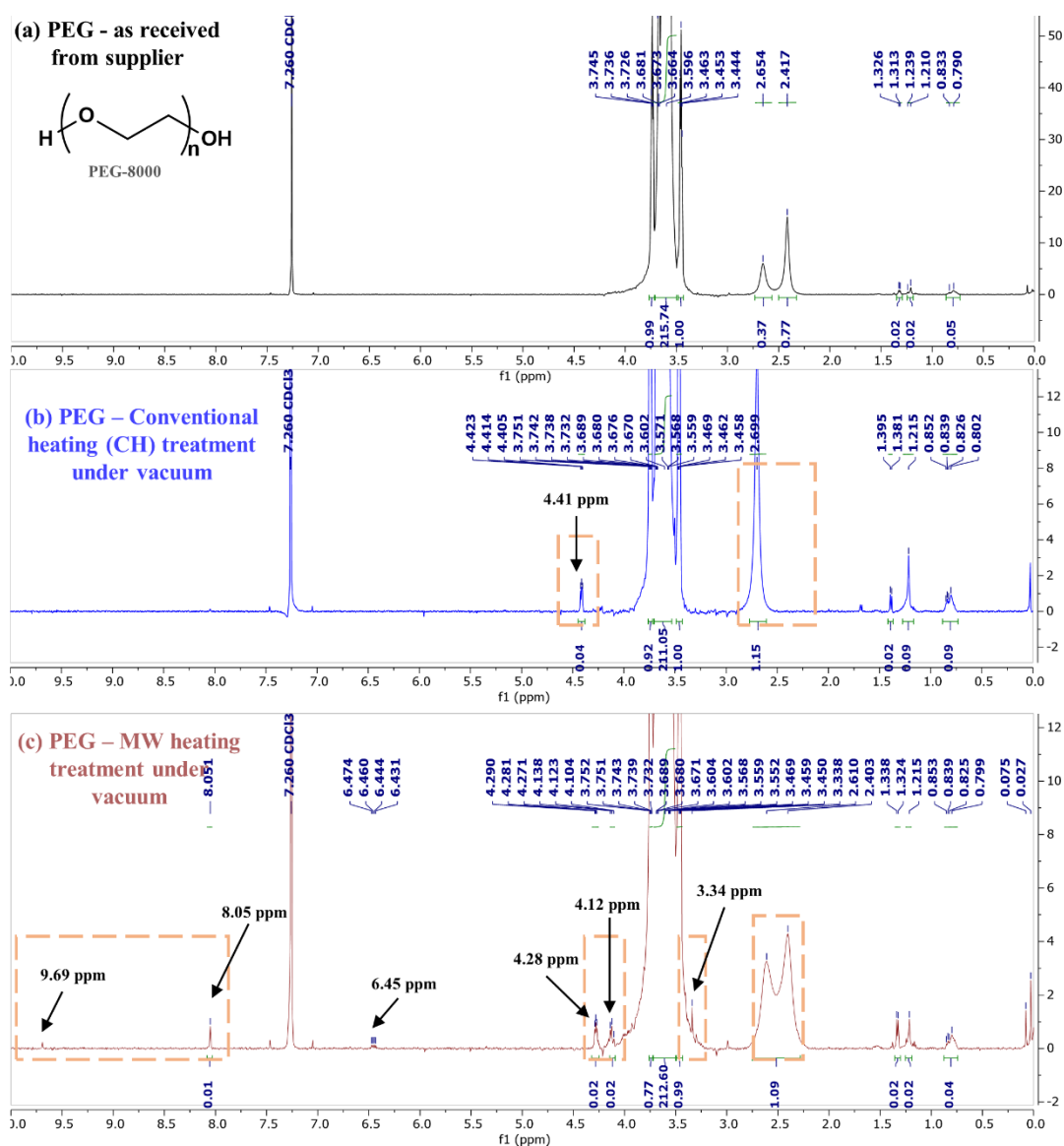


Figure 4.7. ^1H NMR (CDCl_3) spectra of (a) commercial PEG as obtained from supplier and (b) PEG CH and (c) MW heating 110°C for 210 min under vacuum.

Voorhees *et al.* (1994) extensively studied and proposed a series of competitive intermolecular and intramolecular processes to explain the PEG thermal degradation by pyrolysis in a tube furnace (under nitrogen) at elevated temperatures (450 and 550°C) using the GC/MS technique.⁴⁰ According to this study, homolytic cleavage of the C–C and C–O bonds, disproportionation and hydrogen abstraction reactions were proposed as degradation pathways. Regarding this proposed mechanisms, methyl ether products, ethyl ether products, vinyl ether products and aldehyde products are formed. Lattimer (2000) studied the PEG thermal degradation over lower temperature pyrolysis (range 150 – 325°C) and according to this study, at the lowest temperatures hydroxyl and ethyl

ether end groups are the dominant oligomeric products due to the C–O cleavage, while at higher temperatures, methyl ether and vinyl ether end groups are present since C–C cleavage mostly occurs.⁴¹

In this study, according to the ¹H NMR data in Figure 4.7 (c) it seems that products with an aldehyde end group (–O–CH₂–CHO) are formed and their presence is indicated by the appearance of the peak at 9.69 ppm. The peak at 8.05 ppm, could possibly be attributed to a formate ester while the peak at 6.54 ppm indicates the presence of products with a vinyl ether end group (–O–CH=CH₂). The peak at 3.34 ppm can be assigned to the formation of a product with a methyl ether end group (–O–CH₂–CH₃) while the group of peaks at the range of 4.10–4.29 ppm are indicative of to the methylene groups of the degradation end products.

Due to the difficulties in continuously measuring and controlling the bulk PEG temperature under vacuum, the enhanced degradation of PEG with MW under isothermal conditions is most likely attributed to thermal effects (e.g. small temperature oscillations and/or local thermal gradients). It is noted that, depending on the activation energies of the degradation reactions involved, even small differences in the temperature profiles between MW and CH could have significant effects on the kinetics of these reactions. Further experimentation is needed to fully elucidate the origin of the enhanced thermal degradation of PEG with MW under isothermal conditions. However, detailed analysis on this subject is outside the scope of this work, as the main purpose here is to study how MW can be used to intensify the batch HEUR synthesis. For this reason, in the following sections, which examine the effect of MW on the polymerization reaction, PEG was melted and dehydrated with CH to prevent enhanced degradation of PEG, while MW was only applied during the reaction step.

4.3.2. Effect of MW irradiation on the polymerization

4.3.2.1. HEUR Prepolymer synthesis with MW heating at isothermal conditions with CH

A series of experiments was performed to investigate the influence of MW irradiation on the rate of molecular weight evolution of the HEUR's prepolymer under isothermal conditions. The obtained M_n values of the prepolymers over the course of the reaction when the latter is 80°C are shown in Figure 4.8 together with the polydispersity index

(PDI) or the M_w/M_n fraction of the polymers. Based on the results in this graph, it appears that both M_n and PDI values are independent of the heating source used, as no significant differences are found for either, when the same reaction temperature is used.

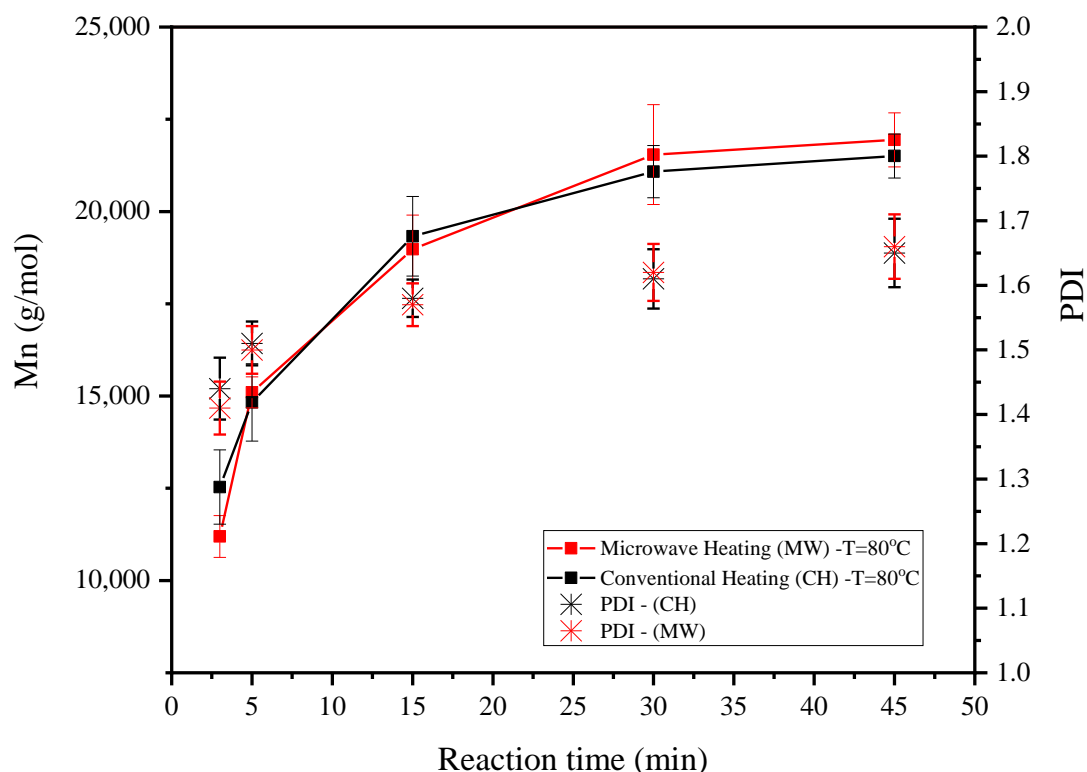


Figure 4.8. The influence of heat source type (oil bath versus MW radiation) on the rate of molecular weight development of the prepolymer during the reaction. MW heated experiments have been performed at least in three repetitions. The error bars represent the standard deviation of the experimental data set. Results of the CH experiments are reproduced from our previous work²⁹ (CC BY-ND 4.0).

Further FTIR tests were performed to determine the chemical composition of the produced prepolymer and to compare the structure-property relationship with the heating source used. Figure 4.9 shows the FTIR spectra of two prepolymers synthesized with MW and CH collected at a polymerization time of 45 minutes. For all analyzed samples, the characteristic $-CH$ stretching band appears at ≈ 2700 to 3000 cm^{-1} and the characteristic absorption peak of the isocyanate group ($N=C=O$) appears at 2265 cm^{-1} .^{29,42,43} The peak at 530 and 730 cm^{-1} is attributed to the chloroform used for the in-situ sampling. Any differences in this range in the spectra of the two prepolymers are

attributed to residual chloroform during the scan. The characteristic absorption bands of polyethylene glycol have been identified as follows: C–O, C–C stretching, CH₂ rocking at 840 cm⁻¹, CH₂ rocking, CH₂ twisting at 960 cm⁻¹, C–O, C–C stretching, CH₂ rocking at 1058 cm⁻¹, C–O, C–C stretching at 1097 cm⁻¹, C–O stretching, CH₂ rocking at 1145 cm⁻¹, CH₂ twisting at 1241 and 1278 cm⁻¹, CH₂ wagging at 1341 cm⁻¹ and CH₂ scissoring at 1466 cm⁻¹.^{43,44} Additionally for both samples, a peak appears at 1715 cm⁻¹, which can be assigned to the disordered hydrogen-bonded carbonyl (C=O) groups in the urethane molecule.^{29,33,45–47}

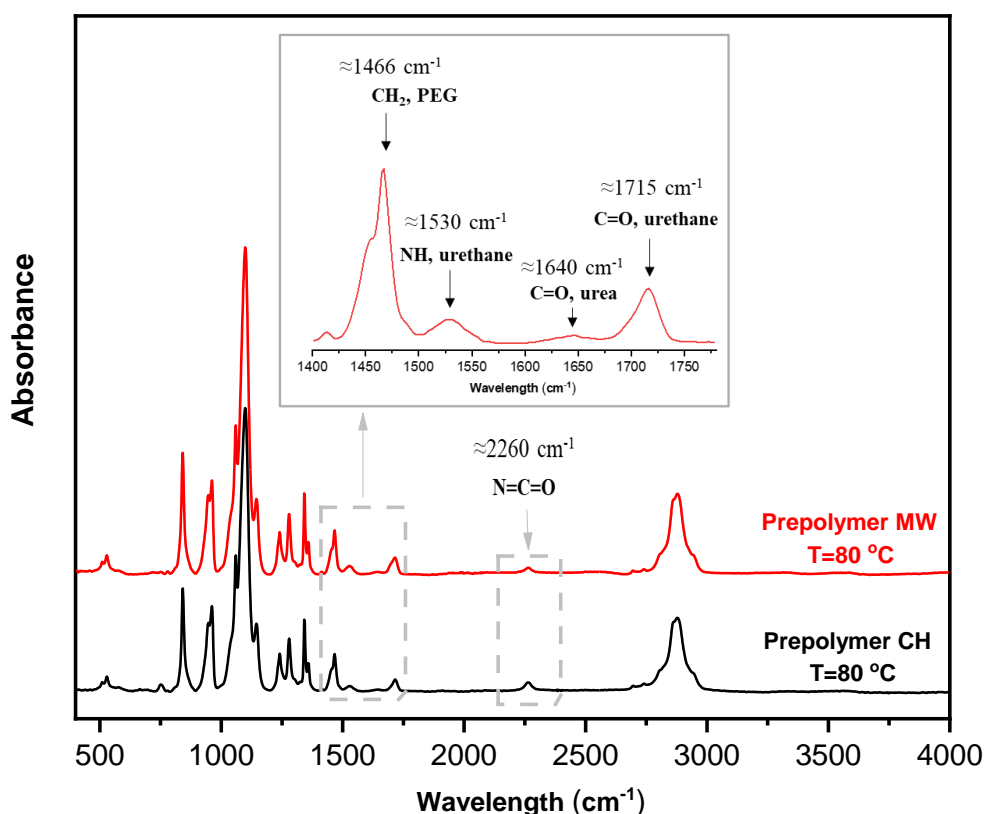


Figure 4.9. FTIR spectra of prepolymers synthesized with MW and CH and collected at a polymerization time of 45 min.

The peak at 1530 cm⁻¹ represents the bending vibrations of the NH in the urethane groups while the peak at 1640 cm⁻¹, is attributed to the traces of ordered hydrogen-bonded urea carbonyl (C=O).^{29,42,43,45,48}

Based on the results obtained, it is confirmed that the chemical composition and structure of the prepolymers produced with MW and CH are identical when using the same reaction temperature, regardless of the heating source used. This observation taken together with the comparable M_n trends and plateau values between the MW and CH experiments indicates that the mechanistic steps and kinetics of the polymerization process remain unaffected when MW are used at isothermal conditions. This observation is consistent with what is now generally accepted, that in most cases the observed effects in MW-assisted organic reactions are the result of purely thermal phenomena.^{49,50}

A detailed analysis of this polymerization process should also include quantitative information on the reaction kinetics. However, there are several factors that make modeling urethane formation kinetics complicated: (a) the number of competing side reactions of diisocyanate; (b) the relative reactivity of the isocyanate groups of the diisocyanate isomers; (c) different reactivity of the isocyanate groups towards the hydroxyl groups of the polyol and the monoalcohol; (d) the different families of polymers formed during step-growth polymerization (dimers, trimers, tetramers, etc.); (e) some reactants and products can catalyze different reaction steps (f) mass transfer limitations due to increase in bulk viscosity when reaching high molecular weights. All in all, to perform a detailed analysis that includes all chemical pathways and species formed, a range of advanced analytical techniques should be used to obtain information on the concentrations of the different reactive species and intermediates, which is beyond the scope of this work.

4.3.2.2. Application of transient temperature profiles with MW heating during the HEUR synthesis

While from a purely kinetic perspective MW heating does not offer a particular advantage during isothermal processing compared to CH, several recent approaches in the literature suggest that many organic reactions could proceed faster to higher product yields if the heating (and cooling) rate is increased, regardless of the heating source used.^{2,49} In this respect, the use of MW is advantageous over CH because the heat transfer rate in CH is limited by the thermal inertia of the heating fluid.² To test the effect of performing the HEUR synthesis with very rapid heating, increasing temperature profiles (at constant MW power) were tested to assess whether transient

temperature profiles could lead to desirable molecular weights in short reaction times. The latter are shown in Figure 4.10 in comparison with isothermal experiments performed with CH. The power levels of 200 and 400 W were selected based on preliminary tests of different constant power levels by assessing the resulting transient temperature profiles of the mixture (not shown here). Too high powers levels led to significant degradation, together with high molecular weight polymers, which featured very high viscosities, and were thus excluded from the analysis. Too low power levels led to insufficient temperature increase. Therefore, the power levels of 200 and 400 W were selected based on the trade-off between significant temperature increase, mixture processability and avoidance of degradation. Additionally, it is worth noting that the MW temperature profile at 200 W features an average temperature of 108 °C which is similar to the isothermal experiment at 110 °C, enabling an effective comparison.

Figure 4.10 (b) shows the molecular weight evolution of HEUR in constant reaction temperature experiments at 80 °C and 110 °C with CH. As can be seen from this figure, a higher reaction temperature leads to reaching the M_n plateau value (~21,000 g/mol) in shorter process times. As reported in our previous work, this M_n plateau value is the maximum HEURs molecular weight (M_n) at the stoichiometry used.²⁹ Regarding HEUR synthesis at 80 °C, the M_n plateau value is reached at 120 min, which is a representative process time when HEUR is synthesized at 80 °C in industrial batch reactors. The same M_n plateau value is reached at 45 min when HEUR is synthesized at 110 °C with CH.

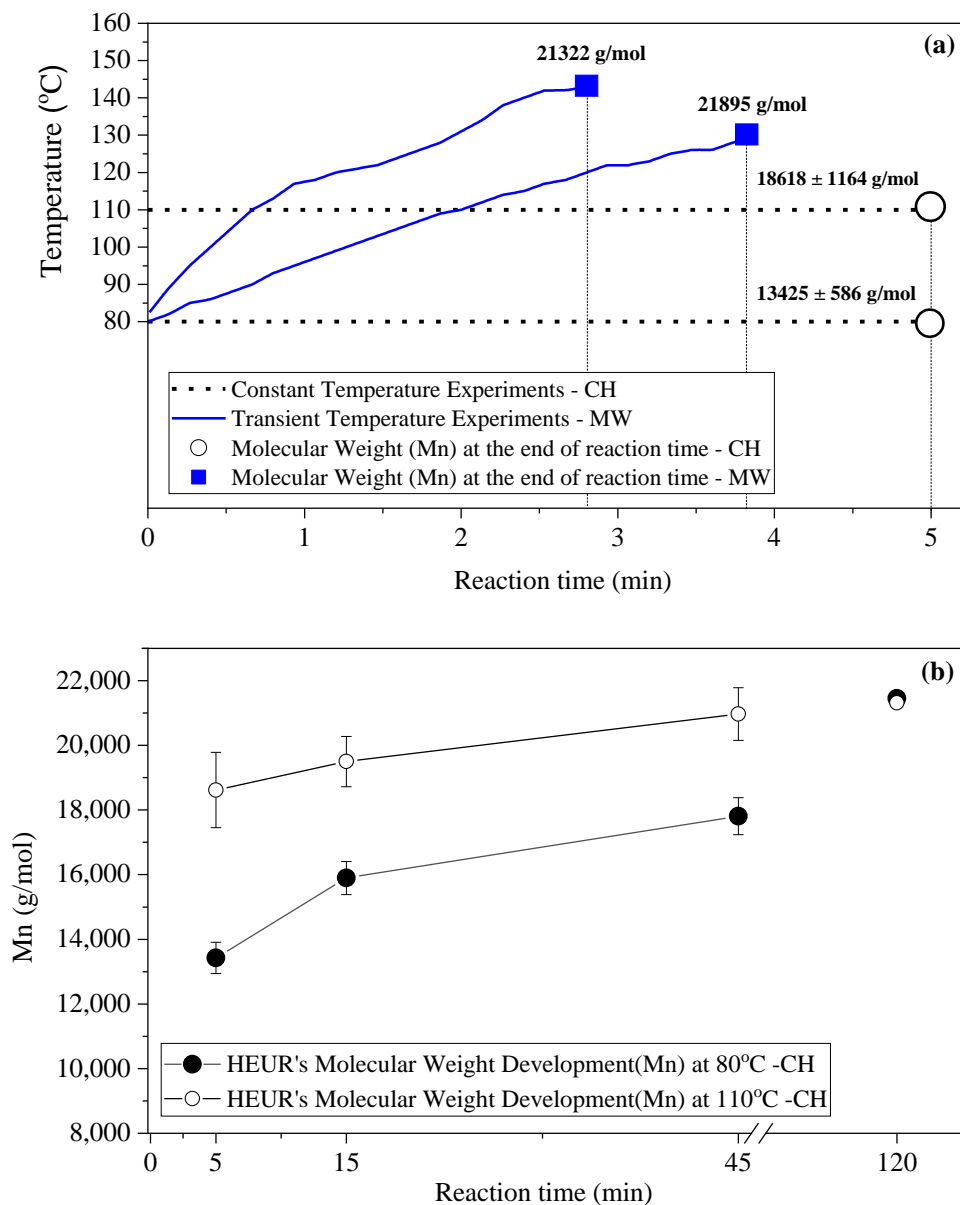


Figure 4.10. (a) Temperature profiles during HEUR synthesis under MW transient heating and CH with the final molecular weights obtained. The average applied power for the transient temperature profiles was 200 W and 400 W for the temperature ramps of 80-129 °C and 80-143 °C, respectively. **(b)** M_n of the produced HEURs obtained for reaction temperatures of 80 and 110 °C with CH. The results of the CH experiments are reproduced from our previous work²⁹ (CC BY-ND 4.0).

The transient temperature profiles obtained with constant MW power of 200 and 400 W are shown in Figure 4.10 (a). This Figure clearly shows that the application of MW to batch HEUR synthesis for less than 5 minutes resulted in a rapid thermal response of

the polymerization mixture, which within a few minutes reached temperature levels well above the nominal reaction temperature in industrial practice (80°C vs. 130-150°C with MW). As shown in Figure 4.10 (a) processing the reacting mixture under intense thermal conditions for short periods of time, as enabled by MWs, resulted in the production of HEURs with comparable molecular weights to those of the industrial product (in the order of 21,000 g/mol) at process times multifold lower compared to CH (4 min vs. 45 and 120 min at a temperature of 110 °C or 80 °C, respectively). This is achieved because the reactor is operating for certain periods of time at higher temperatures than CH, which have a greater impact on the reaction rate, overcompensating for the lower impact of the low temperature periods. Therefore, while the mean temperature of the two profiles is comparable, the “effective temperature” or mean kinetic temperature is higher in MW transient heating. In short, the observed increase in reaction rate during the application of transient temperature profiles is a result of the purely thermal effect of MW heating.

These results prove that regardless of the heating source used, the operation of the batch reactor for the HEUR synthesis in an unsteady-state operating window with transient temperature profiles can favor the polymerization to reach its M_n plateau values in shorter process times. However, due to the inherently slow heat transfer rate to the reactor when a heat transfer fluid is used, such rapid temperature transients cannot be easily attained under CH. In addition, due to the longer residence time of the monomers/reactive mixture at the reaction temperature with CH, such high temperatures achieved by MW heating cannot be used with CH, since the latter both compromise the thermal stability of PEG and favor isocyanate side reactions. In this way, MW is an effective enabling technology for the generation of unsteady state conditions in the batch HEUR synthesis leading to the production of high-quality HEUR in very short reaction times.

While the advantages of a transient heating profile were demonstrated here for batch operation, application of such operating regime goes beyond batch HEUR synthesis, and it could be envisioned as an enabling heating technology in novel continuous HEUR production e.g. via reactive extrusion. Reactive extrusion offers many advantages compared to batch synthesis, the most important in the HEUR case being the intensification of mixing, which helps to overcome the diffusion limitations

imposed by the increase in bulk viscosity in batch mode. Our results mentioned above regarding the thermal response under MW heating, renders MW technology suitable for application in continuous reactive extrusion processes, as the process time scales of the two technologies (MW and reactive extrusion) overlap for polyurethane synthesis (in the order of a few minutes). As such, the temporal transient temperature profiles presented here in a batch mode could mimic the spatial temperature profile of an extruder barrel, when the latter is irradiated with MW.

4.3.3. Estimation and comparison of the theoretical energy requirements for CH and MW heating HEUR synthesis

We have shown that using MW heating we can achieve process times multifold lower compared to CH. The latter applies both in the pretreatment of PEG and during the polymerization. However, a critical evaluation of the process also requires an evaluation of the total energy demand in the two heating modes when comparable mean temperatures are applied for the HEUR synthesis. The actual energy needed for the transformation in the two cases is compared to illustrate the potential of intensifying the HEUR process with MW heating and its conceptual advantage in terms of efficient coupling of MW energy to the polymer mixture. However, it must be emphasized that both lab setups used are not optimized for energy conversion and heat losses and their energy conversion efficiencies are expected to be low.

To simplify the comparison, the total energy requirements were evaluated based on the assumption that prior to the HEUR synthesis, PEG is received dehydrated and in solid form, therefore no vacuum pretreatment is required. Therefore, the transient temperature profile from 80 °C to 129 °C obtained by MW heating (mean temperature ~108 °C) is compared with the constant 110°C CH experiments. Considering this scenario, Table 4.3 is constructed to demonstrate the different energy flows required in the HEUR process.

Table 4.3. Energy input required for the HEUR synthesis with MW and CH

Type of heating	CH	MW
Energy required to heat up the heat transfer fluid	Q_{HF}	-
Energy required to melt PEG	ΔH_f	ΔH_f
Energy required for the HEUR synthesis <i>(in order to achieve the same M_n value)</i>	$Q_{R,CH}$	$Q_{R,MW}$

In the isothermal experiments the total energy required to heat up the oil from ambient temperature to the reaction temperature is calculated by:

$$Q_{HF} = m_{oil} c_{p,oil} (T_{R,CH} - T_A) \quad (1)$$

In Eq. (1), the properties of silicone oil flowing in the jacket of the reactor are, $c_{p,oil} = 1.68 \text{ Jg}^{-1}\text{K}^{-1}$; $\rho_{oil} = 0.89 \text{ gml}^{-1}$, $V_{jacket} = 260\text{mL}$. For the heat capacity and the density of the silicone oil, average values were used based on reported data over the considered temperature range (20 °C-120 °C).⁵¹ Additionally, in Equation (1), $T_{R,CH}$ is the temperature of the reaction mixture and T_A is the temperature of the surroundings.

The latent heat of fusion and the average specific heat capacity of PEG 8000 g/mol above its melting point are equal to: $\Delta H_f = 177.53 \text{ Jg}^{-1}$, $c_{p,PEG} = 16,725 \text{ Jmol}^{-1}\text{K}^{-1}$.⁵² The heat capacity of PEG is assumed to be constant for the tested temperature range since in the work of Yan Kou et al. (2019) the heat capacity of PEG8000 changed by only 2% when the temperature was increased from 72 °C to 127

Chapter 4

°C.⁵² The latent heat of fusion is an energy demand independent of the heating source used.

For the isothermal CH experiment at 110 °C, 45 minutes reaction time is needed to obtain HEURs with a M_n of around 21,000 g/mol as shown in Figure 4.10 (b). The energy required to carry out the isothermal reaction with CH using a thermal fluid corresponds to the total energy losses of the reactor to the environment during the reaction. In that case, $Q_{R,CH} = Q_{L,CH}$, where $Q_{L,CH}$ accounts for the total energy losses to the environment during the reaction with conventional heating. The total heat transferred from the reactor to the surroundings (heat losses) can be calculated from:

$$Q_{L,CH} = U (T_{R,CH} - T_A) t_{R,CH} \quad (2)$$

U [in W/K] is an average (reactor surface area) lumped heat transfer coefficient accounting for conduction and natural convection heat transfer from the glass reactor to the surroundings via the glass wall. In the conventional reactor setup, U has been determined by fitting the exponential decrease of the internal reactor's wall temperature when the oil bath was turned off (cooling curve). It was found to be ~0.15 W/K. Regarding the rest of the parameter values for the calculation of total heat transferred from the reactor to the surroundings: $T_{R,CH} = 110^\circ C$, $T_A = 25^\circ C$ and the reaction time $t_{R,CH} = 45$ min.

In the case of MW heated experiments, the energy required to perform the reaction with a transient temperature profile includes the sensible heat required to raise the temperature during the reaction and the energy required to compensate for the heat losses to the surroundings. In that case, $Q_{R,MW} = Q_{abs} + Q_{L,MW}$, where $Q_{L,MW}$ accounts for the energy required to compensate for the heat losses to the surroundings. The electromagnetic energy converted into heat in the sample is partially absorbed by the sample itself increasing its temperature and thus, its sensible heat Q_{abs} and partially lost to the surroundings via heat conduction and convection. Q_{abs} is calculated by:

$$Q_{abs} = \int_{T_{R,0}}^{T_{R,f}} m_{HEUR} c_{p,HEUR} dT \quad (3)$$

Chapter 4

In Eq. (3), $T_{R,0}$ and $T_{R,f}$ is the initial and final reaction temperature of the transient temperature profile. Since there is no experimental or calculated data on the HEUR specific heat capacity, the latter is approximated by the specific heat capacity of PEG. The total heat transferred from the bulk to the surroundings (heat losses) for the MW heated experiments can be calculated from:

$$Q_{l,MW} = \int_{t_{R,0}}^{t_{R,f}} U(T(t) - T_A) dt \quad (4)$$

In Eq. (4), $t_{R,0}$ and $t_{R,f}$ is the initial and final reaction time of the transient temperature profile. U [in W/K] is an average (reactor surface area) lumped heat transfer coefficient accounting for conduction and natural convection heat transfer from the glass reactor to the surroundings via the glass wall. In the MW cavity, U has been determined, by fitting the exponential decrease in the PEG's temperature when the MW power is off (cooling curve). It was found to be ~ 0.18 W/K. The latter agrees with previously reported values for the average lumped heat transfer coefficient in glass reactor experiments in multimode MW cavities.³⁰ The definite integral in Equation 4 was calculated numerically via the quadrature method. As previously stated for the HEUR synthesis with MW, the transient temperature profile considered for the analysis is that starting from 80°C to 129°C with a total reaction time of 3.8 minutes.

The total energy requirements for the two modes of heating are presented in Table 4.4. Q_P (kJ) accounts for the total energy requirements of the process.

Table 4.4. Calculated energy requirements for the HEUR synthesis with MW and CH.

Type of heating	CH	MW
Q_{HF} (kJ)	33.3	-
ΔH_f (kJ)	8.9	8.9

Q_R	Q_l (kJ)	34.4	13.1
	Q_{abs} (kJ)	-	5.1
Q_P (kJ)		76.6	27.1

The results presented in Table 4.4 show that using CH to produce HEURs with $M_n \sim 21,000$ g/mol requires approximately three times more energy than MW-irradiated synthesis, mainly due to longer process times and additional energy requirements to heat up the heat transfer fluid.

It must be emphasized that the energy conversion efficiencies for the two heating modes (MW, CH) are not reported here as the lab setups used are not optimized for energy conversion and heat losses and these efficiencies are expected to be low. Rather, the actual energy needed for the transformation in the two cases was compared to illustrate the potential of intensifying the HEUR process with MW heating and its conceptual advantage in terms of efficient coupling of MW energy to the polymer mixture. In this context, this information gives a good estimate of the importance of the respective energy consumption values of MW technology regarding industrial practice.

From the operational point of view, higher energy utilization efficiency under MW heating in multimode cavities can be attained by operating at alternative operating frequencies (up to 85% electric-to-MW power efficiency at 915 MHz) and by optimizing the geometric and structural characteristics of the reactor containing the heated load and the resonant cavity, the design and effectiveness of the impedance matching circuit and the dielectric properties of the bulk.^{30,53–58} In addition, scale-up of MW assisted synthesis can take place using either novel, non-cavity based, reactor designs, such as internal transmission line technology fed by solid state generators or continuous flow MW reactors.^{13,55,59}

Collectively, from the operational point of view to fully utilize the effectiveness of MWs, they should be boldly advocated for use in reactions by applying transient temperature profiles for short reaction times in order to minimize heat losses due to long processing times. In the long-term, the potential of using renewable energy sources to power MW (MW) devices (cavities or MW transmitting antennas) makes the technology even more attractive, and potentially addressing the problem of low conversion efficiency of the expensive electrical energy into electromagnetic energy by the magnetron.^{13,60}

4.4. CONCLUSIONS

We investigated for the first time, the effects of MW heating on batch hydrophobically modified ethoxylated urethanes (HEURs) synthesis using polyethylene glycol 8000 g/mol, HMDI and 1-octanol considering all relevant pretreatment and reaction steps. To achieve this, MW heated experiments in a multimode MW cavity were compared with their oil-bath CH counterparts. During the reactant pretreatment step, MW heating can reduce the overall process time through tenfold faster melting of solid PEG. However, in the subsequent PEG dehydration step, use of MWs should be avoided, as faster degradation of PEG was observed compared to the dehydration by CH at a similar bulk temperature. In the polymerization reaction, it was shown that both polymer molecular weight, M_n , and polydispersity index, PDI, of the HEUR prepolymer are independent of the heating source used, as no significant differences are found for either when the same reaction temperature was used.

However, it was concluded that the operation of the batch reactor in a rapid unsteady-state transient temperature profile, only attainable with MW heating, resulted in the production of HEURs with comparable molecular weights as to those produced via isothermal CH experiments at process times multifold lower (4 min vs. 45 or 120 min at a temperature of 110 °C or 80 °C, respectively), due to the rapid thermal response of the polymerization mixture under MW irradiation. An energy analysis and comparison of the transient MW profile versus the CH isothermal one (at comparable mean temperatures) shows that the former needs approximately 3 times less energy to achieve the same molecular weight polymer, due to shorter processing times (and subsequent lower heat losses to the surroundings) and the elimination of the additional energy

needed to heat the transfer fluid. An additional advantage of such novel process operating window is that it can be combined with (low residence time) continuous processing options for polymerizations, such continuous reactive extruders, in which the temporal transient temperature profile can be easily mimicked by a spatial one enabled by MW heating. Overall, our study underscores the potential of MW heating in intensifying HEURs synthesis, a polymerization process with significant industrial relevance.

References

- (1) Quienne, B.; Pinaud, J.; Robin, J. J.; Caillol, S. From Architectures to Cutting-Edge Properties, the Blooming World of Hydrophobically Modified Ethoxylated Urethanes (HEURs). *Macromolecules* **2020**, *53* (16), 6754–6766. <https://doi.org/10.1021/acs.macromol.0c01353>.
- (2) Stefanidis, G. D.; Muñoz, A. N.; Sturm, G. S. J.; Stankiewicz, A. A Helicopter View of Microwave Application to Chemical Processes: Reactions, Separations, and Equipment Concepts. *Reviews in Chemical Engineering*. Walter de Gruyter GmbH 2014, pp 233–259. <https://doi.org/10.1515/revce-2013-0033>.
- (3) Jeon, S.; Kim, J.; Yang, D. Design of Large-Scale Microwave Cavity for Uniform and Efficient Plastic Heating. *Polymers (Basel)*. **2022**, *14* (3). <https://doi.org/10.3390/polym14030541>.
- (4) Komorowska-Durka, M.; Dimitrakis, G.; Bogdał, D.; Stankiewicz, A. I.; Stefanidis, G. D. A Concise Review on Microwave-Assisted Polycondensation Reactions and Curing of Polycondensation Polymers with Focus on the Effect of Process Conditions. *Chemical Engineering Journal*. Elsevier March 5, 2015, pp 633–644. <https://doi.org/10.1016/j.cej.2014.11.087>.
- (5) Stankiewicz, A. Energy Matters: Alternative Sources and Forms of Energy for Intensification of Chemical and Biochemical Processes. *Chem. Eng. Res. Des.* **2006**, *84* (7 A), 511–521. <https://doi.org/10.1205/cherd.05214>.
- (6) Hargreaves, G.; Buttress, A.; Dimitrakis, G.; Dodds, C. The Importance of Ionic

- Conduction in Microwave Heated Polyesterifications. *React. Chem. Eng.* **2019**.
<https://doi.org/10.1039/C9RE00313D>.
- (7) Kalamiotis, A.; Ilchev, A.; Irvine, D. J.; Dimitrakis, G. Sensors and Actuators B: Chemical Optimised Use of Dielectric Spectroscopy at Microwave Frequencies for Direct Online Monitoring of Polymerisation Reactions. *Sensors Actuators B. Chem.* **2019**, *290* (March), 34–40. <https://doi.org/10.1016/j.snb.2019.03.120>.
- (8) D. Bodgal. *Microwave-Assisted Organic Synthesis: One Hundred Reaction Procedures*, 1st ed.; Elsevier Science, 2006.
- (9) Ge, X.; Li, H.; Liu, M.; Zhao, Z.; Jin, X.; Fan, X. Microwave-Assisted Catalytic Alcoholysis of Fructose to Ethoxymethylfurfural (EMF) over Carbon-Based Microwave-Responsive Catalyst. *Fuel Process. Technol.* **2022**, *233* (April), 107305. <https://doi.org/10.1016/j.fuproc.2022.107305>.
- (10) Bogdal, D.; Bednarz, S.; Marcin, Ł.; Kasprzyk, W. Chemical Engineering & Processing : Process Intensification of Oxidation and Epoxidation Reactions — Microwave vs . Conventional Heating. **2018**, *132* (July), 208–217. <https://doi.org/10.1016/j.cep.2018.09.003>.
- (11) Lyu, X.; Li, H.; Xiang, H.; Mu, Y.; Ji, N.; Lu, X.; Fan, X. Energy Efficient Production of 5-Hydroxymethylfurfural (5-HMF) over Surface Functionalized Carbon Superstructures under Microwave Irradiation. **2022**, *428* (July 2021), 1–10.
- (12) Li, H.; Zhao, Z.; Xiouras, C.; Stefanidis, G. D.; Li, X.; Gao, X. Fundamentals and Applications of Microwave Heating to Chemicals Separation Processes. *Renew. Sustain. Energy Rev.* **2019**, *114*, 109316. <https://doi.org/10.1016/J.RSER.2019.109316>.
- (13) Komorowska-Durka, M.; Loo, M. B. t.; Sturm, G. S. J.; Radoiu, M.; Oudshoorn, M.; Van Gerven, T.; Stankiewicz, A. I.; Stefanidis, G. D. Novel Microwave Reactor Equipment Using Internal Transmission Line (INTLI) for Efficient

- Liquid Phase Chemistries: A Study-Case of Polyester Preparation. *Chem. Eng. Process. Process Intensif.* **2013**, *69*, 83–89. <https://doi.org/10.1016/j.cep.2013.03.003>.
- (14) Nagahata, R.; Takeuchi, K. Encouragements for the Use of Microwaves in Industrial Chemistry. *Chem. Rec.* **2019**, *19* (1), 51–64. <https://doi.org/10.1002/tcr.201800064>.
- (15) Nguyen, N. T.; Greenhalgh, E.; Kamaruddin, M. J.; El, J.; Carmichael, K.; Dimitrakis, G.; Kingman, S. W.; Robinson, J. P.; Irvine, D. J. Understanding the Acceleration in the Ring-Opening of Lactones Delivered by Microwave Heating Q. **2014**, *70*, 996–1003. <https://doi.org/10.1016/j.tet.2013.11.031>.
- (16) Bogdal, D.; Lukasiewicz, M.; Pielichowski, J.; Bednarz, S. Microwave-Assisted Epoxidation of Simple Alkenes in the Presence of Hydrogen Peroxide. <https://doi.org/10.1080/00397910500278479> **2006**, *35* (23), 2973–2983. <https://doi.org/10.1080/00397910500278479>.
- (17) Adlington, K.; McSweeney, R.; Dimitrakis, G.; Kingman, S. W.; Robinson, J. P.; Irvine, D. J. Enhanced ‘in Situ’ Catalysis via Microwave Selective Heating: Catalytic Chain Transfer Polymerisation. *RSC Adv.* **2014**, *4* (31), 16172–16180. <https://doi.org/10.1039/C4RA00907J>.
- (18) Kasprzyk, W.; Galica, M.; Bednarz, S. Microwave-Assisted Oxidation of Alcohols Using Zinc Polyoxometalate. **2014**, 2757–2761. <https://doi.org/10.1055/s-0034-1379211>.
- (19) Mu, S.; Liu, K.; Li, H.; Zhao, Z.; Lyu, X.; Jiao, Y.; Li, X.; Gao, X.; Fan, X. Microwave-Assisted Synthesis of Highly Dispersed ZrO₂ on CNTs as an Efficient Catalyst for Producing 5-Hydroxymethylfurfural (5-HMF). *Fuel Process. Technol.* **2022**, *233* (April), 107292. <https://doi.org/10.1016/j.fuproc.2022.107292>.
- (20) Ou, X.; Tomatis, M.; Lan, Y.; Jiao, Y.; Chen, Y.; Guo, Z.; Gao, X.; Wu, T.; Wu,

- C.; Shi, K.; Azapagic, A.; Fan, X. A Novel Microwave-Assisted Methanol-to-Hydrocarbons Process with a Structured ZSM-5/SiC Foam Catalyst: Proof-of-Concept and Environmental Impacts. *Chem. Eng. Sci.* **2022**, *255*, 117669. <https://doi.org/10.1016/j.ces.2022.117669>.
- (21) Valério, A.; Fortuny, M.; Santos, A. F.; Araújo, P. H. H.; Sayer, C. Poly(Urea-Urethane) Synthesis by Miniemulsion Polymerization Using Microwaves and Conventional Polymerization. *Macromol. React. Eng.* **2015**, *9* (1), 48–59. <https://doi.org/10.1002/mren.201400029>.
- (22) Jullien, H.; Valot, H. Polyurethane Curing by a Pulsed Microwave Field. *Polymer (Guildf)*. **1985**, *26* (4), 506–510. [https://doi.org/10.1016/0032-3861\(85\)90149-1](https://doi.org/10.1016/0032-3861(85)90149-1).
- (23) Biswas, A.; Appell, M.; Liu, Z.; Cheng, H. N. Microwave-Assisted Synthesis of Cyclodextrin Polyurethanes. *Carbohydr. Polym.* **2015**, *133*, 74–79. <https://doi.org/10.1016/j.carbpol.2015.06.044>.
- (24) Cheng, H. N.; Biswas, A.; Kim, S.; Appell, M.; Furtado, R. F.; Bastos, M. do S. R.; Alves, C. R. Synthesis and Analysis of Lactose Polyurethanes and Their Semi-Interpenetrating Polymer Networks. *Int. J. Polym. Anal. Charact.* **2022**, *27* (4), 266–276. <https://doi.org/10.1080/1023666X.2022.2064037>.
- (25) Prociak, A.; Michałowski, S.; Bąk, S. Thermoplastic Polyurethane Foamed under Microwave Irradiation. *Polimery/Polymers* **2012**, *57* (11–12), 786–790. <https://doi.org/10.14314/polimery.2012.786>.
- (26) Hiroki, K.; Ichikawa, Y.; Yamashita, H.; Sugiyama, J. I. Rapid Microwave-Promoted Synthesis of Polyurethanes from a Fluorene Unit-Containing Diol and Diisocyanates. *Macromol. Rapid Commun.* **2008**, *29* (10), 809–814. <https://doi.org/10.1002/marc.200700883>.
- (27) Lee, H.; Fang, C. Y.; Pantano, C. G.; Kang, W. Microwave Effect on Curing of Waterborne Polyurethane. *Bull. Korean Chem. Soc.* **2011**, *32* (3), 961–963.

- <https://doi.org/10.5012/bkcs.2011.32.3.961>.
- (28) Kucińska-Lipka, J.; Sienkiewicz, M.; Gubanska, I.; Zalewski, S. Microwave Radiation in the Synthesis of Urethane Prepolymers. *Eur. Polym. J.* **2017**, *88*, 126–135. <https://doi.org/10.1016/j.eurpolymj.2017.01.017>.
- (29) Bampouli, A.; Tzortzi, I.; Schutter, A. De; Xenou, K.; Michaud, G.; Stefanidis, G. D.; Gerven, T. Van. Insight Into Solventless Production of Hydrophobically Modified Ethoxylated Urethanes (HEURs): The Role of Moisture Concentration , Reaction Temperature , and Mixing Efficiency. *ACS Omega* **2022**, No. int. <https://doi.org/10.1021/acsomega.2c04530>.
- (30) Komorowska, M.; Stefanidis, G. D.; Van Gerven, T.; Stankiewicz, A. I. Influence of Microwave Irradiation on a Polyesterification Reaction. *Chem. Eng. J.* **2009**, *155* (3), 859–866. <https://doi.org/10.1016/j.cej.2009.09.036>.
- (31) Barmar, M.; Ribitsch, V.; Kaffashi, B.; Barikani, M.; Sarreshtehdari, Z.; Pfragner, J. Influence of Prepolymers Molecular Weight on the Viscoelastic Properties of Aqueous HEUR Solutions. *Colloid Polym. Sci.* **2004**, *282* (5), 454–460. <https://doi.org/10.1007/s00396-003-0968-0>.
- (32) Choi, J.; Sohn, D.; Lee, Y.; Cheong, C. Self-Diffusion of Hydrophobically End-Capped Polyethylene Oxide Urethane Resin by Using Pulsed-Gradient Spin Echo NMR Spectroscopy. *Macromol. Res.* **2003**, *11* (6), 444–450. <https://doi.org/10.1007/BF03218974>.
- (33) Zhao, X.; Qi, Y.; Li, K.; Zhang, Z. Hydrogen Bonds and FTIR Peaks of Polyether Polyurethane-Urea. *Key Eng. Mater.* **2019**, *815 KEM*, 151–156. <https://doi.org/10.4028/www.scientific.net/KEM.815.151>.
- (34) Najafi, F.; Pishvaei, M. Synthesis and Characterization of a Nonionic Urethane-Based Thickener. *Prog. Color. Color. coatings* **2011**, *4*, 71–77.
- (35) Arnould, P.; Bosco, L.; Sanz, F.; Simon, F. N.; Fouquay, S.; Michaud, G.; Raynaud, J.; Monteil, V. Identifying Competitive Tin-or Metal-Free Catalyst

- Combinations to Tailor Polyurethane Prepolymer and Network Properties. *Polym. Chem.* **2020**, *11* (36), 5725–5734. <https://doi.org/10.1039/d0py00864h>.
- (36) Špírková, M.; Kubín, M.; Dušek, K. Side Reactions in the Formation of Polyurethanes: Stability of Reaction Products of Phenyl Isocyanate. *J. Macromol. Sci. Part A - Chem.* **1990**, *27* (4), 509–522. <https://doi.org/10.1080/00222339009349572>.
- (37) Heintz, A. M.; Duffy, D. J.; Hsu, S. L.; Suen, W.; Chu, W.; Paul, C. W. Effects of Reaction Temperature on the Formation of Polyurethane Prepolymer Structures. *Macromolecules* **2003**, *36* (8), 2695–2704. <https://doi.org/10.1021/ma021559h>.
- (38) Ginsburg, E. J.; Stephens, D. A.; West, P. R.; Buko, A. M.; Robinson, D. H.; Li, L. C.; Bommireddi, A. R. Identification of a Yellow Impurity in Aged Samples of Aqueous Butamben Suspension: Evidence for the Oxidative Degradation of Poly(Ethylene Glycol). *J. Pharm. Sci.* **2000**, *89* (6), 766–770. [https://doi.org/10.1002/\(SICI\)1520-6017\(200006\)89:6<766::AID-JPS8>3.0.CO;2-N](https://doi.org/10.1002/(SICI)1520-6017(200006)89:6<766::AID-JPS8>3.0.CO;2-N).
- (39) Khan, J. A.; He, X.; Khan, H. M.; Shah, N. S.; Dionysiou, D. D. Oxidative Degradation of Atrazine in Aqueous Solution by UV / H₂O₂ / Fe²⁺, Processes : A Comparative Study. *Chem. Eng. J.* **2013**, *218* (ii), 376–383.
- (40) Voorhees, K. J.; Baugh, S. F.; Stevenson, D. N. An Investigation of the Thermal Degradation of Poly(Ethylene Glycol). *J. Anal. Appl. Pyrolysis* **1994**, *30* (1), 47–57. [https://doi.org/10.1016/0165-2370\(94\)00803-5](https://doi.org/10.1016/0165-2370(94)00803-5).
- (41) Lattimer, R. P. Mass Spectral Analysis of Low-Temperature Pyrolysis Products from Poly(Ethylene Glycol). *J. Anal. Appl. Pyrolysis* **2000**, *56* (1), 61–78.
- (42) Auguścik, M.; Kurańska, M.; Prociak, A.; Karalus, W.; Lipert, K.; Ryszkowska, J. Production and Characterization of Poly(Urea-Urethane) Elastomers Synthesized from Rapeseed Oil-Based Polyols Part I. Structure and Properties. *Polimery/Polymers* **2016**, *61* (7–8), 490–498.

- <https://doi.org/10.14314/polimery.2016.490>.
- (43) Delpech, M. C.; Miranda, G. S. Waterborne Polyurethanes: Influence of Chain Extender in FTIR Spectra Profiles. *Cent. Eur. J. Eng.* **2012**, *2* (2), 231–238. <https://doi.org/10.2478/s13531-011-0060-3>.
- (44) Vrandečić, N. S.; Erceg, M.; Jakić, M.; Klarić, I. Kinetic Analysis of Thermal Degradation of Poly(Ethylene Glycol) and Poly(Ethylene Oxide)s of Different Molecular Weight. *Thermochim. Acta* **2010**, *498* (1–2), 71–80. <https://doi.org/10.1016/j.tca.2009.10.005>.
- (45) Yilgör, E.; Burgaz, E.; Yurtsever, E.; Yilgör, I. Comparison of Hydrogen Bonding in Polydimethylsiloxane and Polyether Based Urethane and Urea Copolymers. *Polymer (Guildf)*. **2000**, *41* (3), 849–857. [https://doi.org/10.1016/S0032-3861\(99\)00245-1](https://doi.org/10.1016/S0032-3861(99)00245-1).
- (46) Teo, L. S.; Chen, C. Y.; Kuo, J. F. Fourier Transform Infrared Spectroscopy Study on Effects of Temperature on Hydrogen Bonding in Amine-Containing Polyurethanes and Poly(Urethane-Urea)s. *Macromolecules* **1997**, *30* (6), 1793–1799. <https://doi.org/10.1021/ma961035f>.
- (47) Mattia, J.; Painter, P. A Comparison of Hydrogen Bonding and Order in a Polyurethane and Poly(Urethane-Urea) and Their Blends with Poly(Ethylene Glycol). *Macromolecules* **2007**, *40* (5), 1546–1554. <https://doi.org/10.1021/ma0626362>.
- (48) Stern, T. Conclusive Chemical Deciphering of the Consistently Occurring Double-Peak Carbonyl-Stretching FTIR Absorbance in Polyurethanes. *Polym. Adv. Technol.* **2019**, *30* (3), 675–687. <https://doi.org/10.1002/pat.4503>.
- (49) Strauss, C. R.; Rooney, D. W. Accounting for Clean, Fast and High Yielding Reactions under Microwave Conditions. *Green Chem.* **2010**, *12* (8), 1340–1344. <https://doi.org/10.1039/c0gc00024h>.
- (50) Kappe, C. O.; Pieber, B.; Dallinger, D. Microwave Effects in Organic Synthesis:

- Myth or Reality? *Angew. Chemie - Int. Ed.* **2013**, *52* (4), 1088–1094. <https://doi.org/10.1002/anie.201204103>.
- (51) Dow Corning Corporation. *SYLTHERM 800 Heat Transfer Fluid: Product Technical Data*; 1997. <https://doi.org/http://www.dow.com/heattrans>.
- (52) Kou, Y.; Wang, S.; Luo, J.; Sun, K.; Zhang, J.; Tan, Z.; Shi, Q. Thermal Analysis and Heat Capacity Study of Polyethylene Glycol (PEG) Phase Change Materials for Thermal Energy Storage Applications. *J. Chem. Thermodyn.* **2019**, *128*, 259–274. <https://doi.org/10.1016/j.jct.2018.08.031>.
- (53) Sturm, G. S. J.; Verweij, M. D.; Stankiewicz, A. I.; Stefanidis, G. D. Microwaves and Microreactors: Design Challenges and Remedies. *Chem. Eng. J.* **2014**, *243*, 147–158. <https://doi.org/10.1016/J.CEJ.2013.12.088>.
- (54) Sturm, G. S. J.; Verweij, M. D.; Gerven, T. Van; Stankiewicz, A. I.; Stefanidis, G. D. On the Parametric Sensitivity of Heat Generation by Resonant Microwave Fields in Process Fluids. *Int. J. Heat Mass Transf.* **2013**, *57* (1), 375–388. <https://doi.org/10.1016/J.IJHEATMASSTRANSFER.2012.09.037>.
- (55) Xiouras, C.; Radacsi, N.; Sturm, G.; Stefanidis, G. D. Furfural Synthesis from D-Xylose in the Presence of Sodium Chloride: Microwave versus Conventional Heating. *ChemSusChem* **2016**, *9* (16), 2159–2166. <https://doi.org/10.1002/cssc.201600446>.
- (56) Moseley, J. D.; Woodman, E. K. Energy Efficiency of Microwave- And Conventionally Heated Reactors Compared at Meso Scale for Organic Reactions. *Energy and Fuels* **2009**, *23* (11), 5438–5447. <https://doi.org/10.1021/ef900598m>.
- (57) Kempe, K.; Becer, C. R.; Schubert, U. S. Microwave-Assisted Polymerizations: Recent Status and Future Perspectives. *Macromolecules*. August 9, 2011, pp 5825–5842. <https://doi.org/10.1021/ma2004794>.
- (58) Bermúdez, J. M.; Beneroso, D.; Rey-Raap, N.; Arenillas, A.; Menéndez, J. A.

- Energy Consumption Estimation in the Scaling-up of Microwave Heating Processes. *Chem. Eng. Process. Process Intensif.* **2015**, *95*, 1–8. <https://doi.org/10.1016/j.cep.2015.05.001>.
- (59) Chen, F.; Chen, X.; Warning, A.; Zhu, H. Understanding of Microwave Heating in a Novel Designed Cavity with Monopole Antennas. *Int. J. Appl. Electromagn. Mech.* **2016**, *51* (2), 119–129. <https://doi.org/10.3233/JAE-150123>.
- (60) Chen, T. Y.; Baker-Fales, M.; Vlachos, D. G. Operation and Optimization of Microwave-Heated Continuous-Flow Microfluidics. *Ind. Eng. Chem. Res.* **2020**, *59* (22), 10418–10427. <https://doi.org/10.1021/acs.iecr.0c01650>.

**Tailoring Waterborne Coatings
Rheology with Hydrophobically Modified
Ethoxylated Urethanes (HEURs):
Molecular Architecture Insights Supported
by CG-MD Simulations**

ⁱ This chapter is under review as:

Ioanna Tzortzi, Imane Joundi, Michail Kavousanakis, Theodora Spyriouni, Ariana Bampouli, Guillaume Michaud, Tom Van Gerven, G. D. S. *“Tailoring Waterborne Coatings Rheology with Hydrophobically Modified Ethoxylated Urethanes (HEURs): Molecular Architecture Insights Supported by CG-MD Simulations” (under review)*

ABSTRACT

A novel investigation of the effects of the hydrophilic and hydrophobic segments of Hydrophobically Modified Ethoxylated Urethanes (HEURs) on the rheological properties of their aqueous solutions, latex-based emulsions, and waterborne paints is demonstrated. Different HEUR thickeners were produced by varying the polyethylene glycol (PEG) molecular weight and terminal hydrophobic size. Results reveal that the strength of hydrophobic associations and, consequently, the rheological properties of HEUR formulations can be effectively controlled by modifying the structure of hydrophobic segment, specifically, the combination of diisocyanate and mono-alcohol. This allows for on demand attainment of diverse rheological behaviors ranging from predominantly Newtonian profiles exhibiting lower viscosities to markedly pseudoplastic behaviors with significantly higher viscosities. The length of the hydrophilic group appears to affect viscosity only marginally up to a molecular weight of 23,000 g/mol, with more notable effects at 33,000 g/mol. Additionally, it was indicated that the rheological responses observed in water solutions provide a reliable forecast of their behavior in latex-based emulsions and waterborne paints. Coarse-grained molecular dynamics (CG-MD) simulations were also applied to gain insight into HEUR micelle dynamics in aqueous solutions. Guided by the DBSCAN algorithm, the simulations successfully captured the concentration-dependent behavior and the impact of hydrophilic chain length, aligning with experimental viscosity trends. Various metrics were employed to provide a comprehensive analysis of the micellization process, including the hydrophobic cluster volume, the total micellar volume, the aggregation number, and the number of interconnecting chains with other micelles.

5.1. INTRODUCTION

Waterborne coatings, prevalent in both commercial and residential sectors, owe their unique characteristics to their complex formulation that contain various components like thickeners, latex, dispersing agents, pigments, surfactants, and other ingredients.¹⁻³ The rheological behavior of these paints is dictated by the synergistic interactions among these ingredients. Therefore, the optimization of the ingredient selection at minimum cost is challenging, and understanding of the role of raw materials used and their interactions is essential, as compositional and chemical variations can significantly affect the end product.⁴

In this context, rheology modifiers (or viscosity thickeners), exert significant influence on the rheological properties of waterborne dispersions, despite their relatively low concentration in the paint formulation (1 to 3 wt%).^{1-3,5-7} Among various rheology modifiers, hydrophobically modified ethoxylated urethanes (HEUR) constitute a specific class of non-ionic associative thickeners. They are extensively employed in waterborne paints, inks, emulsions, and coatings due to their superior performance attributes, including excellent flow, leveling, spatter and water resistance and pH insensitivity. Owing to their amphiphilic polymer structure, HEURs facilitate the formation of dynamic transient networks with hydrophobic components like surfactants, latex, and pigments⁸⁻¹⁵, while the structural composition of the employed HEUR can lead to either Newtonian or pseudoplastic rheological behavior in the final product.¹⁶⁻¹⁸

Research on the rheological behavior of HEURs in waterborne systems has mostly focused on investigating the rheology of HEURs in aqueous media, both in the absence and presence of surfactants.^{19,20,29,21-28} These studies aim to assess the effect of various factors, such as the size of hydrophilic and hydrophobic segment, temperature, concentration, and molecular weight distribution of HEUR and the interaction with surfactants. Further, relevant research activity has been extended to examine the rheology and stability of latex emulsions thickened with HEURs, focusing on the effect of latex monomer composition, particle size distribution, surface charge and hydrophobicity.^{6,13,30-37} Bridging mechanisms and associations between HEURs and latex particles have also been studied, particularly focusing on the adsorption of

hydrophobic segments, interparticle bridging and loop formation.^{12,38,39} Despite this extensive research, only few studies have transitioned these findings to waterborne paint formulations^{2,3,9,40}; therefore, a comprehensive analysis linking the HEUR rheological behavior across aqueous solutions, latex-based emulsions and paint formulations is missing. At the same time, the methods for optimizing rheological properties in waterborne dispersions in the industry rely almost exclusively on trial-and-error processes and the experience of formulators, underscoring the necessity for more standardized approaches.

To address the existing knowledge gap in both the scientific and industrial domain, our research analyzes the effects of hydrophilic and hydrophobic segments of HEURs across various waterborne dispersions, including aqueous solutions, latex-based emulsions and commercial waterborne paint formulations. The primary objective is to establish a structure-rheology relationship for HEURs, facilitating the transition from empirical methods to evidence-based optimization of rheological performance in waterborne dispersions. The approach to that end is three-fold. First, we study how different HEUR structures affect the viscosity profile of their aqueous solutions combining experimental methods (Section 5.3.2.1.) and simulation techniques (Section 5.3.2.2.). Steady shear rheological measurements were used to assess the effect of concentration and HEUR structure, complemented by extensive coarse grained MD simulations. These simulations quantify the self-assembly process of HEUR molecules as a function of their structure and thickener concentration using metrics such as the hydrophobic cluster volume, the total micellar volume, the aggregation number (N_{agg}), and the number of interconnecting chains (N_{bridged}) with another hydrophobic cluster. In Section 5.3.3, we integrate the aqueous HEUR solutions from Section 5.3.2.1 into waterborne latex-based emulsions. We examine the effects of HEUR's hydrophilic and hydrophobic segments on emulsion viscosity and underscore the critical role of HEUR's hydrophilic length in the emulsion's phase stability. Finally, in Section 5.3.4, we extend our investigation to waterborne paint formulations, specifically examining how the HEUR structure influences the balance between Newtonian and pseudoplastic rheological behaviors. Given that real world dispersions typically use a mix of HEUR thickeners, identifying optimal structures for levelling and sagging is crucial. For this reason, we link the findings with this particular paint performance. Overall, our research

probes how HEUR's chemical composition impacts rheological behaviors across diverse waterborne dispersions, ranging from aqueous solutions to waterborne coatings.

5.2. MATERIALS, METHODS AND MD SIMULATIONS

5.2.1. Materials

Polyethylene glycol of molecular weight 8000 g/mol with purity of >99.5% was provided by Clariant. H₁₂MDI (4,4-Methylenebis (cyclohexyl isocyanate), mixture of isomers, 90% purity from Acros Organics and 1-Octanol (99% purity) from Alfa Aesar were used as received. Bismuth carboxylate (KKAT XCB221), provided by King Industries, was used as the catalyst. Chloroform (>99.8% purity) stabilized with amylene was purchased from Fisher Chemicals and was dried using 4Å molecular sieves. Acrylic polymer latex emulsion (the solid content is 50%, the particle size is 200 nm and $\eta_{Latex} = 60 \text{ mPa} \cdot \text{s}$ measured at 23 °C with a Brookfield viscometer) and the satin paint base was provided by Arkema group. All reagents were of analytical grade and used without further purification.

5.2.2. Synthesis of HEUR-X and formulation in water

The one-step HEUR synthesis was performed in bulk from the reaction of PEG, a diisocyanate and a mono-alcohol. For all cases, 250 g PEG were initially melted in a conventionally heated reactor where a vacuum pretreatment step was applied limiting the moisture of PEG to 500 ppm. In all experiments, the reaction temperature was 85 °C, the reaction time was 60 min, and the catalyst concentration was set to 0.01% based on the total mass of the reactive mixture. Based on the findings of our previous work⁴², for the one-step HEUR synthesis we utilized a HMDI/PEG ratio of 1.5 and Octanol/PEG of 1. At this reaction stoichiometry, our one-step synthesis maximizes HEUR molecular weight by effectively tripling the molecular weight of the utilized PEG, ensuring complete end-capping. After completion of the polymerization, the entire polymer content of the reactor was diluted with water in 20% w/w solutions by adding water to the reactor, without carrying out prior purification steps in the polymer melt. The water-based HEUR formulations were obtained by stirring the mixture overnight, which resembles an industrial practice for the formulation of a thickener product.

5.2.3. Preparation of the HEUR-latex based emulsion and full paint formulation

Latex-HEUR-X dispersions were prepared following a precise recipe. Initially, 161 g of latex was subjected to gentle homogenization using a submerged stirrer. Subsequently, 45 g of distilled water was added to the mixture. The pH of the dispersion was carefully adjusted by dropwise addition of 28% ammonia solution until it reached a target range of 8.5 to 8.8. Following pH adjustment, 24 g of a 20% aqueous solution of HEUR were introduced to the dispersion, and the mixture was vigorously stirred at a speed of 1100 rpm for 15 minutes. Upon completion of the mixing procedure, the resulting mixture was allowed to equilibrate under ambient conditions for 2 days before conducting further testing.

A satin paint with a pigment volume concentration (PVC) of 32.28 was chosen for the thickener performance study. The formulation of the paint is presented in **Table 5.I**. The preparation of the paint base is performed by introducing in a suitable container, water, two dispersing agents, a defoaming agent, a neutralizing agent (NH_4OH (28%)), a biocide, a pigment, and a filler (TiO_2 and CaCO_3 size $< 1 \mu$). The container is then subjected to strong agitation at 1000 rpm for approximately 15 minutes to break up filler agglomerates and achieve good dispersion. To monitor the grinding of the paint, a fineness gauge is used to measure the size of individual particles after dispersion. Stirring is continued until the size of the agglomerates is below $20 \mu\text{m}$. Once the desired particle size is achieved, the remaining binder, two coalescing agents, water, and a defoaming agent are added to the mixture. The formulation is left under vigorous stirring for 1 hour before the addition of the thickener. The full formulation of the paint is stirred until homogenization is achieved.

Table 5.1. Generalized paint formulation used and their chemical nature for the present study.

Name of ingredients	% wt	Chemical nature
Water	12.0%	-
Dispersing agent	0.6%	Potassium based polyacrylate salt
Defoaming agent 1	0.2%	Polyether siloxane
Neutralizing agent	0.1%	NH ₄ OH (28%)
Biocide	0.2%	2-methyl-2H-isothiazole-3-one and 1,2-benzisothiazol-3(2H)-one
Pigment	18.8%	TiO ₂
Filler	13.0%	CaCO ₃ < 1 μ
Binder	41.6%	Styrene acrylic
Coalescing agent 1	1.0%	Monopropylene Glycol
Coalescing agent 2	1.0%	Ester Alcohol
Water	3.3%	-
Defoaming agent 2	0.2%	Polyether siloxane copolymer
Paint base	92%	
Thickener in water 20% w/w	4.0%	HEUR
Water	4.0%	-
Total paint	100%	
Thickener dry content (% w/w)	0,8%	

5.2.4. Analytical Methods

Gel Permeation Chromatography (GPC): The weight-average molecular weight (M_w) and the number-average molecular weight (M_n), were determined by GPC from Shimadzu, using four Styragel columns from Waters. The polydispersity index, PDI, was calculated as: $PDI = M_w/M_n$. Chloroform was the mobile phase (1 ml/min) at 30 °C operating temperature. Polyethylene glycol/oxide (PEG/PEO) were used as calibration standards. The samples were collected based on the “in-situ” method⁴³, in

which the molten samples were directly dissolved in vials with pre-weighed dry chloroform.

Fourier Transform Infrared Spectroscopy (FTIR): The qualitative analysis of the obtained polymers was performed using attenuated total reflectance-Fourier transform infrared spectroscopy (ATR-FTIR, Perkin Elmer, spectrum 100, USA). At least 16 scans for each sample were conducted in the span range of $4000\text{--}650\text{ cm}^{-1}$. The samples were collected based on the “in situ” method⁴³, in which the molten samples were directly dissolved in vials with pre-weighed dry chloroform. The liquid samples were placed in the analysis cell and the spectra were recorded after total spontaneous solvent evaporation.

Rheological measurements: The rheological properties of HEURs in aqueous solutions were measured on a HAAKE/MARS iQ Air rheometer. A plate - cone (C35 2.0°/Ti), using a cone and plate geometry of 35 mm diameter, 2° angle cone, made of (C35 2°/Ti). The distance of the gap was 0.096 mm. Water-HEUR solutions were prepared by direct addition of water into the reactor after the end of polymerization resulting in 20% w/w aqueous solutions. The solution was stirred overnight to become homogeneous and then the samples were left to rest during the next day. The water amount was selected based on industrial tests performed during the commercialization stage of a thickener product. A range of 17 – 20% dilution in water is normally applied and considered representative of the downstream processing behaviour of the final product. The zero-shear viscosity and the shear stress profiles were obtained for shear rate testing from 0.01 to 1000 s^{-1} . Two types of oscillatory experiments were conducted: (1) frequency sweep at a constant strain and (2) strain sweep at a constant frequency of 1 Hz. The strain sweep experiments were performed initially to determine the critical strain value for each sample, which signifies the point at which the sample structure begins to break down. A strain value below the critical strain was subsequently utilized in the frequency sweep experiments. The 3ITT were performed to evaluate the thixotropy of the samples. All rheological measurements were performed at $23\text{ }^{\circ}\text{C}$.

Anti-Sag Index (ASI) determination ASI was determined with a BYK-Gardner Anti-Sag Meter (BYK-Gardner USA) following the procedure of ASTM D4400–18 [9]. The applicator contains multiple notches with varying clearances spanning 3–12 mils or 4–

24 mils. Each notch is 1/4" (6.4 mm) wide and separated by 1/16" (1.6 mm) spacing. Approximately 10 mL of freshly pre-sheared paint was transferred onto a Leneta Form 9A opacity-display test chart (Leneta, USA), which is made of paper characterized by a black and white, sealed and smooth surface. Then the multi-notched applicator was drawn down across the chart, which generates a series of evenly spaced stripes. The chart was then promptly hanged vertically and left to dry at room temperature. After drying, samples were inspected visually and rated for an ASI, which is defined as the clearance of the gap that produces the thickest film stripe not sagging completely to the stripe below.

Determination of the flow-levelling performance of the paint: Leveling assessments were performed using the Leveling Applicator LTB-2, which adheres to the guidelines outlined in ASTM D4062, the American standard for evaluating leveling properties. This specialized applicator consists of a threaded stainless-steel rod that functions as a grooved doctor blade, enabling the creation of a film with parallel ridges and valleys to simulate brush marks. The LTB-2 features alternating clearances of 300 μm and 100 μm , allowing for the application of stripes with thicknesses of 150 μm and 50 μm , respectively. The resulting wet film thickness of the test drawdown was approximately 100 μm . To assess leveling, three-dimensional plastic cards representing various levels of leveling were utilized, ranging from extremely poor (card 1) to excellent (card 9). This standardized approach using the Leveling Applicator LTB-2 and the plastic cards provides an objective and reliable means for evaluating paint leveling, yielding valuable insights into the performance and quality of the tested coatings.

Accelerated Ageing Test An accelerated test used to predict thermal stability of coatings with time was performed. The test generally involves measuring viscosity change after the paint has been heat-aged for a week at 50°C. This test simulates the stability of the paint over 6 months period. The effect of the loss viscosity of these samples on long-term thermal stability was studied.

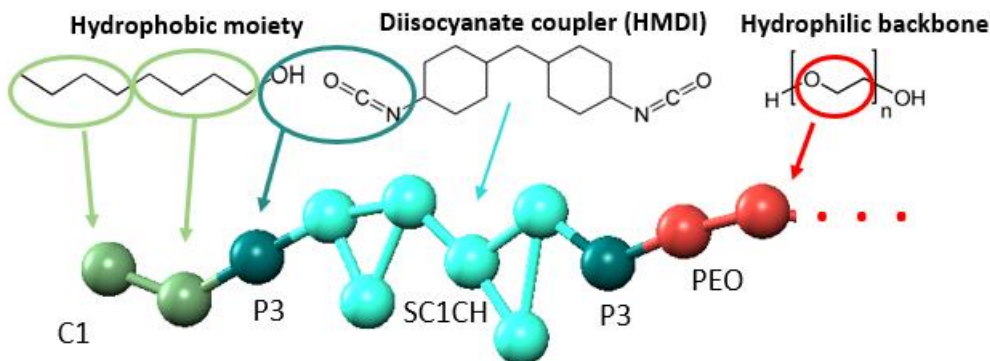
5.2.5. Coarse grained molecular dynamics simulation

Coarse-grained molecular dynamics simulations were performed utilizing the MARTINI framework and force-field⁴³. A schematic illustration of the mapping from

Chapter 5

atomistic to a coarse-grained representation is shown in Scheme 1. A four-to-one mapping was used, i.e., on average four heavy atoms and associated hydrogens were represented by a single bead. Four carbons in the octanol of the example were grouped into one C1 bead.⁴³ For hexanol as hydrophobic moiety, small Martini beads SC1 were used for grouping 3 carbons into one bead. Small beads denoted with ‘S’ have reduced interactions, i.e., the epsilon of the Lennard-Jones potential is scaled to 75% of the original value and sigma is set to 0.43 rather than 0.47 nm.

The hydroxyl reacting with the isocyanate group were mapped onto one P3 bead.⁴³ The cyclohexane rings were modelled by 3 connected beads, noted here as SC1CH. They are SC1 beads with bonding parameters taken from the Martini site⁴⁴, suitable for cyclohexane. The hydrophilic segment of HEURs was represented by a chain of PEO beads adopting the parameterization presented in [44]. Each PEO monomer was mapped onto one CG PEO bead. The PEO polymer chain ends in both sides with the same sequence of beads as shown in **Scheme 5.1** for the left side. Finally, water was modelled with one P4 bead that groups 4 water molecules.⁴³



Scheme 5.1. Mapping from atomistic to coarse-grained representation using Martini beads.

All systems were created and simulated using the MAPS platform (Materials and Processes Simulations Platform, Version 4.5, SCIENOMICS SAS, Paris, France). The initial configurations were produced by random mixing of the components (polymer chains and water) at a density of 0.8 g/cm³, using the Amorphous builder of MAPS, and subsequently energy minimized using LAMMPS (version 29 Sep 2021). The initial configurations were built at a density of 0.8 g/cm³. 70 polymer chains with 362 PEO beads (corresponding to MW equal to 16000), were placed in water so that the

composition of the system was equal to 10, 20 or 35 wt% in polymer. The number of water beads was in the range 60000 to 75000, while the box length was between 210 and 250 Å.

The simulations were performed with LAMMPS at the NPT ensemble for 500 ns at ambient temperature and pressure with a time step of 5 ps. The gromacs pair style of LAMMPS was used with cutoff 12 Å and switching at 9 Å.

5.2.5.1. Automated micelle identification and quantification

In our study, we employ machine learning (ML) techniques to automate the identification and quantification of micelles. This process eliminates the need for manual micelle counting and enables the determination of average aggregation numbers, and average micellar volumes across multiple frames. Specifically, we utilize the unsupervised ML algorithm known as DBSCAN (Density Based Spatial Clustering of Applications with Noise)⁴⁵ which is integrated into the Analysis Tool of the MAPS platform.

DBSCAN relies on two key parameters: the minimum distance for seeking neighboring beads (the ϵ parameter of DBSCAN, set to 10 Å in our computations), and the minimum number of beads required to form a cluster. We set the latter threshold equal to the number of hydrophobic beads per molecule. This automated approach facilitates the identification of the hydrophobic core around which a micelle forms. We leverage the MAPS Analysis Tool's capabilities to measure the volume of each hydrophobic core. In particular, we employ Monte-Carlo based techniques for calculating the volume of irregularly shaped objects^{46,47}

Once we identify the hydrophobic core for each micelle, we proceed to identify the HEUR chains attached to it, and subsequently calculate (again through Monte-Carlo techniques) the volume of each micelle. As part of our analysis, we also identify the bridge chains that connect different micelles to one another.

5.3. RESULTS AND DISCUSSION

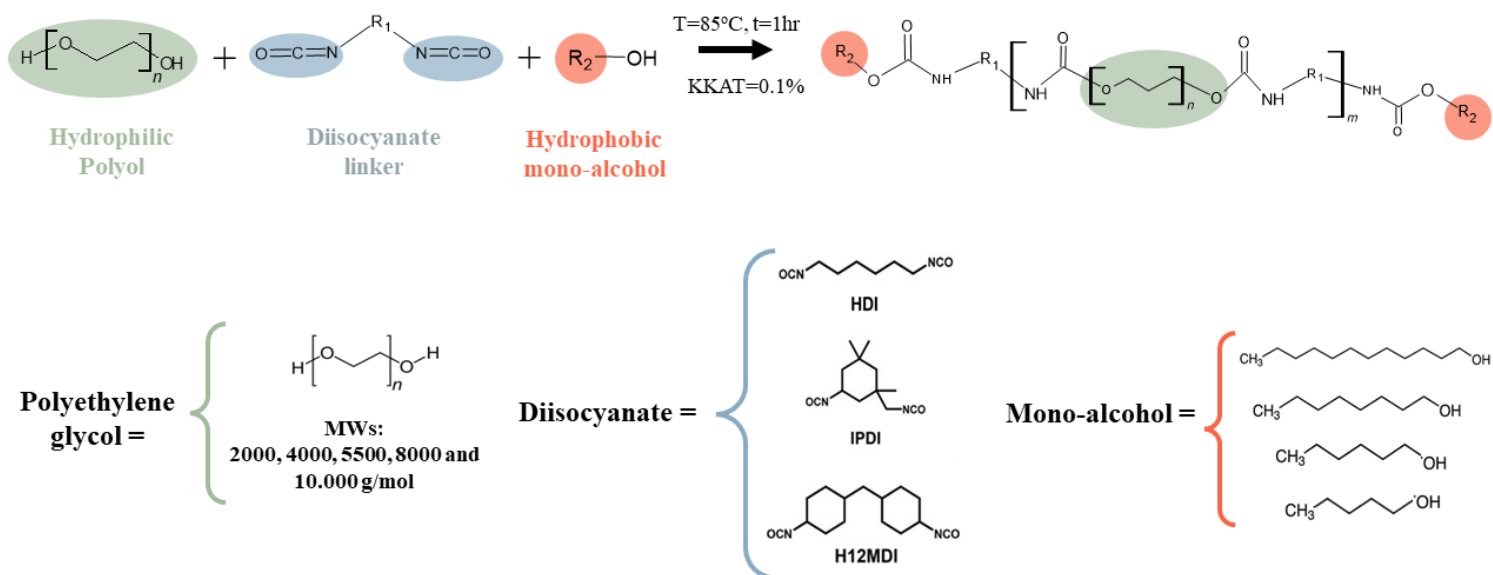
5.3.1. Structural characterization of HEUR

The synthesized HEURs, employing various PEGs, diisocyanates, and mono-alcohols, are detailed in **Table 5.2**, while the one-step synthesis route and corresponding HEUR structures are outlined in **Scheme 5.2**. To assess the individual influence of each segment on the rheological behavior of HEUR formulations, we adhered to the principle of *ceteris paribus* - systematically modifying a single segment in each experiment while other structural factors remained constant. GPC measurements, shown in **Table 5.2**, revealed that the number-average molecular weight (M_n) and the polydispersity index (PDI) of HEUR were effectively controlled. Given the consistent reaction conditions and stoichiometry across all experiments, the M_n remained almost the same ($\approx 23,000$ g/mol) when varying the diisocyanate and mono-alcohol structures. By adjusting the molecular weight of the PEG, we effectively altered the resultant molecular weight – and, consequently, the hydrophilic length of HEUR, tripling the PEG's molecular weight in each case. In the rest of the paper, the term "molecular weight" refers to M_n , albeit this notation will not be used for the sake of simplicity.

FTIR tests were performed to determine the chemical composition of the produced HEUR thickeners and to compare the structure-property relationship with the structural segments of HEUR. **Figure 5.1** shows the FTIR spectra of ten HEUR thickeners synthesized with different (a) mono-alcohols, (b) diisocyanates, and (c) molecular weights. For all analyzed samples, the characteristic absorption bands of polyethylene glycol appear in the range $840\text{-}1466\text{ cm}^{-1}$,^{48,49} and the characteristic -CH stretching band appears in the range $2700\text{-}3000\text{ cm}^{-1}$. Considering that the characteristic absorption peak of the isocyanate group ($\text{N}=\text{C}=\text{O}$) at 2265 cm^{-1} ,^{43,49,50} is absent for all samples, complete end-capping is ensured. Additionally, for all samples, characteristic urethane peaks appear at 1715 cm^{-1} and 1530 cm^{-1} which can be assigned to the disordered hydrogen-bonded carbonyl ($\text{C}=\text{O}$) groups^{43,51-54} and the bending vibrations of the NH ^{43,49,50,52,55} in the urethane polymers. The peak at 1640 cm^{-1} , is attributed to the traces of ordered hydrogen-bonded urea carbonyl ($\text{C}=\text{O}$).^{43,49,50,52,55} Based on the spectra obtained, no structural differences are observed when the mono-alcohol and diisocyanate structure is varied, which is also verified by the identical molecular weights measured with GPC. However, when varying the molecular weight of PEG

Chapter 5

and, as a consequence, the molecular weight of HEUR, differences can be observed in the intensity of the peaks appearing in the range of 1500-1700 cm^{-1} ; these can be attributed to the urethane bond as previously mentioned. The intensity of these peaks is notably more pronounced for the HEURs synthesized using lower molecular weight PEGs due to the relative prominence of the urethane bond's signal when a lower molecular weight PEG is used.



Scheme 5.2. Reaction scheme and structure of reactants used in this study.

Chapter 5

Table 5.2. Structural segments of HEUR, molecular weights (determined by GPC) and PDI values.

	HEUR	Hydrophilic segment	Diisocyanate linker	Hydrophobic segment (mono-alcohol)	Mn (g/mol)	PDI
Hydrophobic segment	HEUR-5: P8-HDI-C8	PEG 8000	HDI	1-Octanol	27,122	1.8
	HEUR-6: P8-IPDI-C8	PEG 8000	IPDI	1-Octanol	23,158	1.7
	HEUR-7: P8-HMDI-C12	PEG 8000	HMDI	1-Dodecanol	22,495	1.7
	HEUR-1: P8-HMDI-C8	PEG 8000	H ₁₂ MDI	1-Octanol	23,233	1.7
	HEUR-2: P8-HMDI-C6	PEG 8000	H ₁₂ MDI	1-Hexanol	22,291	1.7
	HEUR-10: P8-HMDI-C5	PEG 8000	H ₁₂ MDI	1-Pentanol	22,542	1.7
Hydrophilic Segment	HEUR-9: P2-HMDI-C8	PEG 2000	H ₁₂ MDI	1-Octanol	8389	1.8
	HEUR-7: P4-HMDI-C8	PEG 4000	H ₁₂ MDI	1-Octanol	14,078	1.7
	HEUR-3: P5.5-HMDI-C8	PEG 5500	H ₁₂ MDI	1-Octanol	17,788	1.7
	HEUR-4: P10-HMDI-C8	PEG 10000	H ₁₂ MDI	1-Hexanol	32,744	1.8

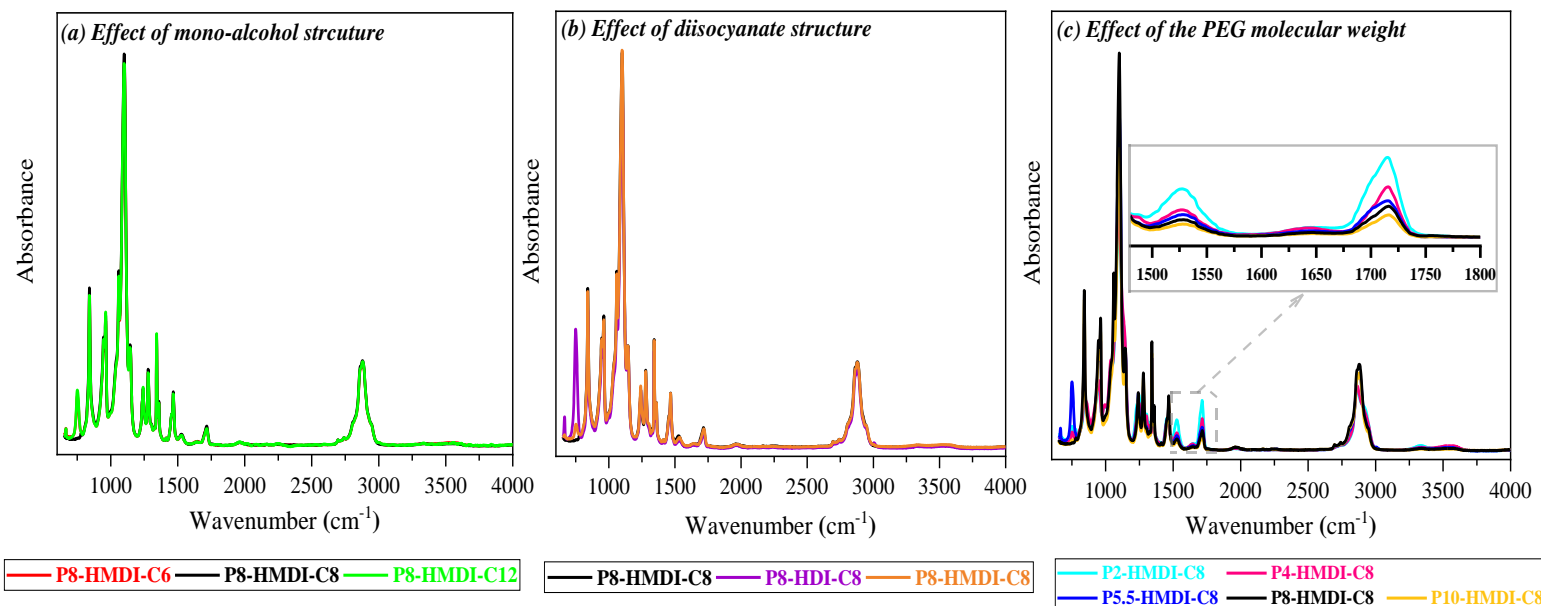


Figure 5.1. FTIR spectra of HEURs synthesized with different (a) mono-alcohols (b) diisocyanates (c) PEG's

5.3.2. Impact of the chemical structure of HEUR on micelle formation and rheological behavior in aqueous solutions

Aqueous HEUR solutions, dependent on polymer concentration, can form distinct micelles characterized by hydrophobic cores and water-soluble PEO corona.^{1,11,25,26,56,57} (see e.g., **Figure 5.2**) Flower-like micelles are formed above a relatively low concentration of HEURs in water, generally between 0.1% and 4% w/w (depending on the polymerization methodology).^{10,11,24,58,59} At these concentrations, viscosity remains relatively low. However, as HEUR concentration increases, a marked increase in viscosity is observed due to the interconnection of bridged clusters, indicating the onset of the percolation transition and the formation of a transient network.^{1,24,59,61} The higher the number of bridges between micelles is, the higher is the network density and, consequently, the solution viscosity. The network density and therefore the rheological properties of HEURs mainly depend on their concentration and chemical composition. Albeit HEUR thickeners exhibit application-oriented performance at concentrations (20% w/w), far exceeding their documented CMC regime, the percolation transition effects, which are responsible for their rheological performance, are understudied. Additionally, there have been many attempts in the literature to understand and predict the impact of hydrophilic and hydrophobic segments of HEURs on the rheology of its

aqueous solutions, yet some findings remain controversial, likely owing to the different synthetic methods applied that influence the end-product behavior.

Our study employs the same synthesis method for all HEUR structures to evaluate the impact of both HEUR concentration and its chemical composition on aqueous rheology. In Section 5.3.2.1, we examine the role of HEUR's hydrophilic and hydrophobic segments in its aqueous thickening behavior and establish the link between the percolation transition and HEUR's molecular structure. Additionally, we study the rheological behavior of 20% w/w HEUR aqueous solutions, a critical concentration for paint manufacturers, to identify HEUR structures exhibiting Newtonian, balanced, or pseudoplastic behavior in water.

Our experimental findings are complemented by Coarse-Grained Molecular Dynamic (CGMD) simulations (see Section 5.3.2.2). This approach enables us to investigate the morphology and structural conformation of micellar clusters as a function of HEUR concentration and chemical structure. CGMD simulations are particularly well-suited for the study of complex molecular systems including biomolecules and polymers. In comparison to atomistic simulations, they are computationally less demanding, allowing us to explore larger and longer time-scale systems. The initial configurations are generated by randomly mixing polymer chains and water, mimicking the initial state of the mixture in our experiments. Given that micelle formation is a process that unfolds over large time scales, conducting simulations at the atomistic level becomes impractical. In contrast, CGMD provides a more efficient sampling of the conformational space facilitating the exploration of the energy landscape of a system and the discovery of phase transitions, while significantly reducing computational costs. This hybrid methodology, combining both macroscopic and microscopic analyses, offers a new perspective that has not been provided in previous studies.

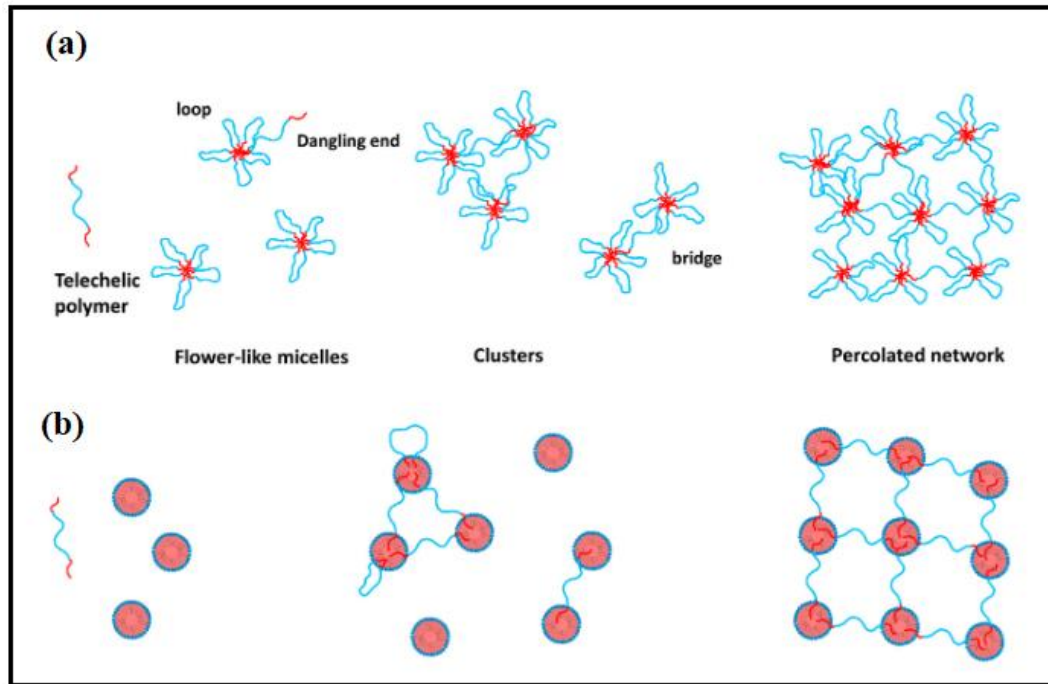


Figure 5.2. Schematic representation of (a) association of HEURs in aqueous solutions and (b) with latex-based emulsions as a function of the polymer concentration. Redrafted with permission.⁶⁰

5.3.2.1. Structure-Concentration Impact on Rheological Properties of Aqueous HEUR Formulations: An Experimental Study

Figure 5.3 illustrates the relationship between viscosity, HEUR concentration and composition. Specifically, Figure 5.3 (a, b, c) in the top row displays how zero-shear viscosity correlates with HEUR concentration for different chemical architectures. The results show that the influence of HEUR concentration on viscosity is subtle at low concentrations, but beyond a certain threshold, viscosity rises sharply for all HEUR structures. This threshold, termed the critical bridging threshold (C_{BT}) in our study, signifies the point where bridging markedly affects viscosity. For each HEUR examined, the C_{BT} was calculated by fitting the viscosity-concentration data with two linear curves, one for low and another for high concentrations. The intersection of these curves denotes the C_{BT} . All determined C_{BT} values are indicated in the labels within **Error! Reference source not found.**(a,b,c).

The bottom row, Figure 5.3 (a', b', c'), presents steady shear viscosity curves for 20% w/w HEUR aqueous formulations. The behavior of specific HEURs, namely P10-HMDI-C8, P5.5-HMDI-C8, and P8-HMDI-C5, is also shown for comparison, even though their respective C_{BT} values have not been determined.

Zero-shear viscosity and HEUR concentration

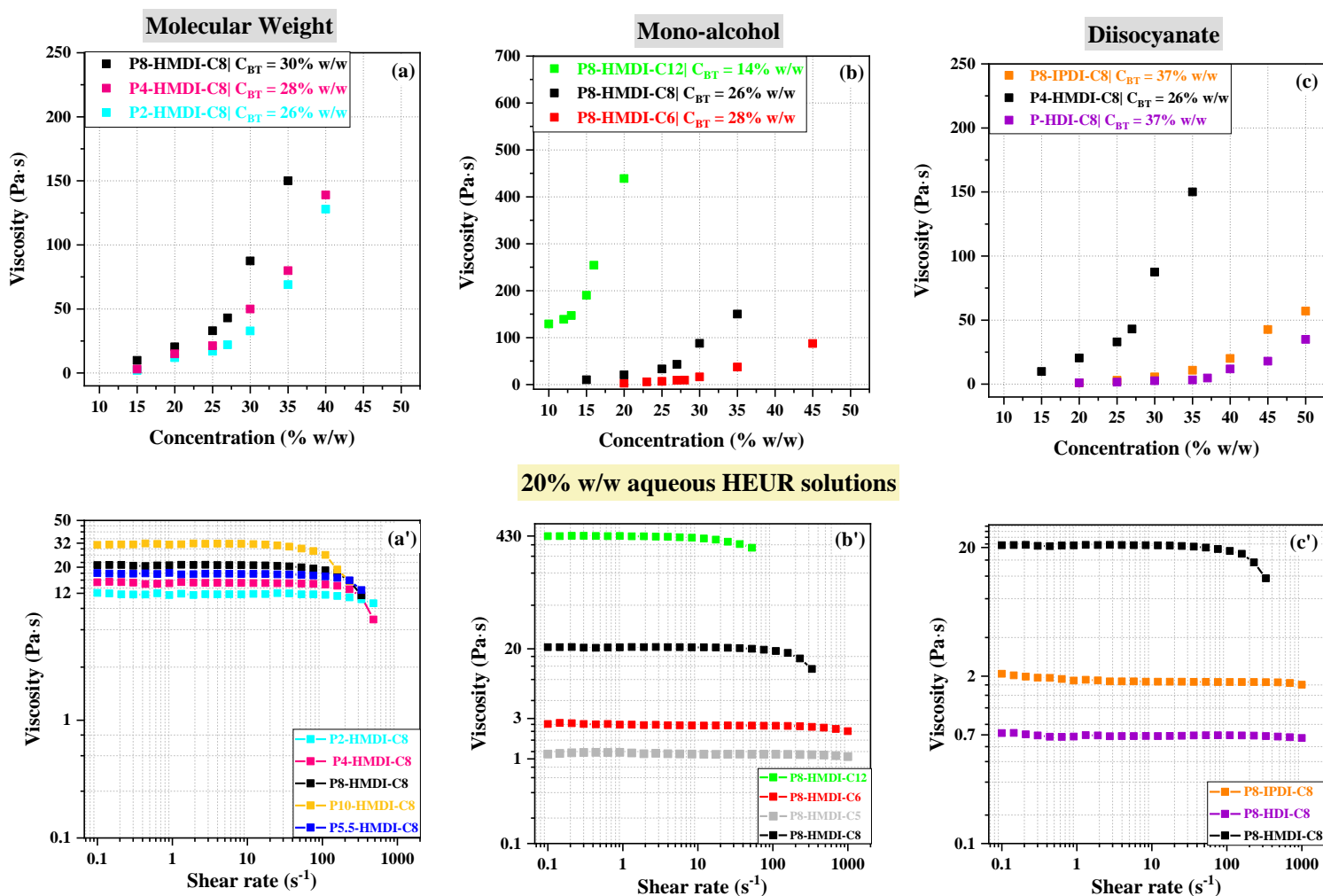


Figure 5.3. (Upper row): Correlation between zero-shear viscosity and HEUR concentration; (Bottom row): steady shear viscosity curves for the 20% w/w HEUR aqueous formulations; (a, a') Impact of PEG molecular weight; (b, b') Influence of mono-alcohol length; (c, c') Effect of diisocyanate structure; Labels contain the measured C_{BT} values for each HEUR tested.

The data presented in Figure 5.3 show that viscosity varies depending on the diisocyanate structure and mono-alcohol length. For instance, the bulkier and more hydrophobic diisocyanate H₁₂MDI (with two cyclohexane rings) yields higher viscosities than IPDI (with a single cyclohexane ring) and HDI (linear structure) across all tested concentrations. HEURs modified with IPDI and HDI exhibit higher C_{BT} values around 37%, compared to HMDI's 26%, indicating that the HMDI-modified HEUR forms a denser network due to its higher hydrophobicity.

Mono-alcohol length also influences viscosity and C_{BT} values. As we transition from C6 to C8 and then to C12, solution viscosity increases with C12 presenting notably higher viscosities and lower C_{BT} values. The latter indicates that the incorporation of C12 as terminal mono-alcohol promotes very strong hydrophobic associations and the higher viscosity values can be ascribed to the enlarged hydrophobic micellar clusters and the slower motions of individual polymer chains as the residence time of the hydrophobic tails in 'polymer micelles' increases.^{25,26,58} Generally, a shift towards longer relaxation times is expected when the polymer chains in a solution become more entangled (due to high polymer concentration, or increased hydrophobicity of the polymer's tail, or higher polymer molecular weight). Figure 5.3 (b', c') illustrates that HEUR solutions with less hydrophobic terminal hydrophobes, such as P8-IPDI-C8, P8-HDI-C8, P8-HMDI-C5, and P8-HMDI-C6, exhibit Newtonian behavior and low viscosities across all tested shear rates. In contrast, HEURs with more hydrophobic terminal groups display increased viscosities and pseudoplastic behavior.

We further explored the impact of HEUR's hydrophilic length by adjusting its molecular weight from 8,000 g/mol (P2-HMDI-C8) to 33,000 g/mol (P10-HMDI-C8), a range selected due to its industrial relevance. As illustrated in Figure 5.3 (a), while there is a discernible increase in viscosity with increasing HEUR molecular weight across all tested concentrations, these increments are subtle, especially when contrasted with the pronounced influence of the hydrophobic segment. Additionally, as the molecular weight increased from 8,000 to 23,000 g/mol, there was a modest reduction in C_{BT} values from 30% to 26% suggesting a denser transient network formed with higher molecular weight HEURs. The steady shear analysis for the 20% w/w HEUR aqueous solutions reveals that an escalation in molecular weight within this range resulted in slightly enhanced viscosities and an earlier onset of the shear thinning effect. Upon

surpassing a molecular weight of 23,000 g/mol, and reaching 33,000 g/mol, significantly higher viscosities were observed compared to lower molecular weights. However, the steady shear viscosity profiles for the tested HEUR molecular weights are more balanced, rather than showing the Newtonian or pseudoplastic trends determined by the hydrophobic segment of HEUR.

It is expected that as the hydrophilic length of HEUR increases, the size of the loops on the floret-shaped aggregates would increase and less looping chains would be involved in a micelle, leading to a lower aggregation number.^{11,58,63} Larger micelles lead to viscosity increase due to the increase in the hydrodynamic polymer volume. With low molecular weight HEURs, intramolecular associations of hydrophobic groups are favored compared to intermolecular ones, because of their proximity. In this context, the observed similarities in C_{BT} values and viscosities of the same order of magnitude could be attributed to aggregates of increased but comparable hydrodynamic volume, which in the case of low HEUR molecular weights would consist of a higher number of loop chains in a micelle. These experimental findings are complemented with CGMD simulations that are presented in the next section.

5.3.2.2. CGMD simulations for the characterization of the HEUR micellar morphology in water

As previously mentioned, CGMD simulations offer a computationally efficient alternative to atomistic simulations allowing for the investigation of larger spatial and longer time scales. In addition, CG models provide an efficient means to sample the conformational space, facilitating the exploration of a system's energy landscape and enabling the monitoring of micellar formation dynamics. In this study, we explore the spontaneous formation of micelles starting from random mixtures of long polymeric chains and water beads. While similar systems have been studied in previous works^{64,65}, our investigation extends to higher molecular weights with polymeric chains reaching up to 32,000 g/mol. To ensure the representativeness of the micellar distribution upon system equilibration, we selected a substantial number of polymeric chains, ranging from 70 to 210 molecules. Notably, in all our simulations micelles form in a spontaneous manner (in contrast to the study in reference⁶⁰, where preassembled flower

like micelles are simulated), and one can observe a diverse range of structural conformations.

Another innovative aspect of our study lies in the automated process of micellar identification and characterization, achieved through the utilization of the unsupervised ML algorithm, DBSCAN. DBSCAN identifies the hydrophobic core of each micelle without requiring any prior knowledge of the number of cores/clusters. As part of this automated process, we also compute aggregation numbers for each micelle (we identify the number of distinct polymeric chains attached to the core), as well as the bridging chains interconnecting different micelles. Finally, we employ Monte-Carlo based techniques to compute both the volume of the hydrophobic cores within each micelle, and the total volume of the entire micelle. These computations are performed using the MAPS' Analysis Tool.

5.3.2.2.1. Micelle formation processes and impact of HEUR concentration and hydrophilic length on micelle formation

First, we studied the self-assembly of HEUR1: P8-HMDI-C8 in a 20% w/w water solution by analyzing molecular configurations and monitoring the time-evolution of the system's energy to determine its equilibrium state. Figure 5.4 (a), (b) and (c) depict the molecular configurations at $t=5$ ns, $t=50$ ns, and $t=500$ ns (final structure), respectively. Figure 5.4(d) shows the system's total energy evolution with the system converging to equilibrium after approximately $t=300$ ns. One can observe the gradual formation of micellar structures, where the hydrophobic end-groups of HEUR (depicted with green spheres in Figure 5.4(a)-(c)) bent inward within the micelle, while the hydrophilic PEG chains (depicted in red) remain exposed to the surrounding water (depicted in blue) (Figure 5.4c). We compute the hydrophobic cluster size distribution by defining a "cluster" as an assembly of terminal hydrophobes, excluding the attached PEO chains. Clusters of hydrophobes are identified using the DBSCAN algorithm. Furthermore, we identify the chains attached to these clusters forming the micelle, and finally we compute the number of chains connecting two distinct micelles (bridge chains).

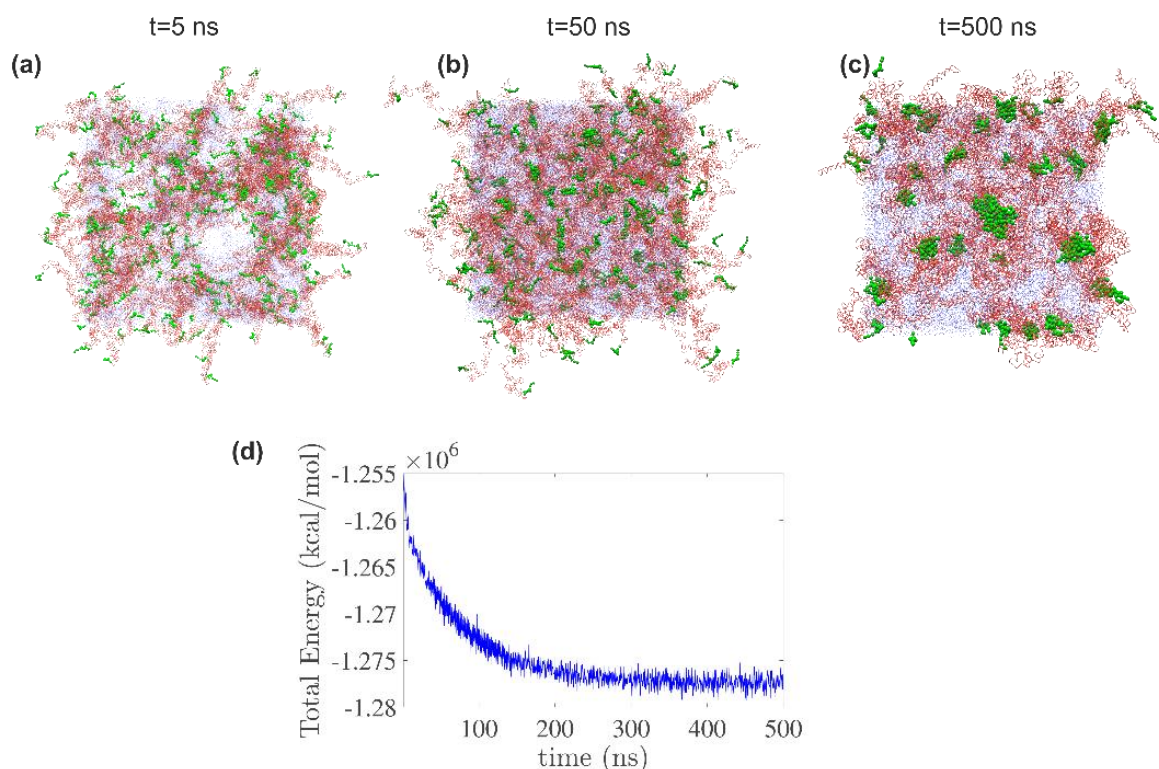


Figure 5.4. CGMD simulation snapshots of HEUR1: P8000-HMDI-C8 in a 20% w/w water solution at (a) $t=5$ ns, (b) $t=50$ ns and (c) $t=500$ ns. Color code: blue represents P4 beads (equivalent to 4 water molecules); red indicates the hydrophilic beads of PEG chains; green spheres represent the hydrophobic end-groups of HEUR (d) Evolution of the system's total energy. The energy reaches a plateau (equilibrium) after approximately $t=300$ ns.

Figure 5.5 presents HEUR1 configurations in water at concentrations of 10%, 20%, and 35% w/w, encompassing concentrations both below and above the experimentally determined critical overlap concentration (C_p) for HEUR1 (26% w/w). The upper layer of Figure 5.5 illustrates the conformation of hydrophobic clusters and PEG chains (water is omitted for clarity), while the lower layer focuses exclusively on the hydrophobic clusters identified by performing the DBSCAN algorithm.

Furthermore, Figure 5.6a and Figure 5.6b provide insights into the self-assembly behavior of HEUR at varying concentrations, highlighting key parameters such as: (a) the micellar volume (the average total volume occupied by micelles), (b) the hydrophobic core volume, (c) N_{agg} which denotes the number of chains forming a micelle, and (d) N_{bridged} denoting the number of hydrophobic chains within a single cluster that are interconnected with another micelle.

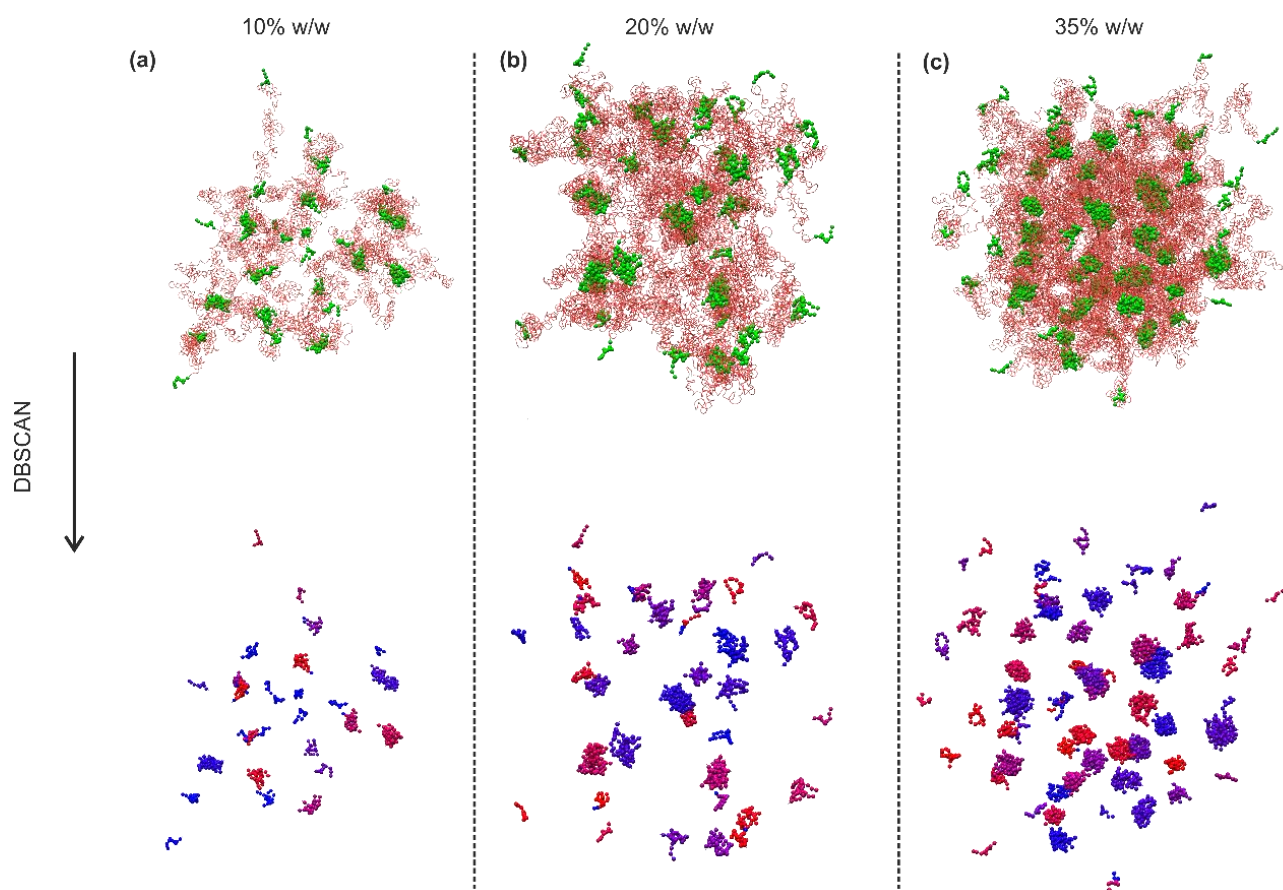
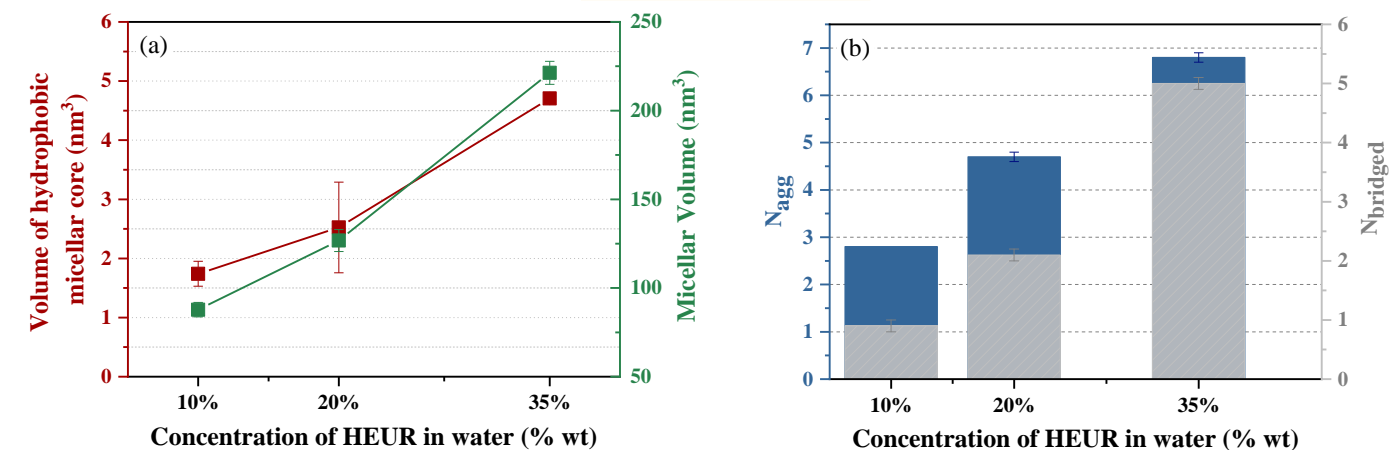


Figure 5.5. Configuration of water-HEUR system at equilibrium for (a) 10% w/w, (b) 20% w/w and (c) 35% w/w concentrations. In the upper panel, PEG chains (in red) and hydrophobic beads (in green) are illustrated; water beads are removed for clarity. The lower panel shows the hydrophobic clusters identified by performing the DBSCAN algorithm (different color for each cluster).

Concentration effect



Chain effect

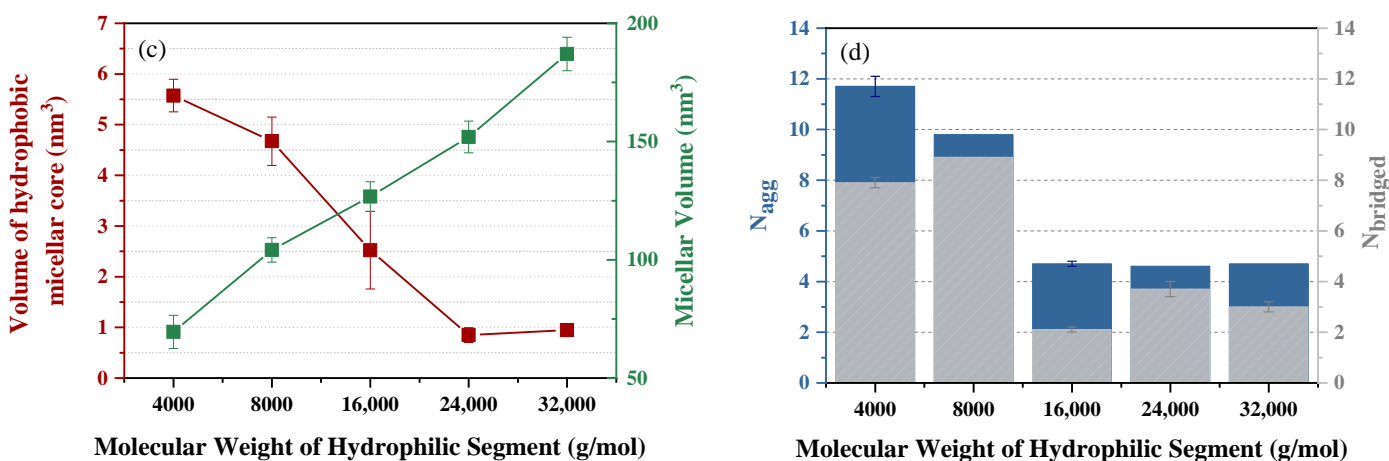


Figure 5.6. Influence of HEUR concentration and hydrophilic chain length on micellar volume, hydrophobic core volume, N_{agg} and $N_{bridged}$.

The molecular configurations of HEUR in Figure 5.5 underscore the concentration-dependent variations in network density. At low HEUR concentrations, the network appears notably sparse, characterized by fewer and smaller hydrophobic clusters. By increasing the HEUR concentration, the network density enhances, evident in the formation of larger hydrophobic aggregates. This phenomenon is quantified in Figure 5.6a and Figure 5.6b. In particular, Figure 5.6a illustrates an increasing trend in both micellar volume and hydrophobic core volume as HEUR concentration increases. Figure 5.6b confirms this trend by displaying simultaneous increase in N_{agg} and $N_{bridged}$ values, indicating both larger hydrophobic clusters and a more interconnected micellar network.

These findings are consistent with the experimental results showing the concentration dependent viscosity trends for HEUR-1, where higher HEUR concentrations correspond to increased viscosities. In addition, a notable correlation is observed between the experimental critical bridging threshold (C_{BT}) of HEUR1 and the percentage of bridged/interconnected chains in the micellar network ($N_{bridged}/N_{agg}$), calculated through GCMD simulations. Interestingly, concentrations below the C_{BT} ($\approx 26\%$) exhibit interconnected chain proportions below 45%; however at 35% w/w HEUR concentration, this percentage sharply rises to 74%, indicating a transition to a densely interconnected micellar network. This transition aligns closely with our experimental data, which shows a marked viscosity increase in viscosity when HEUR concentration surpasses the critical percolation threshold.

Having established that our CG-MD model aligns well with the experimental concentration dependent viscosity trends observed for HEUR-1, we expanded our study to investigate the impact of HEUR's hydrophilic chain length on micelle sizes and morphology. Specifically, we performed simulations for HEUR molecular weights ranging from 4,000 to 32,000 g/mol, in alignment with available experimental data for molecular weights ranging from 8,000 up to 33,000 g/mol.

Figure 5.6c and Figure 5.6d highlight contrasting trends between the impact of HEUR's hydrophilic chain length and HEUR concentration (contrasting with Figure 5.6a and Figure 5.6b). As HEUR molecular weight increases, the hydrophobic core volume decreases, and fewer HEUR chains participate to micelle formation, as evidenced by the decrease in N_{agg} values. In particular, for PEG molecular weights of 4,000 and 8,000 g/mol, N_{agg} ranges from approximately 10 to 12, dropping to around 4.5 for molecular weights between 16,000 and 32,000 g/mol. This decrease in N_{agg} and hydrophobic core volume is attributed to increased repulsive interactions between elongated hydrophilic HEUR chains and the larger steric hindrance of hydrophobic groups. Interestingly, despite the lower N_{agg} values associated with longer hydrophilic segments, the overall micellar volume continues to expand, aligning with the viscosity trends observed experimentally. Regarding the proportion of interconnected hydrophobic clusters, the data does not exhibit a monotonic trend across varying HEUR molecular weights, making it challenging to definitively assess the influence of molecular weight on inter- and intramolecular interactions.

5.3.3. Effects of latex and HEUR chemical structure on rheology and phase stability of waterborne latex–HEUR mixtures

In waterborne paints, the binder, often referred to as latex, typically of acrylic or vinyl-acrylic origin, constitutes 15–40% w/w of the formulation and plays a critical role in the overall paint properties. Given its critical role, industry standards dictate that the effectiveness of newly developed associative thickeners, such as HEURs, should be evaluated based on their incorporation into latex-based emulsions.

Latex is a colloidal system where small hydrophobic polymer particles are dispersed in water. In such system, the hydrophobic segments of HEUR tend to associate with the hydrophobic surface of the latex particles, while the hydrophilic segments remain in the aqueous phase.^{6,8,12} When the latex surface is not saturated by surfactants with higher affinity, and given sufficient thickener concentration, HEUR molecules can bridge latex particles by adsorbing their hydrophobic segments. The strength of these interactions depends on the chemistry of both the HEUR and latex surface.^{6,13,30–37} Previous studies have identified various association mechanisms of HEUR with latex particles.^{6,8,12,13,38,39} These include a single hydrophobe adsorbed on a latex particle with another bridged on a HEUR micellar cluster, adsorption on different latex particles forming bridges, or adsorption to the same latex particle forming loops.^{6,8,12,13,38,39} The favored interactions depend on several factors including latex surface polarity, thickener hydrophobicity, temperature and the concentration of latex and thickener.

To align with industry standards, our study incorporated the 20% aqueous solutions of HEUR in latex emulsions, with a formulation consisting of 70% w/w latex, 2.09% HEUR, and 27.91% water. Notably, mixtures containing lower molecular weight HEURs (P2-HMDI-C8-Mn=8,000 g/mol and P4-HMDI-C8 Mn=14,000 g/mol), led to immediate phase separation, known as syneresis - transforming the liquid emulsion into a non-liquid, foamy texture (Image S1 of the Supporting Information) underlining the importance of the hydrophilic length in stabilizing the emulsion. The rest of the samples did not exhibit phase separation (observed with naked eye) for more than one week.

To expand on this analysis, our investigation utilized dispersion phase diagrams (DPDs), initially introduced by Konstansek^{66,67}, who studied the concentration-dependent nature of syneresis in latex-based emulsions featuring a HEUR thickener,

surfactant, and latex particles. It's worth noting that the presence of surfactants severely affects the phase separation region, as they can associate with HEURs and the latex surface and finally displace the HEUR hydrophobes from adsorbing to the latex particle surfaces. Figure 5.7 reveal distinct stability regions for three HEUR-latex formulations: P2-HMDI-C8, P4-HMDI-C8, and P8-HMDI-C8. The formulation containing P2-HMDI-C8, which has the shortest hydrophilic length, manifested a broad flocculation area (depicted in red) across all tested latex concentrations when the HEUR concentration exceeded 2%. On the other hand, P4-HMDI-C8, featuring a longer hydrophilic segment, displayed a more restricted flocculation region, confined to specific HEUR concentrations between 1-2% and latex concentrations between 50%-85%. Notably, P8-HMDI-C8, with the longest hydrophilic segment, showed no observable macroscopic flocculation. Additionally, as evident from the SEM micrographs in Image 1, the pure-latex has a distinct surface, whereas the tested flocculated samples of P2-HMDI-C8 and P4-HMDI-C8 appear to exhibit regions of agglomerates. These findings emphasize the critical role of the hydrophilic segment length in determining emulsion stability, as it aids in effective interparticle bridging while simultaneously inhibiting the formation of flocculates.

For stable emulsions without syneresis, Figure 5.8(d) demonstrates the impact of HEUR's hydrophilic and hydrophobic segments on rheology of latex-based emulsions. Consistent trends were observed in both the steady shear analysis of HEUR aqueous solutions and the latex emulsions. Enhanced hydrophobicity, attributed to bulkier diisocyanate units or elongated mono-alcohol moieties, promotes the formation of a denser transient network, leading to increased emulsion viscosity. Furthermore, when comparing HEURs with identical hydrophobic structures but variable hydrophilic lengths (from 18,000 to 33,000 g/mol), a direct correlation between higher molecular weight and increased viscosity was evident.

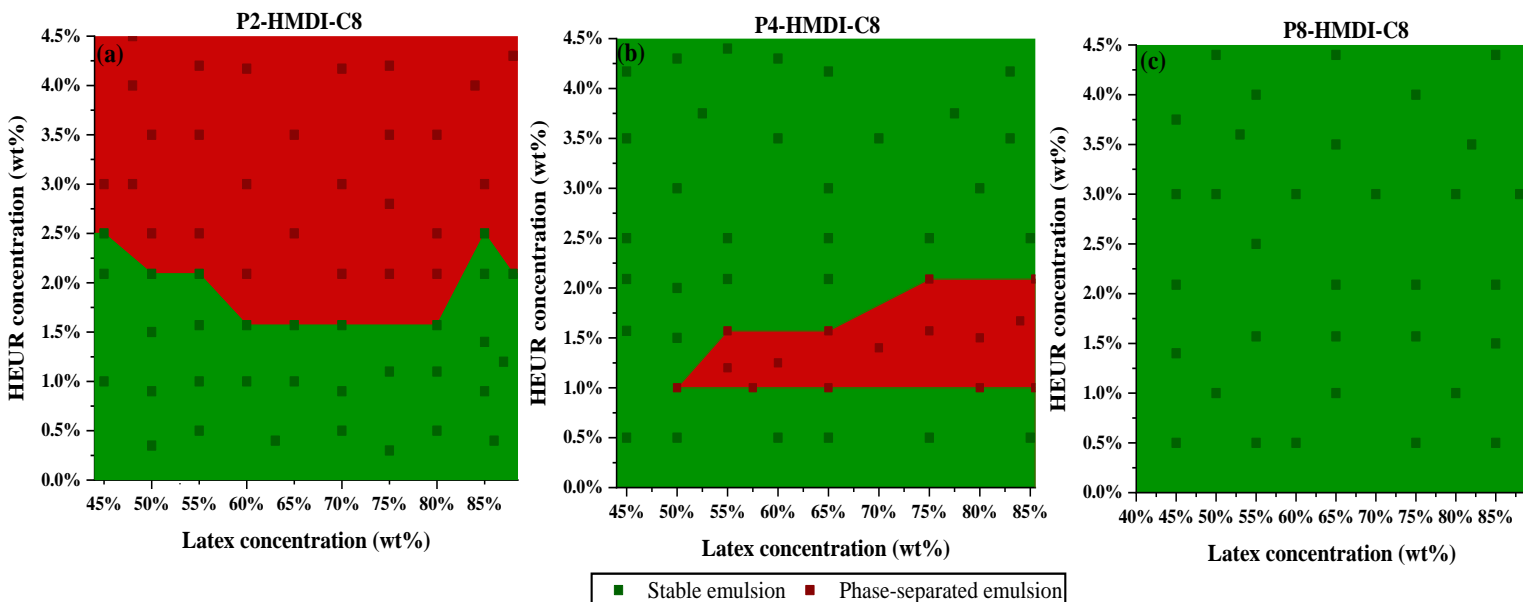


Figure 5.7. DOEs of waterborne HEUR-latex mixtures of (a) Latex 1: formulated with HEUR 8000g/mol from PEG2000 (b) Latex 8: formulated with HEUR 14,000g/mol from PEG4000 (c) Latex 9: formulated with HEUR 23,000g/mol from PEG8000. Scatter points indicate the exact formulations tested in our experiments.

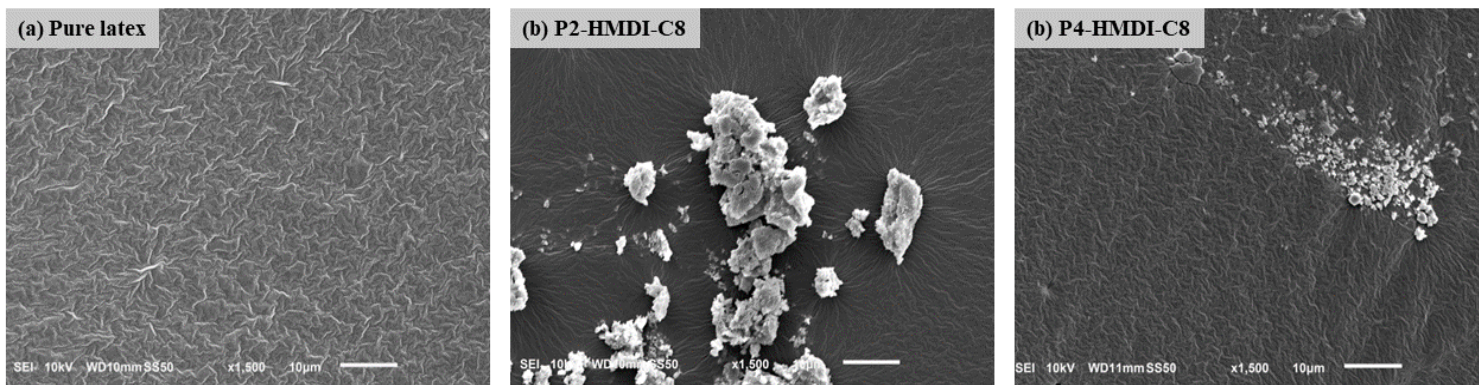


Image 1. SEM Micrographs of the Coatings Formed From: (a) Pure Latex (b) Latex-Based Emulsion of P2-HMDI-C8 from the Flocculated Area (c) Latex-Based Emulsion of P4-HMDI-C8 from the Flocculated Area.

5.3.4. Rheological characterization and performance evaluation of waterborne paints thickened with HEURs: Insights from Steady Shear and Oscillatory Rheology, Levelling, Sagging, and Heat Stability measurements

The aqueous solutions of HEURs were incorporated into waterborne paint formulations to assess the impact of different HEUR chemical structures on the rheological behavior

and overall performance of the thickened paints. The rheological characteristics of these paints were analyzed through steady shear viscosity analysis, oscillatory measurements, 3ITT and thermal stability measurements. Paint performance was further evaluated based on leveling and sagging tests. Detailed results are presented in the following sections.

5.3.4.1. Steady Shear Analysis

Figure 5.8 (a), (b), and (c) depict a shear-thinning behavior for all paint samples, in line with their characteristic nature as highly solid dispersions. Notably, despite the low concentration of HEURs in the paint formulation (1-3% w/w), modifications in HEUR's structural segments impact paint viscosity. Remarkably, despite the different association mechanisms of HEUR in paint formulation (multicomponent system) compared to its self-assembly in aqueous solutions (binary system), the results indicate that the rheological behavior of different HEUR structures in aqueous solutions show the same trend when tested in latex-based emulsions and in the final paint formulation. (Figure 5.8) The Newtonian, balanced and pseudoplastic behavior was effectively retained when incorporating binder and pigment particles. This consistency indicates that the rheological responses observed in water solutions provide a reliable forecast of their behavior in latex-based emulsions and waterborne paints. Higher viscosity values and more pronounced thinning effect was obtained when the effective terminal-hydrophobe size of HEUR was increased based on modifications of the diisocyanate and mono-alcohol structure accordingly. This effect is also demonstrated in the pseudoplasticity index (PI) values depicted in Table S3 of the Supporting Information, where more hydrophobic terminal tail led to higher PI values. By examining the influence of HEUR's hydrophilic length, achieved through altering its molecular weight and PEG length, we observe that paints modified with HEURs having molecular weights of 14,000, 18,000, and 23,000 g/mol exhibit similar PI values and flow characteristics throughout the entire spectrum of shear rates. However, extending the hydrophilic length of HEUR further, as demonstrated in the paint modified with a HEUR possessing a molecular weight of 33,000 g/mol, results in higher PI and viscosity values within the low to mid-shear region, up to 4 s^{-1} .

Effect of HEUR thickener on Waterborne Paints

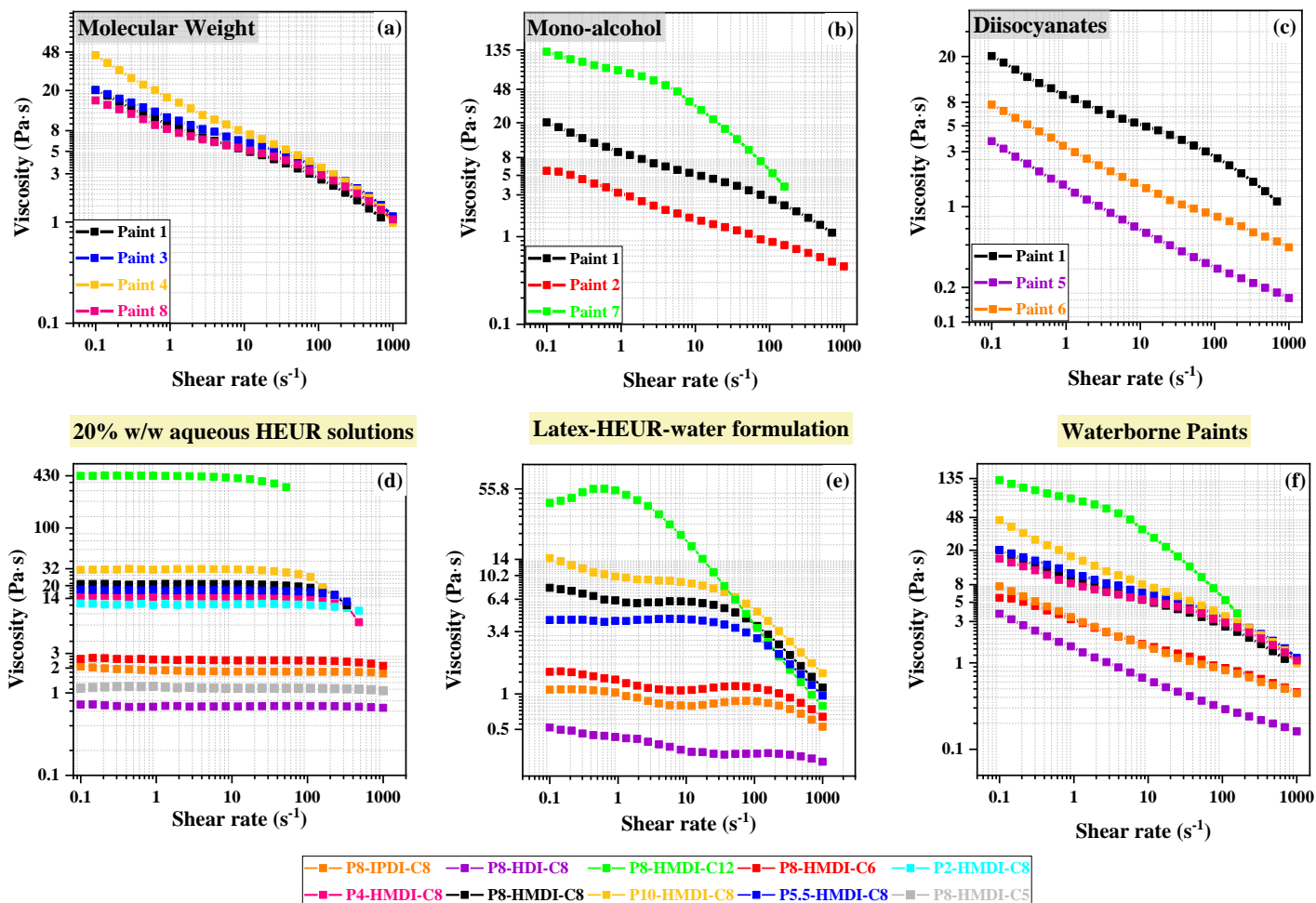


Figure 5.8. Comparative analysis of steady shear viscosity curves for: (Upper row):HEUR-thickened paints: (a) Influence of molecular weight; (b) Impact of mono-alcohol length; (c) effect of diisocyanate structure; and (Bottom row) (d) 20% w/w aqueous HEUR solutions (e) Latex-HEUR-water formulations (f) Waterborne Paints were numbered according to the numbering of HEURs in Table 5.2.

5.3.4.2. Oscillatory measurements

Paints exhibit complex rheological behaviors that go beyond steady shear analysis, requiring evaluation of its viscoelastic properties to gain insight into associative network strength and pigment dispersion quality. The two common oscillatory tests employed are amplitude sweep (AS) and frequency sweep (FS). The AS test establishes a linear viscoelastic range (LVER), where the elastic (G') and viscous (G'') moduli

Chapter 5

remain constant, irrespective of strain, at a set temperature and frequency. Subsequently, within this LVER, an FS test examines the paint's time-dependent properties under minimal stress conditions. Figure 5.9 (a), (b), and (c) showcase oscillatory strain-sweep curves with G' and G'' plotted against strain. Within the LVER, both moduli exhibit stable plateau values until they reach a critical strain or yield point, after which they decline. Yield values for all paints are determined based on a 5% deviation of G' values⁶⁸ from the plateau values, as summarized in Table S3 of the Supporting Information. Complementary FS results, carried out in the LVER, are shown in Figure 5.9 (a'), (b'), and (c'), plotting G' and G'' across a frequency range of 0.1 to 10 Hz at a 1% strain.

Evaluating the impact of mono-alcohol and diisocyanate structure on the frequency and strain-dependent behavior of G' and G'' , the patterns closely mirror those observed in steady shear analysis. A shift of the AS and FS curves to higher G' and G'' values denote a more robust associative network, indicative of a superior structural network within the paint's matrix. This shift is mainly related to interparticle associations, which are strengthened by the incorporation of a bulkier diisocyanate or a longer end-capper into the hydrophobic tail of HEUR. Additionally, the bulkier diisocyanate and the longer mono-alcohol generally lead to a lower crossover frequency ($G' = G''$), illustrating the lower responsiveness of the paint to high-frequency oscillations.

In AS tests, paints with HEUR thickeners of molecular weights between 14,000 and 23,000 g/mol exhibited liquid-like behavior, as indicated by G'' exceeding G' and similar structural strength (similar G' values). In contrast, a molecular weight of 33,000 g/mol led to a solid-like behavior. FS tests further elucidated these findings. Specifically, Paint 8, formulated with the shortest hydrophilic length of HEUR (14,000 g/mol), showed a liquid-like character and lacked a crossover point, indicative of a weaker associative network. Conversely, Paints 1 and 3, featuring HEURs with longer hydrophilic lengths, displayed crossover points at similar frequencies, signifying stronger interparticle associations. Most notably, Paint 4, containing the highest molecular weight HEUR (33,000 g/mol), exhibited a solid-like character.

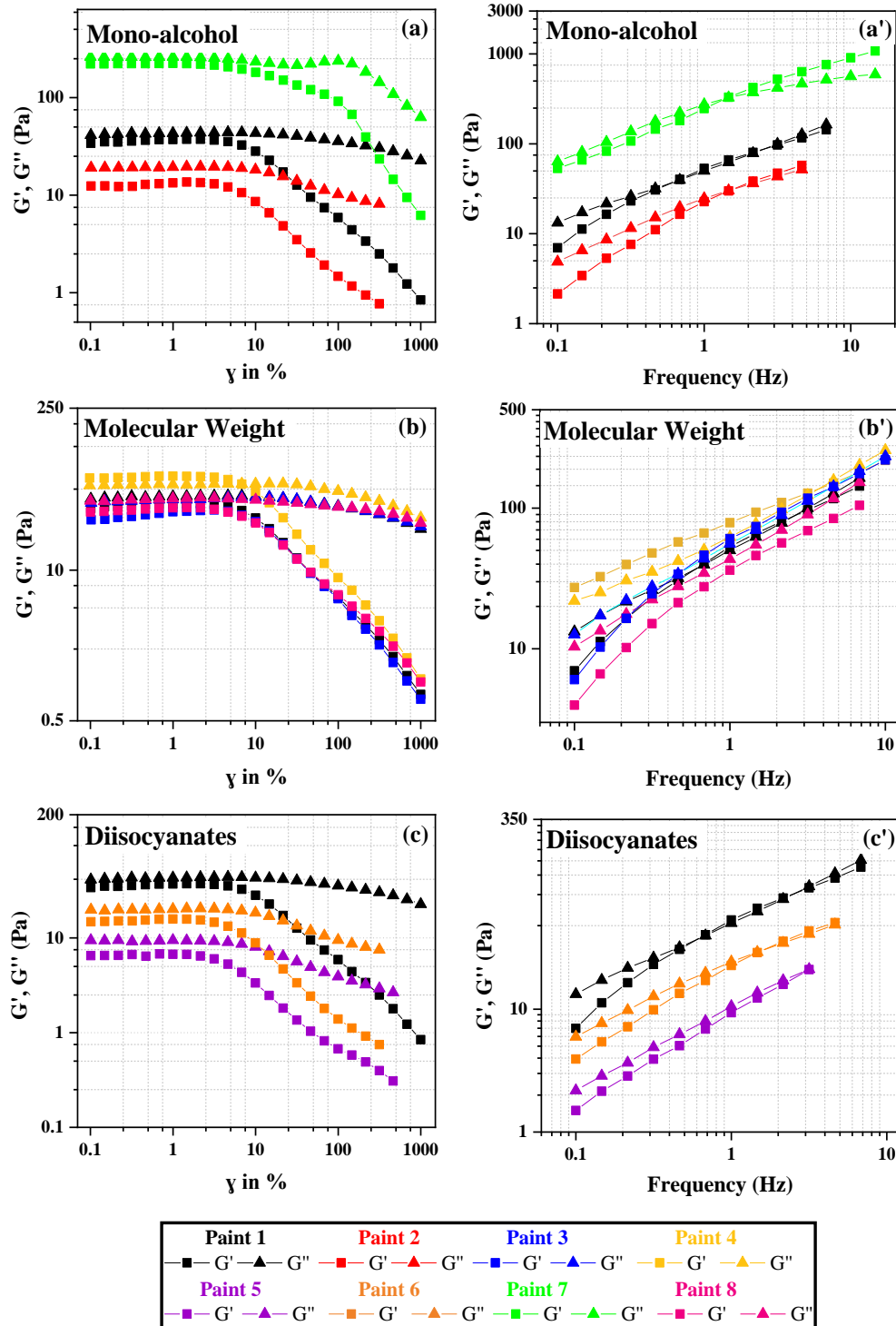


Figure 5.9. Left panel (a, b, c) Oscillatory strain-sweep curves, plotting the elastic (G') and viscous (G'') moduli against strain. Right panel (a', b', c') present frequency sweep results, showing G' and G'' values across a frequency range of 0.1 to 10 Hz, conducted at a 1% strain.

5.3.4.3. Connection of 3ITT with levelling and sagging

We investigated the thixotropic behavior of paints modified with different HEURs using the 3ITT, which is a key method for assessing the time-dependent behavior of paints, simulating conditions from rest to application.^{3,69-72} (Figure 5.10a) This test comprises three intervals simulating a paint's condition at rest, during high shear applications, such as brushing, and the subsequent rest phase. The Thixotropic Index (TI) was calculated to quantify this behavior and the method for this calculation can be found in the Supporting Information.

Our findings reveal that the choice of HEUR significantly affects a paint's viscosity recovery rates and thus its TI values. (Figure 5.10b) For instance, the paint modified with the most hydrophobic HEUR (Paint 7 in Figure 5.10) and the most pseudoplastic behavior exhibited rapid viscosity recovery and the highest TI value, whereas Paints 2, 5, and 6 with the weaker hydrophobic part and the most Newtonian behavior with the lowest viscosities, exhibited the lowest TI values and were slower to recover viscosity. Additionally, molecular weight plays a crucial role; doubling the molecular weight of HEURs from approximately 15,000 to 30,000 g/mol led to an increase in the TI by over eight orders of magnitude, as exemplified by the comparison between Paint 8 modified with a HEUR molecular weight of 14,000 g/mol and Paint 4 with a molecular weight of 33,000 g/mol.

Practical applications of our findings highlight the crucial role of end-use performance in paint formulations, particularly focusing on leveling and sagging properties as key quality indicators. Using standard Leneta charts for evaluation, we found a clear correlation between the molecular structure of HEUR and paint performance. Paint 7 that has the most hydrophobic segment and Paint 4 that has the highest molecular weight showed superior anti-sagging properties but lacked in leveling rating due to their high TI and quick viscosity recovery. On the other hand, Paints 2, 5, and 6 having weaker hydrophobic segment displayed better leveling performance but showed poor sag resistance due to their low TI values. Paints with molecular weights between 14,000 to 23,000 g/mol demonstrated a more balanced performance in both leveling and sagging. These insights are critical as real-world paints often contain more than one

Chapter 5

HEUR thickeners of different chemical structure to achieve optimal performance on both leveling and sagging rating.

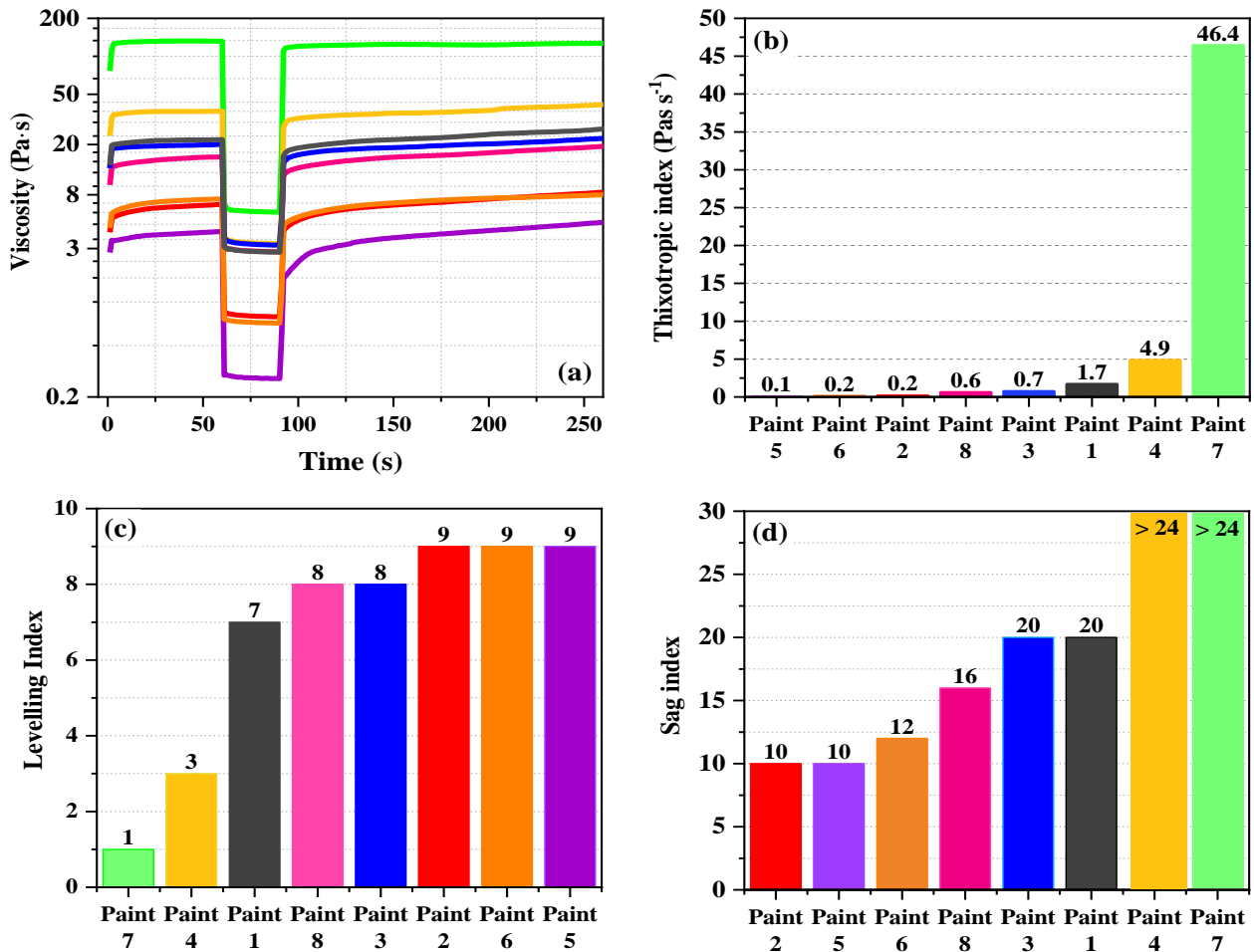


Figure 5.10. Results of Paints 1-8 modified with HEURs 1-8 with varying hydrophilic and hydrophobic structure. (a) 3ITT (Structural recovery greater than 100% occurs when the structure is broken down during high shear, which allows for a new arrangement of molecules resulting in a higher structural strength than before the shear load was applied) (b) TI values (c), (d) Results of Leneta chart for levelling and sagging correspondingly. Flow levelling index: 0 = very poor and 10 = best, Sag index: 4 = poor and 24 = best³

5.3.4.4. Thermal stability measurements

In an accelerated aging test for paint samples, we assessed storage stability and the effects of different HEUR thickeners. Figure 5.11 displays viscosity changes and

Chapter 5

thixotropic indices for both fresh and aged samples. Notably, no phase separation was observed for any of the aged paints. Figure 5.11(a) highlights that aging primarily influences viscosity in low shear regions. Paints 1, 4, 2, and 5 showed low viscosity deviation ($\pm 15\%$) compared to their fresh counterparts with no clear correlation to HEUR structures. Further, a general trend of increased TI values is observed as HEUR molecular weight increases (Figure 11b). The absence of any clear correlation of viscosity change in the aged paints, compared to their fresh counterparts, with the chemical structure of the HEUR thickener, based on the results of Figure 5.11, is not surprising. It can be attributed to the fact that the effect of accelerated paint aging on paint viscosity is paint-specific, that is, it may promote or disrupt interparticle associations, which in turn affect the rheological properties. The enhancement of rheological properties could also result from thermal degradation reactions within the polymer-binder-pigments matrix. Such reactions might cause a molecular recombination, ultimately giving rise to a more robust and chemically stabilized network with enhanced thermal stability. Similar observations regarding thermoplastic polyurethane systems have been made by other authors.⁷³ For a more detailed analysis of the results of steady shear and oscillatory tests between fresh and aged paints, please refer to the Supporting Information.

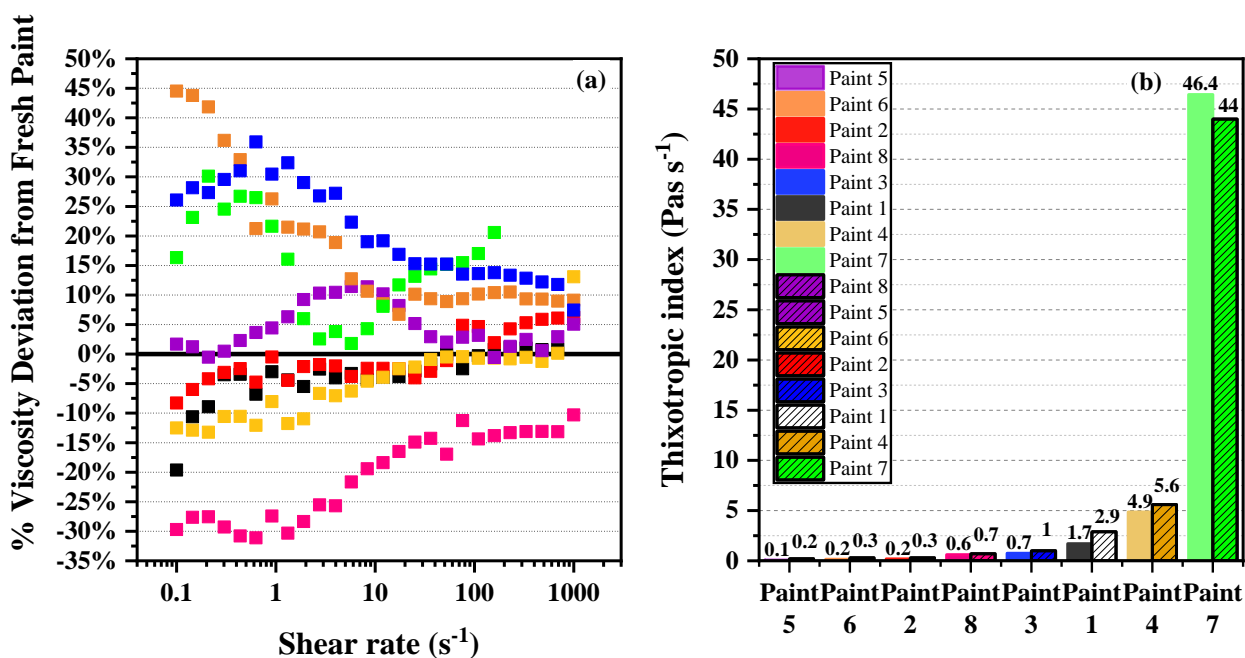


Figure 5.11. (a) % Difference in shear viscosity across the entire shear rate range for fresh and aged paints (Positive values indicate higher viscosities of the aged samples compared to the fresh paints) (b) Thixotropic index for fresh and aged paints

5.3.5. CONCLUSIONS

This work combines experimental and computational approaches to provide a comprehensive evaluation of the impact of HEUR chemical structure on aqueous solutions, latex-based emulsions, and waterborne paints. Linear HEUR thickeners with different hydrophilic and hydrophobic segments were synthesized through a controlled one-step polymerization process by employing PEGs with molecular weights ranging from 2000 to 10,000 g/mol, resulting in HEUR molecular weights ranging from 8,000 to 33,000 g/mol. To investigate variations in molecular weight, we used HMDI-C8 as the terminal hydrophobic group. To investigate the effect of hydrophobic segment, we selected a HEUR molecular weight of 23,000 g/mol. Utilizing diisocyanates such as HMDI, IPDI, and HDI, we standardized the end-capping with C8. When mono-alcohol lengths were altered (C6 to C12), HMDI was retained as the diisocyanate linker.

The rheological analysis demonstrated a significant influence of the hydrophobe's structure on HEUR behavior across all studied formulations. Notably, HEUR samples with increased terminal hydrophobicity, particularly the P8-HMDI-C12, exhibited strongly pseudoplastic behavior in all formulations studied. In paint formulations, these structures demonstrated rapid structural regeneration and high TI values resulting in enhanced sag resistance. However, these benefits were offset by compromised leveling properties. In contrast, HEURs with less effective hydrophobic segments (P8-HDI/IPDI-C8 and P8-HMDI-C5/C6) displayed Newtonian rheological behavior and the corresponding paint formulations showed slower structural regeneration with superior leveling but worse anti-sag performance.

Regarding the hydrophilic segment, gradual increase in HEUR molecular weight up to 23,000 g/mol resulted in marginal viscosity changes in aqueous solutions, while a pronounced viscosity increase was observed with a molecular weight of 33,000 g/mol. In latex emulsions, lower molecular weight HEURs (8000 g/mol) displayed extended flocculated regions, a trend that appeared to be diminished with a 14,000 g/mol HEUR and absent with a 23,000 g/mol HEUR. In paint formulations, molecular weights of

14,000, 18,000, and 23,000 g/mol exhibited similar rheological response in paint formulations, but a molecular weight of 33,000 g/mol deviated, showing a shift towards higher viscosities and solid-like properties.

Finally, to explore HEUR micellar morphology, we employed Coarse-Grained Molecular Dynamics (CG-MD) simulations that effectively captured the spontaneous micelle formation starting from random polymeric chain distributions. We introduced an innovative automated approach for micellar identification using the DBSCAN algorithm accurately computing distinct hydrophobic micelle cores. By performing CG-MD simulations for various concentration values in aqueous solutions, we observed variations in the micellar network density correlating with experimental viscosity trends, while as the hydrophilic length of HEUR increased, the micellar volume continued to grow, in alignment with observed experimental viscosity changes.

References

- (1) Larson, R. G.; Van Dyk, A. K.; Chatterjee, T.; Ginzburg, V. V. Associative Thickeners for Waterborne Paints: Structure, Characterization, Rheology, and Modeling. *Prog. Polym. Sci.* **2022**, *129*. <https://doi.org/10.1016/j.progpolymsci.2022.101546>.
- (2) Bhavsar, R. A.; Nehete, K. M. Rheological Approach to Select Most Suitable Associative Thickener for Water-Based Polymer Dispersions and Paints. *J. Coatings Technol. Res.* **2019**, *16* (4), 1089–1098. <https://doi.org/10.1007/s11998-019-00194-6>.
- (3) Bhavsar, R.; Shreepathi, S. Evolving Empirical Rheological Limits to Predict Flow-Levelling and Sag Resistance of Waterborne Architectural Paints. *Prog. Org. Coatings* **2016**, *101*, 15–23. <https://doi.org/10.1016/j.porgcoat.2016.07.016>.
- (4) Diebold, M.; Backer, S. De; Niedenzu, P. M.; Hester, B. R.; Vanhecke, F. A. C. *Pigments, Extenders, and Particles in Surface Coatings and Plastics: Fundamentals and Applications to Coatings, Plastics and Paper Laminate Formulation*; 2022.
- (5) Patti, A.; Acierno, D. Structure-Property Relationships of Waterborne Polyurethane (WPU) in Aqueous Formulations. *J. Vinyl Addit. Technol.* **2023**, No. November 2022, 589–606. <https://doi.org/10.1002/vnl.21981>.
- (6) Smith, T.; Chisholm, D.; Cheng, A.; Salazar, J. O.; Roccucci, L.; Morales, B.;

- Dombrowski, G.; Rabasco, J.; Hartnett, P.; Fernando, R. Effects of Latex and Thickener Polarities on Rheology and Phase Stability of Latex–HEUR Mixtures. *J. Coatings Technol. Res.* **2023**. <https://doi.org/10.1007/s11998-022-00746-3>.
- (7) Kästner, U. The Impact of Rheological Modifiers on Water-Borne Coatings. *Colloids Surfaces A Physicochem. Eng. Asp.* **2001**, *183–185*, 805–821. [https://doi.org/10.1016/S0927-7757\(01\)00507-6](https://doi.org/10.1016/S0927-7757(01)00507-6).
- (8) Ginzburg, V. V.; Van Dyk, A. K.; Chatterjee, T.; Nakatani, A. I.; Wang, S.; Larson, R. G. Modeling the Adsorption of Rheology Modifiers onto Latex Particles Using Coarse-Grained Molecular Dynamics (CG-MD) and Self-Consistent Field Theory (SCFT). *Macromolecules* **2015**, *48* (21), 8045–8054. <https://doi.org/10.1021/acs.macromol.5b02080>.
- (9) Ginzburg, V. V.; Chatterjee, T.; Nakatani, A. I.; Van Dyk, A. K. Oscillatory and Steady Shear Rheology of Model Hydrophobically Modified Ethoxylated Urethane-Thickened Waterborne Paints. *Langmuir* **2018**, *34* (37), 10993–11002. <https://doi.org/10.1021/acs.langmuir.8b01711>.
- (10) Tripathi, A.; Tam, K. C.; McKinley, G. H. Rheology and Dynamics of Associative Polymers in Shear and Extension: Theory and Experiments. *Macromolecules* **2006**, *39* (5), 1981–1999. <https://doi.org/10.1021/ma051614x>.
- (11) Quienne, B.; Pinaud, J.; Robin, J. J.; Caillol, S. From Architectures to Cutting-Edge Properties, the Blooming World of Hydrophobically Modified Ethoxylated Urethanes (HEURs). *Macromolecules* **2020**, *53* (16), 6754–6766. <https://doi.org/10.1021/acs.macromol.0c01353>.
- (12) Larson, R. G.; Van Dyk, A. K.; Chatterjee, T.; Ginzburg, V. V. Associative Thickeners for Waterborne Paints: Structure, Characterization, Rheology, and Modeling. *Prog. Polym. Sci.* **2022**, *129*, 101546. <https://doi.org/10.1016/j.progpolymsci.2022.101546>.
- (13) Lu, M.; Song, C.; Wan, B. Influence of Prepolymer Molecular Weight on the Rheology and Kinetics of HEUR-Thickened Latex Suspensions. *Prog. Org. Coatings* **2021**, *156* (July 2020), 106223. <https://doi.org/10.1016/j.porgcoat.2021.106223>.
- (14) Abdala, A. A.; Wu, W.; Olesen, K. R.; Jenkins, R. D.; Tonelli, A. E.; Khan, S. A. Solution Rheology of Hydrophobically Modified Associative Polymers: Effects of Backbone Composition and Hydrophobe Concentration. *J. Rheol. (N. Y. N. Y.)* **2004**, *48* (5), 979–994. <https://doi.org/10.1122/1.1773781>.

- (15) Jenkins, R. D.; Bassett, D. R.; Silebi, C. A.; El-Aasser, M. S. Synthesis and Characterization of Model Associative Polymers. *J. Appl. Polym. Sci.* **1995**, *58* (2), 209–230. <https://doi.org/10.1002/app.1995.070580202>.
- (16) Berndlmaier, R. Rheology Additives for Coatings. *Handb. Coat. Addit.* 363–403.
- (17) Wypych, G. *Handbook of Rheological Additives*, First Edit.; Elsevier, 2022; Vol. 1. <https://doi.org/10.1016/C2021-0-00266-2>.
- (18) Shun Xing Zheng. *Principles of Organic Coatings and Finishing*; Cambridge Scholars Publishing, 2019.
- (19) Kaczmariski, J. P.; Glass, J. E. Synthesis and Characterization of Step Growth Hydrophobically-Modified Ethoxylated Urethane Associative Thickeners. *Langmuir* **1994**, *10* (9), 3035–3042. <https://doi.org/10.1021/la00021a029>.
- (20) May, R.; Kaczmariski, J. P.; Glass, J. E. Influence of Molecular Weight Distributions on HEUR Aqueous Solution Rheology. *Macromolecules* **1996**, *29* (13), 4745–4753. <https://doi.org/10.1021/ma9507655>.
- (21) Du, Z.; Wang, F.; Chang, X.; Peng, J.; Ren, B. Influence of Substituted Structure of Percec-Type Mini-Dendritic End Groups on Aggregation and Rheology of Hydrophobically Modified Ethoxylated Urethanes (HEURs) in Aqueous Solution. *Polymer (Guildf)*. **2018**, *135*, 131–141. <https://doi.org/10.1016/j.polymer.2017.12.022>.
- (22) Wang, Y.; Winnik, M. A. Onset of Aggregation for Water-Soluble Polymeric Associative Thickeners: A Fluorescence Study. *Langmuir* **1990**, *6* (9), 1437–1439. <https://doi.org/10.1021/la00099a001>.
- (23) Ma, Z.; Chen, M.; Glass, J. E. Adsorption of Nonionic Surfactants and Model HEUR Associative Thickeners on Oligomeric Acid-Stabilized Poly(Methyl Methacrylate) Latices. **1996**, *112*, 163–184.
- (24) Yekta, A.; Xu, B.; Duhamel, J.; Adiwidjaja, H.; Winnik, M. A. Fluorescence Studies of Associating Polymers in Water: Determination of the Chain End Aggregation Number and a Model for the Association Process. *Macromolecules* **1995**, *28* (4), 956–966. <https://doi.org/10.1021/ma00108a025>.
- (25) Xu, B.; Yekta, A.; Li, L.; Masoumi, Z.; Winnik, M. A. The Functionality of Associative Polymer Networks: The Association Behavior of Hydrophobically Modified Urethane-

- Ethoxylate (HEUR) Associative Polymers in Aqueous Solution. *Colloids Surfaces A Physicochem. Eng. Asp.* **1996**, *112* (2–3), 239–250. [https://doi.org/10.1016/0927-7757\(96\)03558-3](https://doi.org/10.1016/0927-7757(96)03558-3).
- (26) Winnik, M. A.; Yekta, A. Associative Polymers in Aqueous Solution. *Curr. Opin. Colloid Interface Sci.* **1997**, *2* (4), 424–436. [https://doi.org/10.1016/s1359-0294\(97\)80088-x](https://doi.org/10.1016/s1359-0294(97)80088-x).
- (27) Barmar, M.; Barikani, M.; Kaffashi, B. Steady Shear Viscosity Study of Various HEUR Models with Different Hydrophilic and Hydrophobic Sizes. *Colloids Surfaces A Physicochem. Eng. Asp.* **2005**, *253* (1–3), 77–82. <https://doi.org/10.1016/j.colsurfa.2004.06.028>.
- (28) Barmar, M.; Ribitsch, V.; Kaffashi, B.; Barikani, M.; Sarreshtedari, Z.; Pfragner, J. Influence of Prepolymers Molecular Weight on the Viscoelastic Properties of Aqueous HEUR Solutions. *Colloid Polym. Sci.* **2004**, *282* (5), 454–460. <https://doi.org/10.1007/s00396-003-0968-0>.
- (29) Kaffashi, B.; Barmar, M.; Eyvani, J. The Steady State and Dynamic Rheological Properties of Telechelic Associative Polymer Solutions. *Colloids Surfaces A Physicochem. Eng. Asp.* **2005**, *254* (1–3), 125–130. <https://doi.org/10.1016/j.colsurfa.2004.11.031>.
- (30) Jenkins, R. D.; Durali, M.; Silebi, C. A.; El-Aasser, M. S. Adsorption of Model Associative Polymers on Monodisperse Polystyrene Latex. *J. Colloid Interface Sci.* **1992**, *154* (2), 502–521. [https://doi.org/10.1016/0021-9797\(92\)90164-H](https://doi.org/10.1016/0021-9797(92)90164-H).
- (31) Huldén, M. Hydrophobically Modified Urethane-Ethoxylate (HEUR) Associative Thickeners 2. Interaction with Latex. *Colloids Surfaces A Physicochem. Eng. Asp.* **1994**, *88* (2–3), 207–221. [https://doi.org/10.1016/0927-7757\(94\)02835-4](https://doi.org/10.1016/0927-7757(94)02835-4).
- (32) Chen, M.; Wetzel, W. H.; Ma, Z.; Glass, J. E.; Buchacek, R. J.; Dickinson, J. G. Unifying Model for Understanding HEUR Associative Thickener Influences on Waterborne Coatings: I. HEUR Interactions with a Small Particle Latex. *J. Coatings Technol.* **1997**, *69* (867), 73–80. <https://doi.org/10.1007/bf02696149>.
- (33) Svanholm, T.; Molenaar, F.; Toussaint, A. Associative Thickeners: Their Adsorption Behaviour onto Latexes and the Rheology of Their Solutions. *Prog. Org. Coatings* **1997**, *30* (3), 159–165. [https://doi.org/10.1016/S0300-9440\(96\)00682-0](https://doi.org/10.1016/S0300-9440(96)00682-0).

- (34) Quadrat, O.; Šňupárek, J.; Mikešová, J.; Horský, J. Effect of “Hard” Comonomers Styrene and Methyl Methacrylate in Ethyl Acrylate/Acrylic Acid Latices on Their Thickening with Associative Thickener. *Colloids Surfaces A Physicochem. Eng. Asp.* **2005**, *253* (1–3), 163–168. <https://doi.org/10.1016/j.colsurfa.2004.10.098>.
- (35) Quadrat, O.; Horský, J.; Mrkvičková, L.; Mikešová, J.; Šňupárek, J. Thickening of Butyl Acrylate/Styrene/2-Hydroxyethyl Methacrylate/Acrylic Acid Latices with an HEUR Associative Thickener. *Prog. Org. Coatings* **2001**, *42* (1–2), 110–115. [https://doi.org/10.1016/S0300-9440\(01\)00167-9](https://doi.org/10.1016/S0300-9440(01)00167-9).
- (36) Pham, Q. T.; Russel, W. B.; Lau, W. The Effects of Adsorbed Layers and Solution Polymer on the Viscosity of Dispersions Containing Associative Polymers. *J. Rheol. (N. Y. N. Y.)* **1998**, *42* (1), 159–176. <https://doi.org/10.1122/1.550934>.
- (37) Lin, Y.; Song, C.; Xiao, X.; Wan, B. Influence of the Association of Hydrophobic End Groups on the Temperature Insensitivity of HEUR-Thickened Latex/Fe₂O₃/Zn₃(PO₄)₂/BaSO₄ Suspensions. *J. Coatings Technol. Res.* **2023**, *20* (2), 587–601. <https://doi.org/10.1007/s11998-022-00692-0>.
- (38) Santos, F. A.; Bell, T. J.; Stevenson, A. R.; Christensen, D. J.; Pfau, M. R.; Nghiem, B. Q.; Kasprzak, C. R.; Smith, T. B.; Fernando, R. H. Syneresis and Rheology Mechanisms of a Latex-HEUR Associative Thickener System. *J. Coatings Technol. Res.* **2017**, *14* (1), 57–67. <https://doi.org/10.1007/s11998-016-9829-x>.
- (39) Kostansek, E. Using Dispersion/Flocculation Phase Diagrams to Visualize Interactions of Associative Polymers, Latexes, and Surfactants. *J. Coatings Technol.* **2003**, *75* (940), 27–34. <https://doi.org/10.1007/bf02720511>.
- (40) Chatterjee, T.; Linsen, M.; Ginzburg, V. V.; Saucy, D. A.; Nakatani, A. I.; Van Dyk, A. K. Influence of the First Normal Stress Differences on Model Hydrophobically Modified Ethoxylated Urethane-Thickened Waterborne Paints Brush Drag. *Prog. Org. Coatings* **2019**, *135* (March), 582–590. <https://doi.org/10.1016/j.porgcoat.2019.06.029>.
- (41) Procopio, L. To Control the Rheology of Paints and Coatings. *CoatingsTech*.
- (42) Tzortzi, I.; Xiouras, C.; Choustoulaki, C.; Tzani, A.; Detsi, A.; Michaud, G.; Van Gerven, T.; Stefanidis, G. D. One-Step versus Two-Step Synthesis of Hydrophobically Modified Ethoxylated Urethanes: Benefits and Limitations. *Ind. Eng. Chem. Res.* **2023**, *62* (29), 11378–11391. <https://doi.org/10.1021/acs.iecr.3c01107>.

- (43) Bampouli, A.; Tzortzi, I.; Schutter, A. De; Xenou, K.; Michaud, G.; Stefanidis, G. D.; Gerven, T. Van. Insight Into Solventless Production of Hydrophobically Modified Ethoxylated Urethanes (HEURs): The Role of Moisture Concentration , Reaction Temperature , and Mixing Efficiency. *ACS Omega* **2022**, No. int. <https://doi.org/10.1021/acsomega.2c04530>.
- (44) *Bonding Parameters-Martini site.* http://www.cgmartini.nl/images/parameters/ITP/martini_v2.0_solvents.itp (accessed 2023-04-01).
- (45) Ester, M.; Kriegel, H.-P.; Sander, J.; Xu, X. A Density-Based Algorithm for Discovering Clusters in Large Spatial Databases with Noise. In *Knowledge Discovery and Data Mining*; 1996.
- (46) Liu, Y.-S.; Yi, J.; Zhang, H.; Zheng, G.-Q.; Paul, J.-C. Surface Area Estimation of Digitized 3D Objects Using Quasi-Monte Carlo Methods. *Pattern Recognit.* **2010**, *43* (11), 3900–3909. <https://doi.org/10.1016/j.patcog.2010.06.002>.
- (47) Davis, P. J.; Rabinowitz, P.; Rheinbolt, W. *Methods of Numerical Integration*; Computer Science and Applied Mathematics; Elsevier Science, 2014.
- (48) Vrandečić, N. S.; Erceg, M.; Jakić, M.; Klarić, I. Kinetic Analysis of Thermal Degradation of Poly(Ethylene Glycol) and Poly(Ethylene Oxide)s of Different Molecular Weight. *Thermochim. Acta* **2010**, *498* (1–2), 71–80. <https://doi.org/10.1016/j.tca.2009.10.005>.
- (49) Delpech, M. C.; Miranda, G. S. Waterborne Polyurethanes: Influence of Chain Extender in FTIR Spectra Profiles. *Cent. Eur. J. Eng.* **2012**, *2* (2), 231–238. <https://doi.org/10.2478/s13531-011-0060-3>.
- (50) Auguścik, M.; Kurańska, M.; Prociak, A.; Karalus, W.; Lipert, K.; Ryszkowska, J. Production and Characterization of Poly(Urea-Urethane) Elastomers Synthesized from Rapeseed Oil-Based Polyols Part I. Structure and Properties. *Polimery/Polymers* **2016**, *61* (7–8), 490–498. <https://doi.org/10.14314/polimery.2016.490>.
- (51) Zhao, X.; Qi, Y.; Li, K.; Zhang, Z. Hydrogen Bonds and FTIR Peaks of Polyether Polyurethane-Urea. *Key Eng. Mater.* **2019**, *815 KEM*, 151–156. <https://doi.org/10.4028/www.scientific.net/KEM.815.151>.
- (52) Yilgör, E.; Burgaz, E.; Yurtsever, E.; Yilgör, I. Comparison of Hydrogen Bonding in

- Polydimethylsiloxane and Polyether Based Urethane and Urea Copolymers. *Polymer (Guildf)*. **2000**, *41* (3), 849–857. [https://doi.org/10.1016/S0032-3861\(99\)00245-1](https://doi.org/10.1016/S0032-3861(99)00245-1).
- (53) Teo, L. S.; Chen, C. Y.; Kuo, J. F. Fourier Transform Infrared Spectroscopy Study on Effects of Temperature on Hydrogen Bonding in Amine-Containing Polyurethanes and Poly(Urethane-Urea)S. *Macromolecules* **1997**, *30* (6), 1793–1799. <https://doi.org/10.1021/ma961035f>.
- (54) Mattia, J.; Painter, P. A Comparison of Hydrogen Bonding and Order in a Polyurethane and Poly(Urethane-Urea) and Their Blends with Poly(Ethylene Glycol). *Macromolecules* **2007**, *40* (5), 1546–1554. <https://doi.org/10.1021/ma0626362>.
- (55) Stern, T. Conclusive Chemical Deciphering of the Consistently Occurring Double-Peak Carbonyl-Stretching FTIR Absorbance in Polyurethanes. *Polym. Adv. Technol.* **2019**, *30* (3), 675–687. <https://doi.org/10.1002/pat.4503>.
- (56) Grassl, B.; Billon, L.; Borisov, O.; François, J. Poly(Ethylene Oxide)- and Poly (Acrylamide)-Based Water-Soluble Associative Polymers: Synthesis, Characterisation, Properties in Solution. *Polym. Int.* **2006**, *55* (10), 1169–1176. <https://doi.org/https://doi.org/10.1002/pi.2015>.
- (57) Annable, T.; Buscall, R.; Ettelaie, R. Rheology Of Transient Networks Formed By The Association Of Hydrophobically Modified Water Soluble Polymers. *Amphiphilic Block Copolym.* **2000**, 281–304. <https://doi.org/10.1016/B978-044482441-7/50013-X>.
- (58) Annable, T.; Buscall, R.; Ettelaie, R.; Whittlestone, D. The Rheology of Solutions of Associating Polymers: Comparison of Experimental Behavior with Transient Network Theory. *J. Rheol. (N. Y. N. Y)*. **1993**, *37* (4), 695–726. <https://doi.org/10.1122/1.550391>.
- (59) Kaczmarek, J. P.; Glass, J. E. Synthesis and Solution Properties of Hydrophobically-Modified Ethoxylated Urethanes with Variable Oxyethylene Spacer Lengths. *Macromolecules* **1993**, *26* (19), 5149–5156. <https://doi.org/10.1021/ma00071a026>.
- (60) de Molina, P. M.; Gradzielski, M. Gels Obtained by Colloidal Self-Assembly of Amphiphilic Molecules. *Gels* **2017**, *3* (3), 1–27. <https://doi.org/10.3390/gels3030030>.
- (61) Lopes L., Silveira B., M. R. Rheological Evaluation of HPAM Fluids for EOR Applications. *IJET Int. J. Eng. Technol.* **2014**, *14* (03), 35–41.
- (62) Gonzalez-gutierrez, J.; Oblak, P.; Emri, I. Improving Powder Injection Moulding by

- Modifying Binder Viscosity through Different Molecular Weight Variations 12 . 5
Improving Powder Injection Moulding by Modifying Binder Viscosity through
Different Molecular Weight Variations. **2013**, No. January 2014.
- (63) Elliott, P. T.; Xing, L. L.; Wetzel, W. H.; Glass, J. E. Influence of Terminal Hydrophobe Branching on the Aqueous Solution Behavior of Model Hydrophobically Modified Ethoxylated Urethane Associative Thickeners. *Macromolecules* **2003**, *36* (22), 8449–8460. <https://doi.org/10.1021/ma020166f>.
- (64) Wang, S.; Larson, R. G. A Coarse-Grained Implicit Solvent Model for Poly(Ethylene Oxide), CnEm Surfactants, and Hydrophobically End-Capped Poly(Ethylene Oxide) and Its Application to Micelle Self-Assembly and Phase Behavior. *Macromolecules* **2015**, *48* (20), 7709–7718. <https://doi.org/10.1021/acs.macromol.5b01587>.
- (65) Yuan, F.; Larson, R. G. Multiscale Molecular Dynamics Simulations of Model Hydrophobically Modified Ethylene Oxide Urethane Micelles. *J. Phys. Chem. B* **2015**, *119* (38), 12540–12551. <https://doi.org/10.1021/acs.jpcc.5b04895>.
- (66) Kostansek, E. Controlling Particle Dispersion in Latex Paints Containing Associative Thickeners. *J. Coatings Technol. Res.* **2007**, *4* (4), 375–388. <https://doi.org/10.1007/s11998-007-9037-9>.
- (67) Kostansek, E. Latex Polymer Interactions with Associative Thickeners. *Int. latex Conf.* **2006**, 1–14.
- (68) Mezger, T. G. *The Rheology Handbook*; 2009; Vol. 38. <https://doi.org/10.1108/prt.2009.12938eac.006>.
- (69) Antoon-Paar. *3iTT test*. <https://wiki.anton-paar.com/en/3itt-test/> (accessed 2023-08-02).
- (70) Mezger, T. *The Rheology Handbook*; Vincentz Network, 2020. <https://doi.org/doi:10.1515/9783748603702>.
- (71) Malkin, A.; Kulichikhin, V.; Ilyin, S. A Modern Look on Yield Stress Fluids. *Rheol. Acta* **2017**, *56* (3), 177–188. <https://doi.org/10.1007/s00397-016-0963-2>.
- (72) Collivignarelli, M. C.; Todeschini, S.; Bellazzi, S.; Carnevale Miino, M.; Caccamo, F. M.; Calatroni, S.; Baldi, M.; Manenti, S. Understanding the Influence of Diverse Non-Volatile Media on Rheological Properties of Thermophilic Biological Sludge and Evaluation of Its Thixotropic Behaviour. *Appl. Sci.* **2022**, *12* (10).

<https://doi.org/10.3390/app12105198>.

- (73) Boubakri, A.; Haddar, N.; Elleuch, K.; Bienvenu, Y. Influence of Thermal Aging on Tensile and Creep Behavior of Thermoplastic Polyurethane. *Comptes Rendus - Mec.* **2011**, *339* (10), 666–673. <https://doi.org/10.1016/j.crme.2011.07.003>.
- (74) Peroukidis, S. D.; Tsalikis, D. G.; Noro, M. G.; Stott, I. P.; Mavrantzas, V. G. Quantitative Prediction of the Structure and Viscosity of Aqueous Micellar Solutions of Ionic Surfactants: A Combined Approach Based on Coarse-Grained MARTINI Simulations Followed by Reverse-Mapped All-Atom Molecular Dynamics Simulations. *J. Chem. Theory Comput.* **2020**, *16* (5), 3363–3372. <https://doi.org/10.1021/acs.jctc.0c00229>.

**Conclusions and
Recommendations for future work**

6.1. Conclusions

The main findings of this doctoral project related to the research objectives presented in Chapter 1 are summarized below.

Before delving into the details of the process optimization aspects of HEUR synthesis, one of the most important findings was the realization that the sampling method employed for testing polyurethane melts, significantly influences the molecular weight determination and the chemical characterization of polyurethanes. The “solid method” in which the molten sample was collected from the bulk and analyzed after solidification showed molecular weights up to 115% higher than the “in-situ method”, in which the molten sample was directly dissolved in vials with pre-weighed dry chloroform, due to chain-extension reaction between NCO-terminated urethane prepolymers and ambient moisture. Specifically, we found that using the solid method resulted in number-average molecular weights that were 50-77% higher for samples with lower isocyanate content, and even 115% higher for those with elevated isocyanate concentrations, as compared to the in-situ method. This discrepancy is attributed to chain-extension reactions involving NCO-terminated urethane prepolymers and ambient moisture, which led to the formation of urea linkages and an extended polyurea structure. To obtain accurate and reliable data on key product properties like molecular weight, composition, and viscosity, it is imperative to either neutralize residual NCO content or meticulously prevent its exposure to atmospheric moisture.

Regarding the effect of process parameters in the one-step HEUR synthesis we showed that the moisture concentration in the initial polyol used directly impacts the polymerization of HEUR. It's essential to maintain a moisture content below an industry-standard threshold of 1000 ppm to promote the primary urethane reaction and prevent unwanted reactions that subsequently affect the viscosity of HEUR aqueous solutions. Regarding the effect of process parameters in the one-step HEUR synthesis, we found that the moisture concentration in the initial polyol directly impacts the polymerization of HEUR.

Appendix-Supporting Information

Consequently, the initial PEG moisture content should be kept below 1000 ppm to prevent side reactions that subsequently will affect the viscosity of HEUR aqueous solution. Further, when conducting bulk polyurethane polymerizations in batch reactors with overhead stirring, both elevated mixing speeds and higher reaction temperatures (within the range of 80-110 °C) promote faster molecular weight development, but the same molecular weight plateau value is reached in both cases. However, irrespective of the reaction conditions employed during the polymerization, it was found that when the molecular weight of polyurethanes approaches 21,000 g/mol, the polymer becomes a viscous gel that crawls on the agitator rod and keeps rotating, violently hitting the reactor walls, a phenomenon known as the Weissenberg effect. Therefore, an accelerated rate of molecular weight increase, either due to elevated mixing speeds or higher reaction temperatures, leads to an earlier occurrence of the Weissenberg effect, which can jeopardize the homogeneous distribution of reactants within the viscous PEG resulting in variations and inconsistencies between batches. Therefore, our recommendation is to employ moderate mixing speeds tailored to the specific polymerization scale, and, due to PEG's inherent susceptibility to thermal degradation, maintain reaction temperatures between 80-85°C, especially when long polymerization times are employed at industrial scale.

As a next step, we studied the benefits and limitations of utilizing either a one-step (simultaneous chain growth and end-capping) versus a two-step (chain growth followed by end-capping) polymerization process, highlighting their impact on the final HEUR properties. In the conventional one-step process (current industrial practice) there are inherent limitations in producing high molecular weight polymers due to the complex competition between end-capping and polymerization. We found that the two-step method allows for much higher molecular weight polymers than the one-step method, while using less amount of toxic diisocyanates. Additionally, using the two-step method, the polymerization can be simply and efficiently controlled by the addition timepoint of the end-capping agent, which can be tailored to provide HEURs with a wide range of molecular weight and polydispersity index. However, the efficient end-capping of high molecular weight polymers remains a challenge when using conventional mixing equipment in batch reactors, due to mass transfer and mixing limitations associated with the significant

Appendix-Supporting Information

increase in the bulk viscosity of the reaction mixture. To overcome these limitations, alternative and more efficient mixing technologies, such as reactive extruders, should be considered for the efficient end-capping of high molecular weight polymers.

Given that the industrial HEUR synthesis is a slow and energy-intensive polymerization process, due to heat and mass transfer limitations inherent in such highly viscous systems, we investigated the application of microwave (MW) irradiation as an alternative energy source in HEUR synthesis in order to enable fast volumetric heating. Particularly, we investigated the effect of microwave heating on both the HEUR synthesis step and the initial pretreatment step of the reagents prior to the HEUR synthesis. During the reactant pretreatment step, MW heating can reduce the overall process time through tenfold faster melting of solid PEG. However, in the subsequent PEG dehydration step, use of MWs should be avoided, as faster degradation of PEG was observed compared to the dehydration by conventional heating (CH) at similar bulk temperature. In the polymerization reaction, it was shown that both molecular weight, M_n , and polydispersity index, PDI, of the HEUR prepolymer are independent of the heating source, as no significant differences were found when the same reaction temperature was applied. However, it was concluded that the operation of the batch reactor in a rapid unsteady-state (transient) temperature profile, only attainable with MW heating, resulted in the production of HEURs with comparable molecular weights to those produced via isothermal CH experiments at process times multifold lower (4 min vs. 45 or 120 min at a temperature of 110 °C and 80 °C, respectively), due to the rapid thermal response of the polymerization mixture under MW irradiation. A comparison of the energy requirements of the two heating methods, that is, the isothermal CH method and the transient MW heating one, at comparable mean temperatures, shows that the latter needs approximately 3 times less energy to achieve the same molecular weight polymer, due to the shorter processing times (and subsequently lower heat losses to the surroundings) and the elimination of the additional energy needed to heat up the heat transfer fluid.

Given the inherent characteristics of HEUR polymerization, combined with insights from our research and the limitations of batch processing for such viscous systems, we propose

Appendix-Supporting Information

the application of MW in continuous reactive extruders. As such, the temporal (transient) temperature profiles in batch mode could be translated into spatial temperature profiles in extruder barrels, when the latter are irradiated with MW. Application of microwave irradiation in a reactive extrusion process could intensify HEUR production by reducing the overall process time and energy consumption as well as the length and number of modules in reactive extruders for a given throughput. Additionally, microwaves allow for more flexible production since they can be started or shut down quickly. In the long-term, the potential of using renewable energy (wind or solar) to enable MW generation makes the technology even more attractive.

In the last part of the project, the effects of hydrophilic and hydrophobic segments of HEURs on the rheology and properties of various waterborne dispersions, including aqueous solutions, latex-based emulsions, and commercial waterborne paint formulations were investigated using both experimental and computational methodologies. The rheological analysis demonstrated a significant influence of the hydrophobe's structure on HEUR behavior across all studied formulations. Notably, HEUR samples with increased terminal hydrophobicity, particularly the P8-HMDI-C12, exhibited strongly pseudoplastic behavior in all formulations studied. In paint formulations, these structures demonstrated rapid structural regeneration and high TI values resulting in enhanced sag resistance. However, these benefits were offset by compromised leveling properties. In contrast, HEURs with less effective hydrophobic segments (P8-HDI/IPDI-C8 and P8-HMDI-C5/C6) displayed Newtonian rheological behavior and the corresponding paint formulations showed slower structural regeneration with superior leveling but worse anti-sag performance.

Regarding the hydrophilic segment, gradual increase in HEUR molecular weight up to 23,000 g/mol resulted in marginal viscosity changes in aqueous solutions, while a pronounced viscosity increase was observed with a molecular weight of 33,000 g/mol. In latex emulsions, lower molecular weight HEURs (8000 g/mol) displayed extended flocculated regions, a trend that appeared to be diminished with a 14,000 g/mol HEUR and absent with a 23,000 g/mol HEUR. In paint formulations, molecular weights of 14,000,

Appendix-Supporting Information

18,000, and 23,000 g/mol exhibited similar rheological response in paint formulations, but a molecular weight of 33,000 g/mol deviated, showing a shift towards higher viscosities and solid-like properties.

Finally, to explore HEUR micellar morphology, we employed Coarse-Grained Molecular Dynamics (CG-MD) simulations that effectively captured the spontaneous micelle formation starting from random polymeric chain distributions. We introduced an innovative automated approach for micellar identification using the DBSCAN algorithm accurately computing distinct hydrophobic micelle cores. By performing CG-MD simulations for various concentration values in aqueous solutions, we observed variations in the micellar network density correlating with experimental viscosity trends, while as the hydrophilic length of HEUR increased, the micellar volume continued to grow, in alignment with observed experimental viscosity changes.

Appendix-Supporting Information

6.2. Recommendations for future work

Future research should focus on the synthesis of Uni-HEUR thickeners which are characterized by their monomodal molecular weight distribution. These polymers have demonstrated superior thickening efficiency over their polydisperse counterparts (S-G HEURs) and require lower concentrations to achieve desired viscosities. To fully understand the mechanism behind the enhanced thickening properties of Uni-HEUR, it is crucial to utilize advanced characterization techniques. The deployment of two-Dimensional Liquid Chromatography (2D-LC) is particularly promising. The combination of size exclusion chromatography (SEC) with ultra-high-performance Advanced Polymer Chromatography (APC), followed by gradient reversed-phase liquid chromatography (RPLC), will enable a careful analysis of how synthesis conditions affect the structure of Uni-HEUR and its thickening performance.

In addition, the synthesis of sensitive or reactive HEURs is a new way to expand the use of HEURs to new fields of application. In fact, controlling the viscosity of a solution under external stimuli would lead to smart rheological fluids and coating applications. On the other hand, the development of novel structures such as multiarms and dendritics or introducing novel hydrophobic and hydrophilic structures could also lead to the development of more efficient rheological modifiers.

While the synthesis of novel HEUR structures is progressing, parallel advances in computational modeling are essential to complement and accelerate experimental efforts. In the field of computational analysis, refinement of coarse-grained molecular dynamics (CG-MD) models is required. The aim is to improve their ability to capture the nuanced behaviors of HEURs, particularly with regard to hydrophobic interactions. By transitioning to models that utilize shorter polymer backbones, we can improve the accuracy of representing hydrophobic interactions. Furthermore, a two-step approach using CG-MD simulations followed by reverse mapping and subsequent all-atom molecular dynamics simulations can improve the accuracy of quantitative prediction of micelle formation in aqueous solutions when studying the effect of hydrophobic segment structure of HEUR. Additionally, extending the use of CG-MD simulations to model HEUR network formation

Appendix-Supporting Information

in the presence of latex particles can provide important insights for formulators. These simulations will improve our understanding of the influence of HEUR structure on network formation, emulsion stability, and flocculation.

In response to the environmental concerns presented by isocyanate monomers traditionally used in HEUR synthesis, research should also invest in developing non-isocyanate polyurethane alternatives (NIPUs) such as polyhydroxyurethanes (PHUs) through the aminolysis of cyclic carbonates. However, the progress of this method is restrained due to limited commercial availability of cyclic carbonates and the early stage of this technology. Furthermore, there is little current research aimed at increasing the efficiency of solventless aminolysis, and the process often exhibits long reaction times, suboptimal conversions, and inconsistent product quality. Overcoming these obstacles, particularly in achieving high molecular weight PHUs with bulk polymerization in a standard batch reactor, remains a challenge. In this context, the application of MW irradiation could potentially accelerate reaction kinetics and improve the homogeneity of PHUs. This innovative approach could provide a safer and more environmentally friendly alternative to traditional isocyanate-based polyurethane synthesis.

Simultaneously, the development of Hydrophobically Modified PolyEthers (HMPE) should be accelerated. These thickeners, produced without diisocyanates, present a greener substitute, potentially able to replace isocyanate-based thickeners in specific applications. HMPEs exhibit comparable viscosity profiles to HEURs, positioning them as immediate, more sustainable alternatives while NIPU technologies mature.

Supporting Information for all Chapters

SI for Chapter 2

A. Sampling of the produced polymers

The sampling procedure was based on GPC analysis data. More specifically, sampling directly in dry chloroform (GPC solvent) showed lower values of M_n/M_w compared to the analysis performed by diluting the samples after solidification in the same solvent. As an example, data from the mixing study are presented in the current paragraph. The details of the formulation follow in **Table S2.0.1** below:

Table S2.0.1. Reaction conditions for the sampling experiments from the mixing study.

Appendix-Supporting Information

Moisture (ppm)	Reaction Temperature (°C)	Mixing Speed (rpm)	Catalyst (%)	HMDI/ PEG	PEG/ Oct	Sampling Time (min)
700-800	80	30/100/300/750	0.035	1.5	1	3/15

The results from the GPC analysis are shown in **Figure S2.0.2** and **Figure S2.0.3** below for 3 and 15 minutes of reaction respectively:

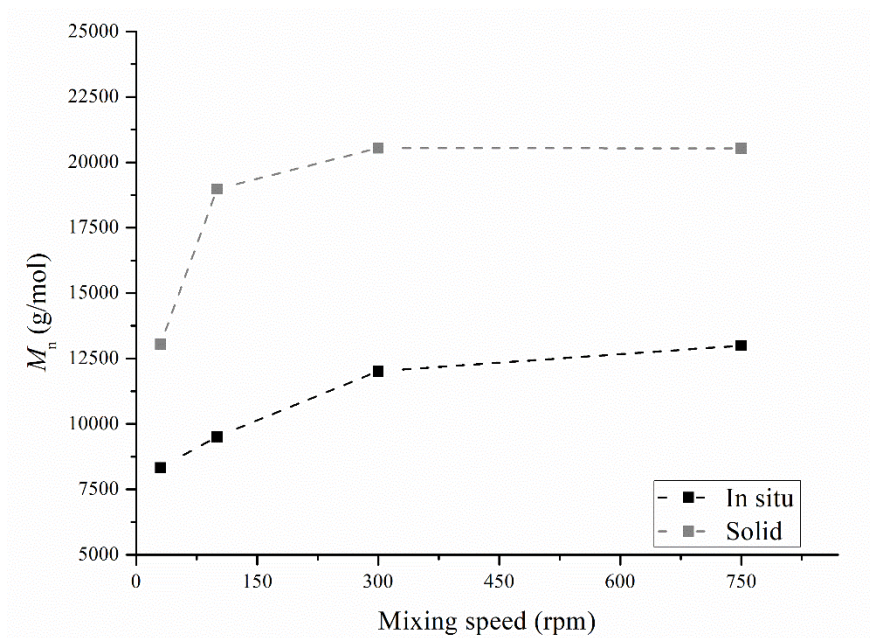


Figure S2.0.1. Results from GPC analysis for solid samples (grey data points) compared to sampling directly in dry chloroform (black data points). The experimental operating conditions are those applied for the mixing speed parametric study, and the samples were collected at 3 minutes after the start of the reaction. The dashed lines have been added to guide the eye.

Appendix-Supporting Information

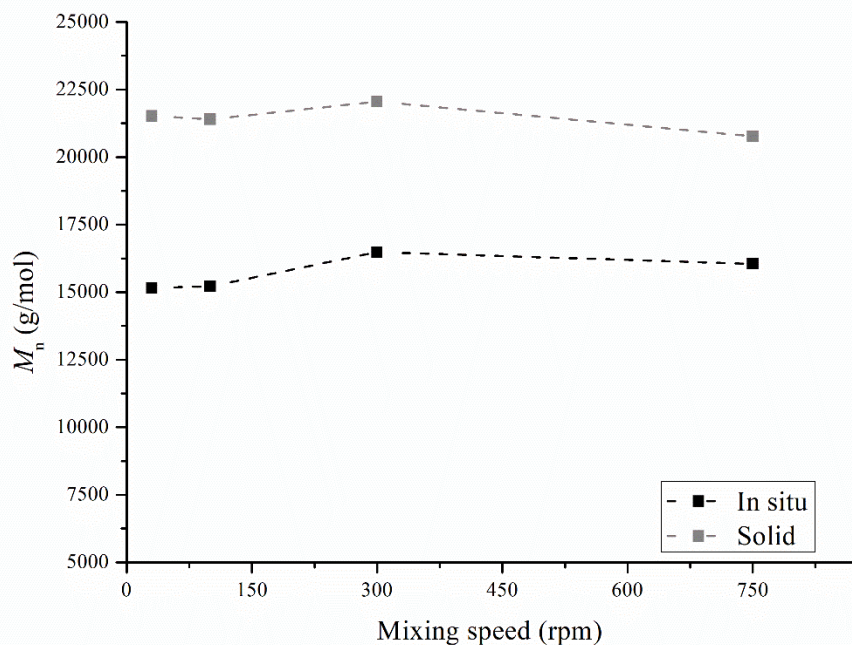


Figure S2.0.2. Results from GPC analysis for solid samples (grey data points) compared to sampling directly in dry chloroform (black data points). The experimental operating conditions are those applied for the mixing speed parametric study, and the samples were collected at 15 minutes after the start of the reaction. The dashed lines have been added to guide the eye.

In the work of Arnould et al.¹, excess of dry methanol was added to the solvent to ensure the end capping of $N = C = O$ terminated polymers in the system. Specifically, in case the produced polymers are terminated with $N = C = O$ groups, side reactions can occur during GPC analysis resulting in different M_n/M_w values. In order to evaluate whether this effect occurs in our system, selected HEUR samples were “in situ” dissolved in the GPC solvent (dry chloroform) containing excess of dry MeOH.

The obtained GPC results of “in situ” sampling in both chloroform and chloroform/MeOH were directly compared. Samples from the moisture and the mixing study were analyzed and are presented below as examples. The details of the formulation follow in Table S2.0.2 (moisture parametric study) and Table S2.0.3 (mixing parametric study) below:

Appendix-Supporting Information

Table S2.0.2. Reaction conditions for the sampling (chloroform / chloroform *MeOH*) experiments based on the moisture parametric study.

Moisture (ppm)	Reaction Temperature (°C)	Mixing Speed (rpm)	Catalyst (%)	HMDI/ PEG	PEG/ Oct	Sampling Time (min)
various	80	100	0.035	1.5	1	45

Table S2.0.3. Reaction conditions for the sampling (chloroform / chloroform *MeOH*) experiments based on the mixing speed parametric study.

Moisture (ppm)	Reaction Temperature (°C)	Mixing Speed (rpm)	Catalyst (%)	HMDI/ PEG	PEG/ Oct	Sampling Time (min)
800	110	100	0.035	1.5	1	5

The results presented in Figure S2.0.3 indicate that the two methods result in very similar M_n values. It was decided that quenching with dry MeOH is not necessary for the produced polymers of the current study.

Appendix-Supporting Information

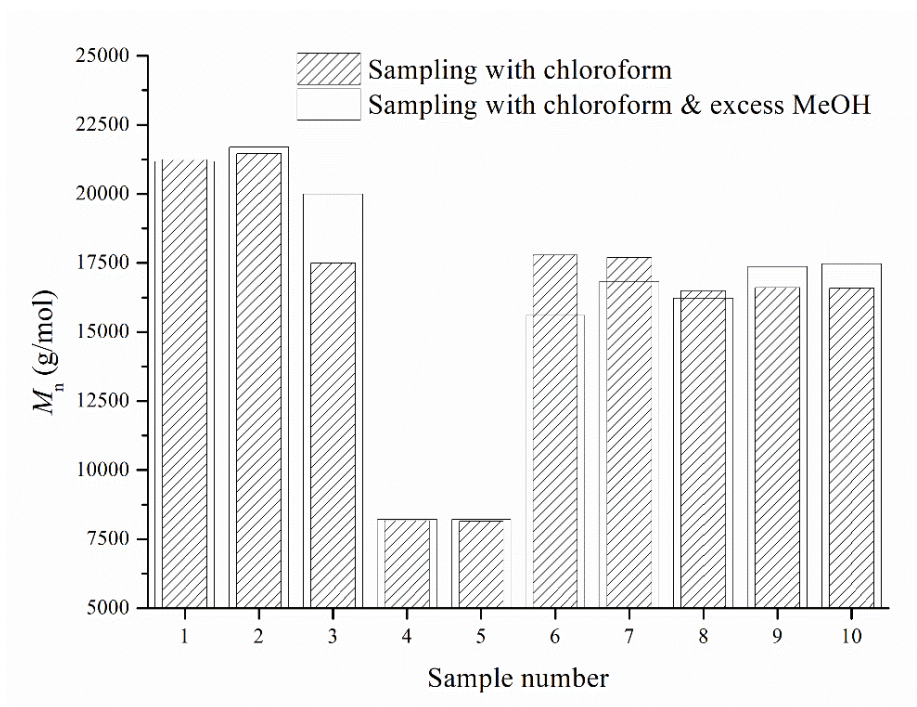


Figure S2.0.3. Results from GPC analysis for sampling directly in dry chloroform (dashed columns) compared to sampling in dry chloroform with methanol excess (solid columns). Examples 1 to 5: samples from the moisture parametric study and 6 to 10: samples from the mixing speed parametric study.

Appendix-Supporting Information

B.Homogeneity of the bulk polymers

In order to evaluate the homogeneity of the polymeric bulk, various samples from the same reaction product were analysed. More specifically, for two different cases from the reaction temperature parametric study, samples from five different spots (perpendicular and a long to the agitator axis) were collected from the bulk at the same reaction times (5 and 15 minutes of reaction). The stoichiometric ratios and other details are presented in Table S2.0.4 for both cases:

Table S2.0.4. Reaction conditions for the homogeneity experiments based on the temperature parametric study.

	Moisture (ppm)	Reaction Temperature (°C)	Mixing Speed (rpm)	Catalyst (%)	HMDI/ PEG	PEG/ Oct	Sampling Time (min)
Case 1	780	110	100	0.035	1.5	1	5
Case 2	760	80	100	0.035	1	1	15

The GPC analysis of the samples from both cases shows that a deviation of up to $\approx 9\%$ (in terms of M_n/M_w values) exists in the bulk mixture. More specifically, in case 1, the M_n range (maximum-minimum M_n) was 1287 g/mol, while the average M_n was 17029 g/mol. In case 2, the corresponding M_n range was 1233 g/mol, while the average M_n was 13995 g/mol. The results are presented in Figure S2. 0.4 and Table S2.0.5.

Appendix-Supporting Information

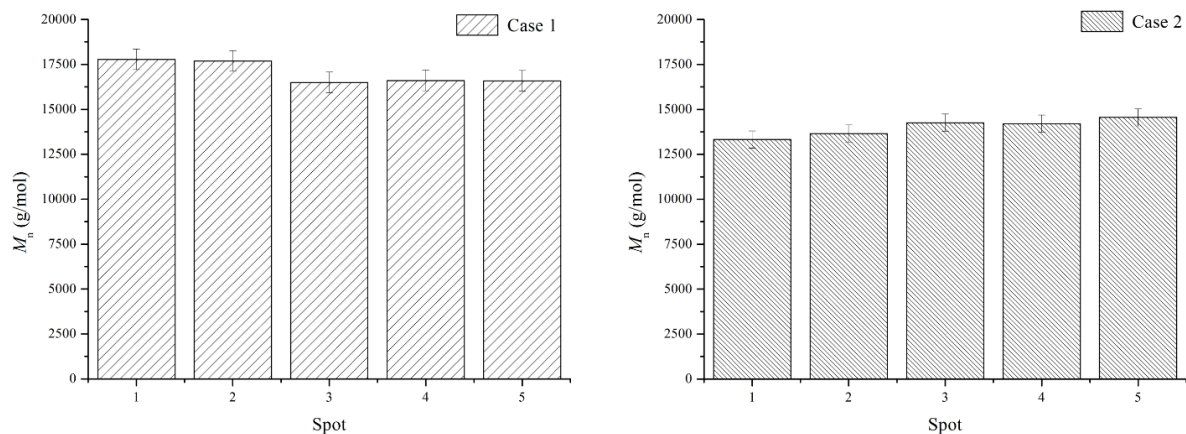


Figure S2.0.4. Results from GPC analysis for the evaluation of the bulk homogeneity.

Table S2.0.5. Results from GPC analysis for the evaluation of the bulk homogeneity: average, STD, min and max values.

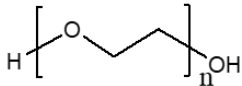
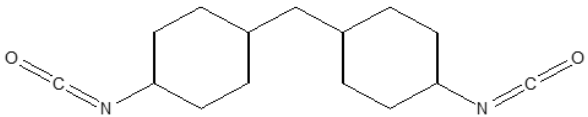
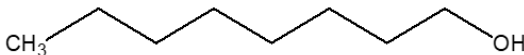
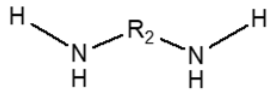
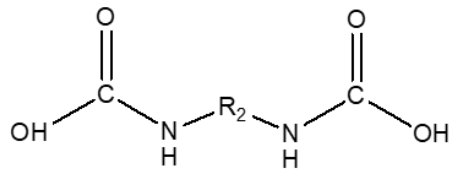
	Case 1	Case 2
Average (g/mol)	17029	13995
STD (g/mol)	577	447
Max M_n	17778	14551
Min M_n	16491	13318
Range=max-min	1287	1233

C. Chemical structures and basic chemical reactions

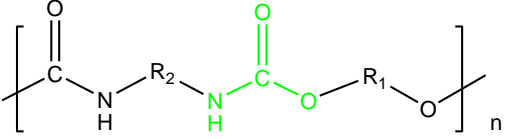
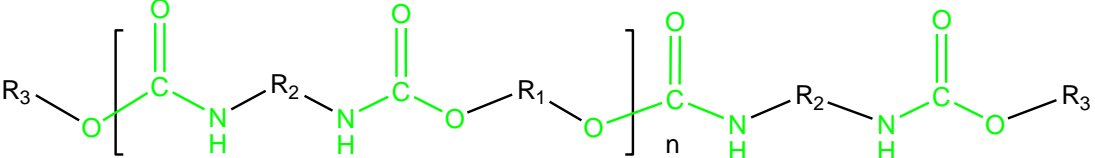
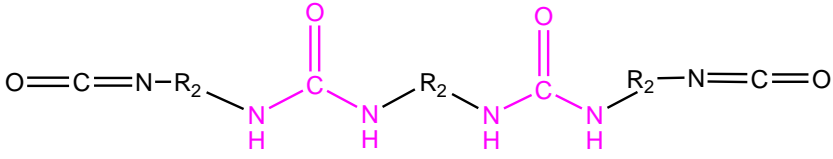
In Table S2.0.6 the chemical structures of the main reactants and (by)products can be found.

Appendix-Supporting Information

Table S2.0.6. List of chemical reactants and major (by)products related to the HEURs production.

Reactant/ (by)product	Simplified structure	Chemical structure
Polyethylene glycol	$\text{HO}-\text{R}_1-\text{OH}$	 $\text{H} \left[\text{O}-\text{CH}_2-\text{CH}_2 \right]_n \text{OH}$
4,4-dicyclohexyl methane diisocyanate	$\text{O}=\text{C}=\text{N}-\text{R}_2-\text{N}=\text{C}=\text{O}$	
Octanol	R_3-OH	 $\text{CH}_3(\text{CH}_2)_6\text{OH}$
Amine	$\text{H}-\text{N}(\text{H})-\text{R}_2-\text{N}(\text{H})-\text{H}$	
Carbamic acid	$\text{HOOC}-\text{N}(\text{H})-\text{R}_2-\text{N}(\text{H})-\text{COOH}$	
Carbon dioxide	$\text{O}=\text{C}=\text{O}$	

Appendix-Supporting Information

Water	$\text{H}-\text{OH}$
Polyurethane (PU)	
HEUR	
Polyurea	

The main possible reactions in the HEUR/ Prepolymer system evaluated in the current work can be summarized in the following five reactions:

- Main polyurethane (PU) reaction: PEG + H₁₂MDI
- Hydrophobic modification of polyurethane (HEUR synthesis): PU + 1-Octanol
- Diisocyanate and hydrophobe reaction: H₁₂MDI + 1-Octanol
- Diisocyanate and water reaction: H₁₂MDI + H₂O
- Diisocyanate and amine reaction: H₁₂MDI + Amine

A simplified representation of this chemistry is presented in the following section. It should be noted that other possible primary (e.g. urea with H₁₂MDI) or secondary reactions (e.g.,

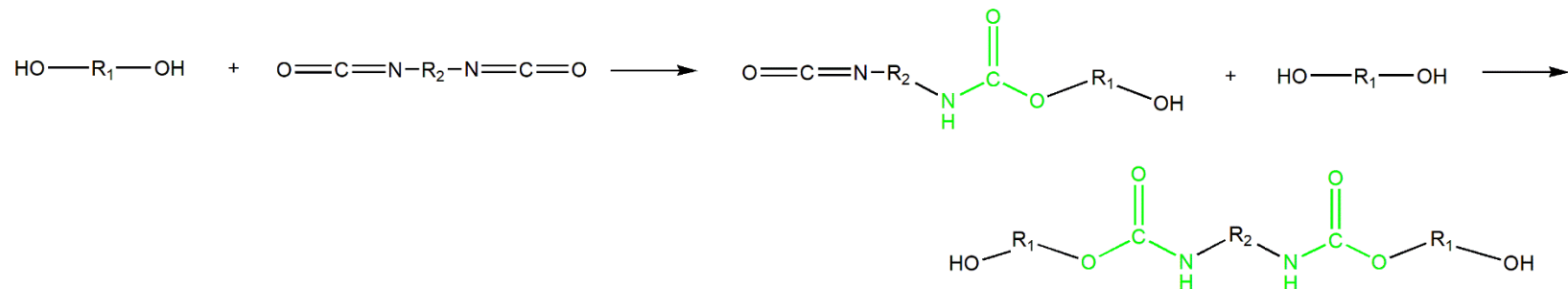
Appendix-Supporting Information

PU or polyurea with H₁₂MDI) have not been considered. For further reactions and details reference to the literature is made.^{2, 3}

Appendix-Supporting Information

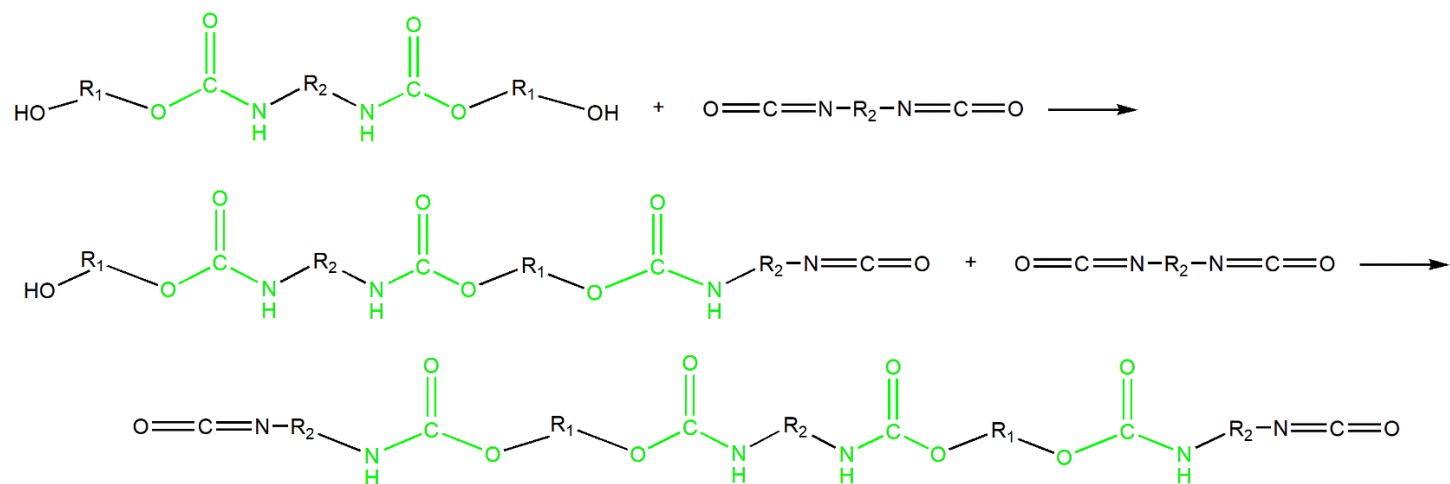
Main polyurethane (PU) reaction: PEG + H₁₂MDI

Step A



Step B

Appendix-Supporting Information



Repeated step A followed by step B for chain build up: polyurethane production

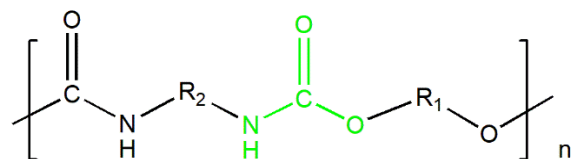
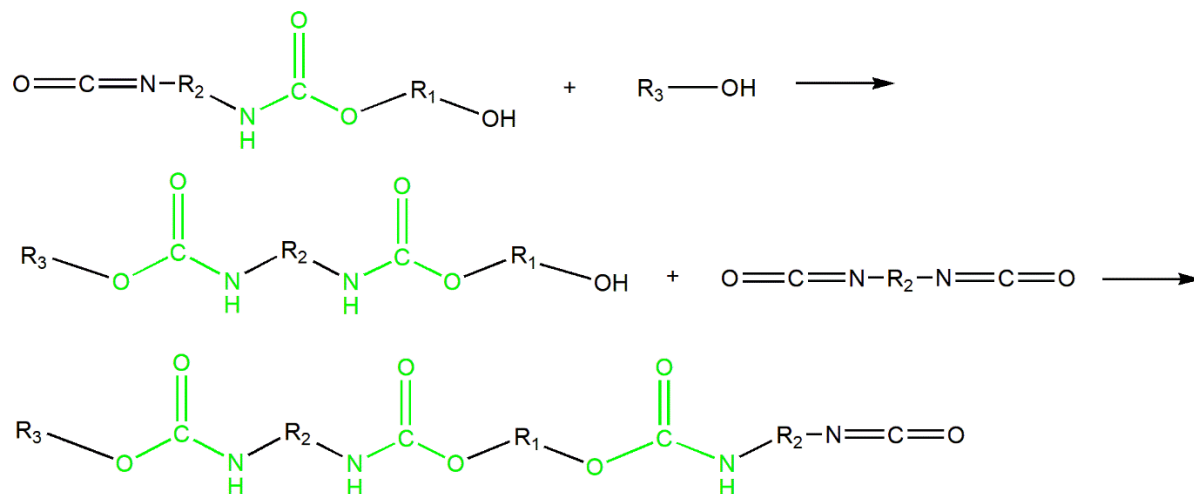


Figure S0.5. Mechanism of main polyurethane (PU) reaction between polyol (PEG) and diisocyanate (H₁₂MDI).

Hydrophobic modification of polyurethane (HEUR synthesis): PU + Octanol

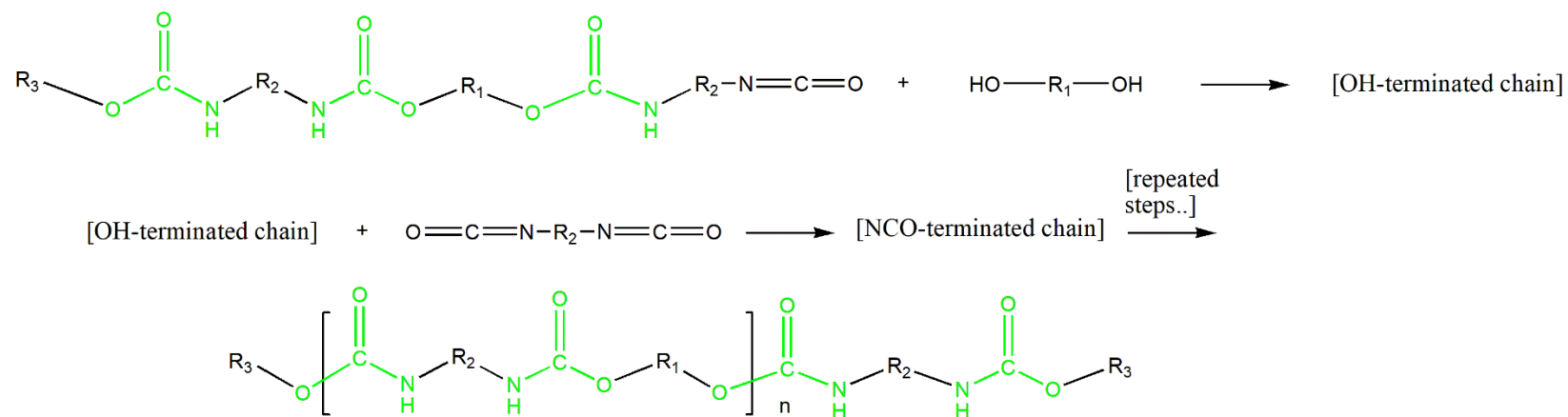
Appendix-Supporting Information

PU: octanol attachment in step A followed by step B



Hydrophobical modification step

Appendix-Supporting Information



PU: octanol attachment in the developed chain (Hydrophobical modification step)

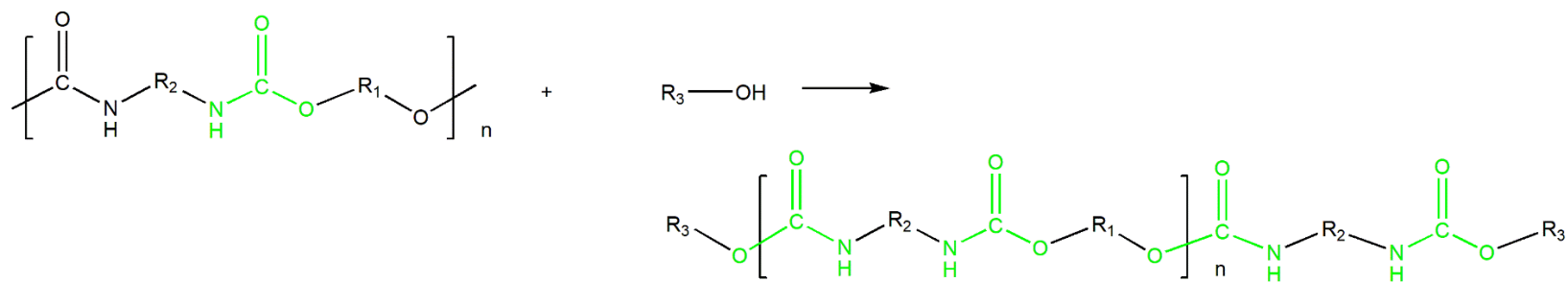


Figure S0.6. Mechanism of the reaction between 1-Octanol and PU during step A or directly at the PU formed polymer.

Appendix-Supporting Information

Diisocyanate and hydrophobe reaction: H₁₂MDI + 1-Octanol

Blocking of HMDI by octanol

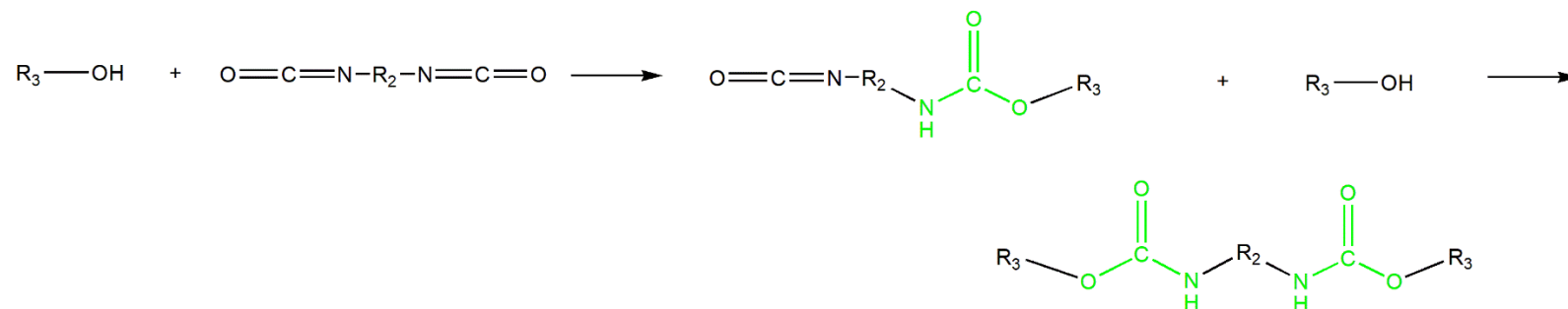
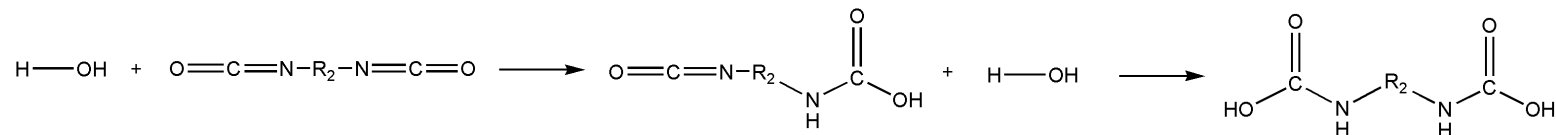


Figure S0.7. Mechanism of the reaction between octanol and diisocyanate.

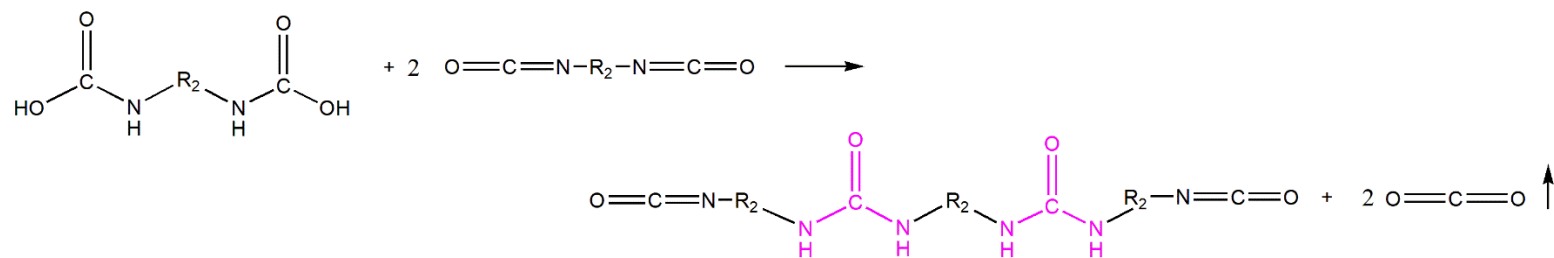
Diisocyanate and water reaction: H₁₂MDI + H₂O

HMDI and water reaction to carbamic acid



Appendix-Supporting Information

Carbamic acid reaction with 2 mol of HMDI: (poly)Urea production



Carbamic acid to amine and CO_2

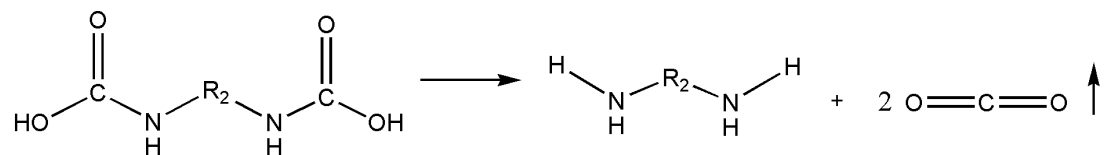


Figure S0.8. Mechanism of the reaction between water and diisocyanate.

Appendix-Supporting Information

It should be noted that carbamic acid is reported to be unstable, therefore its participation in the reaction with diisocyanate is unlikely.³ On the contrary, the most probable route is its decomposition to amine and CO₂. Further on, the amine produced will fast react with isocyanate as described next.

Diisocyanate and amine reaction: H₁₂MDI + Amine

Amine reaction with 2 mol of HMDI: (poly)Urea production

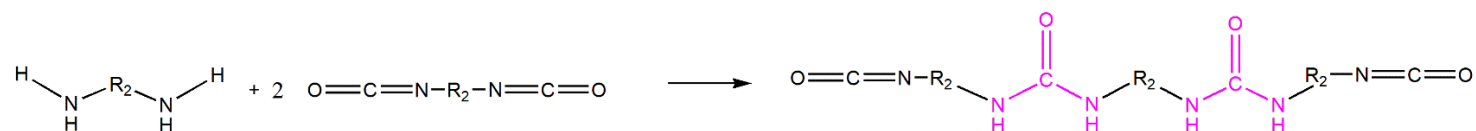
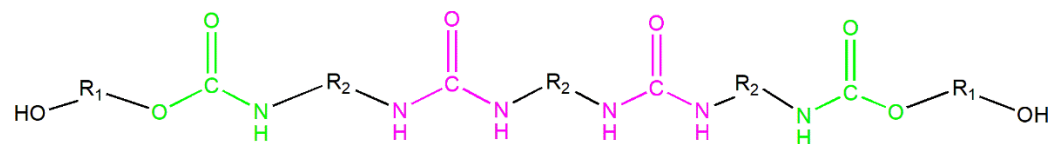
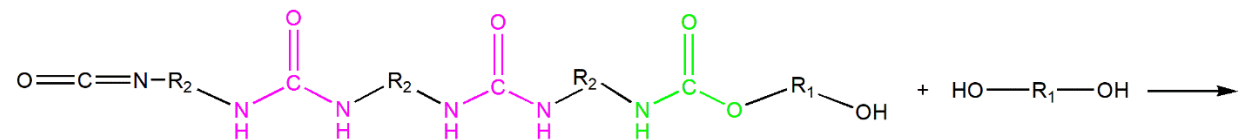
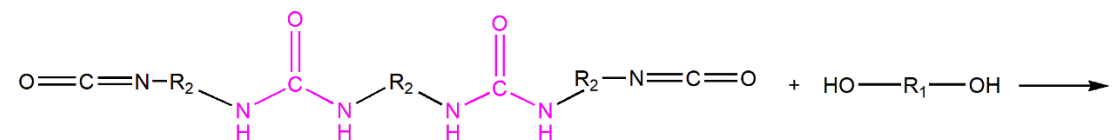


Figure S0.9. Mechanism of the reaction between amine and diisocyanate.

The urea bond containing molecules from Figure S0.8 and Figure S0.9 are N = C = O terminated and could further react with OH containing molecules. The reaction of these molecules with PEG, water (for the higher moisture concentration PEGs) and with octanol would result in the following OH or CH₃ end capped polymers:

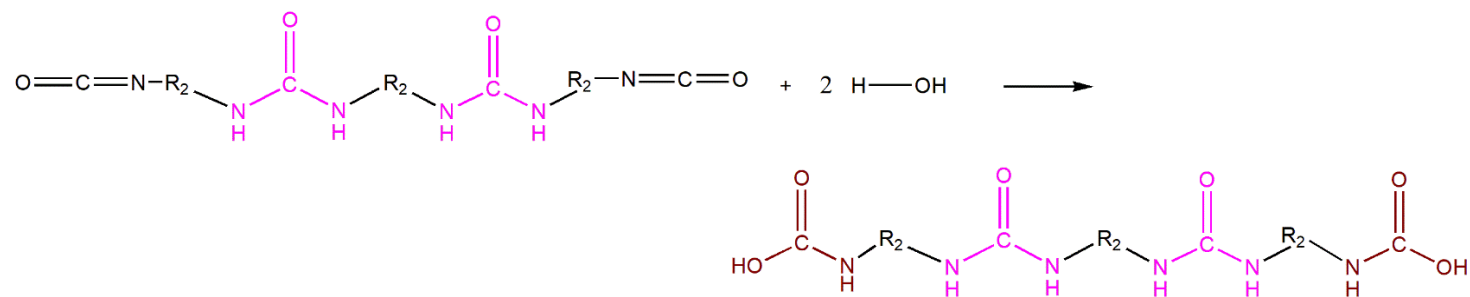
Appendix-Supporting Information

(poly)urea reaction with PEG



(poly)urea reaction with water

Appendix-Supporting Information



(poly)urea reaction with 1- Octanol (Hydrophobic modification step)

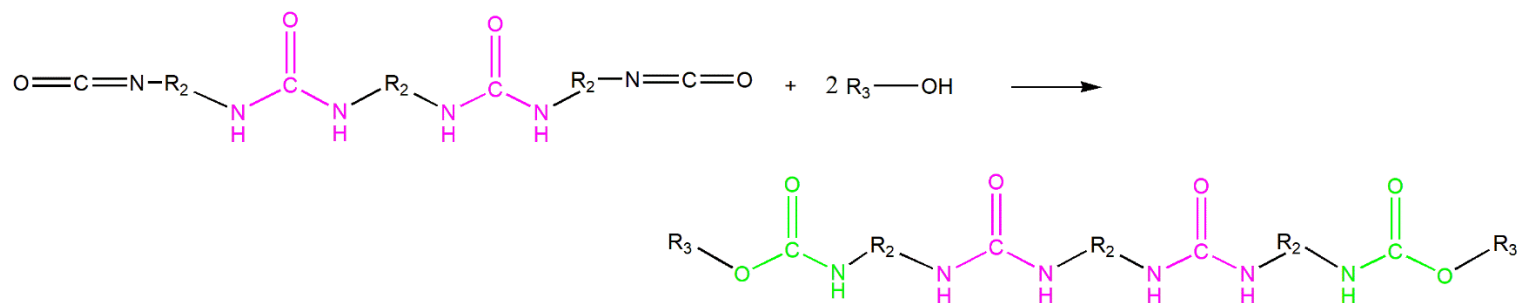


Figure S0.10. Mechanisms of the reaction of the urea containing polymer with PEG, water and 1-Octanol.

D. Analysis results

FTIR spectra

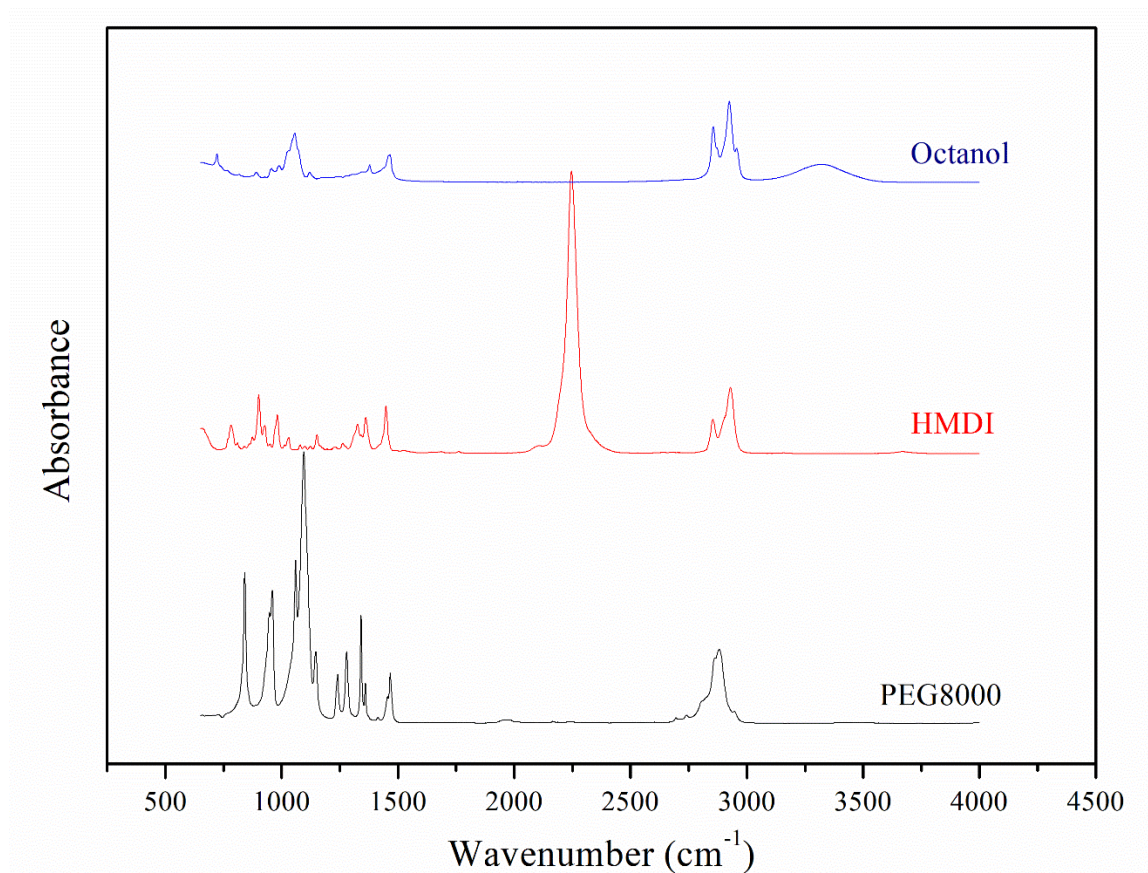


Figure S2.0.11. FTIR spectra of pure reactants (1-Octanol, H₁₂MDI and PEG8000 as received).

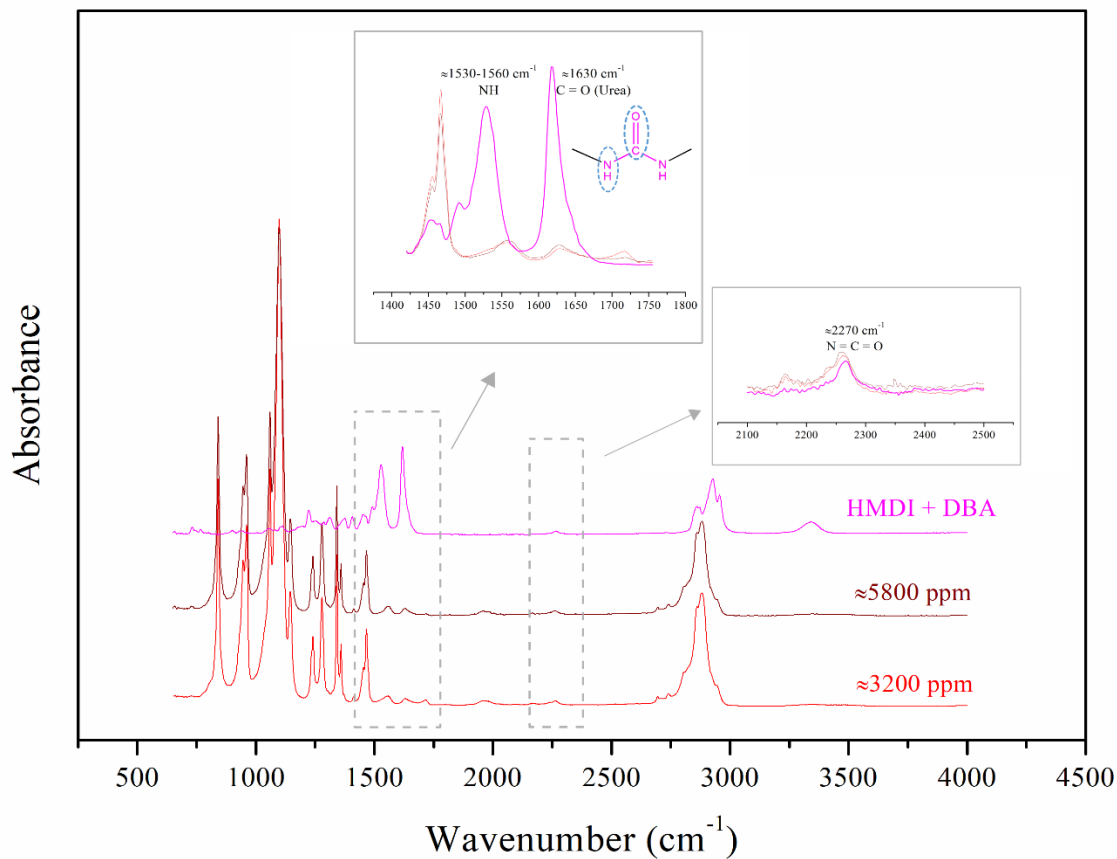


Figure S2.0.12. FTIR spectra of high moisture concentration PEG products compared to the reaction product of H_{12}MDI with dibutylamine (DBA); the peak at 1630 cm^{-1} confirms the type of the $\text{C} = \text{O}$ bond.

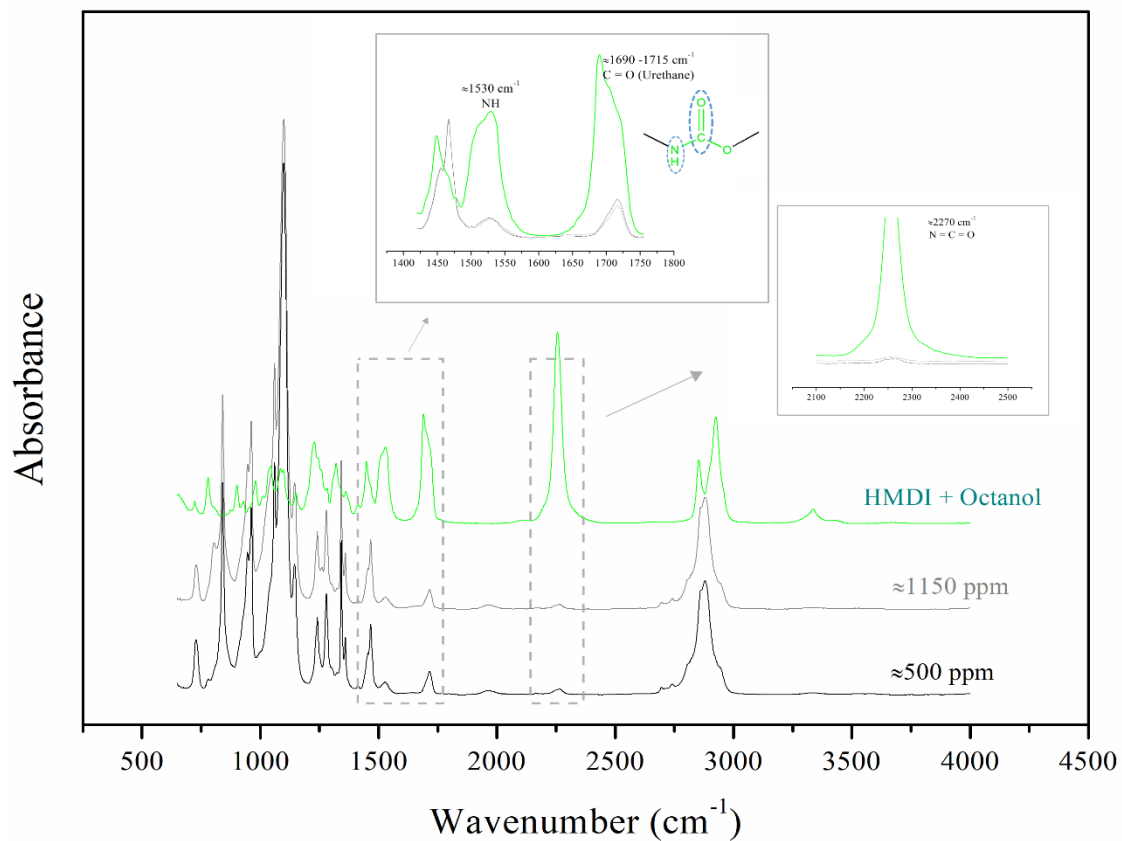


Figure S2.0.13. FTIR spectra of low moisture concentration PEG products compared to the reaction product of H_{12}MDI with 1-octanol; the peak at 1690-1715 cm^{-1} confirms the type of the $\text{C} = \text{O}$ bond.

Appendix-Supporting Information

HMDI/PEG=1.5 & Oct/PEG=1, $t_R=3$ min

HMDI/PEG=4 & Oct/PEG=1, $t_R=3$ min

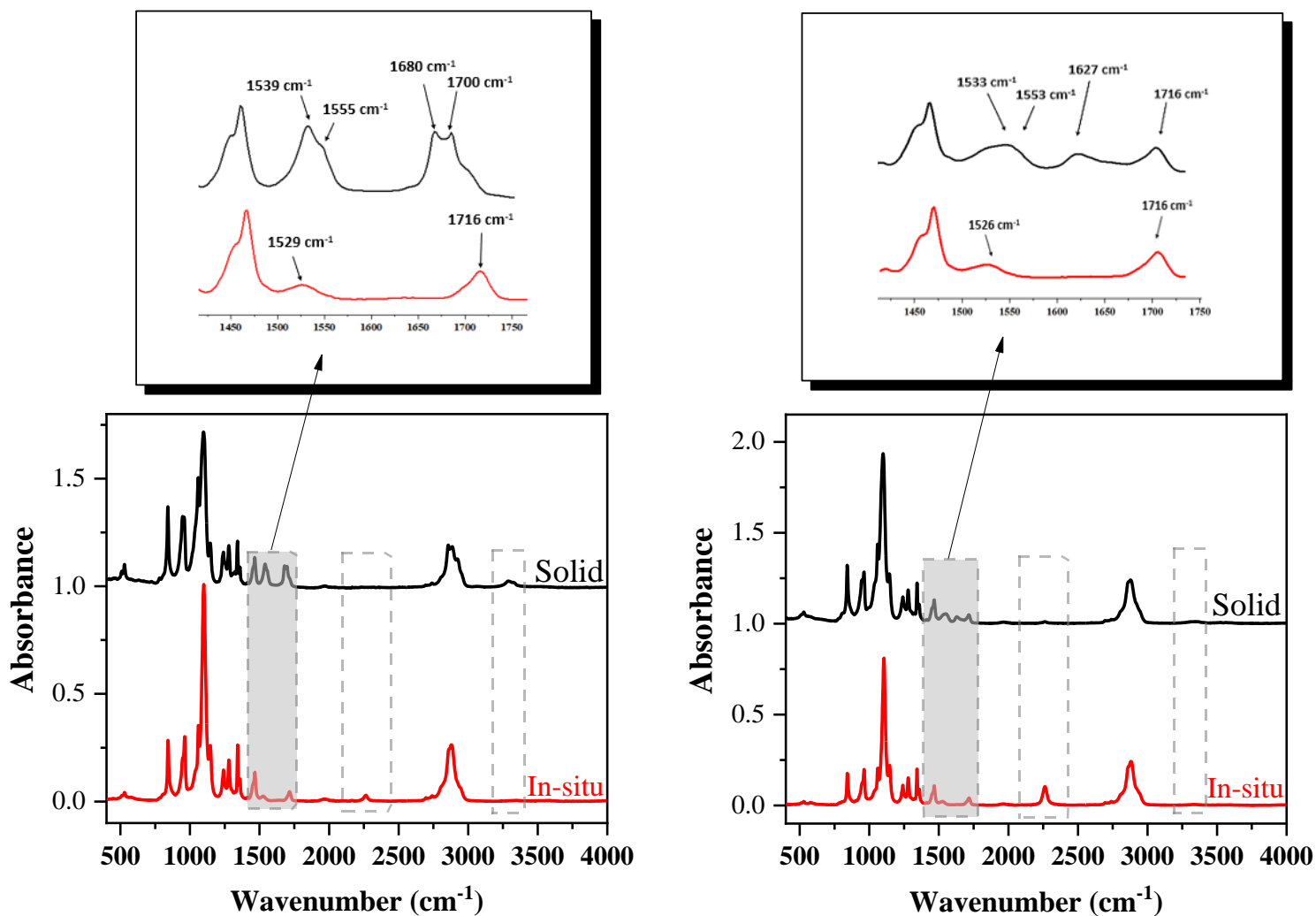


Figure S2.0.14. FTIR spectra of HEUR samples obtained with the in-situ and solid method at HMDI/PEG=1.5 and HMDI/PEG=4. Samples with both methods were taken at reaction times $t_R= 3$ min. For both experiments Oct/PEG=1.

¹H NMR

Appendix-Supporting Information

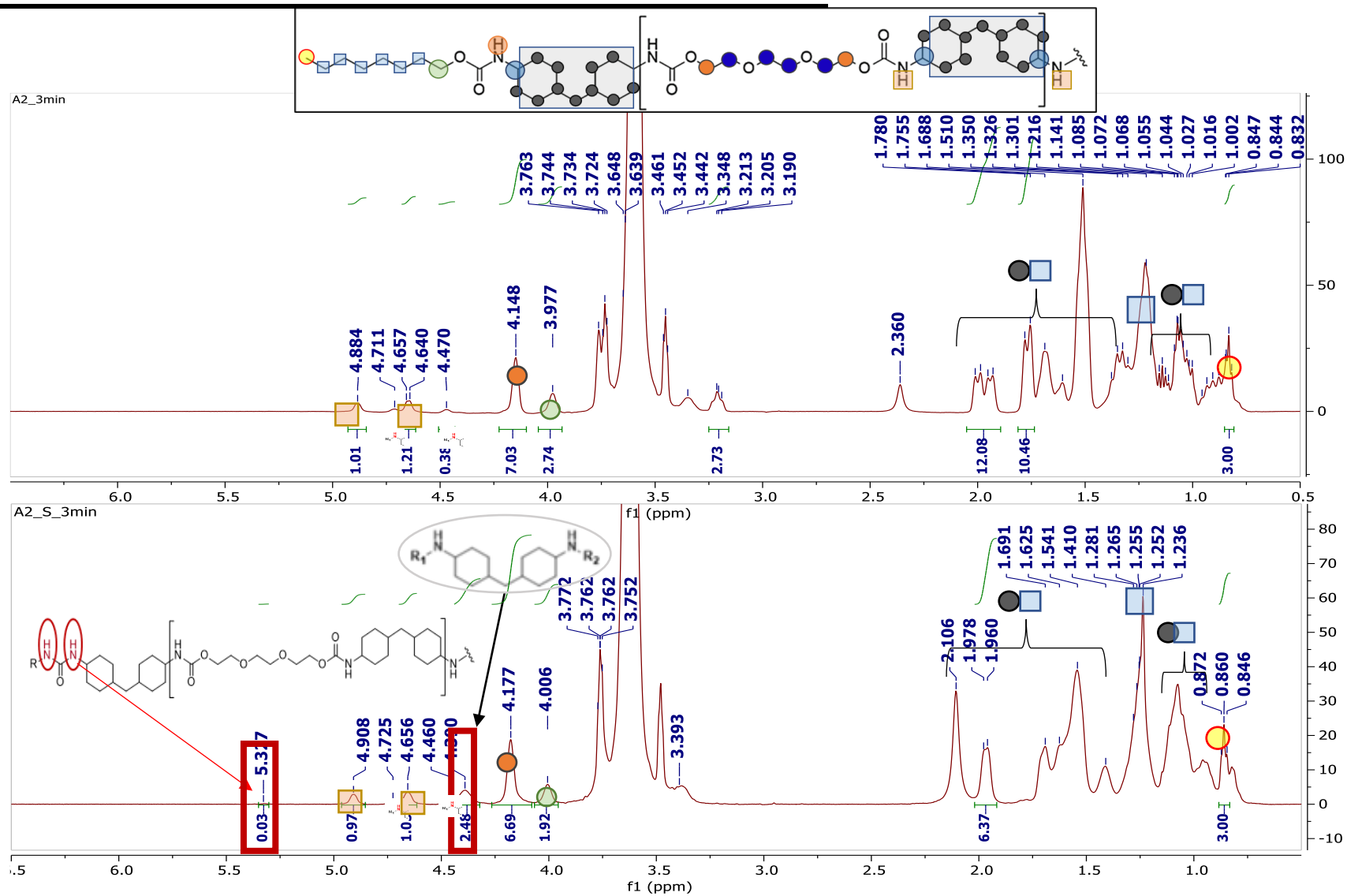


Figure S2.0.16. ^1H NMR spectra of HEUR samples obtained with the in-situ and solid method at HMDI/PEG=4. Samples with both methods were taken at reaction times $t_R=3$ min. For both experiments Oct/PEG=1.

TGA degradation curves

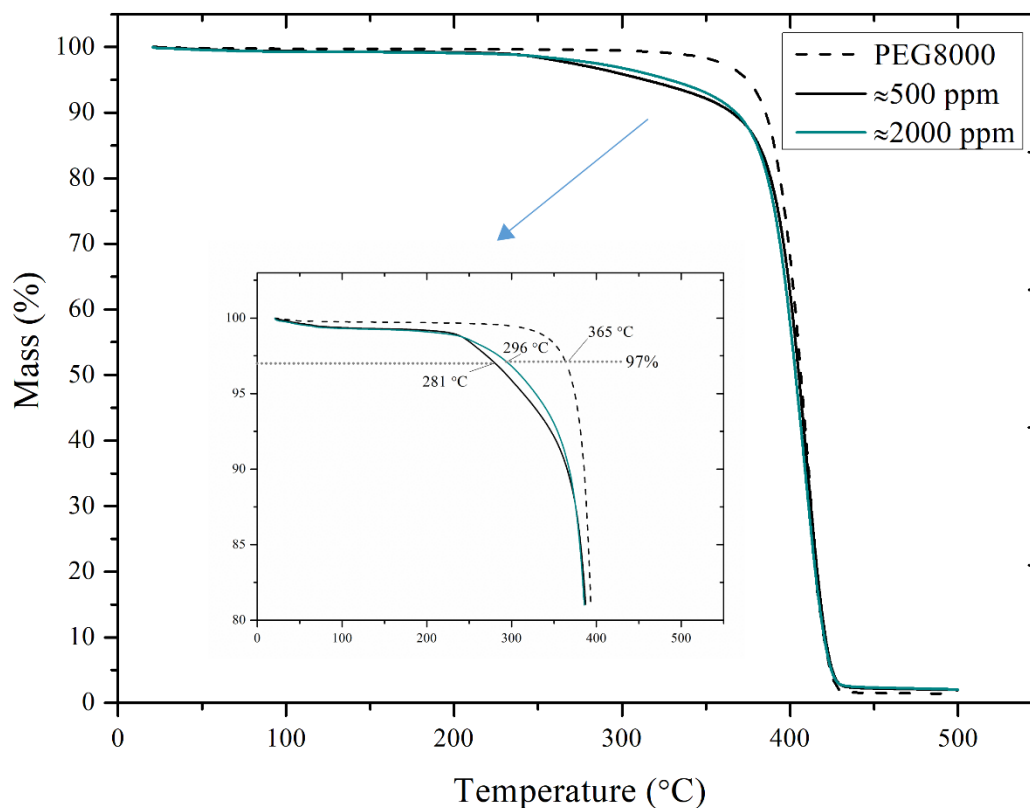


Figure S2.0.17. TGA curves of two selected HEUR samples from the moisture study (500 and 2000 ppm initial moisture concentration of the polyol). The HEUR produced from higher moisture concentration PEG requires higher temperature for mass reduction of 3% compared to the HEUR produced from low moisture concentration PEG. The curve of PEG8000 as received has also been added for reference.

XRD results

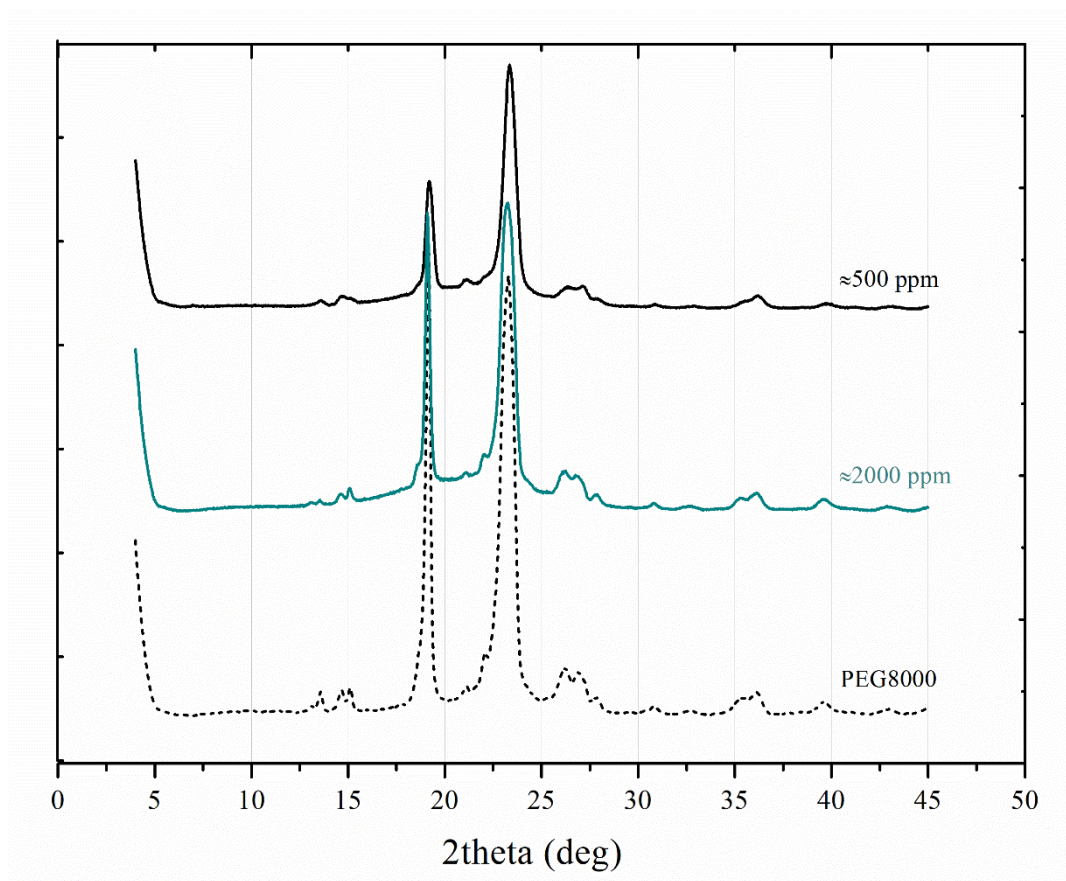


Figure S2.0.18. XRD patterns from PEG8000 and selected HEUR samples from the moisture study.

DSC curves

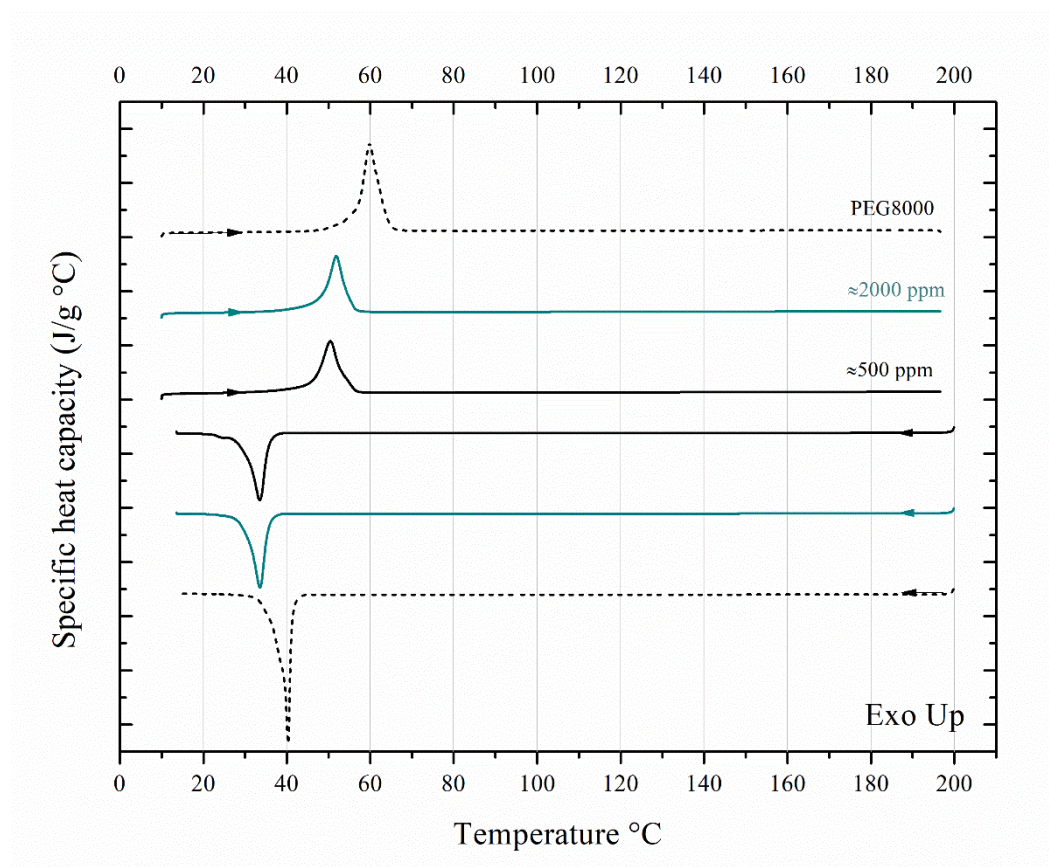


Figure S2.0.19. DSC heating (top) and cooling (bottom) runs at 10 °C/min for PEG8000 and two selected samples from the moisture parametric study (500 and 2000 ppm initial moisture concentration of the polyol). Arrows show the direction of the heating and cooling. The cooling curves have been shifted for clarity. The data are based on the third and fourth cycle in order to compare the materials after being exposed to the exact same thermal history.

Appendix-Supporting Information

SI for Chapter 3

Appendix-Supporting Information

Table S3.0.1. Summary of Two-Step HEUR Synthesis Studies in the literature: Details on the reactants used, operating conditions, reaction time, molecular weight and PDI values

Reactants <i>Type of method used</i>	Reaction medium	Diisocyanate/PEG (molar ratio)	Injection time of the end-capper (min)	Total reaction time (min)	Mn [g/mol]	PDI	Reference
PEG4000/IPDI/1-Tetradecanol					12,700 6900	– 1.3 - 1.2	
PEG6000/IPDI/1-Tetradecanol	Bulk	1.1 – 2.0	120	300	19,300 10,400	– 1.4 - 1.2	Lu et al., 2021 18
PEG8000/IPDI/1-Tetradecanol					25,300 - 8900	1.2 - 1.1	
<i>Two-step process</i>							

Appendix-Supporting Information

PEG6000/HMDI/Cetyl alcohol	Solvent	1.33	-	>120	16,500	1.4	Barmar et al., 2001⁴⁴
<i>Two-step process</i>							
PEG6000/HDI/Alkyl amine	Solvent	1.31	60	90	18,000	1.5	May et al., 1996²⁴
<i>Two-step process</i>							
PEG6000/HMDI/Alkyl amine	Solvent	1.31	60-120	90-150	20,000	1.6	Kaczmariski et al.⁴⁶
<i>Two-step process</i>							
PEG6000/HMDI/Alkyl amine	Solvent	1.50	30	270	24,000	1.4	Kaczmariski et al.⁴⁶
<i>Two-step process</i>							
PEG6000/HDI/Alkyl amine	Solvent	1.16			40,000	1.5	

Appendix-Supporting Information

<i>Two-step process</i>		1.33	30	270	32,000	1.5	
		1.5			28,000	1.4	
PEG8000/HMDI/Octanol	Bulk	1.50	0	45	21,000	1.6	Bampouli et al., 2022³
<i>One-step process</i>							
PEG6000/IPDI/ di(decyloxy)benzyl alcohol	Solvent	1.33	120	300	21,000	1.4	Peng et al., 2014⁴²
<i>Two-step process</i>							
PEG8000/HMDI/Octanol		0.5 -1.5			10,000- 21,000	1.4-1.6	
<i>One-step process</i>	Bulk		0	45			This work
		1.5-3			21,000- 10,000	1.6-1.3	

Appendix-Supporting Information

PEG8000/HMDI/Octanol	1.2	2, 4, 10	23,000	1.6
			30,000	1.7
			34,000	1.8
<i>Two-step process</i>	Bulk			
	1.5	10	22,000	1.7

Appendix-Supporting Information

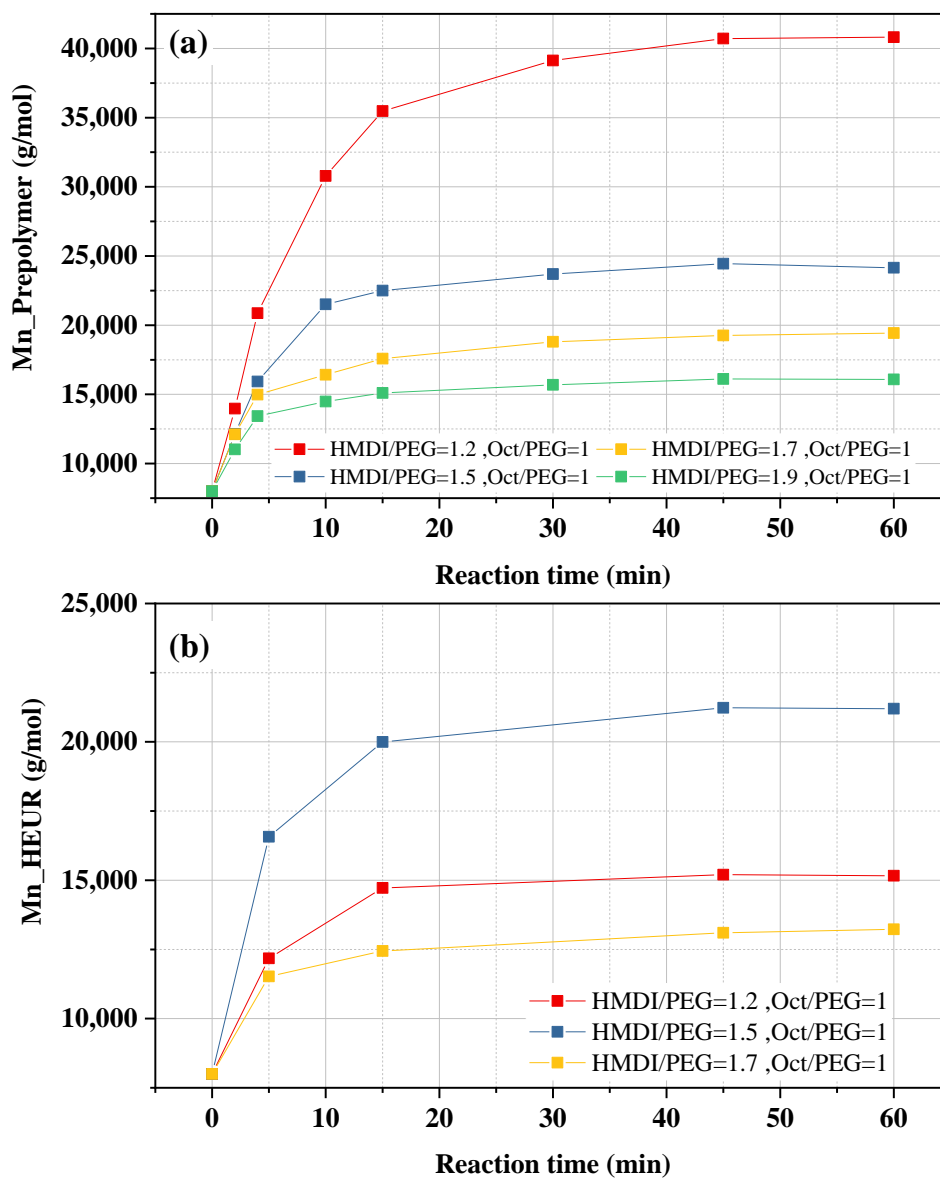


Figure S3.0.1. (a) Mn of the produced prepolymer obtained for HMDI/PEG ratios of 1.2, 1.5, 1.7 (b) Mn of the produced HEUR with one-step synthesis obtained for HMDI/PEG ratios of 1.2, 1.5, 1.7 and Oct/PEG=1. The lines have been added to guide the eye.

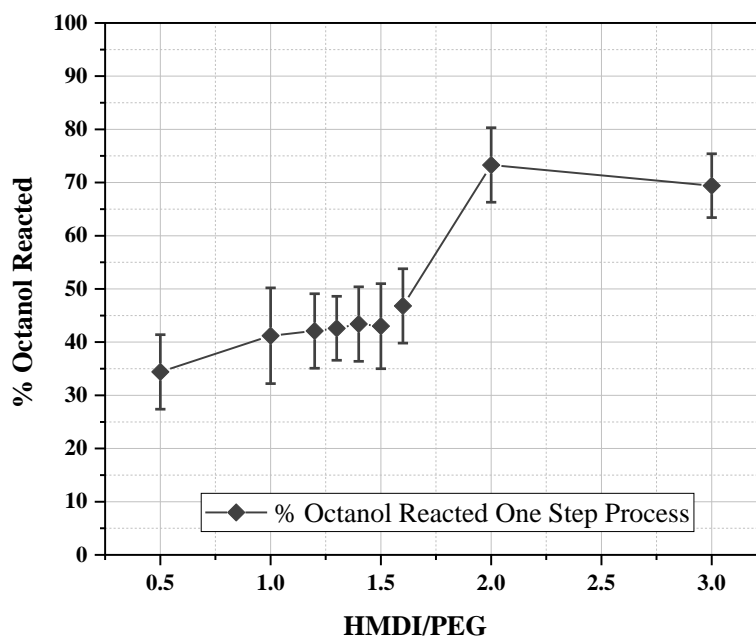


Figure S3.0.2. %Octanol reacted during the one-step HEUR synthesis for various initial HMDI/PEG ratios and Oct/PEG=1. The lines have been added to guide the eye.

Degree of chain extension of NCO terminated prepolymer with water

The high content of residual NCO groups can react with water during the water formulation step (added after the completion of the reaction) potentially leading to chain extension of the NCO-terminated prepolymer leading to urea linkages. This chain extension process can potentially contribute to an increase in the viscosity of the HEUR aqueous solution. To accurately determine the degree of chain extension, we conducted additional GPC analysis on the HEUR sample synthesized using a HMDI/PEG ratio of 3 and an Oct/PEG ratio of 1. This analysis involved measuring the molecular weight of HEUR prior to the addition of water, as well as after drying the aqueous formulation. A subsequent comparison of these measurements (Table S2), showed that the molecular weight values resulting after the chain extension step are still low enough to explain the significant viscosity increase observed in the aqueous solutions. This is also evident from Figure 3 of the main manuscript, which already indicates similar molecular weight values without exhibiting such high viscosity levels.

Appendix-Supporting Information

Table S3.0.2. Molecular weight values of HEUR sample synthesized using a HMDI/PEG ratio of 3 and an Oct/PEG ratio of 1 before and after the water addition.

Sample E59 (One-step HEUR synthesis, HMDI/PEG=3 and Oct/PEG=1)	Mn (g/mol)	Mw (g/mol)
In-situ sampling of the polymer belt before water addition into the reactor)	10,000	13,300
Solid sampling of the dried HEUR aqueous solution	15,300	23,600

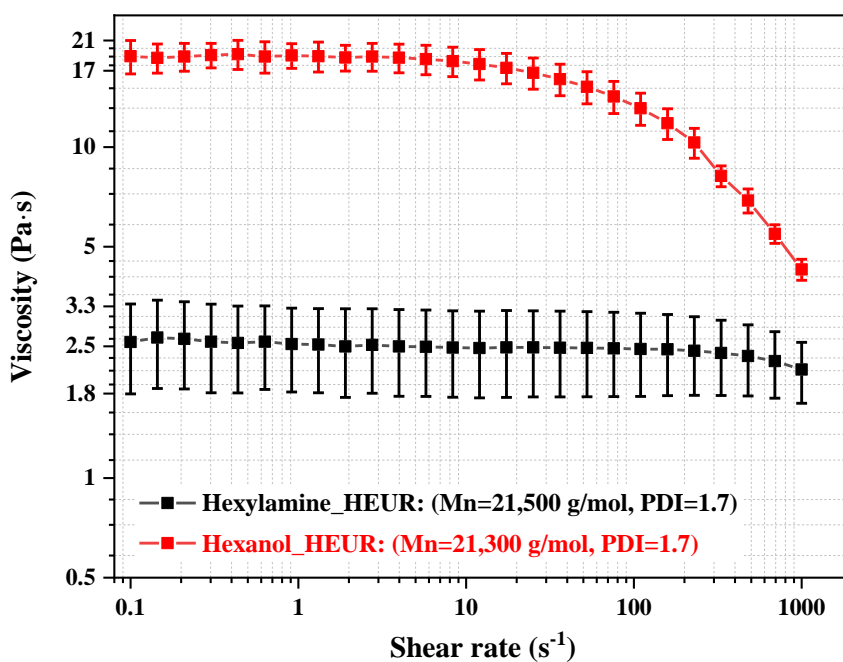


Figure S3.0.3. Steady shear viscosity testing of HEUR synthesized with hexylamine and hexanol via the one-step method (HMDI/PEG=1.5 & Hydrophobe/PEG=1), diluted

Appendix-Supporting Information

in water (20%) and measured at 23 °C. The M_n , PDI values are also indicated in the graph.

Detection of NCO and urea moieties with IR and NMR

The samples for the FTIR spectra of the HEUR synthesized with HMDI/PEG=1.5 and 3 (Oct/PEG=1) (one-step procedure) were collected by the in situ method¹, in which the molten samples were directly dissolved in vials with pre-weighed dry chloroform after the end of the reaction. (*Figure 3.8*)

The samples for the ¹H NMR (CDCl₃) spectra were collected as follows:

- (a) Spectra (a) and (b) were collected by the in situ method¹, in which the molten samples were directly dissolved in vials with pre-weighed CDCl₃ after the end of the reaction
- (b) To obtain spectra (c), the entire polymer content (HMDI/PEG=3, Oct/PEG=1) of the reactor was diluted with water in 20% w/w solutions by adding water to the reactor, after the end of the reaction. After a homogeneous water formulation of HEUR was obtained, an aqueous sample was taken from the bulk and dried under vacuum. Then, this dried sample was directly dissolved in vials with CDCl₃.

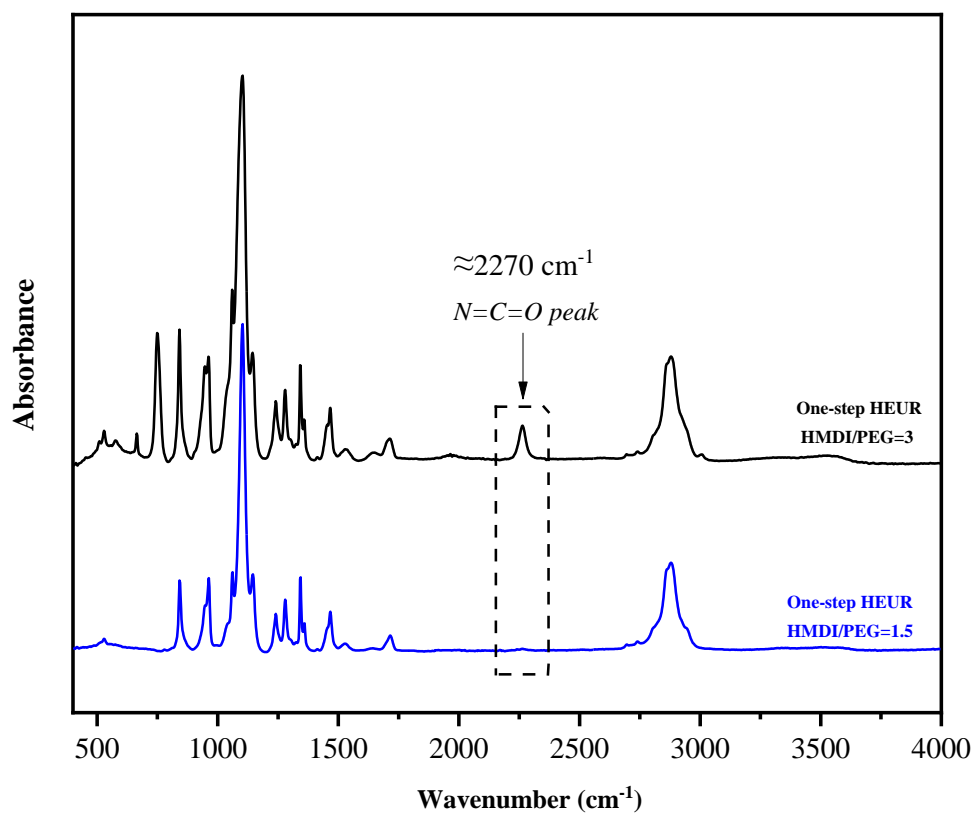


Figure S3.0.4. FTIR spectra of the HEUR (one-step process) synthesized with HMDI/PEG=1.5 and 3, Oct/PEG=1.

Appendix-Supporting Information

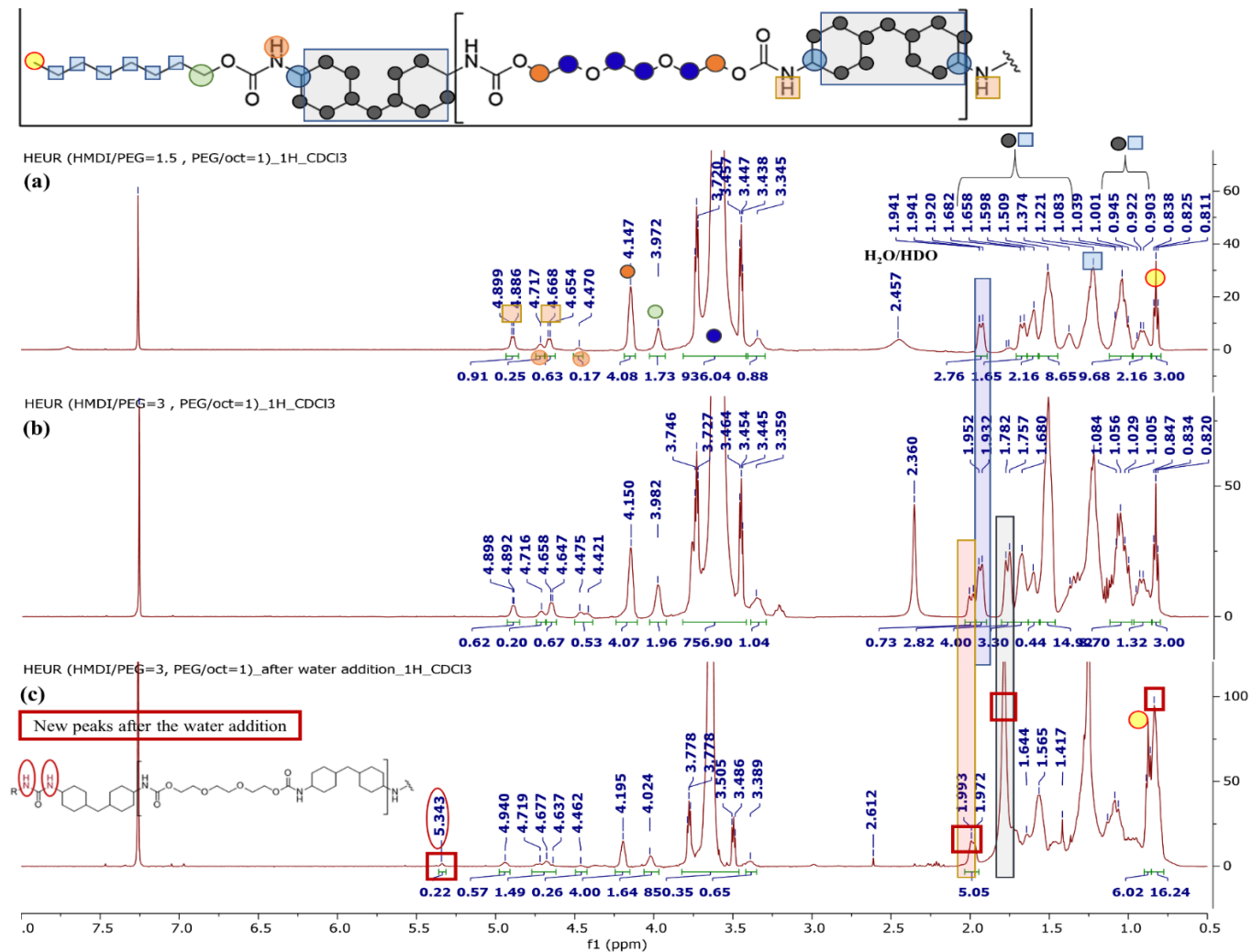


Figure S30.5. ¹H NMR (CDCl₃) spectra of (a) HEUR (one-step synthesis), HMDI/PEG=1.5, PEG/Oct=1 (in situ sampling: melt directly dissolved in CDCl₃) (b) HEUR (one-step synthesis), HMDI/PEG=3, PEG/Oct=1 (in situ sampling: melt directly dissolved in CDCl₃) and (c) HEUR (two-step synthesis) and (c) HEUR (one-step synthesis), HMDI/PEG=3, PEG/Oct=1 (dried solid sampling: the sample was taken after the HEUR was formulated in water, it was dried under vacuum and then directly dissolved in CDCl₃)

Appendix-Supporting Information

Table S3.0.3. Number-average molecular weight and PDI values of prepolymers/HEURs obtained with the two-step (2,4,10 min) method for HMDI/PEG=1.2 and Oct/PEG=1, Oct/PEG=2

Injection time of end-capping agent (Pre-polymerization time) (min)	Number-average molecular weight (g/mol) / PDI			Prepolymer's maximum
	Prepolymer	HEUR at the end of the reaction (Oct/PEG=1)	HEUR at the end of the reaction (Oct/PEG=2)	
2	14,000 / 1.5	22,900 / 1.6	19,000 / 1.6	40,700/1.9
4	20,900 / 1.6	29,900 / 1.7	27,600 / 1.7	
10	30,800 / 1.8	34,200 / 1.8	33,800 / 1.7	

End-capping efficiency in the two-step process

The homogeneity of the bulk in terms of %octanol reacted was investigated by collecting samples from various spots of the reactor. **(Figure S3.0.6)** Sampling included spots from the bulk of the polymer that was on the agitator shaft and some polymer residue at the bottom and sidewalls of the reactor. The molecular weight sampling procedure included only one sample per batch, containing material from various spots of the polymer melt. **(Figure S3.0.7)** After the polymerization was completed, all 6 batches were formulated with water by adding water to the reactor.

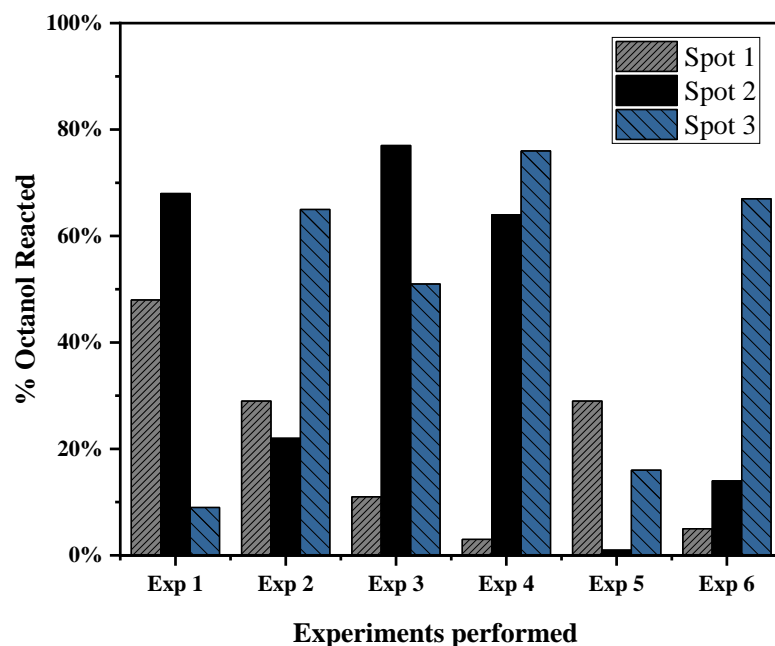


Figure S3.0.6. % Octanol reacted of 6 identical HEURs synthesized with the two-step process with HMDI/PEG=1.5, injection time=10 min and Oct/PEG=1. Three samples were taken per batch. The samples were taken from different spots of the polymer melt (agitator shaft, bottom, and sidewalls of the reactor)

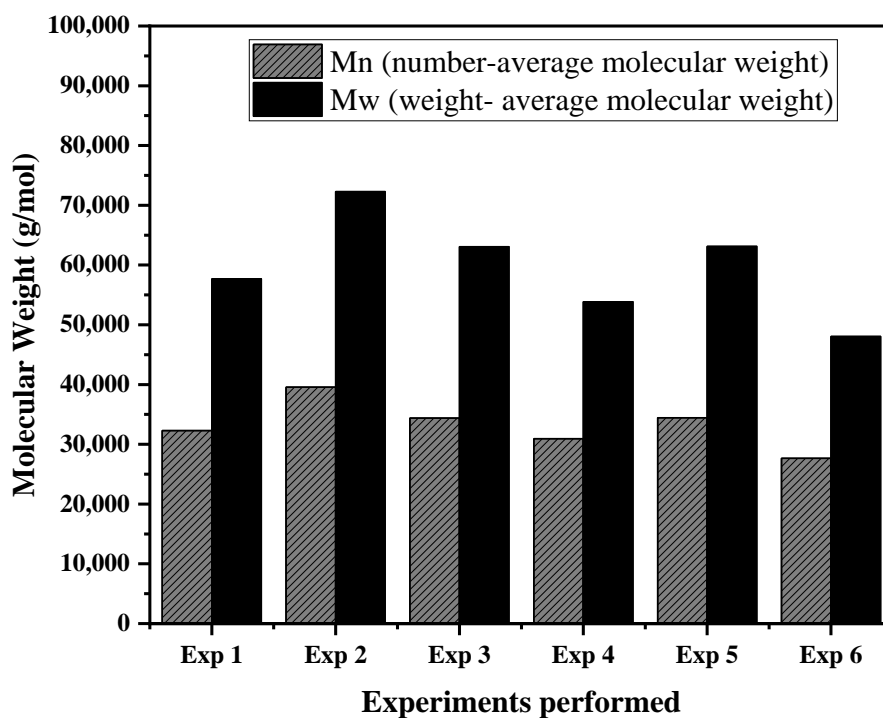


Figure S3.0.7. Number and weight average molecular weight of 6 identical HEURs synthesized with the two-step process with HMDI/PEG=1.5, injection time=10 min and Oct/PEG=1. One GPC sample was taken per batch, containing material from various spots of the polymer bulk.

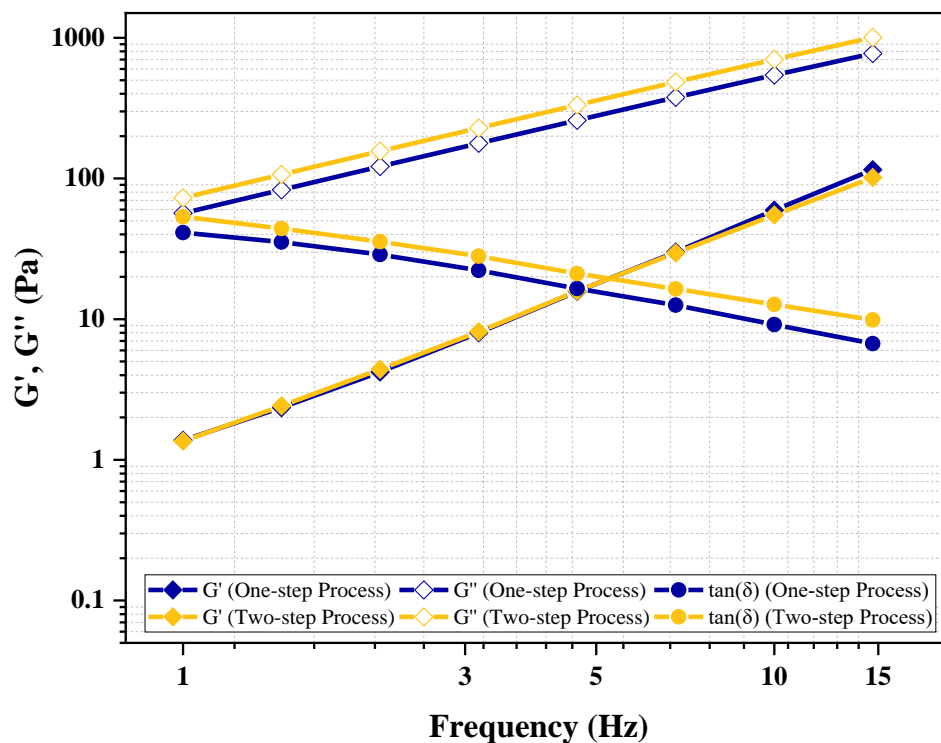


Figure S3.0.8. Storage modulus (G' , solid symbols) and loss modulus (G'' , open symbols) versus frequency for HEUR products synthesized with the one and two-step process.

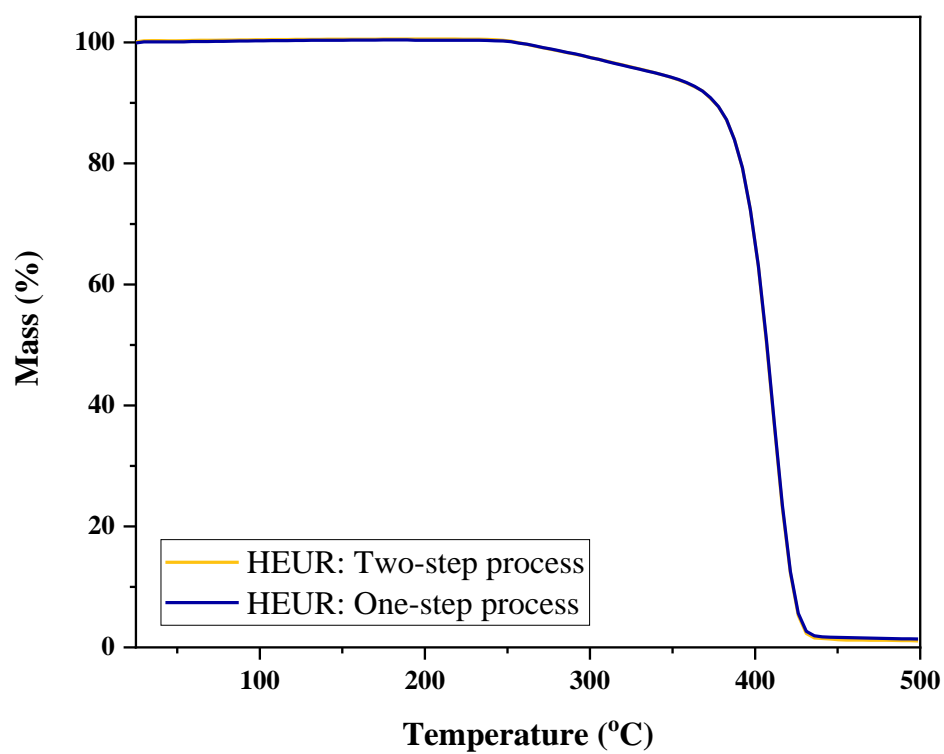


Figure S3.0.9. TGA curves of HEUR products synthesized with the one and two-step process at HMDI/PEG=1.5 and Oct/PEG=1

Appendix-Supporting Information

SI for Chapter 5

Aqueous solutions

Coarse-Grained MD simulations

Table S5.0.1. MARTINI force-field parameters

Bead types and mass	PEO: 44.05 g/mol P3 (Polar – Degree of polarity 3): 57.05 g/mol SC1CH (Cyclohexane bead): 28 g/mol C1 (Apolar – Degree of polarity 1): 58 g/mol P4 (Polar – Degree of polarity 4): 72 g/mol	
Non-bonded Lennard Jones interactions	$U_{ij}(r) = 4\varepsilon_{ij} \left[\left(\frac{\sigma_{ij}}{r} \right)^{12} - \left(\frac{\sigma_{ij}}{r} \right)^6 \right]$	
	$i - j$	ε_{ij} (kJ mol ⁻¹)
	P4-P4	5
	P4-PEO	4
	P4-C1	2
	P4-P3	5
	P4-SC1CH	2
	PEO-PEO	3.77
	PEO-P3	4.5
	PEO-SC1CH	2.026
	PEO-C1	2.7
	P3-P3	5
	P3-SC1CH	2.3
	P3-C1	2.3
	SC1CH-SC1CH	2.625
	SC1CH-C1	3.5
	C1-C1	3.5
Bonded Interactions	$V_b(r) = \frac{1}{2}k_{ij}^b(r - b_{ij})^2$	
	Bond	b_{ij} (nm)
	PEO-PEO	0.33
	PEO-P3	0.47
	P3-SC1CH	0.47
	P3-C1	0.47
	C1-C1	0.47
	SC1CH-SC1CH	5000

Appendix-Supporting Information

Bond angle bending

$$V_a(\theta) = \frac{1}{2} k_{ijk}^a (\cos(\theta) - \cos(\theta_{ijk}))^2$$

Bond angle	k_{ijk}^a (kJ mol ⁻¹ rad ⁻²)	θ_{ijk} (deg)
PEO-PEO-P3	25	179.9
PEO-PEO-PEO	85	130
SC1CH-SC1CH-SC1CH	25	179.9
PEO-P3-SC1CH	25	179.9
SC1CH-SC1CH-P3	25	179.9
P3-C1-C1	25	179.9
C1-P3-SC1CH	25	179.9
P3-SC1CH-SC1CH	25	179.9
SC1CH-P3-C1	25	179.9

Latex-formulations

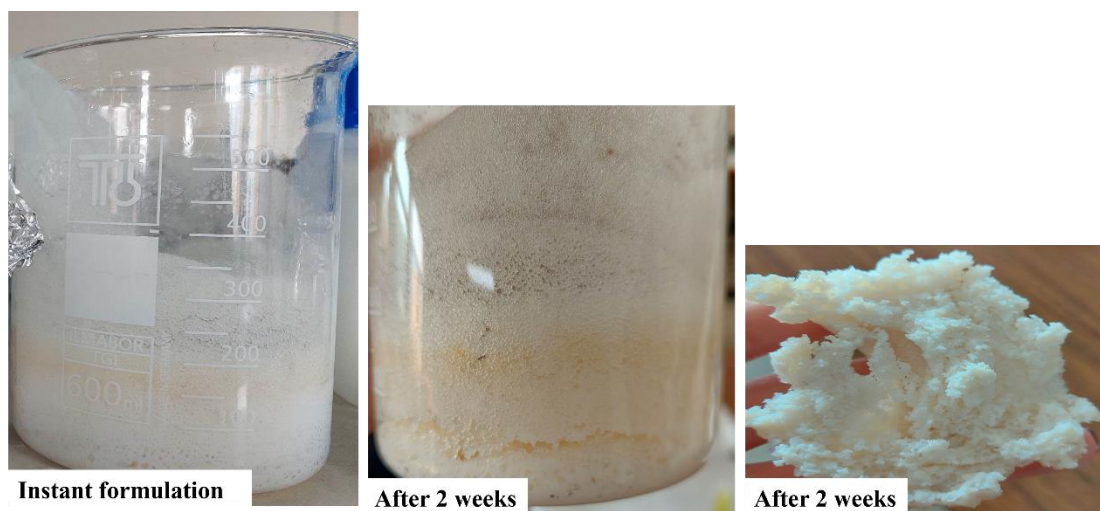


Image S5.0.1. Picture of the instant phase separation of HEUR: P2-HMDI-C8, Mn=8,000 g/mol upon formulation with latex.

Appendix-Supporting Information

Paint formulations

Table S5.0.2. Indices of Pseudoplasticity, Yield Points, G' Values (derived from the linear plateau of the AS test), and Crossover Points (observed in the FS test) for all paints, arranged in ascending order.

	Pseudoplasticity Index $\left(\frac{\eta_{0.1s^{-1}}}{\eta_{10^4s^{-1}}}\right)$		Yield point ($\gamma\%$)		G' (average value calculated within the LVER) (Pa)		Crossover Point (Hz)
Paint 2	23	Paint 5	3,15	Paint 5	6	Paint 8	-
Paint 5	34	Paint 1	4,63	Paint 2	13	Paint 3	0,46
Paint 6	36	Paint 2	4,63	Paint 6	15	Paint 1	0,68
Paint 3	53	Paint 6	4,63	Paint 3	30	Paint 2	1,47
Paint 8	62	Paint 8	6,80	Paint 8	33	Paint 7	1,47
Paint 1	75	Paint 3	6,80	Paint 1	36	Paint 6	1,72
Paint 4	139	Paint 4	6,81	Paint 4	63	Paint 5	3,16
Paint 7	658	Paint 7	14,73	Paint 7	113	Paint 4	3,69

Oscillatory measurements

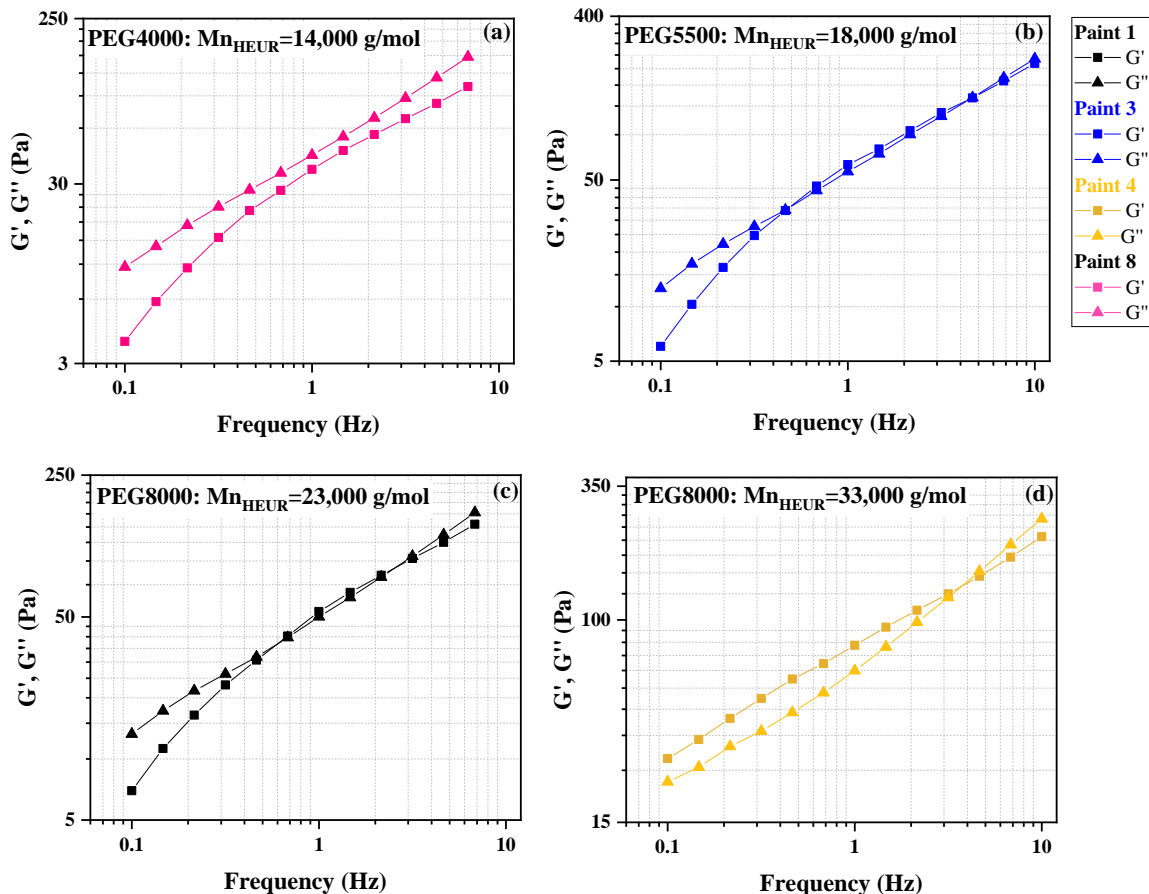


Figure S5.0.1. Frequency sweep tests for paints thickened with HEURs with varying hydrophilic segment (a) 14,000 g/mol (b) 18,000 (c) 23,000 g/mol (d) 33,000 g/mol.

Calculation of Thixotropic Index

The 3ITT test comprises three key intervals:

Interval (1): A very low shear rate is applied to simulate the paint's behavior at rest.

Interval (2): A high shear rate is applied to simulate the structural breakdown of the paint during application processes such as brushing or rolling.

Interval (3): A very low shear rate is reapplied to simulate the paint's structural regeneration at rest.

The TI has previously been defined as:⁶⁴

Appendix-Supporting Information

$$TI = \frac{\eta_{t_R} - \eta_{HS}}{t_R}$$

η_{t_R} : was selected to be 75% of the low shear viscosity.

η_{HS} : viscosity at the end of the high shear interval (2nd interval)

t_R : recovery time to regain η_{t_R}

Thermal Stability of Paints

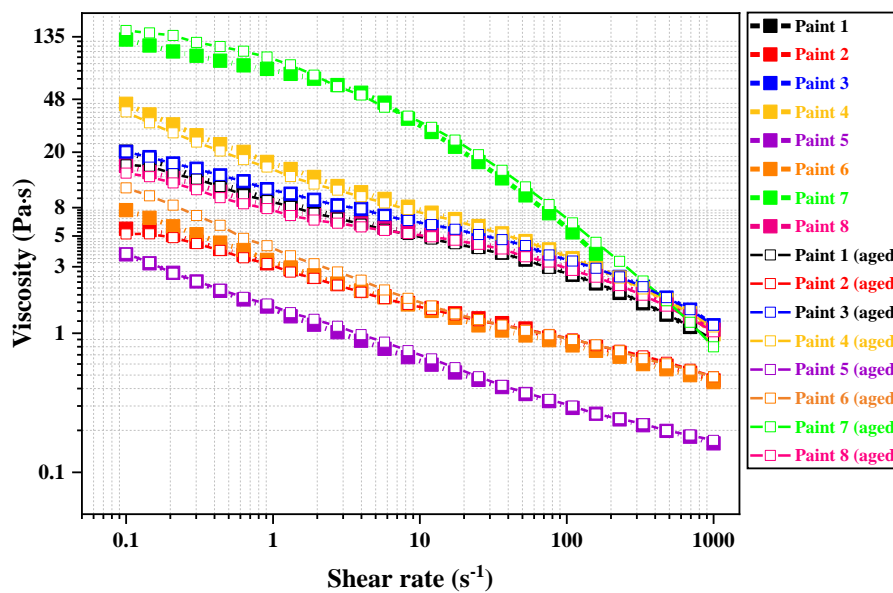


Figure S5.0.2. Steady shear viscosity curves for fresh and aged Paints

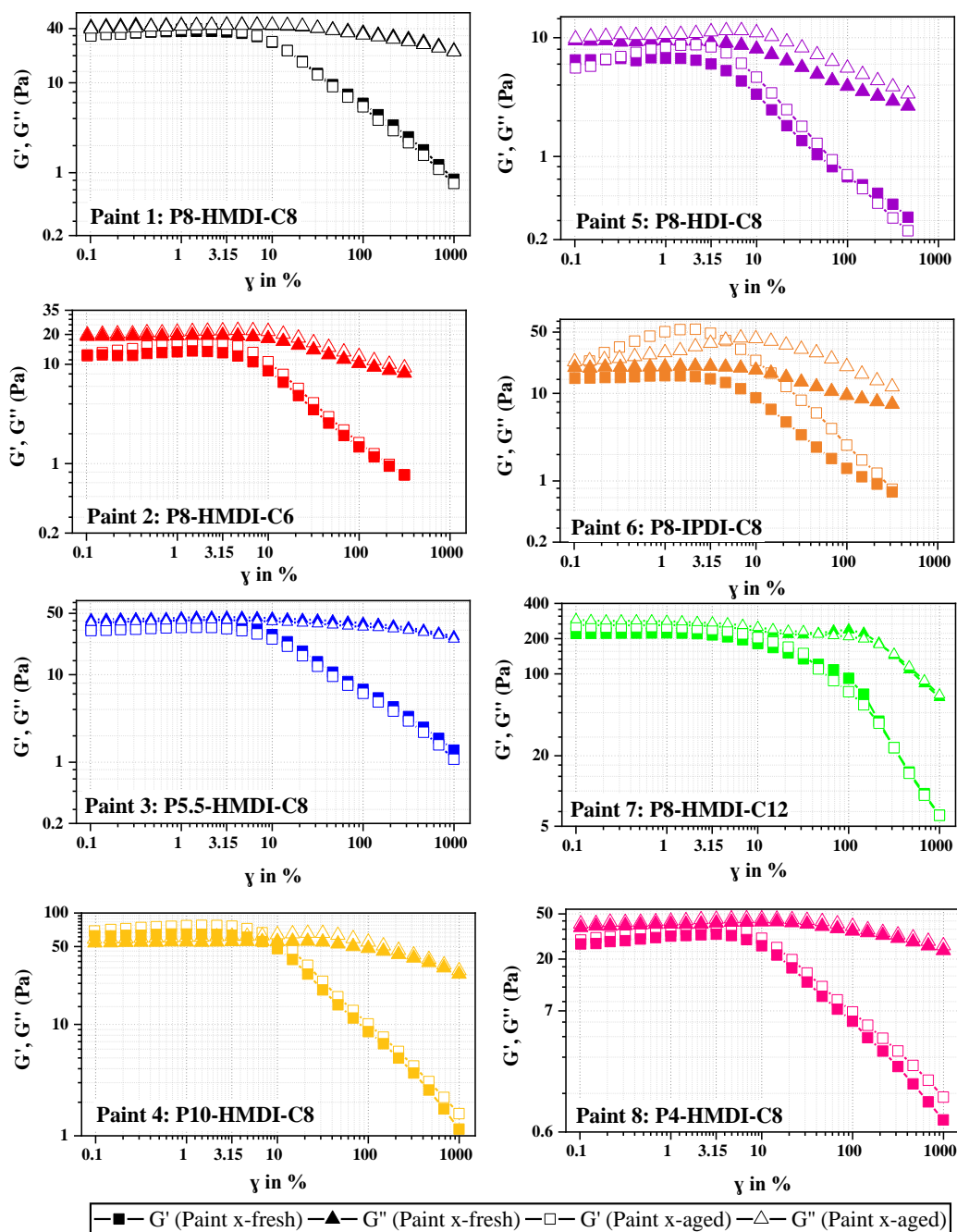


Figure S5.0.3. AS test for fresh and aged Paints

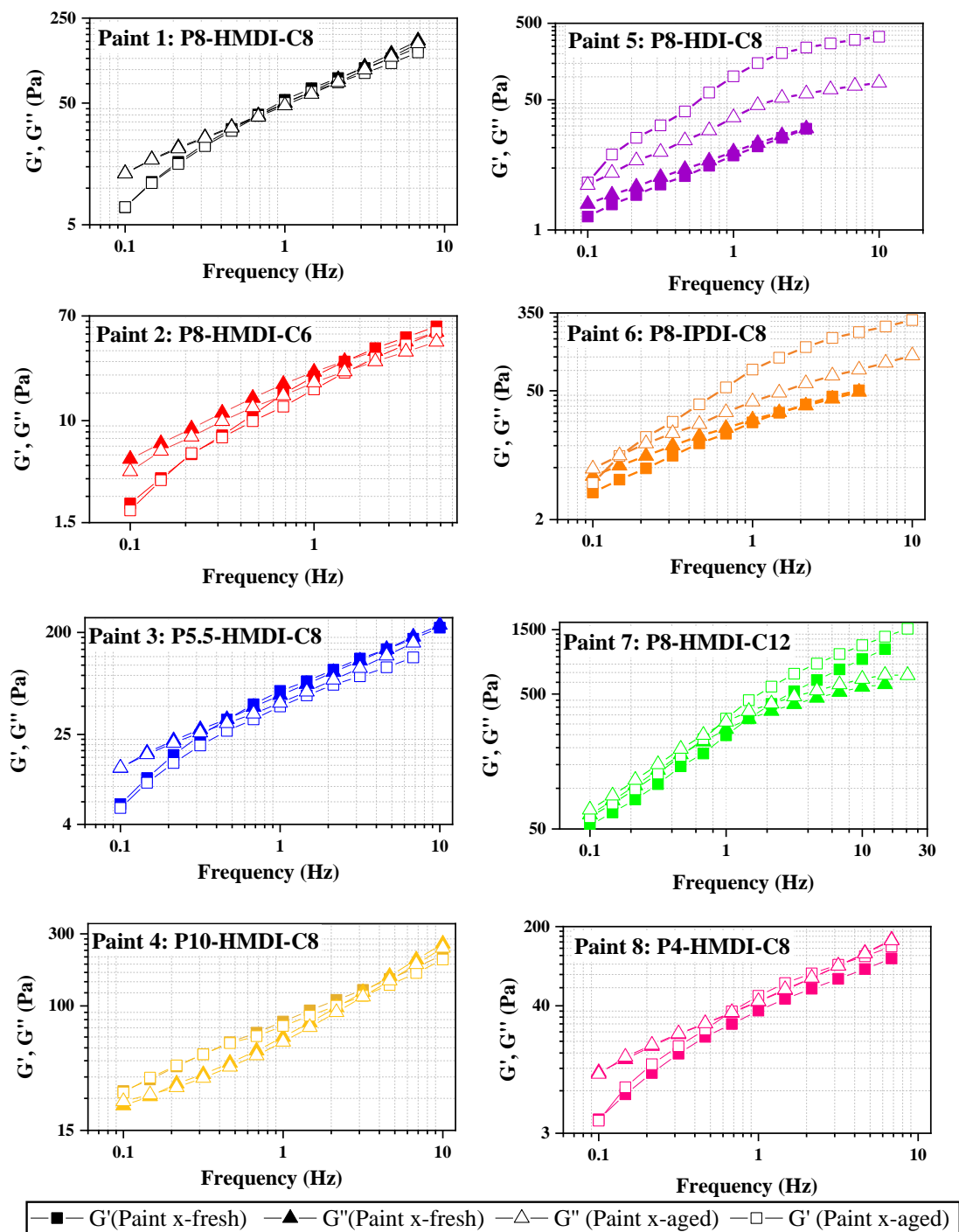


Figure S5.0.4. FS test for fresh and aged Paints

Appendix-Supporting Information

Table S5.0.3 provides a summary of observations derived from the comparisons of the AS and FS tests between the fresh and aged samples. AS and FS test are presented in Figures S5.0.3 and S5.0.4.

The AS results didn't show significant variations; however, the most distinct rheological behavior, indicative of superior structural strength, was evident in Paints 2, 5, and 6. The FS results bolstered these findings. Most notably, Paint 5 and Paint 6 presented superior viscoelastic properties. Both had a crossover point at an exceedingly low frequency, showcasing predominantly solid behavior at the rest of the frequency domain. This solid character implies robust interparticle associations, with superior properties compared to the original network observed in the fresh paints. Overall, taking into consideration the results of all the rheological tests, Paint 1 displayed the most stable behavior, while Paint 4 had the least deviation compared to its fresh counterparts.

Table S5.0.3. Summary of observations derived from the comparisons of the AS and FS tests between the fresh and aged samples.

	Amplitude Sweep	Frequency Sweep
Paint 1	The values of G' and G'' remain consistent and exhibit similar trends throughout the entire % strain range.	The values of G' and G'' remain consistent and exhibit similar trends throughout the entire frequency range. Their crossover points are also identical.
Paint 2	Nearly identical G' and G'' curves were observed, with G' exhibiting an upward trend in the LVER, indicating a thickening effect.	The crossover is observed at the same frequency for both G' and G'' ($f=1.46$ Hz). While the trends of both modulus remain consistent, the aged paint exhibits diminished values.
Paint 3	Nearly identical G' and G'' curves were observed, with a slight tendency towards decreased values.	Compared to the fresh paint, the aged paint lacks a crossover point. Throughout the entire frequency range, the aged paint distinctly exhibits a viscous behavior with G'' consistently greater than G' .

Appendix-Supporting Information

Paint 4	Nearly identical G' and G'' curves were observed, with a slight tendency towards increased values.	Both the fresh and aged paints exhibit the same crossover point. While the G' and G'' curves follow a similar trend for both modulus, the aged paint displays marginally reduced values.
Paint 5	Nearly identical G' and G'' curves were observed, with G' exhibiting an upward trend in the LVER, indicating a thickening effect.	There's a marked effect on the G' , G'' curves. The aged samples exhibit a crossover point at very low frequencies, showcasing a predominantly solid behavior throughout most of the frequency range. Both modulus also tend to reach a plateau value. In contrast, the fresh sample has its crossover point at a higher frequency, displaying a liquid-like behavior in the low-frequency region. At the higher frequency domain, the fresh sample presents equivalent values for both G'' and G' .
Paint 6	A shift from a liquid-like behavior ($G' < G''$) to a solid-like characteristic was noted, accompanied by a thickening effect in both G' and G'' at lower strain values.	Paint 6 shows approximately the same tendency with Paint 5.
Paint 7	Nearly identical G' and G'' curves were observed	The crossover occurs at a lower frequency with elevated G' and G'' values, though the curves largely maintain a similar trend. There's a more pronounced deviation between the G' and G'' curves in the high-frequency domain.
Paint 8	Nearly identical G' and G'' curves were observed, with a slight tendency towards increased values.	In contrast to the fresh sample, which doesn't exhibit a crossover, the aged sample displays a crossover point at $f=0.68$ Hz and primarily demonstrates a liquid behavior at low frequencies. At higher frequencies, the G' and G'' values converge and become closely aligned.

